

**BIOLOGICAL AND CHEMICAL SLUDGE FILTRATION**

**A THESIS SUBMITTED TO  
THE GRADUATE SCHOOL OF NATURAL AND APPLIED SCIENCES  
OF  
MIDDLE EAST TECHNICAL UNIVERSITY**

**BY**

**HANDE YÜKSELER**

**IN PARTIAL FULFILLMENT OF THE REQUIREMENTS  
FOR  
THE DEGREE OF DOCTOR OF PHILOSOPHY  
IN  
ENVIRONMENTAL ENGINEERING**

**JULY 2007**

Approval of the thesis:

**BIOLOGICAL AND CHEMICAL SLUDGE FILTRATION**

submitted by **HANDE YÜKSELER** in partial fulfillment of the requirements for the degree of **Doctor of Philosophy in Environmental Engineering Department, Middle East Technical University** by,

Prof. Dr. Canan Özgen  
Dean, Graduate School of **Natural and Applied Sciences** \_\_\_\_\_

Prof. Dr. Göksel N. Demirer  
Head of Department, **Environmental Engineering** \_\_\_\_\_

Prof. Dr. Ülkü Yetiş  
Supervisor, **Environmental Engineering Dept., METU** \_\_\_\_\_

Prof. Dr. İsmail Tosun  
Co-Supervisor, **Chemical Engineering Dept., METU** \_\_\_\_\_

**Examining Committee Members:**

Prof. Dr. F. Dilek Sanin  
Environmental Engineering Dept., METU \_\_\_\_\_

Prof. Dr. Ülkü Yetiş  
Environmental Engineering Dept., METU \_\_\_\_\_

Prof. Dr. Çetin Hoşten  
Mining Engineering Dept., METU \_\_\_\_\_

Assoc. Prof. Dr. Mehmet Kitiş  
Environmental Engineering Dept., Süleyman Demirel University \_\_\_\_\_

Assist. Prof. Dr. Ayten Genç  
Environmental Engineering Dept., Zonguldak Karaelmas University \_\_\_\_\_

**Date:** \_\_\_\_\_

**I hereby declare that all information in this document has been obtained and presented in accordance with academic rules and ethical conduct. I also declare that, as required by these rules and conduct, I have fully cited and referenced all material and results that are not original to this work.**

Hande Yükseler

## **ABSTRACT**

### **BIOLOGICAL AND CHEMICAL SLUDGE FILTRATION**

Yükseler, Hande

Ph.D., Department of Environmental Engineering

Supervisor : Prof. Dr. Ülkü Yetiş

Co-Supervisor: Prof. Dr. İsmail Tosun

July 2007, 172 pages

Up to date, sludge filterability has been characterized by the Ruth's classical filtration theory and quantified by the well-known parameter specific cake resistance (SCR). However, the complexity of the actual phenomenon is clearly underestimated by the classical filtration theory and SCR is often not satisfactory in describing filterability. Although many scientific studies were conducted for a better analysis and understanding of the filtration theory, still a practically applicable solution to replace the classical theory for a better description of filterability has not been proposed yet. In the present study, blocking filtration laws proposed by Hermans and Bredée, dating back to 1936, which have been extensively used in the membrane literature for the analysis of fouling phenomenon and the multiphase filtration theory developed by Willis and Tosun (1980) highlighting the importance of the cake-septum interface in determining the overall filtration rate have been adopted for the analysis of filterability of sludge systems. Firstly, the inadequacy of the classical filtration theory in characterizing the filterability of real sludge systems and also the lack of the currently used methodology in simulating filtration operation was highlighted. Secondly, to better understand the effect of slurry characteristics and operational conditions on filtration, model slurries of spherical and incompressible Meliodent particles were formed. Finally, a methodology was developed with the gathered filtration data to assess the filterability of the sludge systems by both theories. The results clearly show that both approaches

were superior to the classical approach in terms of characterizing the filterability of sludge systems. While blocking laws yielded a slurry specific characterization parameter to replace the commonly used SCR, the multiphase theory provided a better understanding of the physical reality of the overall process.

**Keywords:** Blocking Filtration Laws, Classical Filtration Theory, Multiphase Filtration Theory, Specific Cake Resistance, Filter Medium Resistance, Sludge Dewatering

## ÖZ

### BİYOLOJİK VE KİMYASAL ÇAMUR FİLTASYONU

Yükseler, Hande

Doktora, Çevre Mühendisliği Bölümü

Tez Yöneticisi : Prof. Dr. Ülkü Yetiş

Ortak Tez Yöneticisi: Prof. Dr. İsmail Tosun

Temmuz 2007, 172 sayfa

Günümüze değin çamur filtrasyonu Ruth tarafından geliştirilen klasik filtrasyon teorisi ile karakterize edilip, özgül kek direnci (ÖKD) parametresi ile değerlendirilmiştir. Ancak, klasik yaklaşım gerçek olgunun karmaşıklığını net olarak gösterememektedir ve ÖKD filtrasyonu tanımlamada yeterli olamamaktadır. Literatürde, filtrasyon prosesini daha iyi analiz edebilmek ve anlayabilmek için birçok bilimsel çalışma gerçekleştirilmiş olmasına rağmen halen klasik teorinin yerini alabilecek pratik olarak uygulanabilir bir çözüm önerilmemiştir. Bu çalışmada, Hermans ve Bredée tarafından 1936 yılında geliştirilen ve membran literatüründe sıklıkla kullanılan tıkanmalı filtrasyon kanunları ile Willis ve Tosun (1980) tarafından geliştirilen, filtrasyon hızının belirlenmesinde kek-filtre ortamı fazının önemini vurgulayan çok-fazlı filtrasyon teorisi çamur filtrasyonu analizinde kullanılmıştır. Öncelikle klasik filtrasyon teorisinin gerçek çamur sistemlerinin filtrasyonunu tayin etmedeki yetersizliği ve mevcutta kullanılan deneysel yöntemin filtrasyon prosesini yansıtmadaki eksiklikleri ortaya konmuştur. İkinci olarak, çamur özelliklerinin ve işletme koşullarının filtrasyon prosesine etkilerini daha iyi anlayabilmek için küresel ve sıkıştırılmayan Meliodent parçacıklarından oluşturulan model çamur sistemleri ile çalışmalar gerçekleştirilmiştir. Son olarak, çamur sistemlerinin filtrasyonunu yorumlayabilmek için, elde edilen filtrasyon dataları her iki teori de kullanılarak yorumlanmıştır. Sonuçlar filtrasyonun karakterize edilmesinde her iki yaklaşım da klasik yaklaşıma göre üstün olduğunu göstermiştir. Tıkanmalı filtrasyon

kanunları ile çamura özgü bir parametre geliştirilirken, çok-fazlı filtrasyon teorisi tüm prosesin fiziksel gerçekliğini açıklamada daha doğru bir yaklaşım getirmiştir.

**Anahtar kelimeler:** Tıkanmalı filtrasyon teorisi, Klasik filtrasyon teorisi, Çok-fazlı filtrasyon teorisi, Özgül kek direnci, Filtre ortamı direnci, Çamur susuzlaştırması

*The important thing is not to stop questioning.*

*Albert Einstein*

## **ACKNOWLEDGEMENTS**

First and foremost, I wish to express my warmest thanks to my supervisor Prof. Dr. Ülkü Yetiş for her endless support, supervision, trust, encouragement and insight which is not limited to this thesis study. She is absolutely a model mentor with her great enthusiasm, kindness, vision and never-ending support. It is a great pleasure for me to be a student of Dr. Yetiş since 1997.

I also wish to express my deepest gratitude to my co-supervisor Prof. Dr. İsmail Tosun for his guidance, excitement, advice and support throughout this thesis study.

The comments and contributions of my committee members Prof. Dr. F. Dilek Sanin and Prof. Dr. Çetin Hoşten throughout the study are greatly acknowledged. The contributions of Assoc. Prof. Dr. Mehmet Kitiş and Assist. Prof. Dr. Ayten Genç are greatly appreciated.

My sincere thanks go to Prof. Dr. Filiz B. Dilek and Dr. Merih Kerestecioğlu for being kind, supportive and encouraging all the time.

The technical assistance of Mr. Kemal Demirtaş with his incredibly brilliant contributions to my experimental set-up (which is worth a special prize!), Mr. Ramazan Demir with his great enthusiasm and never-ending support and Ms. Aynur Yıldırım throughout the experimental studies is gratefully acknowledged. The support and motivation of the department staff-Mrs. Güldane Kalkan, Mrs. Gülşen Erdem and Mr. Cemalattin Akın is greatly appreciated.

My special thanks are extended to my office-mates Vedat Yılmaz and Meltem Ünlü for creating a "Z33 spirit" which is based on honesty, friendship, happiness and joy. They were always by my side, in good times and bad times, offering support and friendship. I am sure time will strengthen the bonds between us, despite wherever we are. I love you both!

The support and motivation of my dearest friend Belgi Kılıç Turan far from USA was incredible. Thank you so much!

My sweetest friends Ahu Pinar Akgöz, Ceren Neşşar, Çiğdem Ömürlü, İlkay Uzun, Meral Mungan, Merve Kocabaş and Samiye Yabanoğlu: I love you all, thanks for everything and making life positive!

I am also thankful for the support and motivation of my friends Cavit Burak Bural, Emre Tokcaer, Erkan Şahinkaya, Ertan Öztürk, Eylem Doğan, Firdes Yenilmez, Gizem Uğurlu, Gülçin Özsoy, Hakan Moral, Onur Güven Apul, Özge Yılmaz, Nevzat Özgü Yiğit, Nimet Varolan Uzal, Nuray Ateş, Serkan Girgin and for all my colleagues and my students, that will be too long to list here, but have been by my side in this period.

And last, but not least, without the encouragement and support of my family nothing would be possible. Mom, dad and Meltoş: Thanks for the inspiration and enthusiasm you have given to me, I am really lucky! I love you...

## TABLE OF CONTENTS

ABSTRACT.....	iv
ÖZ.....	vi
DEDICATION.....	viii
ACKNOWLEDGEMENTS.....	ix
TABLE OF CONTENTS.....	xi
LIST OF TABLES.....	xiv
LIST OF FIGURES.....	xvi
LIST OF SYMBOLS.....	xxi
CHAPTER	
1. INTRODUCTION.....	1
2. THESIS OUTLINE.....	5
3. MATERIALS AND METHODS.....	7
3.1. Materials.....	7
3.1.1. Slurry.....	7
Biological Sludge.....	7
Chemical Sludge.....	7
Model Meliodent Slurry.....	8
3.1.2. Filter Medium.....	8
3.2. Experimental Procedure.....	9
4. REAL SLUDGE SYSTEMS.....	12
4.1. Objective and Experimental Design.....	12
4.2. Theoretical Background.....	14
4.2.1. Fundamentals of Sludge Dewatering.....	14
4.2.2. Classical Filtration Theory.....	16
4.2.3. Drawbacks of the Classical Filtration Theory and the Buchner Funnel Filtration Test Method.....	18
4.2.4. Multiphase Filtration Theory.....	20
4.3. Materials and Methods.....	23
4.3.1. Biological Sludge.....	23
4.3.2. Chemical Sludge.....	23
4.3.3. Filter Medium.....	24
4.3.4. Experimental Procedure.....	24

4.4. Results and Discussion.....	24
4.4.1. Activated Sludge Experiments.....	25
4.4.2. Chemical Sludge (Lead Hydroxide) Experiments.....	27
4.4.3. Comparison of Filtration Behavior of Alum Sludge and Lead Hydroxide Sludge.....	29
4.4.4. Validity of the BF Test.....	31
a. Type of Filter Medium Used.....	31
b. Mode of Filtration Operation.....	32
c. Particle Size-Pore Size Interactions.....	33
4.5. Conclusions.....	35
5. MODEL SLURRY SYSTEMS.....	36
5.1. Objective and Experimental Design.....	36
5.2. Materials and Methods.....	38
5.2.1. Model Slurry.....	38
5.2.2. Filter Medium.....	38
5.2.3. Experimental Procedure.....	38
5.3. Results and Discussion.....	38
5.3.1. Preliminary Investigations.....	38
5.3.2. Effect of particle settling rate.....	42
5.3.3. Effect of particle size distribution.....	44
5.3.4. Effect of slurry concentration.....	46
5.3.5. Effect of particle size and pore size of the filter medium.....	49
5.4. Conclusions.....	55
6. MATHEMATICAL ANALYSIS OF FILTRATION.....	57
6.1. Objective.....	57
6.2. Theoretical Background.....	57
6.2.1. Cake Filtration and Dewatering.....	57
6.2.2. Cake Filtration Literature.....	58
6.2.3. Modeling Approach.....	69
Classical Filtration Theory.....	69
Multiphase Filtration Theory.....	71
Current Practical Approach.....	72
Blocking Filtration Laws.....	72
6.2.4. Expression and Characterization of Filtration by Multiphase Modeling.....	79

6.3. Results and Discussion.....	80
6.3.1. Model Slurry Systems.....	81
6.3.2. Real Sludge Systems.....	91
6.3.3. Blocking Filtration Law Analysis.....	96
6.4. Conclusions.....	103
7. CONCLUSIONS.....	105
REFERENCES.....	108
APPENDICES	
A. FILTRATION TEST RESULTS OF MODEL SLURRY.....	115
B. MULTIPHASE FILTRATION LAW ANALYSIS.....	133
CURRICULUM VITAE.....	169

## LIST OF TABLES

TABLES	
Table 4.1. Experimental studies with real sludge systems.....	12
Table 4.2. SCR values for different types of sludges.....	15
Table 4.3. Activated Sludge-Experimental conditions and filtration test results.....	25
Table 4.4. Chemical Sludge – Experimental conditions.....	28
Table 4.5. Effect of filter medium/down-flow filtration.....	31
Table 4.6. Effect of mode of operation.....	32
Table 4.7. Effect of applied chemical dosage on different filter medium (floc size effect).....	33
Table 5.1. Experimental studies with model slurry systems.....	37
Table 5.2a. Filtration test results-Effect of particle settling rate.....	42
Table 5.2b. V vs. t results for water and sugar solution.....	43
Table 5.3. Filtration test results-Effect of particle size distribution (II).....	46
Table 5.4. Filtration test results-Effect of slurry concentration.....	47
Table 5.5. Filtration test results-Effect of particle-pore size interaction (I).	49
Table 5.6. Filtration test results-Effect of particle-pore size interaction (II).....	51
Table 5.7. Filtration test results-Effect of particle-pore size interaction (III).....	53
Table 6.1. Comparison of filtration theories.....	68
Table 6.2. Blocking filtration laws.....	73
Table 6.3. Model slurry experiments.....	81
Table 6.4. Model slurry-Experimental conditions.....	81
Table 6.5. Experimental conditions-Filter medium effect (I-A).....	83
Table 6.6. MATLAB results for Case I.....	85
Table 6.7. MATLAB results for Case II.....	90
Table 6.8. MATLAB results for Case III.....	91
Table 6.9 Filtration test results-Effect of slurry concentration.....	99
Table 6.10. $K_{CF}$ analysis-Effect of slurry concentration.....	99
Table 6.11. $K_{CF}$ analysis-Effect of filter medium.....	100
Table 6.12. $K_{CF}$ analysis-Effect of pressure.....	100
Table B.1. Experimental conditions-Filter medium effect (I-B).....	138

Table B.2. Experimental conditions-Filter medium effect (I-C).....	145
Table B.3. Experimental conditions-Filter medium effect (I-D).....	150
Table B.4. Experimental conditions-Filter medium effect (I-E).....	155
Table B.5. Experimental conditions-Particle size effect (II-A).....	160
Table B.6. Experimental conditions-Particle size effect (II-B).....	165
Table B.7. Experimental conditions-Pressure effect (III-A).....	170
Table B.8. Experimental conditions-Pressure effect(III-B).....	172

## LIST OF FIGURES

### FIGURES

Figure 3.1. BF filtration test apparatus.....	9
Figure 3.2. BF filtration test apparatus-Down flow mode.....	10
Figure 3.3. BF filtration test apparatus-Up flow mode.....	10
Figure 4.1. Schematic diagram of a one-dimensional cake filtration.....	20
Figure 4.2. $t/V$ versus $V$ for Experiment # 1 and 2.....	26
Figure 4.3. $t/V$ versus $V$ for Experiment # 3 and 4.....	26
Figure 4.4. $t/V$ versus $V$ for Experiment # 5 and 6.....	27
Figure 4.5. $t/V$ versus $V$ for Experiment # 7 and 8.....	28
Figure 4.6. $t/V$ versus $V$ for Experiment # 9, 10 and 11.....	29
Figure 4.7. $t/V$ vs. $V$ -Alum sludge and lead hydroxide sludge.....	30
Figure 5.1. $V$ vs. $t$ plot for sugar-Meliocent slurry (W#40, W#41, W#42).	39
Figure 5.2. $V$ vs. $t$ plot for sugar-Meliocent slurry (W#40, W#41).....	40
Figure 5.3. $V$ vs. $t$ plot for 40 wt. % sugar solution (W#40, W#41, W#42).....	40
Figure 5.4. $V$ vs. $t$ plot for 40 wt. % sugar solution (W#40, W#41).....	41
Figure 5.5. $dt/dV$ vs. $V$ plot- Effect of particle size distribution (I).....	45
Figure 5.6. $dt/dV$ vs. $V$ plot- Effect of particle size distribution (II).....	47
Figure 5.7. $dt/dV$ vs. $V$ plots for slurry concentration (C) of 4, 8, 12 and 16% at 4.5 in-Hg.....	48
Figure 5.8. $dt/dV$ vs. $V$ plots for slurry concentration (C) of 4, 8, 12 and 16% at 9 in-Hg.....	48
Figure 5.9. Effect of particle-pore size interaction (I)-5 in-Hg.....	50
Figure 5.10. Effect of particle-pore size interaction (II)-5 in-Hg.....	51
Figure 5.11. Effect of particle-pore size interaction (III)-5 in-Hg.....	54
Figure 5.12. Effect of particle-pore size interaction (III)-10 in-Hg.....	54
Figure 6.1. Physical interpretation of blocking laws.....	74
Figure 6.2. $d^2t/dV^2$ vs. $dt/dV$ for Bovine Serum Albumin (BSA) solutions...	78
Figure 6.3. $d^2t/dV^2$ vs. $dt/dV$ for natural organic matter (NOM).....	78
Figure 6.4. $dt/dV$ vs. $V$ plot-Filter medium effect (I-A).....	83
Figure 6.5. $dt/dV$ vs. $t$ plot-Filter medium effect (I-A).....	84
Figure 6.6. $dt/dV$ vs. $t$ plot-Filter medium effect (I-A, nylon filter m.).....	84
Figure 6.7. $dt/dV$ vs. $t$ plot-Filter medium effect (I-A, W#41).....	85

Figure 6.8. Comparative $dt/dV$ vs. $t$ plot-Filter medium effect (I-A, W#41).....	86
Figure 6.9. Comparative $dt/dV$ vs. $t$ plot-Filter medium effect (I-A, nylon)	86
Figure 6.10. $d^2t/dV^2$ vs. $t$ plot-Filter medium effect (I-A, W#41).....	87
Figure 6.11. $d^2t/dV^2$ vs. $t$ plot-Filter medium effect (I-A, nylon f.m).....	88
Figure 6.12. $dt^*/dV^*$ vs. $V^*$ plot-Filter medium effect (I-A).....	88
Figure 6.13. $t$ vs. $V$ plot-Activated sludge (up-flow).....	92
Figure 6.14. $d^2t/dV^2$ vs. $t$ plot-Activated sludge (up-flow).....	93
Figure 6.15. $t$ vs. $V$ plot-Activated sludge (down-flow).....	93
Figure 6.16. $d^2t/dV^2$ vs. $t$ plot-Activated sludge (down-flow).....	94
Figure 6.17. $t$ vs. $V$ plot-Chemical sludge (down-flow).....	95
Figure 6.18. $dt/dV$ vs. $t$ plot-Chemical sludge (down-flow).....	95
Figure 6.19. $d^2t/dV^2$ vs. $t$ plot-Chemical sludge (down-flow).....	96
Figure 6.20. $d^2t/dV^2$ vs. $dt/dV$ plot at different slurry concentrations.....	97
Figure 6.21. $V$ vs. $t$ plot for textile wastewater.....	102
Figure 6.22. $d^2t/dV^2$ vs. $dt/dV$ plot for textile wastewater.....	102
Figure A.1. $V$ vs. $t$ for water + Meliodent (A) Up-flow mode (B) Down-flow mode.....	117
Figure A.2. $V$ vs. $t$ for sugar + Meliodent (A) Up-flow mode (B) Down-flow mode.....	117
Figure A.3. $dt/dV$ vs. $V$ plot for different particle sized slurries at 4.5 in-Hg (down-flow mode).....	119
Figure A.4. $dt/dV$ vs. $V$ plot for different particle sized slurries at 9 in-Hg (up-flow mode).....	119
Figure A.5. $dt/dV$ vs. $V$ plot for different particle sized slurries at 9 in-Hg (down-flow mode).....	120
Figure A.6. $V$ vs. $t$ plot for 4% slurry at 4.5 in-Hg- Effect of slurry concentration.....	120
Figure A.7. $V$ vs. $t$ plot for 8% slurry at 4.5 in-Hg- Effect of slurry concentration.....	121
Figure A.8. $V$ vs. $t$ plot for 12% slurry at 4.5in-Hg- Effect of slurry concentration.....	121
Figure A.9. $V$ vs. $t$ plot for 16% slurry at 4.5in-Hg- Effect of slurry concentration.....	122
Figure A.10. $V$ vs. $t$ plot for 4% slurry at 9 in-Hg- Effect of slurry concentration.....	122

Figure A.11. V vs. t plot for 8% slurry at 9 in-Hg- Effect of slurry concentration.....	123
Figure A.12. V vs. t plot for 12% slurry at 9 in-Hg-Effect of slurry concentration.....	123
Figure A.13. V vs. t plot for 16% slurry at 9 in-Hg-Effect of slurry concentration.....	124
Figure A.14. V vs. t plot for steel mesh-Effect of particle size-pore size (I)	124
Figure A.15. V vs. t plot for W#41-Effect of particle size-pore size (I).....	125
Figure A.16. V vs. t plot for W#41 (4%, 5 in-Hg)-Effect of particle size-pore size (III).....	125
Figure A.17. V vs. t plot for nylon filter medium (4%, 5 in-Hg)-Effect of particle size-pore size (III).....	126
Figure A.18. V vs. t plot for steel mesh (4%, 5 in-Hg)-Effect of particle size-pore size (III).....	126
Figure A.19. V vs. t plot for W#41 (4%, 10 in-Hg)-Effect of particle size-pore size (III).....	127
Figure A.20. V vs. t plot for nylon filter medium (4%, 10 in-Hg)-Effect of particle size-pore size (III).....	127
Figure A.21. V vs. t plot for steel mesh (4%, 10 in-Hg)-Effect of particle size-pore size (III).....	128
Figure A.22. V vs. t plot for W#41 (8%, 5 in-Hg)-Effect of particle size-pore size (III).....	128
Figure A.23. V vs. t plot for nylon filter medium (8%, 5 in-Hg)-Effect of particle size-pore size (III).....	129
Figure A.24. V vs. t plot for steel mesh (8%, 5 in-Hg)-Effect of particle size-pore size (III).....	129
Figure A.25. V vs. t plot for W#41 (8%, 10 in-Hg)-Effect of particle size-pore size (III).....	130
Figure A.26. V vs. t plot for nylon filter medium (8%, 10 in-Hg)-Effect of particle size-pore size (III).....	130
Figure A.27. V vs. t plot for steel mesh (8%, 10 in-Hg)-Effect of particle size-pore size (III).....	131
Figure A.28. dt/dV vs. V plot for 8% slurry at 5 in-Hg -Effect of particle size-pore size (III).....	131
Figure A.29. dt/dV vs. V plot for 8% slurry at 10 in-Hg -Effect of particle size-pore size (III).....	132

Figure B.1. dt/dV vs. V plot-Filter medium effect (I-B).....	135
Figure B.2. dt/dV vs. t plot-Filter medium effect (I-B).....	135
Figure B.3. dt/dV vs. t plot-Filter medium effect (I-B, steel mesh).....	136
Figure B.4. dt/dV vs. t plot-Filter medium effect (I-B, nylon filter med.)...	136
Figure B.5. dt/dV vs. t plot-Filter medium effect (I-B, W#41).....	137
Figure B.6. Comparative dt/dV vs. t plot-Filter medium effect (I-B, W#41).....	138
Figure B.7. Comparative dt/dV vs. t plot-Filter medium effect (I-B, nylon)	138
Figure B.8. Comparative dt/dV vs. t plot-Filter medium effect (I-B, steel mesh).....	139
Figure B.9. $d^2t/dV^2$ vs. t plot-Filter medium effect (I-B, #41).....	139
Figure B.10. $d^2t/dV^2$ vs. t plot-Filter medium effect (I-B, nylon f.m).....	140
Figure B.11. $d^2t/dV^2$ vs. t plot-Filter medium effect (I-B, steel mesh).....	140
Figure B.12. dt/dV vs. V plot-Filter medium effect (I-C).....	141
Figure B.13. dt/dV vs. t plot-Filter medium effect (I-C).....	142
Figure B.14. Comparative dt/dV vs. t plot-Filter medium effect (I-C, W#41).....	142
Figure B.15. Comparative dt/dV vs. t plot-Filter medium effect (I-C, nylon f.m).....	143
Figure B.16. Comparative dt/dV vs. t plot-Filter medium effect (I-C, steel mesh).....	143
Figure B.17. $d^2t/dV^2$ vs. t plot-Filter medium effect (I-C, W#41).....	144
Figure B.18. $d^2t/dV^2$ vs. t plot-Filter medium effect (I-C, nylon f.m).....	144
Figure B.19. $d^2t/dV^2$ vs. t plot-Filter medium effect (I-C, steel mesh).....	145
Figure B.20. dt/dV vs. V plot-Filter medium effect (I-D).....	146
Figure B.21. dt/dV vs. t plot-Filter medium effect (I-D).....	146
Figure B.22. Comparative dt/dV vs. t plot-Filter medium effect (I-D, W#41).....	147
Figure B.23. Comparative dt/dV vs. t plot-Filter medium effect (I-D, nylon f.m).....	148
Figure B.24. Comparative dt/dV vs. t plot-Filter medium effect (I-D, steel mesh).....	148
Figure B.25. $d^2t/dV^2$ vs. t plot-Filter medium effect (I-D, W#41).....	149
Figure B.26. $d^2t/dV^2$ vs. t plot-Filter medium effect (I-D, nylon f.m).....	149
Figure B.27. $d^2t/dV^2$ vs. t plot-Filter medium effect (I-D, steel mesh).....	150
Figure B.28. dt/dV vs. V plot-Filter medium effect (I-E).....	151

Figure B.29. dt/dV vs. t plot-Filter medium effect (I-E).....	151
Figure B.30. Comparative dt/dV vs. t plot-Filter medium effect (I-E, W#41).....	152
Figure B.31. Comparative dt/dV vs. t plot-Filter medium effect (I-E, nylon f.m).....	153
Figure B.32. Comparative dt/dV vs. t plot-Filter medium effect (I-E, steel mesh).....	153
Figure B.33. $d^2t/dV^2$ vs. t plot-Filter medium effect (I-E, W#41).....	154
Figure B.34. $d^2t/dV^2$ vs. t plot-Filter medium effect (I-E, nylon f.m).....	154
Figure B.35. $d^2t/dV^2$ vs. t plot-Filter medium effect (I-E, steel mesh).....	155
Figure B.36. dt/dV vs. V plot-Particle size effect (II-A).....	156
Figure B.37. dt/dV vs. t plot-Particle size effect (II-A).....	156
Figure B.38. Comparative dt/dV vs. t plot-Particle size effect (II-A, 53- 75 $\mu$ m).....	157
Figure B.39. Comparative dt/dV vs. t plot-Particle size effect (II-A, 250- 425 $\mu$ m).....	158
Figure B.40. Comparative dt/dV vs. t plot-Particle size effect (II-A,mixed)	158
Figure B.41. $d^2t/dV^2$ vs. t plot-Particle size effect (II-A, 53-75 $\mu$ m).....	159
Figure B.42. $d^2t/dV^2$ vs. t plot-Particle size effect (II-A, 250-425 $\mu$ m).....	159
Figure B.43. $d^2t/dV^2$ vs. t plot-Particle size effect (II-A, mixed).....	160
Figure B.44. dt/dV vs. V plot-Particle size effect (II-B).....	161
Figure B.45. dt/dV vs. t plot-Particle size effect (II-B).....	161
Figure B.46. Comparative dt/dV vs. t plot-Particle size effect (II-B, 75- 100 $\mu$ m).....	162
Figure B.47. Comparative dt/dV vs. t plot-Particle size effect (II-B, 200- 210 $\mu$ m).....	163
Figure B.48. Comparative dt/dV vs. t plot-Particle size effect (II-B, 250- 425 $\mu$ m).....	163
Figure B.49. $d^2t/dV^2$ vs. t plot-Particle size effect (II-B, 75-100 $\mu$ m).....	164
Figure B.50. $d^2t/dV^2$ vs. t plot-Particle size effect (II-B, 200-210 $\mu$ m).....	164
Figure B.51. $d^2t/dV^2$ vs. t plot-Particle size effect (II-B, 250-425 $\mu$ m).....	165
Figure B.52. dt/dV vs. V plot-Pressure effect (III-A).....	166
Figure B.53. dt/dV vs. t plot-Pressure effect (III-A).....	166
Figure B.54. dt/dV vs. V plot-Pressure effect (III-B).....	167
Figure B.55. dt/dV vs. t plot-Pressure effect (III-B).....	168

## LIST OF SYMBOLS

$A$	Cross-sectional area of filter, $m^2$
$c$	Mass of solids per unit volume of filtrate, mg/L
$d_{particle}$	Particle diameter, $\mu m$
$d_{pore}$	Pore diameter, $\mu m$
$F$	Filtrate flux, $L/m^2-h$
$F_d$	Drag force, N
$F_o$	Initial flowrate, mL/s
$G$	Function of average cake porosity and the volume fraction of liquid in the slurry, dimensionless
$J_o$	Dimensionless pressure gradient at the cake-septum interface
$J_S$	Correction factor introduced by Shirato <i>et al.</i> (1969) to average cake resistance to account for the relative velocity between the solid and liquid phases
$J_T$	Correction factor introduced by Tiller and Huang (1961) to average cake resistance for the internal flow rate variation
$k$	Constant of the fluid
$K$	Permeability of the cake
$K_o$	Permeability at the cake-septum interface
$\underline{\underline{K}}^{TP}$	Permeability tensor based on two-phase theorem, $m^2$
$K_{CB}$	Complete blocking filtration constant, $s^{-1}$
$K_{CF}$	Cake filtration constant, $s^{-1}$
$K_{IB}$	Intermediate blocking filtration constant, $s^{-1}$
$K_{SB}$	Standard pore blocking filtration constant, $s^{-1}$
$q$	Superficial liquid velocity, m/s
$q_L$	Superficial liquid velocity at the exit of filter cake (superficial filtrate velocity), m/s
$q_S$	Superficial solid velocity, m/s
$L(t)$	Cake thickness, m
$n$	Filtration number (characterizes the dominant filtration mechanism)
$P^*$	Dimensionless pressure
$P_A$	Applied pressure, Pa
$P_{atm}$	Atmospheric pressure, Pa
$P_L$	Liquid pressure averaging over entire cross-sectional area, Pa

$P_o$	Pressure at the cake-septum interface, Pa
$P_S$	Solid pressure averaging over entire cross-sectional area, Pa
$r$	Superficial solid velocity, m/s
$R_c$	Resistance of the cake, 1/m
$R_m$	Filter medium (septum) resistance, 1/m
$s$	Mass fraction of solids in the slurry
$t$	Time, s
$t^*$	Time for the cake filtration phase determined after Hermia's analysis, s
$u_L$	Superficial liquid velocity, m/s
$u_o$	Superficial liquid velocity at the exit of filter cake (superficial filtrate velocity), m/s
$u_s$	Superficial solid velocity, m/s
$V$	Filtrate volume, mL
$V^*$	Filtrate volume for the cake filtration phase determined after Hermia's analysis, mL
$z$	Spatial coordinate, m
$W_s$	Total mass of solids within the cake, kg

*Greek letters*

$\Delta P_C$	Pressure drop across the filter cake ( $P_A - P_o$ ), Pa
$\Delta P_T$	Total pressure drop across the filter ( $P_A - P_{atm}$ ), Pa
$\varepsilon$	Cake porosity
$\langle \varepsilon \rangle$	Average cake porosity
$\varepsilon_L$	Porosity at cake-slurry interface
$\varepsilon_{sl}$	Volume fraction of liquid in the slurry
$\varepsilon_s$	Solidosity
$\xi$	Dimensionless distance
$\lambda$	Resistance function
$\langle \alpha \rangle$	Average specific cake resistance, m/kg
$\mu$	Filtrate viscosity, N.s/m <sup>2</sup>
$\rho$	Liquid density, kg/m <sup>3</sup>
$\rho_s$	Solid density, kg/m <sup>3</sup>

## **CHAPTER 1**

### **INTRODUCTION**

Sludge is a semi-solid material produced by various biological and chemical processes in water and wastewater treatment plants that needs further treatment prior to its disposal into the environment. The requirement for further treatment is due to its high organic content, nutrient content, pathogenic organisms and high amounts of water. More importantly, the water in sludge is not only in one form in terms of its binding characteristics to solids. The form of water in sludge determines the effectiveness of sludge treatment operations to separate the water associated with the solids.

Before ultimate disposal, the water content of sludge should be decreased both from environmental and economical point of view. Sludge dewatering, commonly achieved through vacuum/pressure filtration or centrifugation, is a paramount process in water and wastewater treatment systems as it reduces the volume of sludge, and consequently, the costs for transporting the sludge to its ultimate disposal site. In general, efficiency of dewatering depends on the dewaterability of the sludge which is affected by particle charge, pH, solids concentration, organic content, floc density, and size and cellulose content. The characterization of the sludge to be dewatered is the key factor for the design and operation of sludge filters. The performance of a dewatering process lies beneath the correct assessment of the dewaterability of the sludge and selection of appropriate operational conditions.

Sludge dewaterability is quantified mainly by two parameters: capillary suction time (CST) and specific cake resistance (SCR), of which the latter is the most commonly used one. SCR measurements are carried out by Buchner funnel (BF) filtration test apparatus. In this method, a well-mixed slurry is poured into the BF in which the liquid portion is separated from the solids via a filtering medium by the application of a vacuum. The volume of filtrate collected is recorded as a function of time. The slope of the straight line resulting from the plot of  $t/V$  versus  $V$  is related to the average SCR which is a measure of dewaterability, i.e., the flatter the slope, the better the dewaterability.

The SCR concept stems from the classical filtration theory developed by Ruth (1935) employing a heuristic analogy with Ohm's Law proposing a two-resistance theory. According to Ruth's theory, the total resistance in filtration comprises of a series of the resistances of the medium and of the formed cake. Combination of the electric analogy with the mass balance yields the well-known constant pressure filtration equation; which further assumes that the controlling factor is the resistance of the cake and the medium resistance is negligible.

The experimental time-volume data are used to generate plots of  $t/V$  vs.  $V$  from which the slope and the intercept give the average SCR and the filter medium resistance, respectively. The average SCR evaluated using the constant pressure filtration equation is considered to be the key factor in the characterization of sludge dewaterability. In the literature, certain values are tabulated as the typical SCR values for some types of sludges (Tchobanoglous, 1979; Eckenfelder, 1989; Casey, 1997).

One of the major drawbacks of the SCR concept is that, a single value of SCR is assigned to a sludge. However, it is a well-known fact that the sludge particle size distribution is one of the key factors in controlling sludge dewaterability (Karr and Keinath, 1978). Besides, SCR is also influenced by the operational conditions such as filtration area, applied vacuum, filter medium and the mode of filtration, i.e., up-flow or down-flow. In standard down-flow filtration tests, once the slurry is poured into the funnel, most of the solids settle down and form a loose cake as a result of both applied vacuum and sedimentation. After a certain period of time, the supernatant liquid at the top of the filter cake is almost free of solids and from that point on, the process resembles flow through a packed bed rather than filtration. For biological sludges, for example, settling of flocs is rather fast. It is also important to note that once the level of the supernatant liquid reaches the top surface of the cake, the process is no longer filtration but cake dewatering, and the start of this period is very difficult to determine.

Tosun *et al.* (1993) was the first to question the methodology used in BF filtration experiments. Their results indicated that the slope of the  $t/V$  versus  $V$  plot is strongly affected by the mode of filtration. They concluded that the down-flow tests can be used to get qualitative information on the dewaterability of sludges but quantitative results are subject to question. It should be noted that

up-flow filtration tests are superior to down-flow tests not only for eliminating the particle settling by sedimentation but also for mimicking the full scale dewatering applications as rotary drums. Thus, when expressing results using SCR, it is important to note that these are only comparative and qualitative information about the dewaterability of the sludges; and quantitative results are subject to question since they are valid only for the operational conditions under which the test is being carried out.

Another important failure of the classical approach is that the medium resistance is negligible and that the overall rate of filtration is controlled only by the cake itself. The filtration tests conducted, however, revealed the importance of the filter medium used in determining the overall filtration performance. Contrary to classical filtration theory, the multiphase filtration theory developed by Willis and Tosun (1980), indicates that the region of high drag which occurs at the cake-septum interface controls the filtrate rate. Thus, besides the slurry characteristics, the pore size of the filter medium should also be taken into consideration. Since the sludge dewaterability is dependent on the cake-septum interface, it is crucial to specify the type of septum used in the filtration tests. Although some investigators report the type of filter medium used in the BF experiments, i.e., Whatman #2 with a pore size of  $8\mu\text{m}$  (Tchobanoglous, 1979; Eckenfelder, 1989), most of the filtration studies do not report the filter medium. Thus, the SCR values reported in the literature without indicating the type of filter medium used do not give any practical value. Moreover, the filter cloths used at industrial scale dewatering applications have much larger pore sizes than the filter papers used in the laboratory tests. In that respect, it is evident that current laboratory dewatering tests do not actually represent the real plant scale applications. Currently, with all of its well-known deficiencies, the classical filtration theory is still being used to quantify the filterability of sludge systems for practical purposes.

This study firstly highlights the failure of the classical filtration theory and the SCR concept in expressing the filterability of real sludge systems and the lack of currently used experimental methodology in representing real scale dewatering operations. Secondly, the effects of slurry characteristics and operational conditions on the overall filtration performance were explored to better understand the physical reality behind the filtration process.

The overall objective of the study is to develop a correct mathematical analysis of the filterability of sludge systems via the blocking laws approach and the multiphase filtration theory. To achieve this objective, firstly, up-flow and down-flow BF tests with real sludge systems and synthetic slurries using different filter media were conducted. The blocking law analysis revealed a slurry-specific filtration number to characterize the overall filterability. Multiphase filtration theory, on the other hand, yielded a modified experimental methodology and data analysis technique for the correct assessment of the filterability of sludge systems.

## **CHAPTER 2**

### **THESIS OUTLINE**

This chapter provides the general outline of the thesis. Chapter 1 is the introduction part of the thesis. The materials used and the experimental procedure followed are outlined in Chapter 3.

The filtration studies are grouped under three study phases based on the differences in the objectives of each phase of the study:

1. Filtration tests with real sludge systems (Chapter 4),
2. Filtration tests with model slurry systems (Chapter 5),
3. Mathematical analysis of filtration and filterability of sludge systems (Chapter 6).

To make each study phase clearer, chapters were divided into subsections: objective and experimental design, theoretical background, materials and methods, results and discussion and finally conclusions are outlined at the end of each chapter.

Chapter 4 covers the first phase of the studies which aimed at showing the failure of the classical filtration theory in expressing the filterability of real sludge systems. Moreover, the validity of the currently used testing method was also assessed in terms of its reliability in representing the actual phenomena.

Since real sludge systems are very complex in nature, it was not possible to use those systems to come up with a mathematical expression that will correctly assess the filterability. For this purpose, spherical and incompressible Meliodent particles were used to form model slurries.

Chapter 5 covers the second phase of the studies which were conducted to analyze the effects of operational conditions and slurry characteristics on the expression of filterability of sludge systems. Model slurries were used to better understand the factors affecting the overall filtration performance.

Chapter 6 covers the last stage of the studies. The aim was to come up with a correct mathematical analysis of the cake filtration process. For this purpose, multiphase filtration theory and blocking filtration laws were used to describe the filterability. Multiphase filtration theory, yielded a modified experimental methodology and data analysis technique for the correct assessment of the filterability of sludge systems. The blocking law analysis, on the other hand, revealed a slurry-specific filtration number to characterize the overall filterability.

Chapter 7 outlines the conclusions drawn from the present study. Supplementary information and data for Chapter 5 are given in Appendix A and for Chapter 6 given in Appendix B.

## CHAPTER 3

### MATERIALS AND METHODS

#### 3.1. Materials

The characteristics of the slurries and filter media used during BF filtration tests are presented below.

##### 3.1.1. Slurry

The filtration tests were conducted with two types of slurries: real sludges and model synthetic slurries. As real sludge systems, filtration behavior of both biological and chemical sludges was investigated. As to better understand the phenomena behind cake filtration, well-defined slurries of incompressible and spherical Meliodent particles were prepared. The slurry characteristics are given below.

##### *Biological Sludge*

Biological sludge experiments were conducted with samples taken from the recycle line of activated sludge unit of Ankara Sincan Municipal Wastewater Treatment Plant. The mixed liquor suspended solids (MLSS) concentration of the sludge sample was set to 10 g/L during experiments. Both raw and chemically conditioned activated sludges were used during filtration experiments. A cationic polyelectrolyte (Zetag 7635, CIBA Chemicals) was utilized as the chemical conditioner.

##### *Chemical Sludge*

Chemical sludge experiments were conducted with two different types of sludges, namely lead hydroxide and aluminum hydroxide (alum), prepared under laboratory conditions. Lead hydroxide sludge was prepared by first dissolving lead nitrate in water and then precipitating it as lead hydroxide at a pH of 11. Alum sludge was prepared by the addition of aluminum sulfate to a clay

suspension. The alkalinity of the clay suspension was checked and found to be enough to have reaction go to completion producing aluminum hydroxide precipitates.

#### *Model Meliodent Slurry*

In order to better understand the phenomena behind filtration, well-defined slurries with known particle size distributions and incompressible particles were utilized.

In the literature, Leonard and Brenner (1965) used the slurry of Lucite 4F particles dispersed (by the help of Triton X-100) in a 40 wt. % sugar solution in their filtration studies. The purpose was to eliminate the settling effect of particles during the course of filtration since the particles have a low sedimentation rate in sugar solution. Lucite 4F is a type of PMMA (polymethyl methacrylate) particle with a specific gravity of 1.19 and the density of the 40 wt. % sugar solution is reported as 1.16 g/ cm<sup>3</sup>.

In this study, instead of Lucite particles, another type of PMMA particle "Meliodent" which is a trademark manufactured by Bayer Dental and used in dental applications was used. Meliodent particles were dispersed in 40 wt. % sugar solution (density ranged between 1.13-1.15 g/cm<sup>3</sup>). Not only slurries with sugar but also those with water were prepared. The concentration of Meliodent slurries prepared ranged from 2 wt. % to 16 wt. % depending on the test for which the slurry was subjected to. Slurries with particle size ranges of 53-75µm, 75-100µm, 100-175µm, 175-250µm, 100-250µm, 200-210 µm and 250-425µm were used.

The Meliodent particles do not uniformly disperse in sugar solution and water. For this reason, a drop of Triton X-100 is added to 1 L of solution. Triton X-100 causes foaming problem when applied more than a drop. Triton X-100 is fully miscible in water and has a density of 1.05 g/cm<sup>3</sup>.

#### **3.1.2. Filter Medium**

Different types of filter media were used to assess the effect of filter medium on the overall performance of filtration. Whatman # 40 (8 µm), # 41 (20-25 µm)

and # 42 (2.5  $\mu\text{m}$ ) filter papers; Millipore nylon filter media of 41 $\mu\text{m}$  and 333 $\mu\text{m}$  pore sizes; steel mesh of 200 $\mu\text{m}$  and real scale filter cloths were used.

### 3.2. Experimental Procedure

The BF filtration test apparatus is shown in Figure 3.1. The test set-up used in the experiments both in the direction (down-flow) and in the opposite direction (up-flow) of gravity is shown in Figures 3.2 and 3.3, respectively.

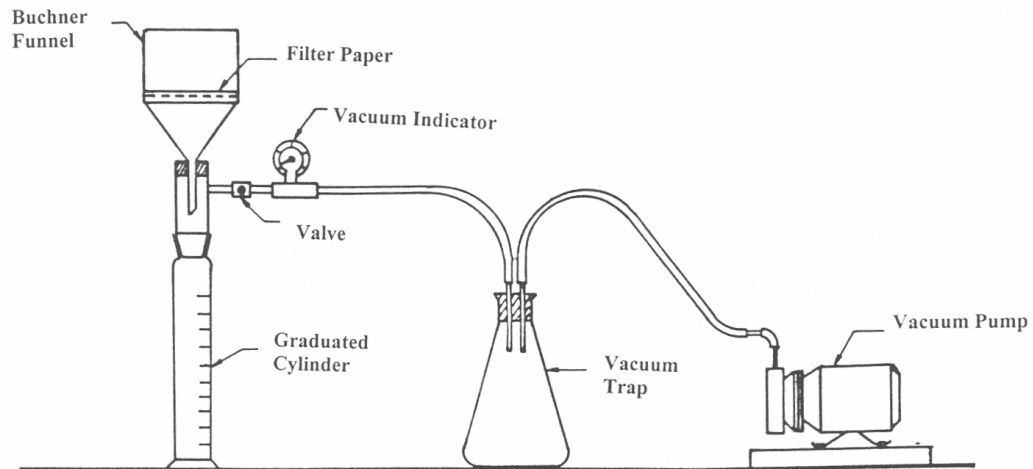


**Figure 3.1.** BF filtration test apparatus

In a typical BF test, well-mixed slurry is poured into the funnel in which filter paper is placed. Vacuum is applied and the filtrate is collected into a calibrated reservoir where the volume of filtrate ( $V$ ) is recorded as a function of time ( $t$ ). Monitoring of the filtrate volume is continued until no more filtrate comes out of the unit. The mass of filtrate collected with time is recorded by a computer and the data are converted to  $t$  vs.  $V$  by using the density of the filtrate. The values of the SCR and filter medium resistance are determined from the plot of  $t/V$  vs.  $V$ .

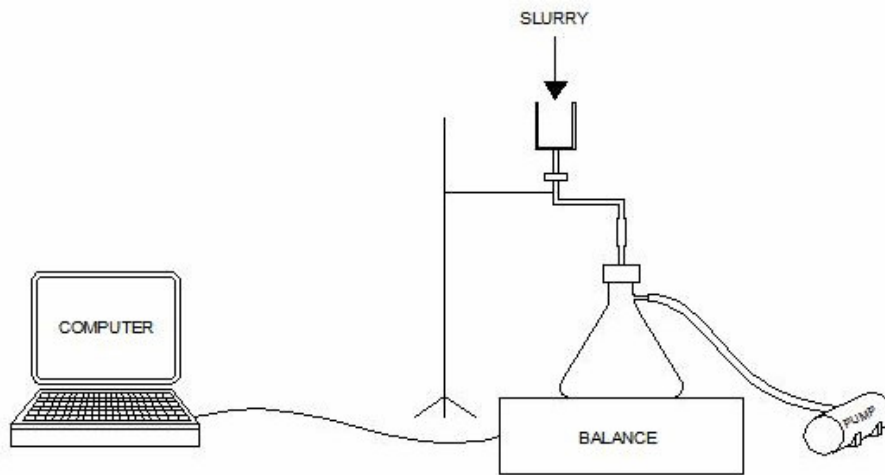


**Figure 3.2.** BF filtration test apparatus-Down flow mode

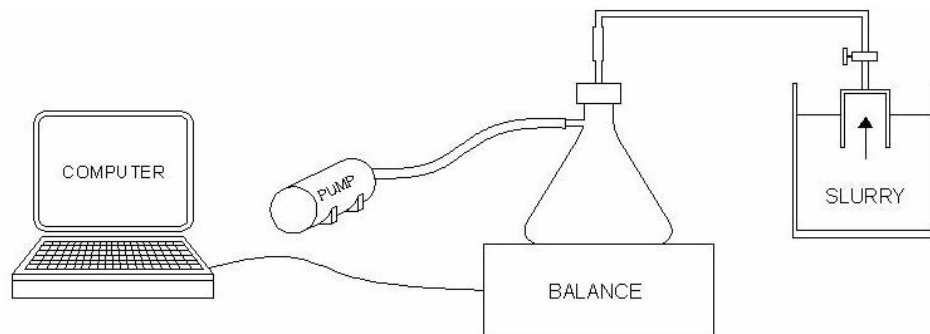


**Figure 3.3.** BF filtration test apparatus-Up flow mode

In standard down-flow BF tests, once the slurry is poured into the funnel, most of the solids settle down and form a loose cake as a result of both applied vacuum and sedimentation. For biological sludges, for example, settling of flocs is rather fast. It is also important to note that once the level of the supernatant liquid reaches the top surface of the cake, the process is no longer filtration but dewatering, and the start of this period is very difficult to determine.

The aim of using different modes of filtration was both to eliminate the effect of sedimentation during filtration and also to mimic rotary drum filters.

To investigate the effect of filtration area on the filterability, two different BF's with diameters 40 mm ( $A = 12.6 \text{ cm}^2$ ) and 90 mm ( $A = 63.6 \text{ cm}^2$ ) were used. To have comparable results, the mass of solids accumulated on the filter medium per unit area was kept constant throughout the experiments. The vacuum applied vary between 5 in-Hg to 22 in-Hg during the experiments conducted.

Each experiment was repeated at least two times for real sludge systems and three times for Meliodent slurries and the experimental data represent the arithmetic average of the results.

## CHAPTER 4

### REAL SLUDGE SYSTEMS

#### 4.1. Objective and Experimental Design

The objective of the initial phase of the study was to show the inadequacy of the constant pressure filtration equation in representing filterability of real sludge systems, i.e., biological and chemical sludges, under different operational conditions.

The validity of the currently used testing method in representing the actual phenomena was also assessed. The rationale behind this investigation is the fact that lab scale experiments actually do not correctly represent the field scale dewatering units in terms of the filter medium and the mode of filtration operation.

To investigate the effect of operational conditions on filterability, data were analyzed from  $t/V$  vs.  $V$  relationships and resistances were evaluated accordingly. The experimental data for testing the validity of the BF test were analyzed from  $dt/dV$  vs.  $V$  relationship. One should note that,  $dt/dV$  vs.  $V$  analysis is the correct way to analyze data since  $t/V$  vs.  $V$  results from integration of  $dt/dV$  vs.  $V$  assuming constant concentration, SCR and filter medium resistance values.

Table 4.1 summarizes the experimental studies covered in this chapter.

**Table 4.1.** Experimental studies with real sludge systems

Exp.	Sludge	Operational parameters*		Data analysis
		Constant	Variable	
<b>Effect of operational conditions</b>	Activated	C: 10 g/L $\Delta P$ : 15in-Hg, 22in-Hg M: down-flow BF:40 mm, 90 mm	<b><u>Filter medium</u></b> W#40 (8 $\mu$ m) W#41 (20-25 $\mu$ m) W#42 (2.5 $\mu$ m)	t/V vs. V
	Activated	C: 10 g/L $\Delta P$ : 15in-Hg, 22in-Hg M: down-flow FM: W#40, W#41, W#42	<b><u>Filtration Area</u></b> BF diameter: 40 mm 90 mm	t/V vs. V
	Chemical (Lead Hyd.)	$\Delta P$ : 18in-Hg, 22in-Hg M: down-flow BF:40 mm, 90 mm	<b><u>Filter medium</u></b> W#40 (8 $\mu$ m) W#41 (20-25 $\mu$ m) W#42 (2.5 $\mu$ m)	t/V vs. V
	Chemical (Lead Hyd.)	C: 10 g/L $\Delta P$ : 15in-Hg, 22in-Hg M: down-flow FM: W#40, W#41, W#42	<b><u>Filtration Area</u></b> BF diameter 40 mm 90 mm	t/V vs. V
<b>Validity of the BF test</b>	Activated	C: 10 g/L $\Delta P$ : 5 in-Hg M: down-flow BF: 40 mm Raw and 1% cond.	<b><u>Filter medium</u></b> W#40 (8 $\mu$ m) Filter cloth (50-100 $\mu$ m)	dt/dV vs. V
	Activated	C: 10 g/L $\Delta P$ : 5 in-Hg BF: 40 mm Raw and 1% cond. FM: Cloth	<b><u>Mode of filtration</u></b> Down-flow Up-flow	dt/dV vs. V
	Activated	C: 10 g/L $\Delta P$ : 5 in-Hg M: up-flow BF: 40 mm 1%, 5% and 7% cond. sludge	<b><u>Filter medium</u></b> Steel mesh (200 $\mu$ m) Nylon filter medium (333 $\mu$ m)	dt/dV vs. V

\* C: Solids concentration (by wt. %), FM: Filter medium, M: Mode of filtration, BF: Buchner funnel diameter

## **4.2. Theoretical Background**

### *4.2.1. Fundamentals of Sludge Dewatering*

Sludge is a semi-solid material produced by water and wastewater treatment that needs further treatment prior to its disposal into the environment. The form of water in sludge determines the effectiveness of sludge treatment operations to separate the water associated with the solids.

Sludge dewatering is accomplished by a variety of ways: drying beds, lagoons, vacuum and pressure filters, belt filter presses and centrifuges. Among these, vacuum and pressure filters are the most commonly used dewatering techniques in water and wastewater treatment. Mechanical dewatering typically removes about 20% of all the water in the sludge. Dewaterability of sludges depends on many factors, such as, particle charge, pH, solids concentration, organic content, floc density and size, mechanical strength of the particles and cellulose content.

The characterization of the sludge to be dewatered is the key factor for the design and operation of sludge filters. Sludge dewaterability is quantified mainly by two parameters: capillary suction time (CST) and specific cake resistance (SCR).

The CST test indicates the time (in seconds) required for a small volume of filtrate to be withdrawn from conditioned sludge when subjected to the capillary suction pressure of dry filter paper. The CST test is a rapid and simple method of screening dewatering aids. It relies on the capillary suction of a piece of thick filter paper (Whatman #17) to draw out the water from a small sample of conditioned sludge. The sample is placed in a cylindrical cell on top of chromatography grade filter paper. The time it takes for the water in the sludge to travel 10 mm in the paper between two fixed points is recorded electronically as CST. CST is measured after sludge is mixed with varying conditioner dosages. A typical CST for an unconditioned sludge is approximately 200 seconds or more. Sludges that hold water more tenaciously may exhibit CST values in thousands of seconds. A conditioned product that will readily dewater should yield a CST value of 10 seconds or less to produce good cake either from belt filter presses or centrifuges (Vesilind, 2003).

The disadvantage of the CST (especially in comparison to SCR) is that the test is specific only to the sludge being tested. While it gives comparative data, it is not a fundamental measure of dewaterability (Vesilind, 2003). Moreover, since no pressure is applied in the case of CST, it does not simulate the actual process. For example, Wu *et al.* (1997) reported that CST measurements lead to excess use of conditioners for sludges.

SCR measurements, on the other hand, are carried out by BF filtration test apparatus. In this method, a well-mixed slurry is poured into the BF in which the liquid portion is separated from the solids via a filtering medium by the application of vacuum. The volume of filtrate collected is recorded as a function of time. In the literature, certain values are tabulated as the typical specific cake resistance values for some types of sludges (Tchobanoglous, 1979; Eckenfelder, 1989; Casey, 1997). Table 4.2 gives a comparison of SCR values of different types of sludges. Typical SCR values reported for municipal sludges are from 3 to  $40 \times 10^{11}$  m/kg for conditioned digested wastewater solids and 1.5 to  $5 \times 10^{14}$  m/kg for primary sludge (Vesilind, 2003).

**Table 4.2.** SCR values for different types of sludges  
(Tchobanoglous, 1979)

<b>Sludge type</b>	<b>SCR (m/kg)</b>
Primary	$1.5 - 5 \times 10^{14}$
Activated	$1 - 10 \times 10^{13}$
Digested	$1 - 6 \times 10^{14}$
Digested, coagulated	$3 - 40 \times 10^{11}$

SCR and CST are good comparative techniques for the prediction of trends in dewatering for a given sludge system. However, the results do not produce a characterization parameter that is independent of the starting solids concentration (in the case of CST) and/or the applied pressure (in the case of SCR) (Scales *et al.*, 2004). Scales *et al.* (2004) highlighted that techniques such as CST and SCR, which lack to exploit the long filtration time behavior, are not only inadequate but probably misleading.

Although the results are subject to question, currently, for the characterization of sludge filterability and/or dewaterability, SCR has been the commonly used parameter.

The concept of SCR stems from the empirical filtration theory of Ruth, based on the experimental observation that filtrate volume is usually a parabolic function of time for a constant applied pressure filtration.

#### 4.2.2. Classical Filtration Theory

The classical filtration theory developed by Ruth (Ruth *et al.*, 1933; Ruth, 1935) is based on heuristic analogy with Ohm's Law in which the filtrate rate is related to the ratio of the driving force, i.e., the total pressure drop across the filter ( $\Delta P_T$ ), to the total resistance, i.e., the summation of the cake resistance ( $R_c$ ) and the filter medium resistance ( $R_m$ ):

$$\mu u_o = \frac{\Delta P_T}{R_c + R_m} \quad (4.1)$$

where  $u_o$  is the superficial liquid velocity defined by

$$u_o = \frac{1}{A} \frac{dV}{dt} \quad (4.2)$$

The resistance of the cake,  $R_c$ , is generally assumed to be proportional to the mass of solids in the filter cake per unit area,  $W_s/A$ , with  $\langle \alpha \rangle$  being the proportionality constant:

$$R_c = \langle \alpha \rangle \frac{W_s}{A} \quad (4.3)$$

where  $\langle \alpha \rangle$  is the average SCR. Substitution of Eqs. (4.2) and (4.3) into Eq. (4.1) gives;

$$\frac{1}{A} \frac{dV}{dt} = \frac{1}{\mu \langle \alpha \rangle W_s + AR_m} A(\Delta P_T) \quad (4.4)$$

The macroscopic mass balance expressed in the form

$$\text{Mass of slurry filtered} = [\text{Mass of wet cake}] + [\text{Mass of filtrate}] \quad (4.5)$$

relates the volume of filtrate,  $V$ , to the mass of solids in the filter cake,  $W_s$ , as

$$W_s = cV \quad (4.6)$$

where  $c$  represents the mass of solids per unit volume of filtrate and is given by

$$\frac{1}{c} = \left[ \frac{1}{s} - 1 \right] \frac{1}{\rho} - \left[ \frac{\langle \varepsilon \rangle}{1 - \langle \varepsilon \rangle} \right] \frac{1}{\rho_s} \quad (4.7)$$

where  $s$  represents the weight fraction of solids in the slurry.

Elimination of  $W_s$  between Eqs. (4.4) and (4.6) and rearrangement of the resulting equation leads to:

$$\frac{dt}{dV} = \left( \frac{\mu \langle \alpha \rangle c}{A^2 \Delta P_T} \right) V + \frac{\mu R_m}{A \Delta P_T} \quad (4.8)$$

For a constant pressure filtration, i.e.,  $\Delta P_T = \text{constant}$ , it is customary to integrate Eq. (4.8) by assuming  $c$ ,  $\langle \alpha \rangle$  and  $R_m$  constant. The result is

$$\frac{t}{V} = \left[ \frac{\mu \langle \alpha \rangle c}{2A^2 \Delta P_T} \right] V + \frac{\mu R_m}{A \Delta P_T} \quad (4.9)$$

If a plot of  $t/V$  versus  $V$  yields a straight line, then Equation (4.9) indicates that the average SCR,  $\langle \alpha \rangle$ , and the medium resistance,  $R_m$ , can be obtained from the slope and the intercept, respectively.

The application of constant pressure filtration equation in the determination of the dewaterability and/or filterability of sludge systems, for the most of the time, resulted in variable average SCR values and negative filter medium resistances which cannot be explained by the classical filtration theory.

#### *4.2.3. Drawbacks of the Classical Filtration Theory and the Buchner Funnel Filtration Test Method*

Classical filtration theory, for a specific slurry, assumes SCR to be independent of the operational conditions. Moreover, it considers the medium resistance to be negligible and assumes that the controlling factor is the resistance of the cake. However, the pore size of the filter medium relative to the size of the solids in the slurry is a major factor influencing the magnitude of the average SCR (Tosun *et al.*, 1993).

The standard BF filtration test apparatus simulates filtration only in downward direction. However, in real-life applications using rotary drum filters, the mechanism is more like of up-flow filtration in which the submerged disc which is covered with the filter cloth sucks the particles out of the slurry. Besides, the high settling rate of biological and chemical sludges results in the interference of filtration operation with sedimentation. Tosun *et al.* (1993) have shown that the mode of filtration operation affected the slope values of the  $t/V$  vs.  $V$  plots of activated sludge samples, which is a direct measure of the SCR value. They concluded that the down-flow tests can be used to get qualitative information on the dewaterability of sludges but quantitative results are subject to question. More recently, Wu *et al.* (2000) performed filtration tests with upward, sideward and downward filter orientations. They have concluded that each orientation yields different SCR value and thus it is evident that SCR is affected by the mode of filtration operation.

The dependence of SCR on filter orientation could be attributed to particle settling and pile up during filtration. The distribution of particles within the cake will differ by changing the filter orientation. In down-flow mode, larger particles will settle first and accumulate on the cake-septum interface. In up-flow mode, however, the particle orientation will be reversed, i.e., smaller particles pile up on the cake-septum interface. Thus, particle size and distribution within the slurry becomes an important point to be taken into consideration. Also, the

relative sizes of the particles within the slurry and the pore openings of the filter medium is another factor to be considered. If the sizes are close to each other then the pores of the filter medium may be easily clogged, resulting in a higher resistance. The settling effect of solids was also highlighted by Benesch *et al.* (2004) by modeling cake filtration with superimposed zone as well as classifying sedimentation.

In a typical BF test, the major operational parameters are the type of filter paper used, the filtration area, and the applied vacuum. Although these parameters are not standardized in a BF test, Vesilind (2003) reports that the laboratory apparatus required to perform the BF test consists of a 9-cm diameter BF, a 250 mL lipless graduated cylinder filtrate receiver, a timer, and a vacuum pump. However, no specification is given for the type of filter medium used. On the other hand, Tchobanoglous (1979) and Eckenfelder (1989) specify the filter medium as Whatman #2 with a pore size of 8  $\mu\text{m}$ . For the BF test procedure, Eckenfelder (1989) also mentions the volume of sludge sample as 200 mL and that the sludge transferred to the BF should be kept there for a sufficient time of 5 to 10 seconds for a cake to form prior to application of the constant vacuum.

In field scale applications of sludge dewatering, filter cloths used have larger pore sizes as compared to the ones used at lab scale tests. Thus, it is evident that lab scale tests do not actually mimic the field scale applications. As the importance of the filter medium in assessing the dewaterability of sludges have been shown (Tosun *et al.*, 1993), this fact becomes even more significant.

The size distribution of the particles in the sludge relative to the pores of the filter medium is an important factor in the determination of the overall filtration rate. In the literature, several workers have shown that high levels of smaller particles decrease filtration rate (measured by the specific resistance to filtration) (Higgins and Novak, 1997; Karr and Keinath, 1978; Lawler *et al.*, 1986; Mikkelsen and Keiding, 2002). Karr and Keinath (1978) found that particles in the range of 1-100  $\mu\text{m}$  had the most significant effect on dewaterability.

Guan *et al.* (2001) have tested activated sludge systems and concluded that effects of differences in floc structure on SCR were most marked for flocs of

small size. In their study, the size and structure of flocs within the samples were modified by addition of cationic polymer.

These results are very important in assessing the dewaterability of sludges. They clearly emphasize the importance of particle size and its distribution within the slurry. However, not only the size of the particles but also the relative size of the particles with respect to the pore size of the filter medium should be taken into consideration. When the size of the particles within the slurry are close to the pore size of the filter medium, a blockage of the pores by the particles is expected yielding a higher resistance to flow. Thus, the resistance developed at the cake-septum interface is the controlling factor in filtration.

#### 4.2.4. Multiphase Filtration Theory

The multiphase filtration theory, developed by Willis and Tosun (1980), combines the volume-averaged equations of change with the experimental observations to deduce the filtration mechanism.

For a one-dimensional cake filtration shown in Figure 4.1, the volume averaged equations of continuity for the liquid and solid phases are given by

$$\frac{\partial \varepsilon}{\partial t} = \frac{\partial q}{\partial z} \quad (4.10)$$

$$-\frac{\partial \varepsilon}{\partial t} = \frac{\partial r}{\partial z} \quad (4.11)$$

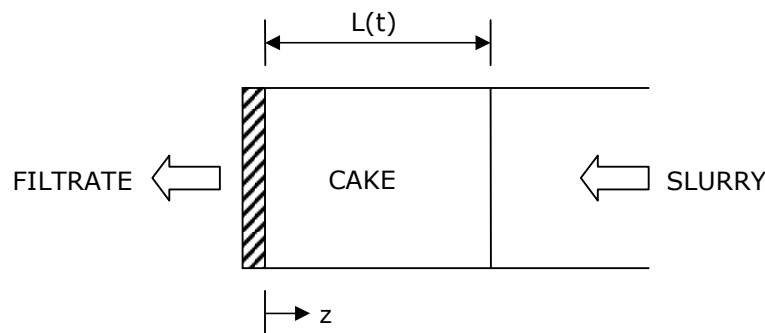


**Figure 4.1.** Schematic diagram of a one-dimensional cake filtration

The volume averaged equation of motion, on the other hand, consists of the inertial, viscous, pressure, gravity and drag forces. In porous media flows the dominant terms are the drag, pressure, and gravity forces. Thus, the equation of motion is given by

$$F_d = \varepsilon \frac{\partial P}{\partial z} \quad (4.12)$$

A constitutive equation for the drag force can be postulated in the form

$$F_d = \lambda \left( \frac{q}{\varepsilon} - \frac{r}{1-\varepsilon} \right) \quad (4.13)$$

in which  $\lambda$  is the resistance function. It is inversely related to the permeability,  $K$ , of the cake by

$$\lambda = \frac{\varepsilon^2 \mu}{K} \quad (4.14)$$

Combination of Eqs. (4.12), (4.13) and (4.14) leads to

$$q - \frac{\varepsilon}{1-\varepsilon} r = \frac{K}{\mu} \frac{\partial P}{\partial z} \quad (4.15)$$

If the porosity distribution is known, then the distribution of liquid and solid superficial velocities can be determined from the continuity equations, i.e., Eqs. (4.10) and (4.11). This leaves Eq. (4.15) as a first-order differential equation. Therefore, the process correlation for cake filtration does not require the simultaneous solution of the continuity and motion equations. It can simply be obtained by specifying the boundary condition at the cake-septum interface where the least permeable part of the cake is most likely to occur. At the cake-septum interface, the liquid and solid velocities are given by

$$\text{At } z = 0, \quad q = \frac{1}{A} \frac{dV}{dt} \quad \text{and } r = 0 \quad (4.16)$$

Therefore, evaluation of Eq. (4.15) at  $z = 0$  yields

$$\frac{1}{A} \frac{dV}{dt} = K_o \left( \frac{\partial P}{\partial z} \right)_{z=0} \quad (4.17)$$

where  $K_o$  is the permeability at the cake-septum interface. It is not determined solely by the solid-liquid combination but includes the interaction of the septum with the filter cake. Therefore, the value of  $K_o$  is not only affected by the nature and the particle size distribution of the solid particles, but also with the pore size distribution of the filter medium.

Introduction of the dimensionless variables

$$P^* = \frac{P - P_o}{\Delta P_c} \quad \text{and} \quad \xi = \frac{z}{L} \quad (4.18)$$

reduces Eq. (4.17) to

$$\frac{1}{A} \frac{dV}{dt} = K_o J_o \frac{\Delta P_c}{L} \quad (4.19)$$

where  $J_o$  is the dimensionless pressure gradient at the cake-septum interface defined by

$$J_o = \left. \frac{\partial P^*}{\partial \xi} \right|_{\xi=0} \quad (4.20)$$

The relationship between cake length and filtrate volume is obtained from the macroscopic mass balance as

$$L = \left( \frac{G}{A} \right) V \quad (4.21)$$

The term  $G$  is expressed as a function of average cake porosity,  $\langle \varepsilon \rangle$ , and the volume fraction of liquid in the slurry,  $\varepsilon_{sl}$ , as

$$G = \frac{1 - \varepsilon_{sl}}{\varepsilon_{sl} - \langle \varepsilon \rangle} \quad (4.22)$$

in which the term  $\varepsilon_{sl}$  is calculated from

$$\varepsilon_{sl} = \frac{(1-s)\rho_s}{\rho_s - s(\rho_s - \rho)} \quad (4.23)$$

Substitution of Eq. (4.21) into Eq. (4.19) leads to

$$\frac{dt}{dV} = \frac{1}{K_o J_o} \left( \frac{G}{A^2 \Delta P_c} \right) V \quad (4.24)$$

Therefore, when  $dt/dV$  versus  $V$  is plotted, the slope of the straight line is proportional to  $K_o J_o$ . The intercept, simply indicates the initial reciprocal rate through a clean filter medium.

### 4.3. Materials and Methods

#### 4.3.1. Biological Sludge

Biological sludge experiments were conducted with the slurry taken from the recycle line of activated sludge unit from a nearby municipal wastewater treatment plant. The mixed liquor suspended solids (MLSS) concentration of the sludge sample was set to 10 g/L during filtration experiments. Chemical conditioning of the activated sludge samples was made by a commercially available cationic polyelectrolyte (Zetag 7635, CIBA Chemicals).

#### 4.3.2. Chemical Sludge

Chemical sludge experiments were conducted with two different types of sludges, namely lead hydroxide and aluminum hydroxide (alum), prepared under laboratory conditions. Lead hydroxide sludge was prepared by first dissolving lead nitrate in water and then precipitating it as lead hydroxide at a pH of 11. Alum sludge was prepared by the addition of aluminum sulfate to a clay suspension. The alkalinity of the clay suspension was checked and found to be

enough to have reaction go to completion producing aluminum hydroxide precipitates.

#### *4.3.3. Filter Medium*

To assess the effect of filter medium on the overall performance of filtration, Whatman # 40, # 41 and # 42 filter papers with pore sizes of 8  $\mu\text{m}$ , 20-25  $\mu\text{m}$  and 2.5  $\mu\text{m}$ , respectively, were used. Besides the laboratory filter papers; a filter cloth, a steel mesh and a nylon filter medium were used with pore sizes of 50-100  $\mu\text{m}$ , 200  $\mu\text{m}$  and 333  $\mu\text{m}$ , respectively.

To investigate the dependence of average SCR value on the filtration area, two different BFs with diameters 40 mm ( $A = 12.6 \text{ cm}^2$ ) and 90 mm ( $A = 63.6 \text{ cm}^2$ ) were used.

#### *4.3.4. Experimental Procedure*

The BF filtration apparatus used in the experiments were shown in Figures 3.2 and 3.3. Filtration experiments were conducted both in the same and opposite directions to the gravity.

Each experiment was repeated at least twice and the experimental data represent the arithmetic average of the results.

### **4.4. Results and Discussion**

In order to show the inadequacy of the constant pressure filtration equation in analyzing filterability of real sludge systems, filtration experiments were carried out under different operational conditions using activated and chemical sludges as summarized in Table 4.1. Moreover, the filtration performances of two different chemical sludges were also compared. Finally, the reliability of the BF test method was explored in terms of the effect of filter medium used (lab filter papers versus plant scale filter cloths) and the mode of filtration. The importance of particle size-pore size interactions were highlighted via chemical conditioning of activated sludge at different dosages to have dominance of different particle size distributions.

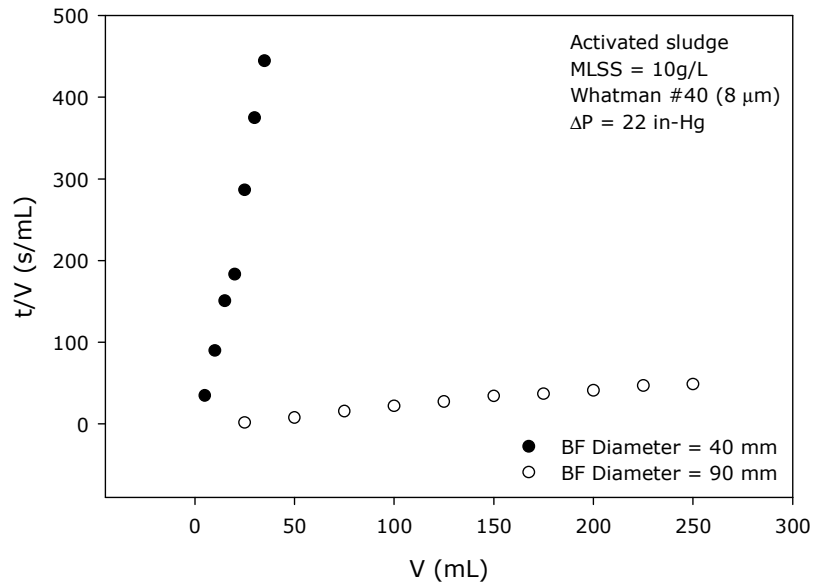
#### 4.4.1. Activated Sludge Experiments

Table 4.3 summarizes the experimental conditions and the resulting SCR and filter medium resistance values for the activated sludge runs.

**Table 4.3.** Activated Sludge-Experimental conditions and filtration test results

Parameter	Experiment #					
	1	2	3	4	5	6
Filter Medium	W#40	W#40	W#42	W#42	W#40	W#41
Pore size ( $\mu\text{m}$ )	8	8	2.5	2.5	8	20-25
BF diameter (mm)	40	90	40	90	40	40
$\Delta P$ (in-Hg)	22	22	22	22	15	15
SCR ( $\times 10^{-14}\text{m/kg}$ )	2.85	1.12	0.93	1.33	0.78	0.17
$R_m$ ( $\times 10^{-10}\text{1/m}$ )	- 435	- 45	- 8.6	346	- 27	- 44

Figure 4.2, 4.3 and 4.4 are the  $t/V$  vs.  $V$  plots of experiments 1-2, 3-4 and 5-6, respectively. The results showed that, under the same operational conditions and keeping mass of solids per unit area constant, changing the filtration area resulted in 1.5 to 2.5 times higher SCR values for experiments 3-4 and 1-2, respectively. On the other hand, keeping everything constant and decreasing the pore size of the filter medium from 20-25  $\mu\text{m}$  to 8  $\mu\text{m}$  resulted in 4.6 times higher SCR value for the same sludge as given in Table 4.3. As to analyze the effect of applied pressure on the SCR value, experiment 1 and 5 can be compared. As the pressure was increased about 1.5 times, the SCR value increased 3.7 times as tabulated in Table 4.3.



**Figure 4.2.**  $t/V$  versus  $V$  for different BF diameter

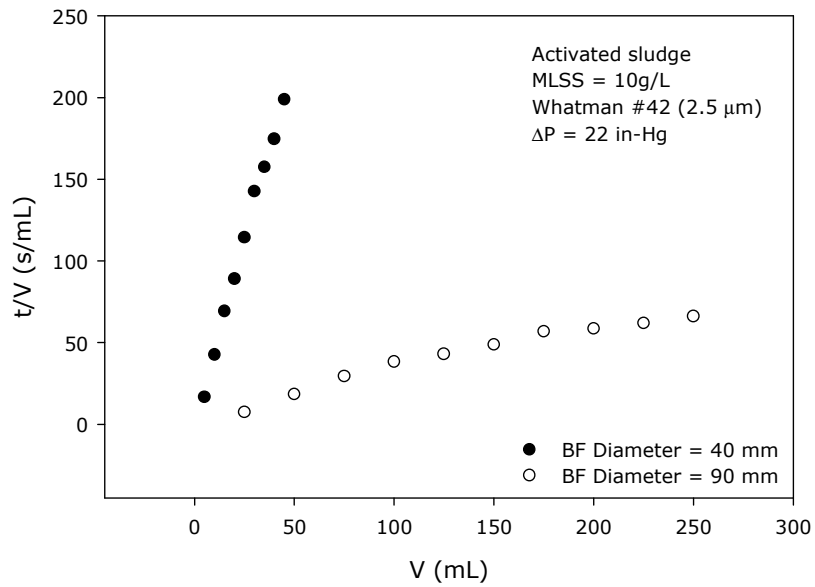


**Figure 4.3.**  $t/V$  versus  $V$  for different BF diameter

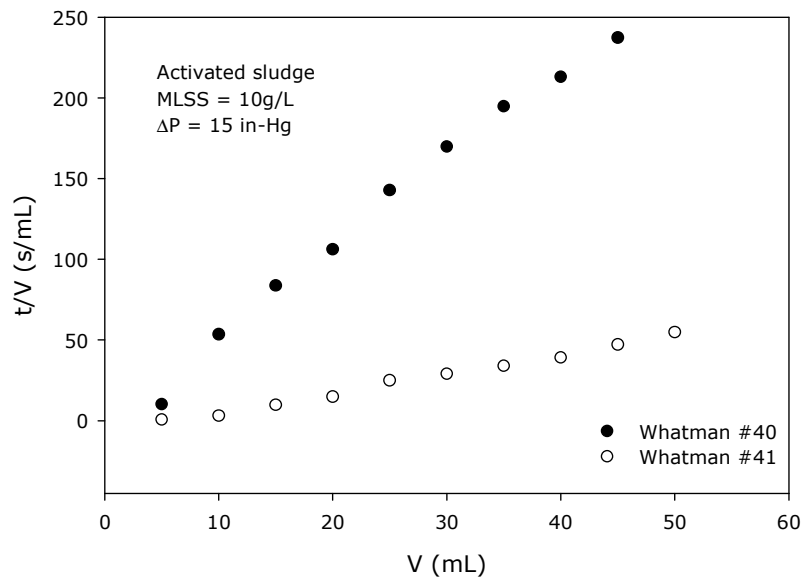


**Figure 4.4.**  $t/V$  versus  $V$  for different filter medium

The filtration experiments conducted with activated sludge have shown that SCR values are highly dependent on operational conditions besides the slurry characteristics; and it is erroneous to give typical values of SCR for sludges. Moreover, negative filter medium resistance values were obtained for most of the filtration runs as given in Table 4.3. It is physically meaningless to have negative resistance values and this point is not emphasized in filtration studies since filter medium resistance is taken as negligible by the Ruth's classical approach.

The incapability of the classical approach in representing the filterability of biological sludges could be attributed to the complex nature of these sludge systems. For this purpose, the behavior of less complicated chemical sludge systems was investigated. Two different chemical sludges, lead hydroxide and alum, were prepared under laboratory conditions.

#### 4.4.2. Chemical Sludge (Lead Hydroxide) Experiments

The filtration test results of lead hydroxide sludge were used to generate plots of  $t/V$  vs.  $V$ . The experimental conditions are given in Table 4.4.

**Table 4.4.** Chemical Sludge – Experimental conditions

Parameter	Experiment #				
	7	8	9	10	11
Filter Medium	W#42	W#42	W#40	W#41	W#42
Pore size ( $\mu\text{m}$ )	2.5	2.5	8	20-25	2.5
BF diameter (mm)	40	90	40	40	40
$\Delta\text{P}$ (in-Hg)	18	18	22	22	22

Figure 4.5 and 4.6 are the  $t/V$  vs.  $V$  plots of experiments 7-8 and 9-10-11, respectively. Analysis of the figures again show a variation in the slope values of  $t/V$  vs.  $V$  plots which is a measure of the SCR. Moreover, the straight line trend was not even seen as shown in Figure 4.6.

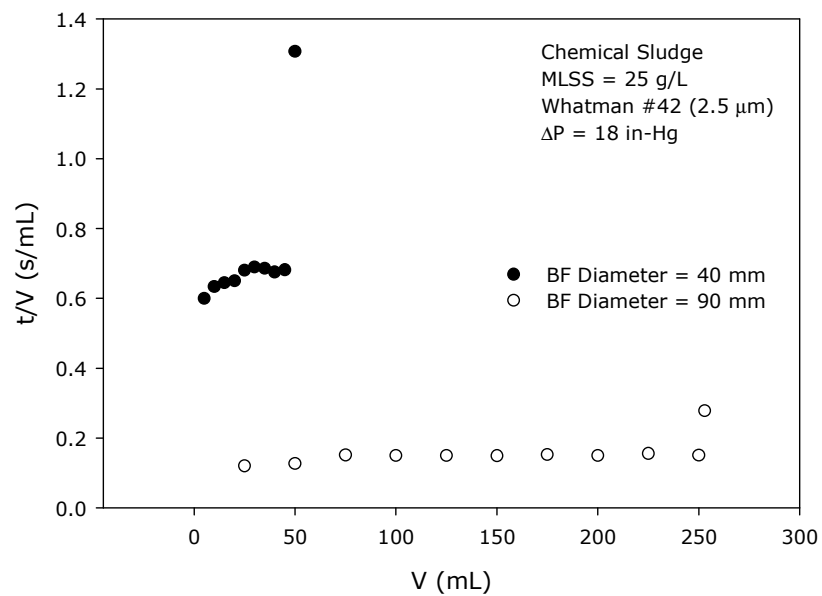


**Figure 4.5.**  $t/V$  versus  $V$  for Experiment # 7 and 8

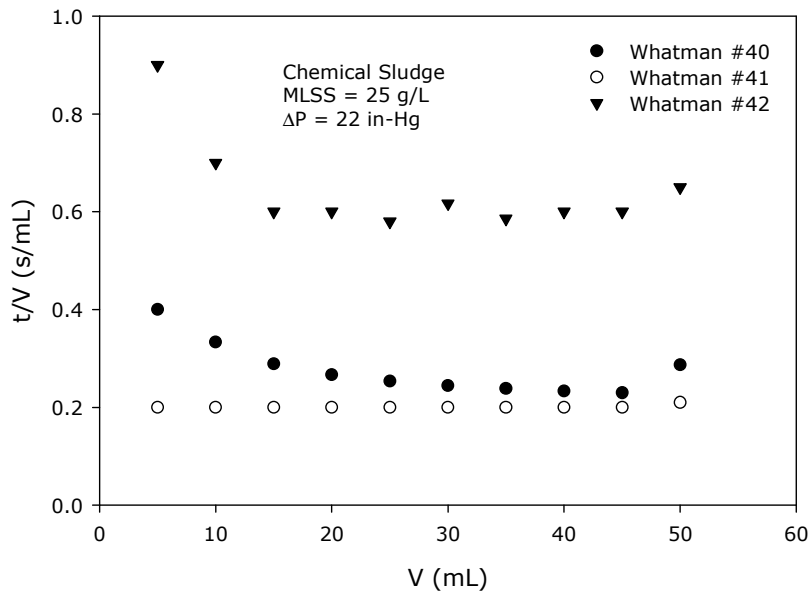


**Figure 4.6.**  $t/V$  versus  $V$  for Experiment # 9, 10 and 11

Although chemical sludge systems are less complicated than biological sludge systems, filtration test results of lead hydroxide sludge revealed even worse results.

#### 4.4.3. Comparison of Filtration Behavior of Alum Sludge and Lead Hydroxide Sludge

A comparison for the filtration behavior of two different chemical sludges was made. Figure 4.7 is the  $t/V$  vs.  $V$  plot for alum and lead hydroxide sludge filtered under the same operational conditions.

Although chemical sludge systems are less complicated than biological sludge systems, filtration tests revealed that:

- The straight line trend of  $t/V$  vs.  $V$  plot as depicted by Ruth's approach cannot be obtained for lead hydroxide sludge
- Alum sludge yielded a straight line trend after a certain point

It should be noted that, although alum sludge is better described by the classical approach as compared to lead hydroxide sludge, this does not mean that the

classical theory is successful in representing filterability of sludge systems. A single sludge that shows deviation from the expected trends of the classical approach clearly points out the failure of the theory. A theory should be universal and cannot be applicable to certain types of sludges while it fails to represent the others.

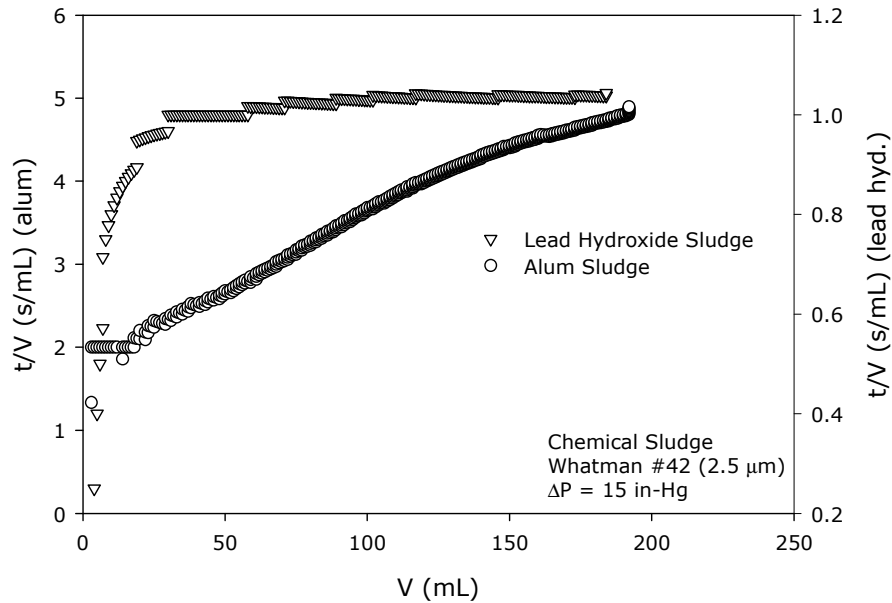


**Figure 4.7.** t/V vs. V-Alum sludge and lead hydroxide sludge

In the literature, Scales *et al.* (2004) performed filtration tests with sewage sludge and alum based potable water treatment sludge. They compared filtration test results for both types of sludges and concluded that the alum based potable water treatment sludge could be characterized using a classical approach. This outcome actually highlights the failure of the classical theory.

The difference in the filterability of alum and lead hydroxide sludges could be best explained by the differences in the particle size distributions, floc shapes and sizes. As the sizes and the relative distributions of the flocs change, the overall filtration behavior of the slurries differs greatly.

#### 4.4.4. Validity of the BF Test

Further studies with real sludge systems were conducted to investigate the validity of the currently used experimental method in assessing the sludge dewaterability.

##### a. Type of Filter Medium Used

Activated sludge experiments with a commercial filter cloth (50-100  $\mu\text{m}$  pore size) and laboratory filter paper, i.e. Whatman # 40 with a pore size of  $8\mu\text{m}$ , were conducted at a vacuum of 5 in-Hg in down-flow mode. The  $dt/dV$  vs.  $V$  results of filtration tests conducted with both raw and conditioned sludge are given in Table 4.5.

**Table 4.5.** Effect of filter medium/down-flow filtration  
(values in brackets are for filtrate turbidities)

Sludge Type	Filter Medium	
	W#40 (8 $\mu\text{m}$ )	Filter Cloth
Raw Sludge (no conditioning)	$\frac{dt}{dV} = 5.07 \times 10^{-2} V + 0.57$ (<4 NTU)	$\frac{dt}{dV} = 1.27 \times 10^{-2} V + 1.04$ (<4 NTU)
1% chemical conditioned sludge	$\frac{dt}{dV} = 2.61 \times 10^{-2} V + 0.93$ (<2 NTU)	$\frac{dt}{dV} = 0.94 \times 10^{-2} V + 1.83$ (<2 NTU)

The results revealed that, for filtration tests with filter cloth, the slope values, which are an indication of the resistance to filtration, are lower than those for laboratory filter paper, i.e., Whatman #40. Upon application of chemical conditioning, the slope values decreased for both types of filter media used. Besides, the effluent quality showed no variation in terms of turbidity for the filter cloth and Whatman #40. Thus, having a constant filtrate quality, smaller resistance to filtration was experienced with the filter cloth both for

unconditioned and conditioned cases. This result is a clear indication of the over-estimation of lab scale experiments in determination of the overall resistance to filtration.

According to the classical approach, whatever medium is used, same sludge should yield same SCR value when filtered through a filter cloth or a Whatman #40 filter paper since SCR is believed to be a slurry specific parameter. Although the classical theory ignores the importance of the filter medium used, the results gathered so far indicated that SCR value is not a sludge-specific value, and more importantly, the operational conditions under which the test is carried out affects the filtration test results. Since the filter medium plays an important role in sludge dewaterability, it is crucial to specify the type of filter medium used in the filtration tests.

#### **b. Mode of Filtration Operation**

A detailed discussion on the effects of mode of filtration operation on the overall filterability was given in Section 4.2.3.

The effect of mode of operation for both raw activated sludge and conditioned activated sludge filtered through a commercial filter cloth was investigated and the results are given in Table 4.6.

**Table 4.6.** Effect of mode of operation during dewaterability analysis  
(values in brackets are for filtrate turbidities)

<b>Mode of operation</b>	<b>Filter cloth</b>	
	<b>Raw sludge (no conditioning)</b>	<b>1% chemical conditioned sludge</b>
Down-flow	$\frac{dt}{dV} = 1.27 \times 10^{-2} V + 1.04$ ( <4 NTU)	$\frac{dt}{dV} = 0.94 \times 10^{-2} V + 1.83$ ( <2 NTU)
Up-flow	$\frac{dt}{dV} = 7.98 \times 10^{-2} V + 2.07$ ( <4 NTU)	$\frac{dt}{dV} = 0.82 \times 10^{-2} V + 1.47$ ( <2 NTU)

### c. Particle Size-Pore Size Interactions

The up-flow filtration test results at 1%, 5% and 7% by wt. conditioner dosage rates with steel mesh (200 μm) and nylon filter medium (333 μm) are given in Table 4.7. It should be noted that, at each conditioner dosage applied, the size of the flocs formed differ greatly resulting in dominance of different floc sizes.

**Table 4.7.** Effect of applied chemical dosage on different filter medium (floc size effect) (values in brackets are for filtrate turbidities)

<b>Chemical Dosage Rate</b>	<b>Medium # 1 (steel mesh, 200 μm)</b>	<b>Medium # 2 (nylon filter, 333 μm)</b>
1%	$\frac{dt}{dV} = 1.94 \times 10^{-3} V + 1.29$ ( < 5 NTU)	$\frac{dt}{dV} = 0.42 \times 10^{-3} V + 0.09$ ( ≈ 350 NTU)
5%	$\frac{dt}{dV} = 0.41 \times 10^{-3} V + 0.84$ ( < 5 NTU)	$\frac{dt}{dV} = 2.07 \times 10^{-3} V + 0.06$ ( < 5 NTU)
7%	$\frac{dt}{dV} = 0.19 \times 10^{-3} V + 0.64$ ( < 5 NTU)	$\frac{dt}{dV} = 0.22 \times 10^{-3} V + 0.09$ ( < 5 NTU)

Upon conditioning the sludge at different chemical dosage rates, the particle size distribution within the slurry differed greatly. As can be seen from the slope values of dt/dV vs. V fit equations in Table 4.7, changing the particle size distribution within the slurry relative to the pore size of the filter medium resulted in 10 times higher SCR values for steel mesh from going 7% to 1% chemical conditioning. Although the same filter medium is used, the intercept value of the steel mesh shows variation. This implies that, the intercept is also affected by the particle and/or floc concentration within the slurry.

At 1% chemical conditioning, the size of the flocs formed were relatively smaller in size. As seen in Table 4.7, the flocs were found to clog the 200 μm pores of the steel mesh whilst they were found to escape from the 333 μm nylon filter yielding very high filtrate turbidity. One should note that, the filtrate turbidity is not a design parameter for sludge dewatering facilities as the filtrate is

ultimately diverted to the head of the treatment plant for subsequent treatment within the wastewater line. It can be concluded that, at 1% chemical conditioning, the flocs formed were mainly at the size of 200  $\mu\text{m}$  and exactly clog the pores of the filter medium.

Chemical conditioning at 5% resulted in larger flocs which were found to yield higher resistance to filtration for the 333  $\mu\text{m}$  nylon filter. This may be due to existence of flocs which were comparable in size to the pores of the nylon filter medium. On the other hand, for the 7% conditioning rate the slope values were found to be close to each other, implying that the flocs formed and the two filter media have similar interactions.

It is important to remember that the BF test is used to assess the performance of conditioners in dewatering a particular sludge; the best dosage, i.e. the dosage that gives the lowest SCR, for each of the conditioners may be obtained and compared. Based on the cost of the conditioning chemicals tested and their optimum doses, the cost for conditioning a given sludge quantity with each of the conditioners tested can be evaluated and compared. However, Table 4.7 clearly indicates that the optimum dosage obtained for a specific conditioner highly depends on the filter medium used. Thus, the results obtained from lab scale BF tests to determine the filterability of sludges and optimum conditioner dosages are subject to question. The results are valid only for the operational conditions under which the test is being carried out, i.e., type of filter medium, filtration area, mode of filtration, and applied vacuum.

The results obtained so far with real sludge systems indicate that the currently used approach should be modified. As activated sludge systems are complex in terms of its wide range of particle size distribution with high non-uniformity having compressible and different shaped particles it is not possible to modify or develop a filtration model based on data from such systems.

#### 4.5. Conclusions

The initial phase of the study has revealed several important conclusions:

- The results obtained from activated sludge and chemical sludge experiments indicate that the slopes of the  $t/V$  vs.  $V$  plots are strongly affected by the operational conditions.
- SCR is not a slurry specific characterization parameter as depicted by the classical filtration theory. Moreover, it provides only qualitative and comparative information. Quantitative results are subject to question since they are valid only for the conditions under which the test is being carried out, i.e. vacuum applied, filter medium used, mode of filtration operation, and also the characteristics of the slurry.
- The lab scale BF test does not actually represent the field scale applications of dewatering in terms of the filter medium used and mode of filtration operation. Hence, the SCR values obtained at lab scale studies do not reflect the real plant scale performance.
- Real sludge systems are so complex in nature that it is impossible to correctly analyze the effect of slurry characteristics and operational conditions on the overall performance of the filtration process. First, model slurries should be used to explore the physical reality behind the filtration process; and afterwards the applicability to real sludge systems should be tested.

## CHAPTER 5

### MODEL SLURRY SYSTEMS

#### 5.1. Objective and Experimental Design

The objective of the second phase of the studies was to analyze the effects of operational conditions and slurry characteristics on the expression of filterability of sludge systems. To better understand the factors affecting the overall filtration performance, model slurries of spherical and incompressible Meliodent particles were used.

The experiments conducted with Meliodent slurries can be grouped under 4 topics:

- A. Effect of particle settling rate (buoyant vs. non-buoyant slurries)
- B. Effect of particle size distribution
- C. Effect of slurry concentration
- D. Effect of particle size and pore size of the filter medium

The filtration test data were analyzed in terms of  $dt/dV$  vs.  $V$  relationships evaluated directly from the experimental time-volume data. The experimental data presented are the average of at least three coincident filtration tests conducted under the same experimental conditions.

Table 5.1 summarizes the experimental studies covered in this chapter.

**Table 5.1.** Experimental studies with model slurry systems

Case	Operational parameters*		Data analysis
	Constant	Variable	
A-Effect of particle settling rate	C: 8% PS:100-250 $\mu\text{m}$ FM:Whatman#41 $\Delta\text{P}$ : 4.5, 9 and 18 in-Hg M: up-, down-flow	<b><u>Slurry</u></b> Buoyant slurry (40 wt. % sugar sol.) Non-buoyant slurry (water)	dt/dV vs. V
B-Effect of particle size distribution	C: 8% FM:Whatman#41 $\Delta\text{P}$ : 4.5, 9 in-Hg M: up-flow	<b><u>Particle size</u></b> 75-100 $\mu\text{m}$ 175-250 $\mu\text{m}$ Mixed	dt/dV vs. V
	C: 2% FM:Whatman#41 $\Delta\text{P}$ : 5 in-Hg M: up-flow	<b><u>Particle size</u></b> 53-75 $\mu\text{m}$ 250-425 $\mu\text{m}$ Mixed	dt/dV vs. V
C-Effect of slurry concentration	PS: 175-250 $\mu\text{m}$ FM:Whatman#41 $\Delta\text{P}$ : 4.5, 9 in-Hg M: up-flow	<b><u>Slurry conc.</u></b> (by wt.) 4%, 8%, 12%, 16%	dt/dV vs. V
D- Effect of particle size and pore size of the filter medium	C: 4% PS: 250-425 $\mu\text{m}$ $\Delta\text{P}$ : 5 in-Hg M: up-flow	<b><u>Filter Medium</u></b> Whatman#41 Steel mesh	dt/dV vs. V
	C: 2% PS: 53-75 $\mu\text{m}$ $\Delta\text{P}$ : 5 in-Hg M: up-flow	<b><u>Filter Medium</u></b> Whatman#41 Nylon filter medium	dt/dV vs. V
	C: 4% and 8% PS: 200-210 $\mu\text{m}$ $\Delta\text{P}$ : 5 and 10 in-Hg M: up-flow	<b><u>Filter Medium</u></b> Whatman#41 Nylon filter m. Steel mesh	dt/dV vs. V

\* C: Solids concentration (by wt. %), FM: Filter medium, M: Mode of filtration, PS: Particle size distribution

## **5.2. Materials and Methods**

### *5.2.1. Model Slurry*

The model slurry samples were prepared by perfectly spherical and incompressible Meliodent particles in distilled water and in 40 wt. % sugar solution. The viscosity of the 40 wt. % sugar solution was measured as 1.40 cP at 20<sup>0</sup>C (Brookfield DV-II+ Viscometer). In the literature, the viscosity of 80 wt. % sucrose solution at 21<sup>0</sup>C is reported as 1.92 cP (Geankoplis, 1982).

### *5.2.2. Filter Medium*

In this phase of the study, Whatman #40 (8 μm), #41 (20-25 μm) and #42 (2.5 μm) filter medium; Millipore nylon filter media of 41μm pore size and steel mesh of 200μm pore size were used.

### *5.2.3. Experimental Procedure*

The BF filtration test apparatus was used both in standard down-flow mode and in up-flow mode of operation.

In up-flow mode of operation, the slurries were continuously stirred so as to have a homogeneous mixture. The volume of filtrate collected as a function of time was recorded by a computer. The filtrate data was recorded for every 2 seconds. Each experiment was repeated at least three times and the experimental data represent the arithmetic average of the results.

## **5.3. Results and Discussion**

### *5.3.1. Preliminary Investigations*

Prior to the analysis of effect of slurry characteristics and operational conditions on the overall filtration performance, preliminary studies were carried out with sugar-Meliodent slurries.

Initially, Meliodent particles were fractionated by sieving through 100 μm sieve so that two different particle size fractions were formed. Sugar-Meliodent slurries

composed of particles larger than  $100\ \mu\text{m}$  were used to form model slurries of 8% particle concentration. The slurry samples were filtered through Whatman #40, #41 and #42 filter papers at a constant applied vacuum of 18 in-Hg. The tests were conducted in standard down-flow mode of operation. Figure 5.1 is the V vs. t plot for the slurry filtered through three different filter media.

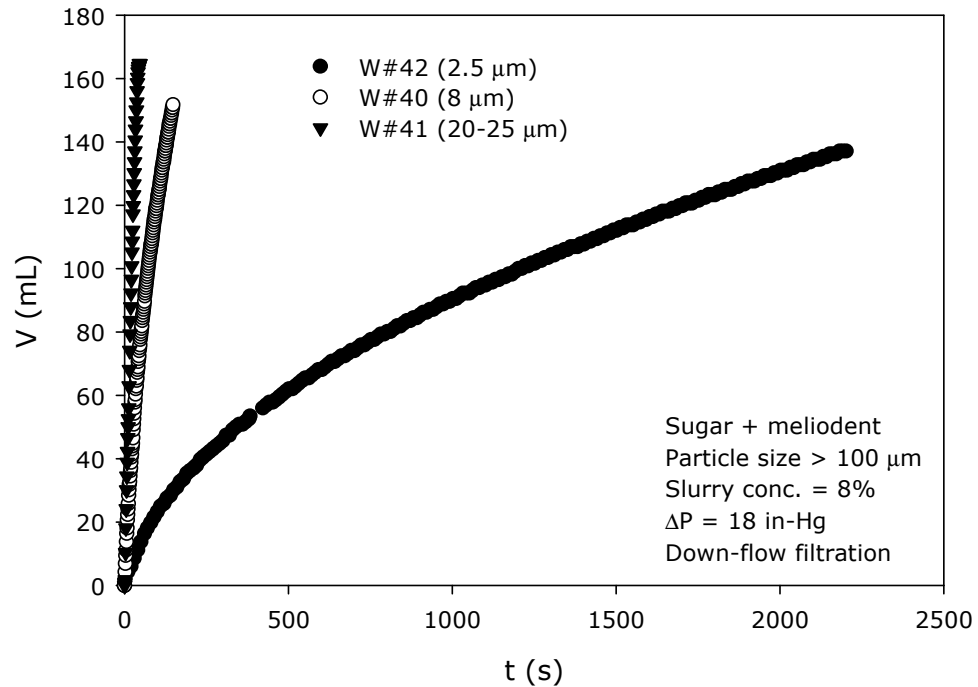


**Figure 5.1.** V vs. t plot for sugar-Melioident slurry (W#40, W#41, W#42)

Figures 5.1 and 5.2 clearly emphasize the effect of filter medium used on the overall filtration performance. As the pore size of the filter medium increased, the filtration rate of the slurry became faster. This finding clearly emphasizes the importance of cake-septum interface in the determination of the resistance to flow as predicted by the multiphase filtration theory. The particle-free 40 wt. % sugar solution was also filtered through the same filter papers under the same vacuum of 18 in-Hg. Figure 5.3 shows the volume-time relationships for the particle-free sugar solution.

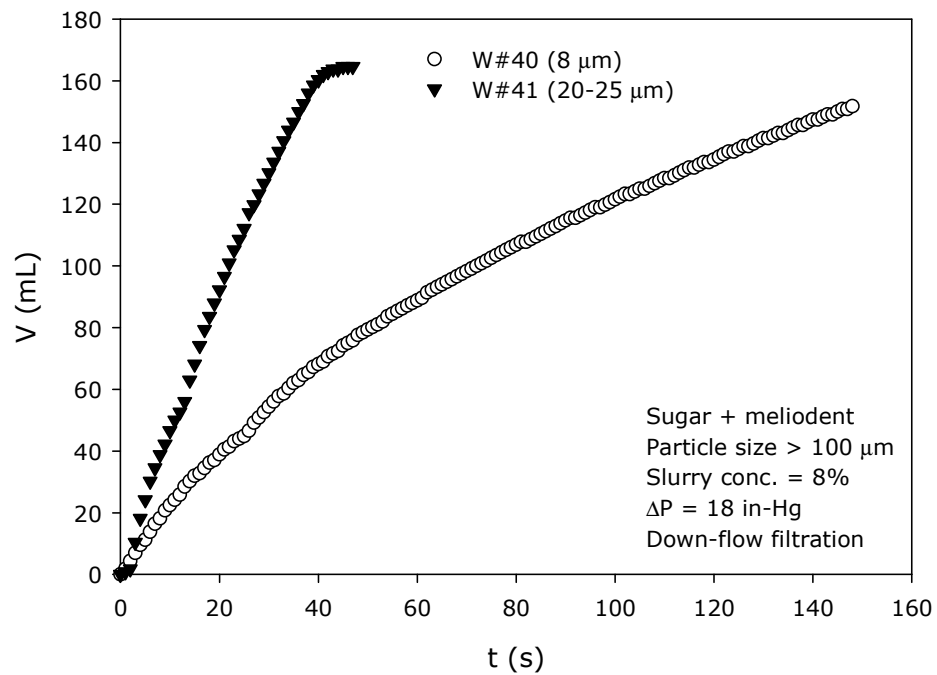


**Figure 5.2.** V vs. t plot for sugar-Melioident slurry (W#40, W#41)

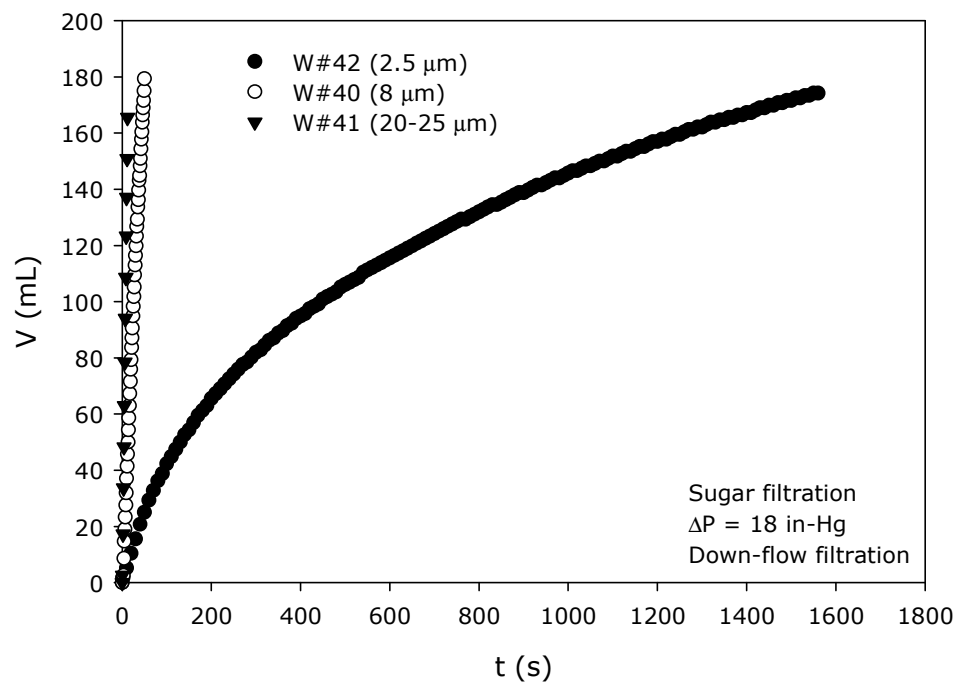


**Figure 5.3.** V vs. t plot for 40 wt. % sugar solution (W#40, W#41, W#42)

When the V vs. t trends for W#40 and W#41 are analyzed separately as in Figure 5.4, it is seen that they yield a linear V vs. t trend, as expected. However, the non-linear behavior of W#42 filter paper was unexpected and was seen for all sugar solutions prepared either by tap water or by distilled water. In order to eliminate the possibility of this behavior due to impurities in commercial sugars, sucrose was used throughout the study. However, the non-linear behavior did not change and this behavior was attributed to a possible formation of polymer structures by the sucrose particles that somehow cover or clog the pores.

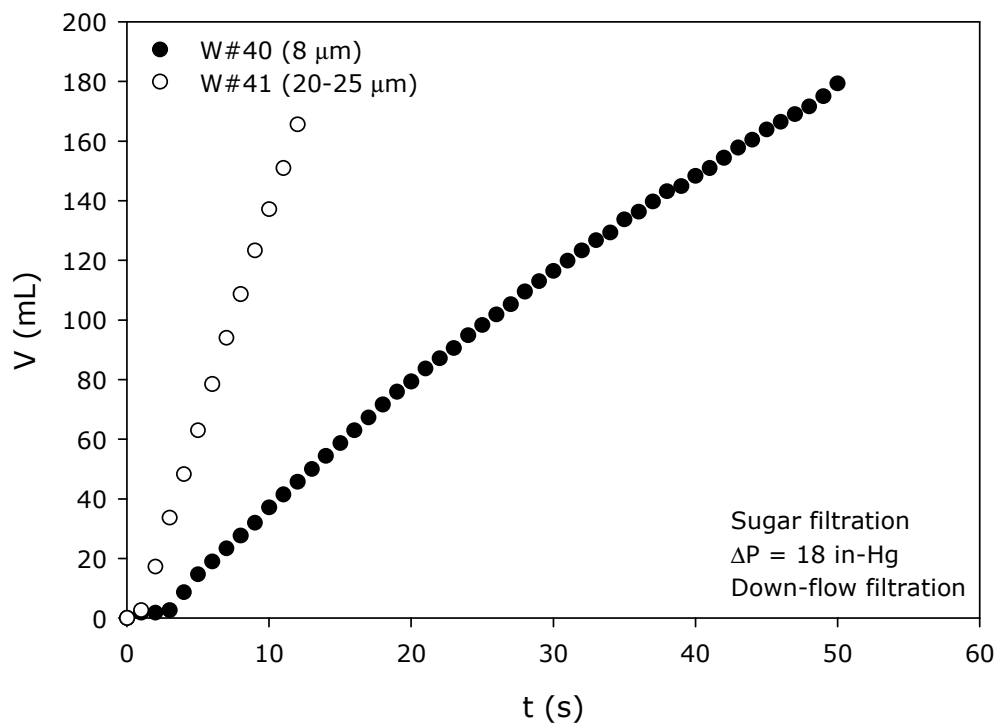


**Figure 5.4.** V vs. t plot for 40 wt. % sugar solution (W#40, W#41)

As a result of this observation, W#42 filter paper was not used in any further analysis throughout the study. Among the Whatman filter papers, #41 filter paper with the largest pore size was selected which will be closer to real life applications as it is the coarsest one of all.

5.3.2. Effect of particle settling rate (buoyant vs. non-buoyant slurries)

The filtration test results are presented in Table 5.2a. The  $dt/dV$  vs.  $V$  results are the average of at least three coincident tests. As an example,  $V$  vs.  $t$  test results for both modes of operation under 4.5 in-Hg vacuum for both slurries are given in Appendix A (Figures A.1 and A.2).

**Table 5.2a.** Filtration test results-Effect of particle settling rate

<b>P (in-Hg)</b>	<b>Mode</b>	<b>Water + Meliodent</b>	<b>Sugar + Meliodent</b>
<b>4.5</b>	<b>Up</b>	$\frac{dt}{dV} = 1.3 \times 10^{-3}V + 0.2$	$\frac{dt}{dV} = 4.3 \times 10^{-3}V + 0.3$
	<b>Down</b>	$\frac{dt}{dV} = 6.2 \times 10^{-3}V + 0.2$	$\frac{dt}{dV} = 5.2 \times 10^{-3}V + 0.2$
<b>9</b>	<b>Up</b>	$\frac{dt}{dV} = 0.6 \times 10^{-3}V + 0.1$	$\frac{dt}{dV} = 1.2 \times 10^{-3}V + 0.2$
	<b>Down</b>	$\frac{dt}{dV} = 3.2 \times 10^{-3}V + 0.1$	$\frac{dt}{dV} = 2.3 \times 10^{-3}V + 0.1$
<b>18</b>	<b>Up</b>	$\frac{dt}{dV} = 0.2 \times 10^{-3}V + 0.1$	$\frac{dt}{dV} = 0.6 \times 10^{-3}V + 0.1$
	<b>Down</b>	$\frac{dt}{dV} = 0.8 \times 10^{-3}V + 0.1$	$\frac{dt}{dV} = 0.9 \times 10^{-3}V + 0.1$

Table 5.2b summarizes the volume-time relationships for particle-free water and sugar solutions under 4.5, 9 and 18 in-Hg applied vacuum. The tests were conducted in up-flow mode of operation to have more reliable results as the volume of slurry to be filtered is nearly 5 times as much as that for the down-flow mode of operation.

**Table 5.2b.** V vs. t results for water and sugar solution

<b>Pressure</b>	<b>Water</b>	<b>Sugar Solution (40 wt. %)</b>
	$V = 6.95t$	$V = 6.27t$
4.5 in-Hg	$\frac{t}{V} = 0.14$	$\frac{t}{V} = 0.16$
	$V = 14.27t$	$V = 11.40t$
9 in-Hg	$\frac{t}{V} = 0.07$	$\frac{t}{V} = 0.09$
		$V = 22.50t$
18 in-Hg	-	$\frac{t}{V} = 0.04$

Results revealed that, for a constant applied vacuum, up-flow and down-flow modes of filtration yielded different slope values, i.e., different resistances to filtration, and this difference is more pronounced for non-buoyant slurries. However, a difference still exists for buoyant slurries and this indicates that the effect of particle settling during the course of filtration is not a major factor affecting overall filtration performance. For example, at an applied vacuum of 4.5 in-Hg, the slope value is approximately 4.8 times larger in down-flow mode of operation as compared to up-flow mode with water-Meliodont slurry (non-buoyant); however, the difference is only 1.2 times for the sugar-Meliodont slurry (buoyant). Moreover, as the applied vacuum was increased to 18 in-Hg, the slope of down-flow operation for non-buoyant slurry became 3.5 times that of up-flow mode. When Table 5.2a is analyzed; a slope value for down-flow mode of approximately 1.2 to 1.9 times larger than up-flow mode is obtained for buoyant slurry. Thus, it may not be correct to attribute the difference observed for non-buoyant slurries directly to buoyancy effect.

Although the same slurry was filtered, the mode of filtration operation affected the initial deposition of the particles over the filter medium, and consequently, the particle size distribution within the cake. The accumulation of different particle sizes over the filter medium will affect the resistance developed at the

cake-septum interface, which in turn results in a totally different filterability performance.

When the slope values for the buoyant slurry given in Table 5.2a are normalized for viscosity (dividing slope values by 1.40 cP), although the viscosity affect is diminished, still a difference will be observed between the slurries. This may be due to the different particle-fluid behaviors during the filtration tests, i.e. for non-buoyant slurry particles settle faster in down-flow operations as compared to the buoyant slurry and in up-flow mode the particles are more easily sucked out of the buoyant slurry since the particles are already buoyant in the slurry even in the absence of mixing.

The results obtained so far indicate that the overall filtration rate is mainly affected by how the particles deposit over and cover the filter medium. Although the buoyancy effect was normalized, it is mainly the individual particle-filter medium interaction that determines the overall performance of the filtration process.

When the intercept values given in Table 5.2a are compared with Table 5.2b, it is seen that the values for the slurries are higher than those given for the particle-free liquids, as expected.

For particle-free water and sugar solutions, the initial passage rate ( $V/t$  value) is the maximum value that can be achieved for that filter medium. Thus, for slurries being filtered, the intercept values, which are the reciprocals of the initial passage rates, should always be higher than that for the particle-free liquid.

At 18 in-Hg vacuum, the filtration operation was so fast that the balance could not read the values accurately for water. Thus, it was decided not to use this pressure in the forthcoming filtration tests since the number of filtration data that can be gathered at this operating pressure will not be sufficient to have reliable results.

### 5.3.3. Effect of particle size distribution

Second group of experiments were conducted to analyze the effect of particle size distribution on the overall filtration performance. The filtration test results are given in Table A.1 (Appendix A).

The  $dt/dV$  vs.  $V$  plot for 4.5 in-Hg test (up-flow mode) is given in Figure 5.5 and  $dt/dV$  vs.  $V$  plot for 9 in-Hg test (up-flow mode) and down-flow modes are given in Appendix A (Figures A.3, A.4 and A.5).

As can be seen from the results presented in Table A.1 (Appendix A) and Figure 5.5, for the given particle size ranges, since the relative sizes of the particles used and the pores of the filter medium were not so distinct, a significant effect of different particle size distributions could not be observed. To better understand the effect of particle size distribution, slurries were formed with particle size fractions closer to the pore size of the filter medium.

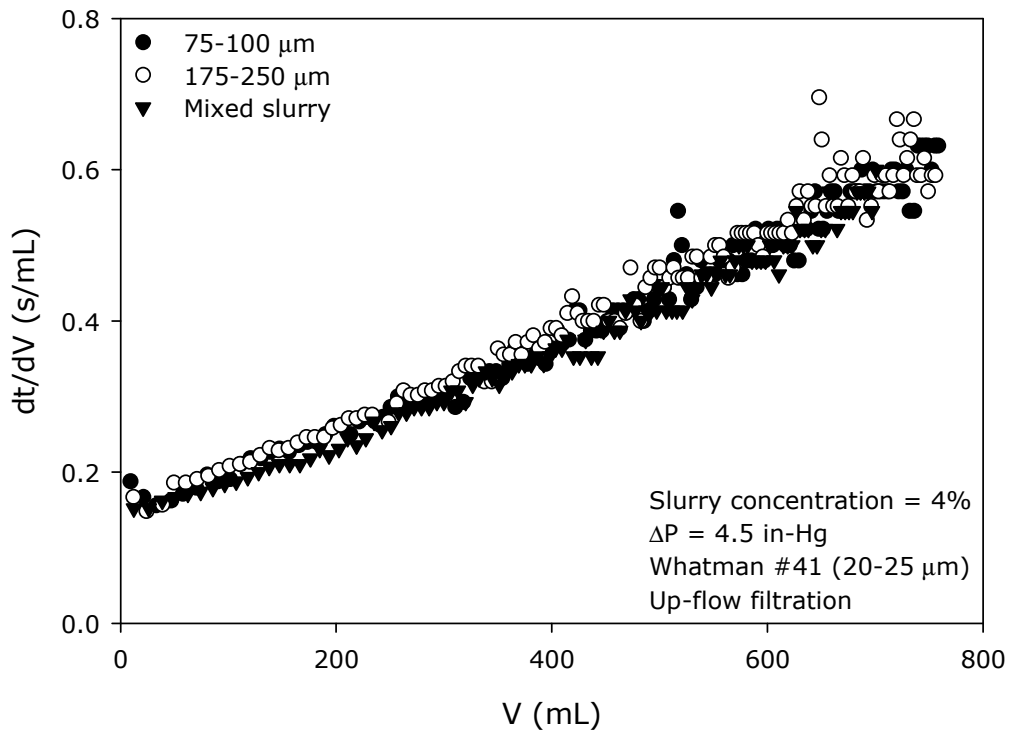


**Figure 5.5.**  $dt/dV$  vs.  $V$  plot- Effect of particle size distribution (I)

Slurries of particle size ranges of 53-75  $\mu\text{m}$  and 250-425  $\mu\text{m}$  were formed. The filtration test results are given in Table 5.3 and the  $dt/dV$  vs.  $V$  plot is given in Figure 5.6.

**Table 5.3.** Filtration test results-Effect of particle size distribution (II)

<b>Operational Conditions</b>	<b>Water + Meliodent</b>
Slurry concentration	2%
Pressure	5 in-Hg
Filter Paper	W#41 (20-25 $\mu\text{m}$ )
Mode of filtration	Up-flow
<b>Particle Size Distribution</b>	
53-75 $\mu\text{m}$	$\frac{dt}{dV} = 4.6 \times 10^{-4}V + 0.12$
250-425 $\mu\text{m}$	$\frac{dt}{dV} = 0.9 \times 10^{-4}V + 0.11$
Mixed	$\frac{dt}{dV} = 4.2 \times 10^{-4}V + 0.14$
	$V = 6.95t$
<b>Water filtration</b>	$\frac{t}{V} = 0.14$

As seen from Figure 5.6, the  $dt/dV$  vs.  $V$  trends of the mixed slurry and the fine slurry are nearly the same. This trend can be explained by the possible particle pile-up over the filter medium during filtration process. For the mixed slurry, the small size fraction is believed to be sucked out first and deposit over the filter medium which yields a similar trend as the fine slurry. Here, the wide range of particle sizes used makes the results clearer to assess the effect of particle size range on the filterability.

#### 5.3.4. Effect of slurry concentration

Another important factor to consider was the effect of slurry concentration on the overall filtration performance. The filtration results given in Table 5.4 are the average of at least three coincident filtration tests. The  $V$  vs.  $t$  plots are given in Appendix A (Figures A.6-A.13). The  $dt/dV$  vs.  $V$  plots are given in Figure 5.7 and Figure 5.8.

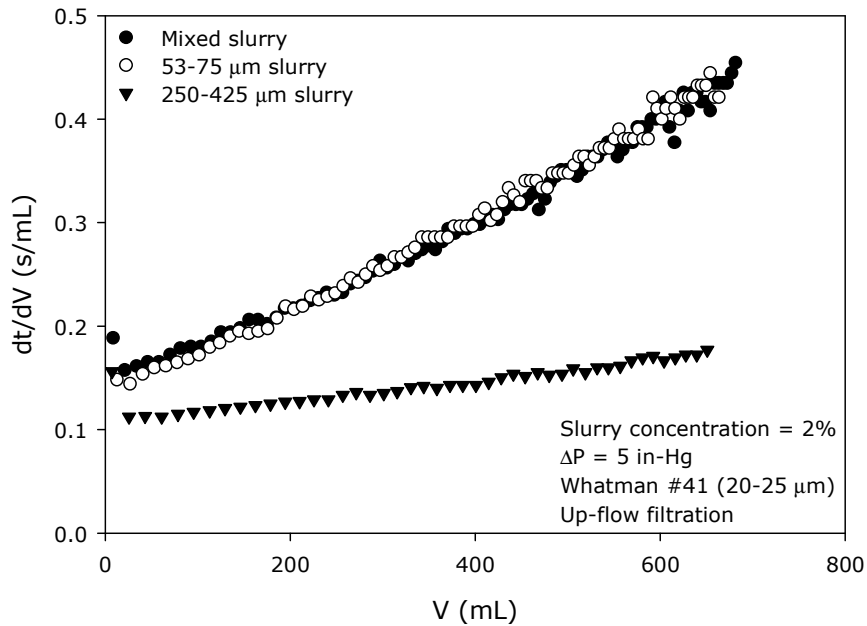


**Figure 5.6.** dt/dV vs. V plot- Effect of particle size distribution (II)

**Table 5.4.** Filtration test results-Effect of slurry concentration

<b>Operational conditions</b>	<b>Water+Meliodent</b>	<b>Water+Meliodent</b>
Particle Size Distribution	175-250 $\mu\text{m}$	175-250 $\mu\text{m}$
Pressure	4.5 in-Hg	9 in-Hg
Filter Paper	W#41 (20-25 $\mu\text{m}$ )	W#41 (20-25 $\mu\text{m}$ )
Mode of filtration	Up-flow	Up-flow
<b>Slurry concentration</b>		
4%	$\frac{dt}{dV} = 1.2 \times 10^{-3} V + 0.15$	$\frac{dt}{dV} = 1.1 \times 10^{-3} V + 0.12$
8%	$\frac{dt}{dV} = 1.6 \times 10^{-3} V + 0.21$	$\frac{dt}{dV} = 1.4 \times 10^{-3} V + 0.18$
12%	$\frac{dt}{dV} = 2.2 \times 10^{-3} V + 0.25$	$\frac{dt}{dV} = 1.6 \times 10^{-3} V + 0.15$
16%	$\frac{dt}{dV} = 4.7 \times 10^{-3} V + 0.46$	$\frac{dt}{dV} = 3.1 \times 10^{-3} V + 0.31$
	$V = 6.95t$	$V = 14.27t$
<b>Water filtration</b>	$\frac{t}{V} = 0.14$	$\frac{t}{V} = 0.07$

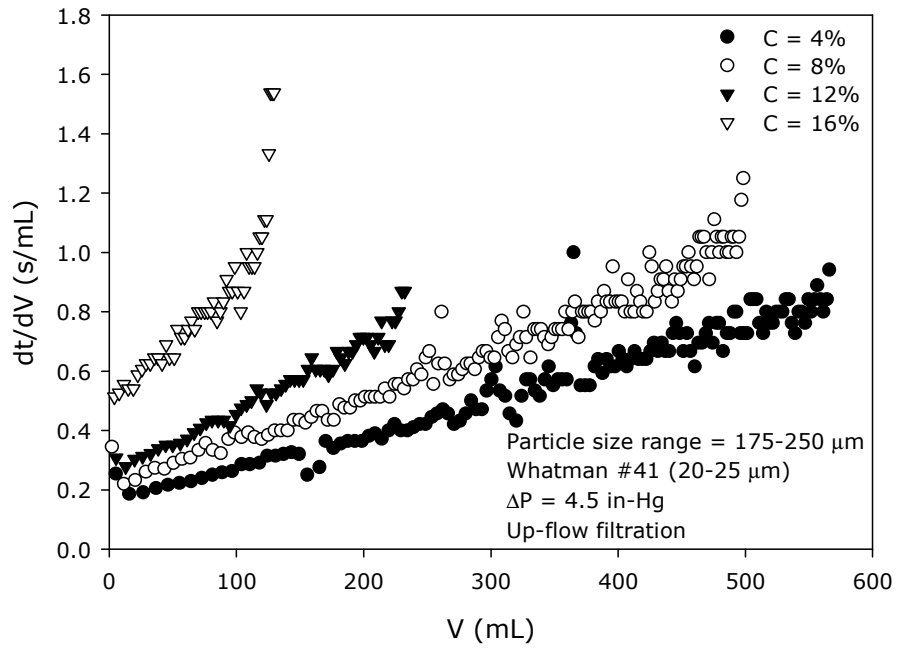


**Figure 5.7.** dt/dV vs. V plots for slurry conc. of 4, 8, 12 and 16% at 4.5 in-Hg

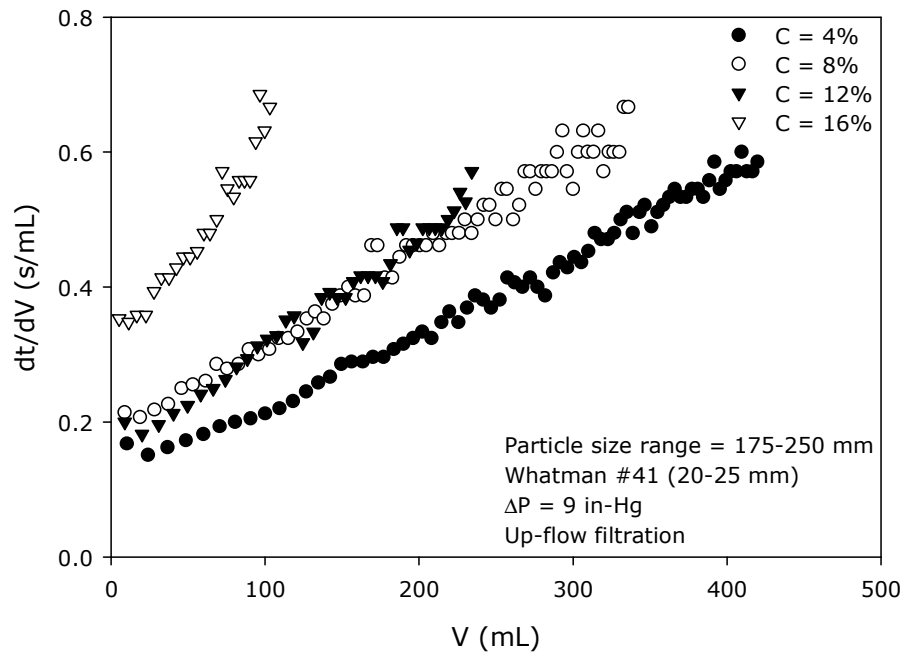


**Figure 5.8.** dt/dV vs. V plots for slurry conc. of 4, 8, 12 and 16% at 9 in-Hg

The results presented in Figure 5.7 and Figure 5.8 showed that the intercept of  $dt/dV$  vs.  $V$  plots is a function of the slurry concentration. The results showed that the intercept value, which is the inverse of initial passage rate, is not only affected by the filter medium but also by the slurry concentration.

Practically, at low slurry concentrations, the intercept value will be close to the inverse rate of passage of particle-free liquid. As the slurry concentration gets higher, it is expected to have larger intercept values (since passage rates will be smaller).

As seen in Table 5.4 and in Figures 5.7 and 5.8, as the slurry concentration increases, the intercept of  $dt/dV$  vs.  $V$  plots gets larger, as expected. The classical filtration theory assumes the intercept to be the filter medium resistance which is practically expected to be constant and depend only on the pore size of the filter medium. The results, contrary to the classical approach, show that the intercept value is also a function of the slurry concentration.

### 5.3.5. Effect of particle size and pore size of the filter medium

The filtration test results are given in Table 5.5. The volume-time plot for the steel mesh is provided in Figure A.14 and for Whatman #41 in Figure A.15 (Appendix A). The  $dt/dV$  vs.  $V$  plots are given in Figure 5.9.

**Table 5.5.** Filtration test results-Effect of particle-pore size interaction (I)

<b>Operational Conditions</b>	<b>Water + Meliodent</b>	<b>Water + Meliodent</b>
Particle size distribution	250-425 $\mu\text{m}$	250-425 $\mu\text{m}$
Slurry concentration	4%	4%
Filter paper	W#41 (20-25 $\mu\text{m}$ )	Steel mesh (200 $\mu\text{m}$ )
Mode of filtration	Up-flow	Up-flow
<b>Pressure (in-Hg)</b>		
5	$\frac{dt}{dV} = 4.5 \times 10^{-4}V + 0.14$	$\frac{dt}{dV} = 0.2 \times 10^{-4}V + 0.08$
	$V = 6.95t$	$V = 13.43t$
<b>Water filtration</b>	$\frac{t}{V} = 0.14$	$\frac{t}{V} = 0.075$

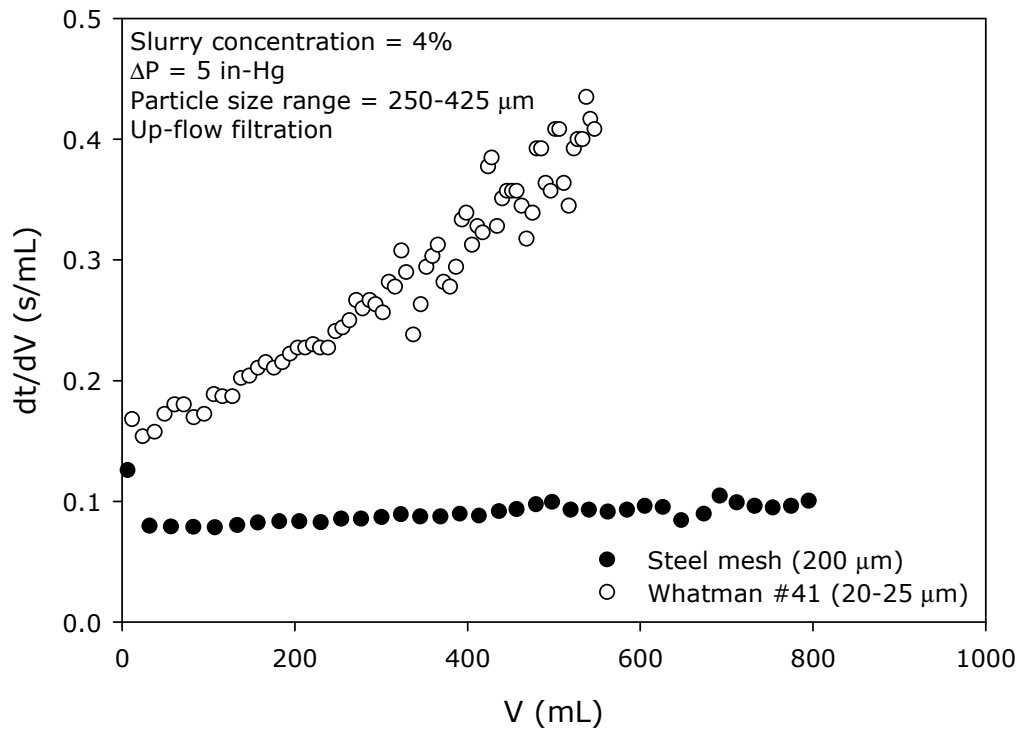


**Figure 5.9.** Effect of particle-pore size interaction (I)-5 in-Hg

The  $dt/dV$  vs.  $V$  results presented in Figure 5.9 showed a higher slope value, i.e. higher resistance to filtration, for the Whatman #41 filter paper. At first, as the particle size range of the slurry was closer to the coarser filter medium, a higher slope value was expected for the coarser medium due to possible initial pore blockage and coverage. However, the results revealed a different trend as shown in Figure 5.9. This result could be due to the wide range of particles within the slurry and the relative fraction of fine particles (around 250  $\mu\text{m}$ ) to the total particle size distribution of the slurry. The fine particles are closer to the pore size of the steel mesh (200  $\mu\text{m}$ ) and their fraction within the total particle size range will definitely affect the resistance developed at the cake-septum interface. In the above case, probably the fraction of particles around 250  $\mu\text{m}$  did not overwhelm and thus did not result in a significant cake-septum resistance as expected. Hence, it was decided to narrow the particle size range of the model slurry to better analyze the effect of particle size-pore size interactions. For this purpose, slurry with a particle size range of 53-75  $\mu\text{m}$  was formed. The filtration test results are given in Table 5.6.

**Table 5.6.** Filtration test results-Effect of particle-pore size interaction (II)

<b>Operational Conditions</b>	<b>Water + Meliodent</b>	<b>Water + Meliodent</b>
Particle size distribution	53-75 $\mu\text{m}$	53-75 $\mu\text{m}$
Slurry concentration	2%	2%
Filter paper	W#41 (20-25 $\mu\text{m}$ )	Nylon filter medium (41 $\mu\text{m}$ )
Mode of filtration	Up-flow	Up-flow
<b>Pressure (in-Hg)</b>		
5	$\frac{dt}{dV} = 4.5 \times 10^{-4} V + 0.13$	$\frac{dt}{dV} = 10.2 \times 10^{-4} V + 0.09$
	$V = 6.95t$	$V = 12.93t$
<b>Water filtration</b>	$\frac{t}{V} = 0.14$	$\frac{t}{V} = 0.077$

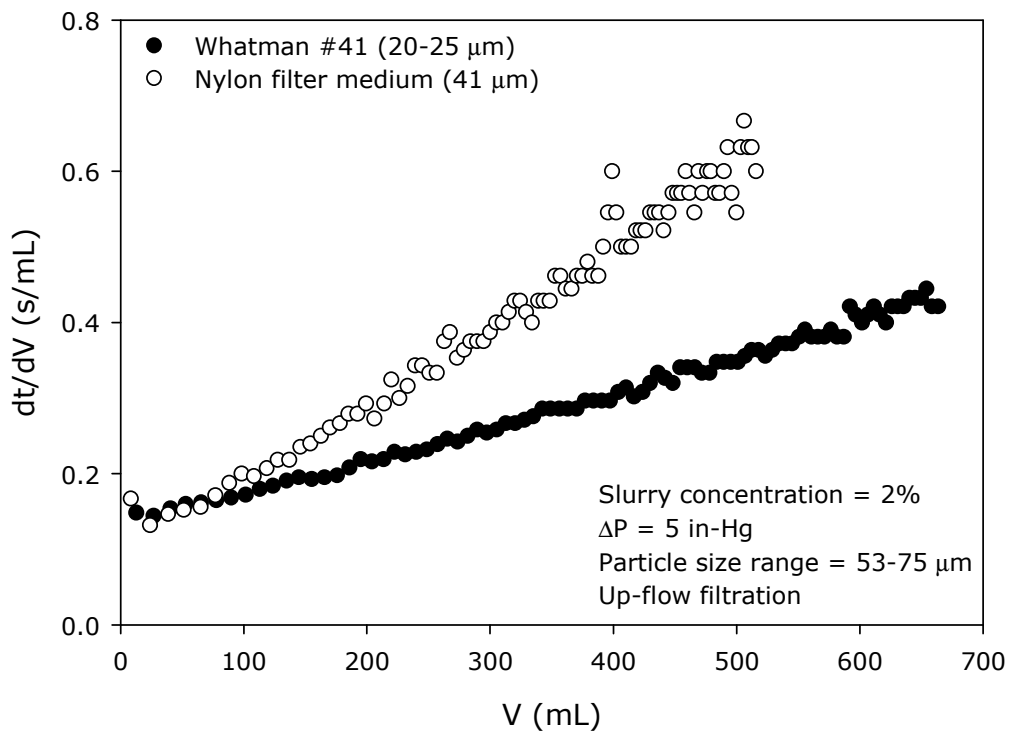


**Figure 5.10.** Effect of particle-pore size interaction (II)-5 in-Hg

As seen from Figure 5.10, as the particle sizes gets closer to the filter medium pore sizes, the slope of  $dt/dV$  vs.  $V$  plot increases which indicates an increasing resistance at the cake-septum interface. Thus, it is evident that particle size-pore size interaction determines the overall filtration rate.

To better understand the particle-pore interactions, slurry with particles of 200-210  $\mu\text{m}$  were formed. The results are given in Table 5.7. The  $V$  vs.  $t$  plots are provided in Appendix A (Figures A.16-A.27). The  $dt/dV$  vs.  $V$  plots for 4% slurry are given in Figures 5.11 and 5.12; and those for 8% slurry are given in Appendix A, Figures A.28 and A.29.

**Table 5.7.** Filtration test results-Effect of particle-pore size interaction (III)

Operational conditions	Water + Meliodent		Water + Meliodent		Water + Meliodent	
	W#41 (20-25 μm)		Nylon filter medium (41 μm)		Steel Mesh (200 μm)	
Filter paper	W#41 (20-25 μm)		Nylon filter medium (41 μm)		Steel Mesh (200 μm)	
Particle size distribution	200-210 μm	200-210 μm	200-210 μm	200-210 μm	200-210 μm	200-210 μm
Slurry concentration	4%	8%	4%	8%	4%	8%
Mode of filtration	Up-flow	Up-flow	Up-flow	Up-flow	Up-flow	Up-flow
<b>Pressure</b>						
5 in-Hg	$\frac{dt}{dV} = 6.48 \times 10^{-4}V + 0.17$	$\frac{dt}{dV} = 9.03 \times 10^{-4}V + 0.21$	$\frac{dt}{dV} = 4.36 \times 10^{-4}V + 0.10$	$\frac{dt}{dV} = 8.56 \times 10^{-4}V + 0.12$	$\frac{dt}{dV} = 4.34 \times 10^{-4}V + 0.11$	$\frac{dt}{dV} = 8.59 \times 10^{-4}V + 0.22$
10 in-Hg	$\frac{dt}{dV} = 2.77 \times 10^{-4}V + 0.09$	$\frac{dt}{dV} = 4.17 \times 10^{-4}V + 0.10$	$\frac{dt}{dV} = 2.40 \times 10^{-4}V + 0.06$	$\frac{dt}{dV} = 4.56 \times 10^{-4}V + 0.07$	$\frac{dt}{dV} = 1.64 \times 10^{-4}V + 0.08$	$\frac{dt}{dV} = 4.12 \times 10^{-4}V + 0.09$
<b>Water filtration</b>						
5 in-Hg	$V = 6.95t$	$\frac{t}{V} = 0.144$	$V = 12.93t$	$\frac{t}{V} = 0.077$	$V = 13.43t$	$\frac{t}{V} = 0.075$
10 in-Hg	$V = 14.27t$	$\frac{t}{V} = 0.07$	$V = 20.42t$	$\frac{t}{V} = 0.049$	$V = 20.73t$	$\frac{t}{V} = 0.048$

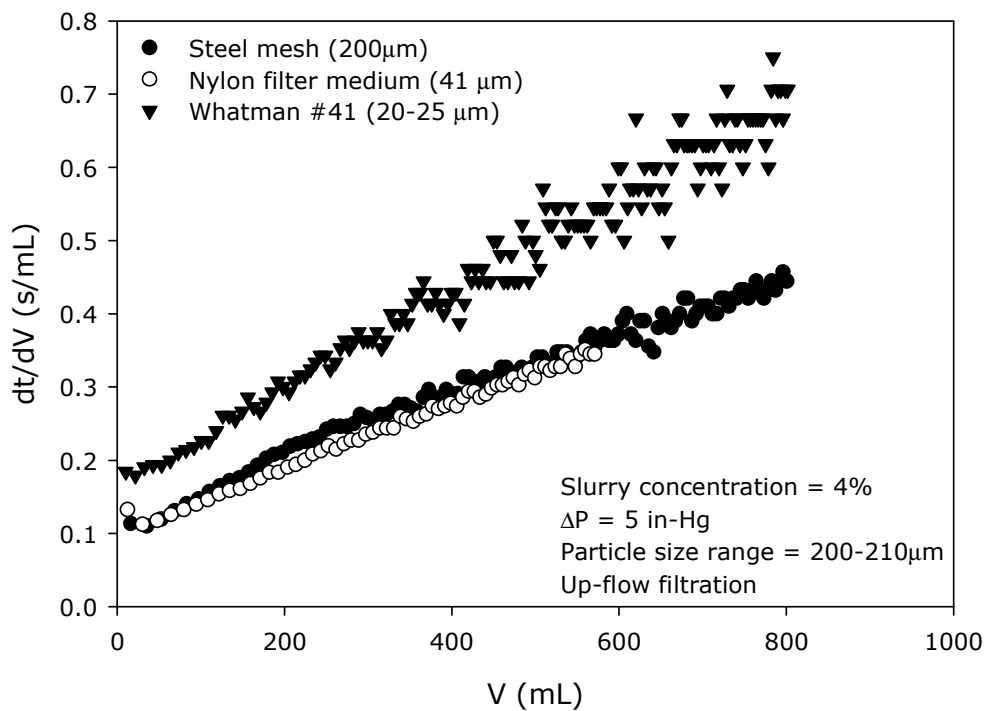


**Figure 5.11.** Effect of particle-pore size interaction (III)-5 in-Hg

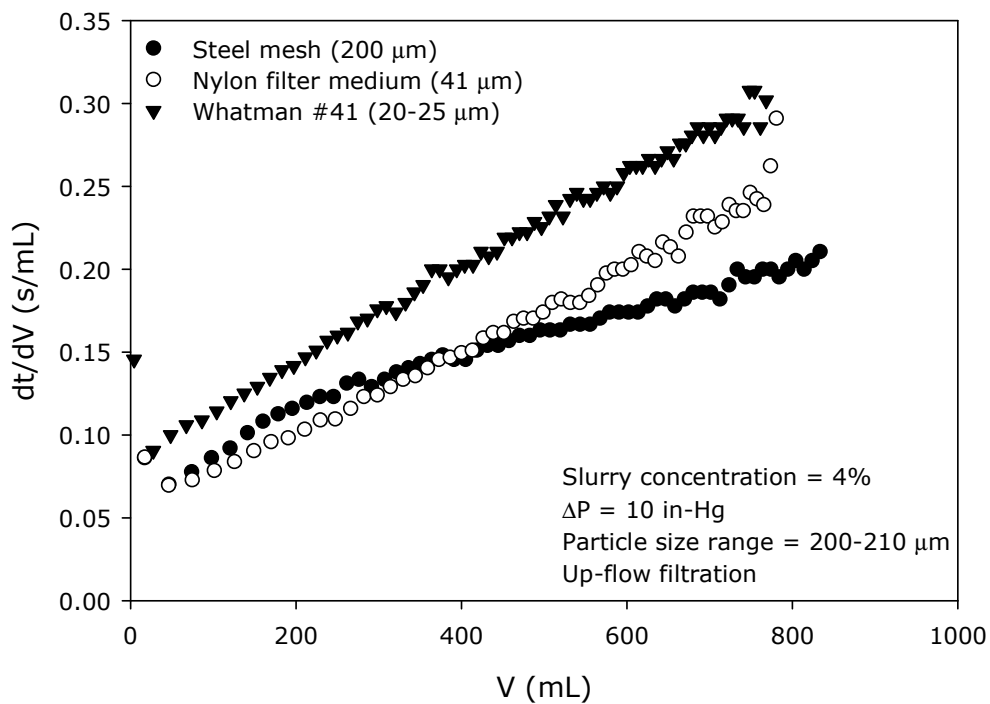


**Figure 5.12.** Effect of particle-pore size interaction (III)-10 in-Hg

Figures 5.11 and 5.12 yield an interesting result. Although the particles within the slurry are close in size to the pores of the steel mesh,  $dt/dV$  vs.  $V$  trends for both the steel mesh and the nylon filter medium were observed to be the same; and moreover, the data for both runs were coincident as shown in Figure 5.11. On the other hand, the results for Whatman #41 filter medium yielded the highest slope for  $dt/dV$  vs.  $V$  plots which indicates the highest resistance at the cake-septum interface. Thus, an initial blockage of the pores of the steel mesh by the Meliodent particles was not experienced as expected. A similar trend was also observed for filtration at 10 in-Hg with a deviation after a certain point for steel mesh and nylon filter medium as given in Figure 5.12.

These results highlight an important feature of the filtration process. The initial pore coverage, pore blockage and initial particle deposition over the filter medium greatly affects the overall process. The major rate determining part is the cake-septum interface. Moreover, it is very hard to predict the variations that will be encountered at this stage. Not only the particle size distribution of the slurry, but also the pore size of the filter medium plays an important role.

#### **5.4. Conclusions**

The filtration tests conducted with model slurries have revealed several important conclusions:

- The filterability of a specific slurry is a strong function of the filter medium used; moreover, the particle size distribution relative to the pore size of the filter medium is found to affect the overall filtration performance as predicted by the multiphase filtration theory.
- Up-flow and down-flow filtration tests revealed different filterability characteristics for the same sludge filtered under the same operational conditions. This outcome was attributed to the different particle deposition and pile up over the filter medium.
- The intercept value of  $dt/dV$  vs.  $V$  plots is defined as the reciprocal rate of the initial passage of slurry through the clean filter medium. The filtration test results showed that, the magnitude of the intercept is affected not

only by the pore size of the filter medium but also by the concentration of the slurry being filtered.

- The results obtained so far have shown that, filtration is a very complex phenomena even for the model slurries since it is very hard to predict the particle-pore interactions at the cake-septum interface which is the major rate determining part.
- The fact that the filterability of slurries is a strong function of the filter medium used makes the existence of a unique filterability parameter for a specific slurry prone to question.

## CHAPTER 6

### MATHEMATICAL ANALYSIS OF FILTRATION

#### 6.1. Objective

The aim of the last stage of studies is to come up with a correct mathematical analysis of the cake filtration process via the blocking laws approach and the multiphase filtration theory.

Up to now, the inadequacy of the Ruth's classical approach was highlighted with real sludge systems. Moreover, the effects of operational parameters on the filterability of sludge systems were explored by using Meliodent slurries.

#### 6.2. Theoretical Background

This section provides an in-depth analysis of the current mathematical approaches to the cake filtration problem.

##### 6.2.1. Cake Filtration and Dewatering

In cake filtration, the particles larger than the pores of the filter medium are retained at the surface of the medium, whereas, smaller particles enter the pores of the medium. These smaller particles may (1) block the pore opening of the medium completely, or (2) adhere to the walls of the pores thus progressively reducing the internal diameter of the pore, or (3) pass through the filter medium. As the filtration proceeds the particles retained on the filter medium will form a porous structure and the smaller particles which are able to pass through the pores initially will get trapped in this porous cake formed by the deposited particles. This is observed practically as the initial filtrate obtained with a new or washed filter medium is often found to be cloudy, but becomes clearer as time progresses (Gala and Chiang, 1980).

In the filtration operation, a cake containing filtrate trapped in the void spaces between the particles is obtained at the end of the operation. In many cases where the recovery of solids is desirable it is necessary that the liquid content of

the solids be as low as possible. In order to reduce the liquid content of the cake, the cake is subjected to dewatering (Gala and Chiang, 1980).

Cake dewatering is a process in which the filtrate within the voids of the filter cake is displaced by air in the presence of a pressure gradient across the filter cake or by mechanical squeezing. The two characteristics of cake dewatering are the permeability and the final moisture content (Chi *et al.*, 1985).

Filtration and dewatering are distinct in the sense that filtration leads to the formation of a cake containing a relatively low proportion of residual filtrate, while dewatering is used to affect further liquid content reduction of the cake itself. The fundamental principles underlying the two processes are entirely different.

Importance of the dewatering process can be realized in the applications where the final product is the solid particles which are generally required to be transported over long distances. Thus, it is necessary that they be as dry as possible.

### *6.2.2. Cake Filtration Literature*

Cake filtration, which is one the most frequently used separation techniques, is an example of a flow through porous media problem. As applicable to all fluid mechanics problems, equation of continuity and equation of motion are the basic equations describing the overall phenomena. In the filtration field, the most important problem is the lack of scientific basis and that the cake filtration problem has been treated heuristically by the researchers. The development of the constant pressure filtration equation is based solely on heuristic analogy with Ohm's Law and nowhere in the derivation of the equation was Darcy's Law used. Carman (1938) was the first to recognize that Darcy's Law is applicable to filtration and introduced Kozeny's expression for the SCR; so that, a relation between permeability and SCR was obtained.

Any theory without the support of experimental evidence is incomplete. Most of the data found in the filtration literature are obtained from an experimental device called compression-permeability (CP) cell which is first introduced by Ruth

(1946) "to narrow the gap between theory and practice". CP cell is a vertical cylinder with a movable piston through which a mechanical load is applied at the top of a confined bed of solids. The simulation of filtration by using this device is dependent on two assumptions. The first assumption states that if  $P_A$  is the applied pressure and  $P_L$  is the pore liquid pressure, then when this pressure difference is equal to the applied pressure in the CP cell, the porosity,  $\epsilon$ , and the specific resistance,  $\alpha$ , obtained from this device are equal to the porosity and specific resistance of the differential volume element within the filter cake. The difference between the applied pressure and the pore liquid pressure is called the compressive stress,  $P_s$ , and derived heuristically using a simple force balance, which involves the assumption of point contact between the particles. The second assumption states that the local porosity (or, solidosity) and the specific resistance values are uniquely expressed as functions of the compressive stress. However, it should be noted that the compressive stress is not a directly measured parameter in actual filtration or flow through porous media. It is an operational variable of the CP cell only.

For a constant pressure filtration, the filtrate time-discharge is usually a parabolic function of time. Deviations from the expected parabolic behavior are usually attributed to the variation of the average SCR during the course of filtration and modifications on Ruth's expression (1946) for SCR is proposed. Ruth's expression for evaluation of the SCR values obtained from the CP cell neglects the medium resistance. Tiller and Cooper (1960) introduced a new definition which is a function of time if the septum resistance is not negligible and proposed that the average SCR is not constant but that it decreases and squeezes liquid out of the cake causing the exit flow to exceed the entrance flow. Afterwards, Tiller and Huang (1961) introduced a correction factor,  $J_T$ , into the definition of the average cake resistance to account for internal flow rate variation. Later, Shirato *et al.* (1969) introduced another correction factor,  $J_S$ , into the definition of the average cake resistance to account for the relative velocity between the solid and liquid phases. Both  $J_T$  and  $J_S$  are evaluated from the CP data.

The use of CP cell has received so much attention that experimentalists overlooked the possibility of inaccurate representation of filtration by this test device. Willis (1959) was the first to question the reproducibility of the SCR

values obtained from the CP cell. His results indicate that the SCR values depend on how the cake is deposited in the CP cell and that CP resistances are inversely proportional to the length-to-diameter ratio of the deposited cake. However, at that time his results were ignored since they were not in agreement with the current acceptance of CP concept. Later, Lu *et al.* (1970) and Rawling *et al.* (1970) confirmed Willis' (1959) earlier finding that CP resistances are inversely proportional to the length-to-diameter ratio of the deposited cake in the CP cell. Shirato *et al.* (1968) showed that neglecting side-wall friction in CP cell leads to significant errors in estimating filtration characteristics and that CP porosities and resistances are not uniform as previously assumed. Afterwards, researchers have directed their effort in criticizing the validity and applicability of CP cell data in the simulation of filtration. Tiller *et al.* (1972) proposed a simplified wall friction theory for CP cells and itemize the variations in CP methodology that have a significant effect on CP results. Tiller and Green (1973) pointed out that it is virtually impossible to obtain accurate values of resistance and porosity from CP cells at low pressure, which further complicates the methodology of the CP cell. Despite these efforts, so far no corrections have been made on the previously published results because there is not sufficient data available to make the necessary corrections.

Besides the aforementioned experimental works, researchers have put efforts for a better description of the filtration theory. The constant pressure cake filtration is a moving boundary problem which constitutes the combination of the equations of continuity and motion together with the relevant boundary and initial conditions. This moving boundary problem can be treated via two different approaches to get a basic differential equation for cake filtration: Eulerian and Lagrangian. These different approaches have led to development of different filtration theories; however, the basic equations describing the overall phenomenon are the same for all modeling studies: equation of continuity for solid and liquid phases and the equation of motion for liquid (or the Darcy's Law) and solid phases.

Wakeman (1978) used the Eulerian approach and obtained a set of non-linear partial integro-differential equations. However, there is a flaw in his development of the boundary condition at the moving interface as indicated by Tosun (1986).

Smiles (1970) is the first to derive the filtration equation in the form of a diffusion equation using the Lagrangian approach. His formulation of cake filtration via the Lagrangian approach is referred to as the '*Diffusional Modeling*' in the filtration literature. However, his formulation has two drawbacks (Tosun, 1986): (i) as pointed out by Wakeman (1978), the development is conceptually difficult and ignores accepted filtration terminology; (ii) the boundary condition used at the cake-slurry interface indicated no liquid flux at this point. Afterwards, Atsumi and Akiyama (1975) also formulated cake filtration as a moving boundary problem using the Lagrangian approach and solved the resulting equation numerically.

The Eulerian and Lagrangian formulations of cake filtration are presented below.

#### *Eulerian Formulation*

For one dimensional cake filtration, the differentiation of the liquid-phase equation of motion (i.e. Darcy's law), Eq. 4.15, with respect to position, and substitution of equations of continuity for liquid (Eqn. 4.10) and solid phases (Eqn. 4.11) yield

$$\frac{\partial \varepsilon}{\partial t} - \frac{r}{1-\varepsilon} \frac{\partial \varepsilon}{\partial x} = (1-\varepsilon) \frac{\partial}{\partial x} \left( \frac{K}{\mu} \frac{\partial P}{\partial x} \right) \quad (6.1)$$

The identity

$$(1-\varepsilon) \frac{\partial}{\partial x} \left( \frac{K}{\mu} \frac{\partial P}{\partial x} \right) = \frac{\partial}{\partial x} \left[ (1-\varepsilon) \frac{K}{\mu} \frac{\partial P}{\partial x} \right] - \frac{K}{\mu} \frac{\partial P}{\partial x} \frac{\partial (1-\varepsilon)}{\partial x} \quad (6.2)$$

can be rewritten, with the aid of Eq. (4.15), in the form

$$(1-\varepsilon) \frac{\partial}{\partial x} \left( \frac{K}{\mu} \frac{\partial P}{\partial x} \right) = \frac{\partial}{\partial x} \left[ (1-\varepsilon) \frac{K}{\mu} \frac{\partial P}{\partial x} \right] + \left( q - \frac{\varepsilon}{1-\varepsilon} r \right) \frac{\partial \varepsilon}{\partial x} \quad (6.3)$$

so that Eq. (6.1) becomes

$$\frac{\partial \varepsilon}{\partial t} = \frac{\partial}{\partial x} \left[ (1-\varepsilon) \frac{K}{\mu} \frac{\partial P}{\partial x} \right] + \frac{1}{A} \frac{dV}{dt} \frac{\partial \varepsilon}{\partial x} \quad (6.4)$$

It is generally accepted that the porosity variation is due primarily to interfacial momentum transfer (i.e. drag) which depends on the fluid pressure gradient. Therefore, making use of the relationship

$$\left[ \frac{K}{\mu} \frac{dP}{d\varepsilon} \frac{\partial \varepsilon}{\partial x} \right]_{x=0} = \frac{1}{A} \frac{dV}{dt} \quad (6.5)$$

Eq. (6.4) takes the form

$$\frac{\partial \varepsilon}{\partial t} = \frac{\partial}{\partial x} \left( E \frac{\partial \varepsilon}{\partial x} \right) + \left[ \frac{E}{1-\varepsilon} \frac{\partial \varepsilon}{\partial x} \right]_{x=0} \frac{\partial \varepsilon}{\partial x} \quad (6.6)$$

where the compressibility coefficient,  $E$ , is given by

$$E = \frac{K(1-\varepsilon)}{\mu} \frac{dP}{d\varepsilon} \quad (6.7)$$

*Boundary condition at the moving interface*

When Eq. (6.6) is multiplied by  $dx$  and integrated from 0 to  $L(t)$ , the result is

$$\int_0^L \frac{\partial \varepsilon}{\partial t} dx = \left[ E \frac{\partial \varepsilon}{\partial x} \right]_{x=L} - \left[ E \frac{\partial \varepsilon}{\partial x} \right]_{x=0} + \left[ \frac{E}{1-\varepsilon} \frac{\partial \varepsilon}{\partial x} \right]_{x=0} (\varepsilon_L - \varepsilon_0) \quad (6.8)$$

Application of Leibnitz's rule to the left-hand side of Eq. (6.8) gives

$$\frac{d}{dt} \int_0^L \varepsilon dx - \varepsilon_L \frac{dL}{dt} = \left[ E \frac{\partial \varepsilon}{\partial x} \right]_{x=L} - (1-\varepsilon_L) \left[ \frac{E}{1-\varepsilon} \frac{\partial \varepsilon}{\partial x} \right]_{x=0} \quad (6.9)$$

The macroscopic mass balance

$$[\text{Mass of slurry filtered}] - [\text{Mass of filtrate}] = [\text{Mass of wet cake}]$$

can be written in symbolic form as

$$\frac{V}{A} = \frac{(1 - \langle \varepsilon \rangle)(1 - s)\rho_s - \rho_s \langle \varepsilon \rangle}{s\rho} L \quad (6.10)$$

where the average porosity,  $\langle \varepsilon \rangle$ , is defined by

$$\langle \varepsilon \rangle = \frac{1}{L} \int_0^L \varepsilon dx \quad (6.11)$$

The slurry porosity,  $\varepsilon_{sl}$ , is related to the mass fraction of solids in the slurry,  $s$ , by Eqn. 4.23.

Rearranging yields Eq. (6.5) as

$$\left[ \frac{E}{1 - \varepsilon} \frac{\partial \varepsilon}{\partial x} \right]_{x=0} = \frac{\varepsilon_{sl} - \langle \varepsilon \rangle}{1 - \varepsilon_{sl}} \frac{dL}{dt} \quad (6.12)$$

Substitution of Eqs. (6.11) and (6.12) into Eq. (6.9) yields

$$E \frac{\partial \varepsilon}{\partial x} = \frac{\varepsilon_{sl} - \varepsilon_L}{1 - \varepsilon_{sl}} (1 - \langle \varepsilon \rangle) \frac{dL}{dt} \quad \text{at } x = L(t) \quad (6.13)$$

which is the boundary condition at the moving interface. With the help of Eq. (6.7), Eq. (6.13) takes the form

$$\frac{\partial \varepsilon}{\partial x} = \frac{1 - \langle \varepsilon \rangle}{1 - \varepsilon_L} \frac{\varepsilon_{sl} - \varepsilon_L}{1 - \varepsilon_{sl}} \frac{\mu}{K} \frac{d\varepsilon}{dP} \frac{dL}{dt} \quad \text{at } x = L(t) \quad (6.14)$$

Wakeman (1978), using a different approach, derived the boundary condition as

$$\frac{\partial \varepsilon}{\partial x} = \frac{\varepsilon_{sl} - \varepsilon_L}{1 - \varepsilon_{sl}} \frac{\mu}{K} \frac{d\varepsilon}{dP} \frac{dL}{dt} \text{ at } x = L(t) \quad (6.15)$$

Comparison of Eq. (6.14) with Eq. (6.15) indicates a flaw in Wakeman's development of the boundary condition. The correct form of the boundary condition, Eq. (6.14), reduces to Eq. (6.15) if  $\langle \varepsilon \rangle = \varepsilon_L$ , which can only be true for a uniform porosity distribution throughout the filter cake.

### *Lagrangian Formulation*

First, a new dependent variable  $e$ , void ratio, is introduced which is defined by

$$e = \frac{\varepsilon}{1 - \varepsilon} \quad (6.16)$$

so that Eqs. (6.6) and (6.13) take the form

$$\frac{\partial e}{\partial t} = (1 + e)^2 \frac{\partial}{\partial x} \left( C \frac{\partial e}{\partial x} \right) + \left[ C(1 + e) \frac{\partial e}{\partial x} \right]_{x=0} \frac{\partial e}{\partial x} \quad (6.17)$$

and

$$C \frac{\partial e}{\partial x} = (1 - \langle \varepsilon \rangle) \left( \frac{e_{sl} - e_L}{1 + e_L} \right) \frac{dL}{dt} \text{ at } x = L(t) \quad (6.18)$$

where

$$C = \frac{E}{(1 + e)^2} \quad (6.19)$$

The material coordinate  $m$  is related to  $x$  by the relation

$$m(x,t) = \int_0^x (1 - \varepsilon) dx \quad (6.20)$$

By using the chain rule, it can be shown that

$$\frac{\partial e}{\partial x} = \frac{1}{1+e} \frac{\partial e}{\partial m} \quad (6.21)$$

and

$$\left( \frac{\partial e}{\partial t} \right)_x = \left( \frac{\partial e}{\partial t} \right)_m + r \frac{\partial e}{\partial m} \quad (6.22)$$

Substitution of Eqs. (6.21) and (6.22) into Eqs. (6.17) and (6.18) results in

$$\frac{\partial e}{\partial t} = \frac{\partial}{\partial m} \left( C \frac{\partial e}{\partial m} \right) \quad (6.23)$$

and

$$C \frac{\partial e}{\partial m} = (e_{sl} - e_L) \frac{dm_L}{dt} \text{ at } m = m_L \quad (6.24)$$

The initial and boundary conditions, besides Eq. (6.24), are

$$e = e_{sl} \quad \text{at} \quad t = 0, \quad \text{for all } m \quad (6.25)$$

$$e = e_o \quad \text{at} \quad m = 0, \quad t > 0 \quad (6.26)$$

$$e = e_L \quad \text{at} \quad m = m_L, \quad t > 0 \quad (6.27)$$

Smiles (1970) used the Lagrangian approach and come up with a general flow equation in the form of a diffusion equation, Eq. (6.23). Instead of using the term  $C$ , they have named it as  $D_m$ , the diffusivity, which is defined by

$$D_m = \frac{K_h}{(1+e)} \frac{d\psi}{de} = K_m \frac{d\psi}{de} \quad (6.28)$$

where  $K_h$  is the hydraulic conductivity (m/s) and  $\psi$  is the liquid potential component of the total potential (m).

Smiles (1970) set the void ratio of the feed as equal to that at the cake surface, which signifies no liquid flux at the cake surface. This indicates the limited applicability of Smiles' work to real systems. Thus, the solution given by Smiles is applicable only to a limited case and may be considered as a limiting case of cake filtration (Atsumi and Akiyama, 1975).

Atsumi and Akiyama (1975) formulated the cake filtration as a Stefan problem. They have introduced a similarity variable to transform the governing equation into an ordinary one, which in turn is solved numerically via fourth-order Runge-Kutta method. Wakeman (1978) also used the same mathematical approach.

Multi-phase theory is an approximation to modeling transport processes in multi-phase systems such as in a porous medium. The volume-averaged multiphase equations of change provide a fundamental basis for the analysis of porous media flow systems. The volume averaging technique smooths functional discontinuities between phases by appropriately defined averages and generates a continuum at the scale of local measurements in multiphase systems. Considering filtration problem as composed of solid particulate phase and continuous liquid phase; then there are two continuity conditions and two motion equations. Darcy's Law can be obtained from the liquid phase equation of motion by making appropriate assumptions.

Later, Lu and Hwang (1993) develop the particle dynamics approach for modeling cake filtration. They adopt the concept of critical friction angle between spherical particles to simulate the structure of the deposited filter cake. They

predict the profiles of local cake properties, such as porosity, specific filtration resistance, and hydraulic pressure from a set of simple filtration data by considering the compression effect caused by the liquid drag. A force analysis considering drag forces, gravity force and interparticle forces (such as Van der Waals' force, electrostatic force) of particles is carried from the cake surface toward the filter septum. By taking a force balance for a depositing particle, the value of the critical friction angle is determined, and the structure of cake is simulated numerically. A numerical program is also designed to evaluate the growth of cake, hydraulic pressure distribution, local cake porosity, and local specific filtration resistance from the experimental data of filtration rate versus time.

A brief comparison of filtration theories is given in Table 6.1.

**Table 6.1.** Comparison of filtration theories (Lee and Wang, 2000)

<b>Theory</b>	<b>Classical</b>	<b>Diffusional</b>	<b>Multi-phase</b>	<b>Particle-dynamics</b>
Gravity/inertial effects	Neglected	Neglected	Neglected	Considered
Steady-state/transient	Steady-state	Transient	Steady-state	Transient
Particle interactions	Point-contact	Not specified	Not specified	Point-contact
Mass equations	$\left(\frac{\partial q_L}{\partial x}\right)_t = \left(\frac{\partial \varepsilon_L}{\partial x}\right)_t \left(\frac{\partial q_s}{\partial x}\right)_t = \left(\frac{\partial \varepsilon_s}{\partial x}\right)_t$	$\left(\frac{\partial q_L}{\partial x}\right)_t = \left(\frac{\partial \varepsilon_L}{\partial x}\right)_t$	$\left(\frac{\partial q_L}{\partial x}\right)_t = \left(\frac{\partial \varepsilon_L}{\partial x}\right)_t \left(\frac{\partial q_s}{\partial x}\right)_t = \left(\frac{\partial \varepsilon_s}{\partial x}\right)_t$	Conservation of particle number
Momentum equations	$\frac{dP_L}{dx} = \frac{dP_s}{dx} = \frac{\mu \varepsilon_L}{k(u_L - u_s)}$	$\frac{dP_L}{dx} = \frac{\mu \varepsilon_L}{k(u_L - u_s)}$	$\nabla(P_L/\varepsilon_L) = -\varepsilon_L \mu_L / K^{TP} (\vec{u}_L - \vec{u}_s)$	Newton's 2nd law of motion for particles; contact-angle assumption
Constitutive equations	Power-law and derivatives	No; experimentally measured	No; experimentally measured	Power-law and Kozeny equation
Boundary conditions (x = 0)	Ps = ΔPc (filtration); dPs/dx = 0 (consolidation)	Ps = ΔPc (filtration)	None for particle location; Ps = ΔPc (filtration)	
Boundary conditions (x = L)	Ps = 0	Ps = 0	Ps = 0	None for particle location; Ps = 0
Initial conditions	None	$\varepsilon = \phi_o$	None	No particles exist

### 6.2.3. Modeling Approach

#### *Classical Filtration Theory*

The derivation of the classical filtration theory developed by Ruth (Ruth *et al.*, 1933; Ruth, 1935) is presented in Section 4.2.2. Mathematically, it is expressed as

$$\frac{dt}{dV} = \left( \frac{\mu \langle \alpha \rangle c}{A^2 \Delta P_T} \right) V + \frac{\mu R_m}{A \Delta P_T} \quad (6.29)$$

For a constant pressure filtration, i.e.,  $\Delta P_T = \text{constant}$ , it is customary to integrate Eq. (6.29) by assuming  $c$ ,  $\langle \alpha \rangle$  and  $R_m$  constant. The result is

$$\frac{t}{V} = \left[ \frac{\mu \langle \alpha \rangle c}{2A^2 \Delta P_T} \right] V + \frac{\mu R_m}{A \Delta P_T} \quad (6.30)$$

Classical theory assumes a straight line fit with a positive slope for the plot of  $t/V$  versus  $V$ .

The analysis of filtration process by the use of Eqn. (6.30) requires a continuous supply of slurry with constant solids concentration. On the other hand, once the slurry is poured into the BF, most of the solids settle down and form a filter cake as a result of both applied vacuum and sedimentation.

The constant pressure filtration equation, Eqn. (6.30), is used as the basic equation for cake filtration of incompressible cakes. For compressible cakes, the assumption of constant SCR is not valid and researchers have suggested an empirical relation taking into account the pressure gradient across the cake and the compressibility coefficient of the cake. At this point, the terminology used as “compressible cake” is generally misunderstood; and cake compressibility and particle compressibility is confused.

The Filtration Dictionary (1975) defines incompressible and compressible filter cake as follows:

“The forces acting on particles within a filter cake vary throughout the depth or thickness of the cake. When a fluid flows through a filter cake there is a pressure drop through the depth or thickness of the cake; a particle in the peripheral or uppermost layer of the cake will be subject to a force which is proportional to the pressure differential causing fluid to flow around and/or through the particles. This force will in turn be transmitted to the adjacent particles in the direction of flow; but in addition, these adjacent particles will also be influenced by the force due to the liquid pressure differential around each particle; these total forces will then be transmitted to the next adjacent particles in the direction of flow; hence the forces exerted on the particles in the cake will increase through the depth or thickness of the cake.

If the cake is incompressible these forces will not alter the structure of the cake and the pressure gradient will be uniform through the cake.

If the particles are compressible and become deformed under the influence of these forces, the particles at the surface or in the uppermost layer of the cake will be subject to the least deformation and the degree of deformation will increase through the depth or thickness of the cake; the pressure gradient will not be linear, such deformation will reduce the porosity of the cake and increase the specific resistance.”

The pore liquid pressure distribution is linear (or, pressure gradient is uniform) only for flow through a packed bed with uniform porosity distribution. Therefore, according to the definition given in the literature, an incompressible cake is one in which porosity is independent of position and time. On the other hand, a compressible cake is one in which porosity is both dependent on position and time (Tosun, 2005).

In the literature, however, the compressibility of the cake or solid matrix is often confused with the compressibility of the solid particles. For example, the definition given by the Filtration Dictionary implies that compressible cakes are only formed by deformable particles. In fact, non-deformable particles can form either a compressible cake if fine particles migrate into the interstices between larger particles, or an incompressible cake if they are all the same size and do not move. Therefore, the porosity change, which is the key factor to the

definition of compressible and incompressible cakes, is not only dependent on the elastic behavior of the particle itself but also on the particle size distribution (Tosun, 2005).

Thus, slurry of biosolids which is composed of compressible particles will certainly produce a compressible cake; but, slurry composed of incompressible particles may also produce a compressible cake depending on the particle size distribution within the slurry.

The classical filtration theory for most of the time underestimates the actual phenomena due to its underlying assumptions as negligible solid particle velocity, existence of only point contacts between particles and major resistance to flow being the cake itself. The drawbacks of the classical filtration theory are discussed in details in Chapter 4.

In the literature, alternatives to classical filtration theory are proposed as given in Table 6.1. Among these, the multiphase filtration theory is the one that focuses on the importance of the particle size distribution and type of filter medium used in determining the overall filtration rate. Thus, it is the one among the proposed theories that best explains the actual phenomenon.

#### *Multiphase Filtration Theory*

The derivation of the multiphase filtration theory is given in Section 4.2.4. Mathematically, it is expressed as.

$$\frac{dt}{dV} = \frac{1}{K_o J_o} \left( \frac{G}{A^2 \Delta P_c} \right) V \quad (6.31)$$

Therefore, when  $dt/dV$  is plotted versus  $V$ , the slope of the straight line is proportional to  $K_o J_o$ . The intercept, simply indicates the initial reciprocal rate through a clean filter medium.

### *Current Practical Approach*

Currently, for filtration and dewatering of solid/liquid suspensions, with all of its erroneous results and questionable assumptions, Ruth's classical approach is still being used. Although the drawbacks of the Ruth's classical approach are well-known and well-accepted, since there is no alternative parameter to characterize the filterability in practical usage, the filter designs and operational conditions are estimated on the basis of this classical approach at the industrial scale. The users of this classical two-resistance approach should be very careful in analyzing the results since it only gives comparative and qualitative information about the filterability of slurries.

In the analysis of filtration process, it is important to note that the process is dynamic and the phenomena at short filtration times and that at long filtration times is different. Thus, it is important to differentiate between the regions of different characteristics in terms of particle-pore interactions. Studies considering this major fact date back to 1930's. This approach, namely blocking filtration laws, is used in the membrane filtration literature for fouling analysis.

### *Blocking Filtration Laws*

As early as 1936, Hermans and Bredée, studied the principles of the mathematical treatment of constant pressure dead end filtration realizing the fact that cake filtration is not the only type of filtration encountered at industrial scale. It is interesting to note that, this approach takes into account the particle size distribution of slurry and also its relation to filter pore size which is not considered in Ruth's approach. Later in 1982, based on this study, Hermia published the derivation of the four blocking filtration laws. These laws are derived assuming homogeneous feed, spherical particles, cylindrical parallel homogeneous pores and grouped as:

1. *Complete Blocking*: every single particle blocks a single pore without superimposition,  $d_{\text{particle}} \cong d_{\text{pore}}$
2. *Intermediate Blocking*: every single particle blocks a single pore, or deposits on the filter surface (superimposition is possible),  $d_{\text{particle}} \cong d_{\text{pore}}$
3. *Standard Blocking*: particles deposit on the internal pore walls decreasing the pore diameter,  $d_{\text{particle}} \ll d_{\text{pore}}$

4. *Cake Filtration*: particles larger than the membrane pores deposit onto the membrane surface,  $d_{\text{particle}} > d_{\text{pore}}$

Mathematically, the characteristic form of the filtration laws derived by Hermia (1982) is expressed as:

$$\frac{d^2t}{dV^2} = k \left( \frac{dt}{dV} \right)^n \quad (6.32)$$

The exponent  $n$  is the filtration number and characterizes the filtration fouling mechanism. Table 6.2 summarizes the four filtration laws and Figure 6.1 gives the physical interpretation of the four laws.

**Table 6.2.** Blocking filtration laws (Austin *et al.*, 2001)

Law	n	Equation
Complete Blocking	2	$V = \frac{F_o}{K_{CB}} (1 - e^{-K_{CB}t})$
Standard Blocking	3/2	$\frac{t}{V} = \frac{1}{F_o} + \frac{K_{SB}}{F_o} t$
Intermediate Blocking	1	$V = \frac{F_o}{K_{IB}} \ln(1 + K_{IB}t)$
Cake Filtration	0	$\frac{t}{V} = \frac{K_{CF}}{4F_o^2} V + \frac{1}{F_o}$

In the literature, this approach is extensively used for fouling analysis during membrane filtration of a wide variety of suspensions. Some examples of studies using Hermia's approach can be listed as: Bowen *et al.* (1995) and Iritani *et al.* (1995) with protein suspensions; Roorda (2004) with wastewater treatment plant effluents, Mohammadi *et al.* (2003) with oil in water emulsions, Yuan *et al.* (2002) with humic acid, Konieczny and Rafa (2000) and Costa *et al.* (2006) with natural organic matter. But, none of the investigators used this approach to describe cake filtration or for concentrated suspensions.

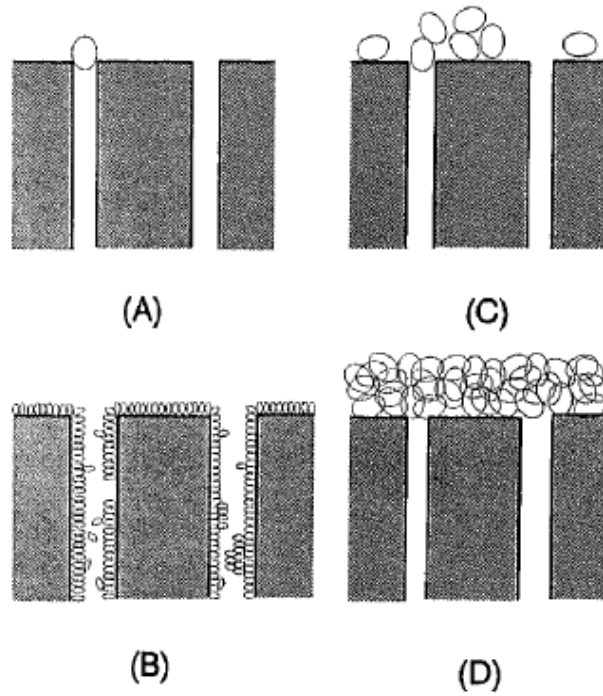


**Figure 6.1.** Physical interpretation of blocking laws: (A) Complete blocking, (B) Standard blocking, (C) Intermediate blocking, (D) Cake filtration (Bowen *et al.*, 1995).

In this method, first the gathered filtration data is analyzed in terms of Eq. (6.32). The experimental data of filtrate flux versus time is analyzed to generate plots as suggested by Eq. (6.32). The derivatives are evaluated as:

$$\frac{dt}{dV} = \frac{1}{JA} \quad (6.33)$$

$$\frac{d^2t}{dV^2} = -\frac{1}{J^3 A^2} \frac{dJ}{dt} \quad (6.34)$$

The  $dJ/dt$  value in Eq. (6.34) is generally evaluated by differentiating the adjusted polynomial that best fitted the experimental data of filtrate flux versus time.

The plot of Eq. (6.32) on a log-scale gives the flux decline analysis for the slurry being filtered. The relationship for low values of  $dt/dV$ , which correspond to short filtration times and for high values of  $dt/dV$  corresponding to long filtration times, reveals the dominant fouling mechanism. It is important to note that change of dominant mechanism during the filtration process emphasizes that the overall process is dynamic and it is incorrect to represent the whole phenomena with a single equation. In developing a filtration model, one of the most important issues is to recognize that the process is performed in stages, which do not necessarily involve the same fundamental principles (Bürger *et al.*, 2001).

When Eq. (6.32) is plotted, the transition of the dominant fouling mechanism is generally observed with a peak in the curve. Normally, the value of  $n$  is defined to be 0 for cake filtration, however, negative values for  $n$  is also encountered beyond the cake filtration phase which cannot be explained by any of the current blocking filtration laws described above.

The negative  $n$ -parameter is found by many membrane researchers (Bowen *et al.*, 1995; Roorda, 2004; Costa *et al.*, 2006; Ho and Zydney, 2000), however, a clear identification for this phase has not been made yet. What is important to note is that this negative “ $n$ ” region is a physical fact that is encountered during certain filtration operations. Physically, for a constant pressure and constant area filtration,  $dt/dV$  is proportional to the “total resistance to flow” and thus,  $d^2t/dV^2$  is proportional to the “change in the total resistance to flow”. At the beginning of filtration, upon deposition of particles above the filter medium, change in the resistance increases continuously up to a certain point which is the climax observed in  $d^2t/dV^2$  vs.  $dt/dV$  plots. For this phase,  $n$  values are positive and greater than zero. The magnitude of the  $n$ -value at this blocking stage is affected by the particle size-filter medium pore size interactions. At the climax,  $n = 0$ , meaning that the change in the resistance is constant, i.e.  $d^2t/dV^2 = \text{constant}$ , and also at its maximum value. In continuous operations where the slurry is continuously fed to the system which results in an increase in the total resistance to flow; as a result of particle deposition, a considerable cake is built up upon reaching the climax. Afterwards, a shift in the mechanism towards a negative  $n$ -parameter is physically a case where there is an already formed cake layer and particle deposition above this layer is still continuing. At this stage, cake filtration mechanism is still ongoing and probably coupled with a

compression phase either due to particle compressibility or cake compressibility as a result of migration of incompressible particles within the cake.

This negative  $n$ -parameter can physically be explained as a condition at which upon arrival of particles to the already deposited layers (deposition of particles means increasing  $dt/dV$ ) the change in resistance ( $d^2t/dV^2$ ) is decreasing. For the experimental studies where a considerable cake is being built up, this period theoretically should correspond to both the cake filtration and the cake compression phases. However, one should note that, compressibility of the cake does not require particles to be compressible. Particles may be incompressible; however, their dislodging within the cake matrix may result in the change of the porosity of the cake. Hence, incompressible particles may result in a compressible cake. Moreover, practically, for the characterization of sludge filterability, the effect of both cake filtration and cake compression phases are of interest.

On the other hand, after the filtration process is ceased, if one is to pass particle-free liquid through the formed cake structure, then it is obvious that a zero  $d^2t/dV^2$  will be achieved. This point was also highlighted by Bowen *et al.* (1995) that at a finite  $dt/dV$  a linear dependence of  $V$  on time should occur, equivalently a plateau in flow curves, resulting in a zero  $d^2t/dV^2$ .

Researchers have carried out experimental studies for the determination of the filtration mechanisms involved and assess the dominant mechanism by analyzing the correlation coefficients for the fitted equations at different values of  $n$  (Table 6.2). The relation yielding the maximum correlation is believed to be the dominant filtration mechanism. However, this is not the case all the time, in some circumstances the correlation coefficients are found to be so close to each other which makes it hard to make a clear differentiation. In this case, it is believed that the filtration is carried out by the mixed effect of the mechanisms involved. This point also highlights how complicated is the overall phenomena during filtration. Thus, it will be erroneous to represent the whole process by a single equation since it is dynamic and the conditions are subject to change in time.

In filtration of concentrated slurries, the dominant mechanism is generally cake filtration; this feature is especially more emphasized at long filtration times.

However, at short filtration times, the cake-septum interface plays an important role in the determination of the overall filtration resistance. The cake-septum interface plays an important role which is influenced both by the particle size distribution within the slurry and the pore size of the filter medium. It is suspicious to call the initial phase of filtration as "cake filtration" since there exists no cake at short filtration times. Cake formation is a time dependent phenomena, thus, it is for sure that after a certain point the cake filtration mechanism will dominate. The major mechanism responsible for the initial flux decline is dependent not only on the particles comprising the cake but also on the filter medium and its pore size. However, this point is ignored in the derivation of the constant pressure filtration equation developed by Ruth and data regarding sludge filtration is treated by this classical approach so far.

It should be noted that the users of the blocking filtration laws do consider concentrated slurries and slurries of particles larger than the pore sizes of the filter medium directly as "cake filtration" and assume no other dominant mechanism to prevail at short filtration times. Contrary to this general trend, Bowen *et al.* (1995) explained the consecutive steps in the whole process of filter medium blocking in terms of the successive or simultaneous presence of the following stages:

- (i) The smallest pores are blocked by all particles arriving to the filter medium.
- (ii) The inner surfaces of bigger pores are covered.
- (iii) Some particles arriving to the filter medium cover other pre-arrived particles while others directly block some of the pores.
- (iv) Finally a cake starts to be built.

In practice, the four phases are superimposed. If there is only a single pore size and the pore is greater than the molecule to be deposited, blocking should start with a standard process followed by a complete blocking, an intermediate and a cake filtration. While, if the molecule is much greater than the pore, it should start with a complete blocking followed by an intermediate and a cake filtration process. Figure 6.2 and 6.3 are some examples of  $d^2t/dV^2$  vs.  $dt/dV$  plots from the literature.

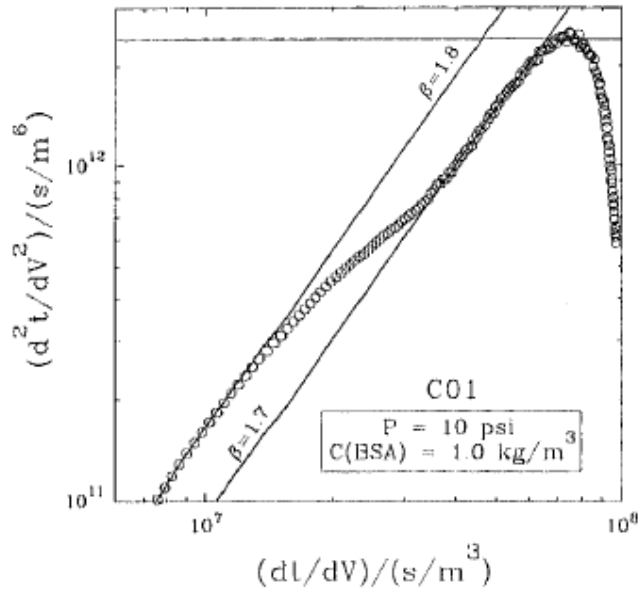


**Figure 6.2.**  $d^2t/dV^2$  vs.  $dt/dV$  for Bovine Serum Albumin (BSA) solutions (Bowen *et al.*, 1995)

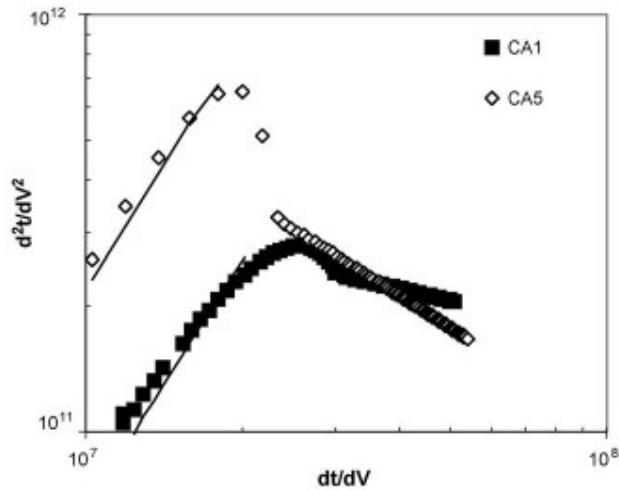


**Figure 6.3.**  $d^2t/dV^2$  vs.  $dt/dV$  for natural organic matter (NOM) (Costa *et al.*, 2006)

The major drawback of the blocking filtration law analysis is the determination of the flux-time relationships from the experimental volume-time data. The data should be carefully interpreted as flux versus time fitting requires extra care and

will greatly affect the  $d^2t/dV^2$  trend. Researchers use different best fits of flux versus time data such as polynomial fits (Bowen *et al.*, 1995; Costa *et al.*, 2006) and cubic spline fits (Yuan *et al.*, 2002). Some others use numerical differentiation methods to evaluate  $dJ/dt$  such as 5-points forward difference derivative formula (Orsello *et al.*, 2006).

The goodness of fit for the resulting functional relationship should be examined carefully before selecting the appropriate fit as it will directly affect the magnitude of the filtration number " $n$ ". Bowen *et al.* (1995) also highlighted that smoothing of the experimental data strongly affects the accuracy of the numerical derivations.

#### *6.2.4. Expression and Characterization of Filtration by Multiphase Modeling*

The successful mathematical treatment of filtration lies beneath the correct assessment of the physical reality of the overall phenomena. The filtration tests conducted with Meliodent slurries have revealed the importance of both the particle size distribution of the slurries and the pore size of the filter medium. Moreover, the complexity of understanding and expressing the initial stages of filtration were also highlighted. At short filtration times, when the filter medium pores are clean, upon arrival of particles onto the surface of the medium, pores are either covered or blocked by the particles and it is very cumbersome to predict which particle size fraction will arrive first or upon arrival how will they arrange themselves on the filter medium. More importantly, this hard to predict initial phase of the process actually represents the controlling resistance of the overall process, i.e. the resistance at the cake-septum interface.

Mathematically, this hard to predict initial phase is observed with an initial deviation when  $dt/dV$  vs.  $t$  plots are generated. It is clearly analyzed that as the filtration begins up to a certain time  $t^*$  the process somehow shows variation. This period is actually the phase at which the cake-septum resistance develops as a result of the combined effect of both the filter medium and the layer of particles that deposit over the filter medium up to  $t^*$ .

### 6.3. Results and Discussion

The filtration test results gathered for model slurries and for real sludge systems were analyzed with the multiphase modeling approach and the blocking filtration laws to come up with a correct mathematical treatment of the filtration data.

A first application of blocking law analysis to filtration data of concentrated slurries was made and as a result of this analysis, a slurry-specific filtration constant,  $K_{CF}$ , was found for the model slurries being tested.

In the multiphase analysis of filtration data of both model slurries and real sludge systems, the following procedure is followed:

1. The experimental volume-time relationship is used to generate  $dt/dV$  vs.  $t$  plots ( $dt/dV$  values are calculated from experimental data as the ratio of time difference to volume difference). These plots indicate the deviation in the initial phase of the filtration process.
2. Time-volume data is best fitted in MATLAB and the resulting equations in the form  $t = aV^m + bV$  are obtained (the constraint for the parameter "b" is set by considering the passage of particle-free water through the clean filter medium). It should be noted that, the parameter "a" is related to the total resistance to flow.
3. The  $d^2t/dV^2$  vs.  $t$  plots are generated from the fitted time-volume relationship ( $d^2t/dV^2$  physically represents the "change in resistance to flow", thus, the change of this value with time shows the change of resistance developed at cake-septum interface with time). The time after which a nearly constant  $d^2t/dV^2$  value is reached is the  $K_oJ_o$  value that characterizes the overall filtration process (Eqn. 6.31).
4. The data belonging to this constant  $d^2t/dV^2$  phase predicts the filterability of the slurry under the defined operational conditions.

The experimental data presented in Chapters 4 and 5 are transformed according to the above mentioned procedure. The results are presented below first for the model slurries and then for real sludge systems. Afterwards, results for the blocking law analysis of model slurry data are presented.

### 6.3.1. Model Slurry Systems

The model slurry results are presented under three main topics as given in Table 6.3. The data analysis procedure outlined above is adapted to every data set covered under the three experimental cases given in details in Table 6.4 Detailed graphical analysis is provided for a single data set, the rest is given in Appendix B.

**Table 6.3.** Model slurry experiments

Case #	Filter Medium	Particle Size	Applied Pressure
<b>I</b>	<b>Variable</b>	Constant	Constant
<b>II</b>	Constant	<b>Variable</b>	Constant
<b>III</b>	Constant	Constant	<b>Variable</b>

**Table 6.4.** Model slurry-Experimental conditions

Case No.	Experiment No.	Operational parameters*		Data analysis
		Constant	Variable	
<b>I</b>	Exp. I-A	C: 2% $\Delta P$ : 5 in-Hg PS: 53-75 $\mu\text{m}$ M: upflow	<b><u>Filter medium</u></b> W#41 (20-25 $\mu\text{m}$ ) Nylon f.m.(41 $\mu\text{m}$ )	dt/dV vs. V dt/dV vs. t t vs. V $d^2t/dV^2$ vs. t
	Exp. I-B	C: 4% $\Delta P$ : 5 in-Hg PS: 200-210 $\mu\text{m}$ M: upflow	<b><u>Filter medium</u></b> W#41 (20-25 $\mu\text{m}$ ) Nylon f.m.(41 $\mu\text{m}$ ) Steel mesh (200 $\mu\text{m}$ )	dt/dV vs. V dt/dV vs. t t vs. V $d^2t/dV^2$ vs. t
	Exp. I-C	C: 4% $\Delta P$ : 10 in-Hg PS: 200-210 $\mu\text{m}$ M: upflow	<b><u>Filter medium</u></b> W#41 (20-25 $\mu\text{m}$ ) Nylon f.m.(41 $\mu\text{m}$ ) Steel mesh (200 $\mu\text{m}$ )	dt/dV vs. V dt/dV vs. t t vs. V $d^2t/dV^2$ vs. t
	Exp. I-D	C: 8% $\Delta P$ : 5 in-Hg PS: 200-210 $\mu\text{m}$ M: upflow	<b><u>Filter medium</u></b> W#41 (20-25 $\mu\text{m}$ ) Nylon f.m.(41 $\mu\text{m}$ ) Steel mesh (200 $\mu\text{m}$ )	dt/dV vs. V dt/dV vs. t t vs. V $d^2t/dV^2$ vs. t
	Exp. I-E	C: 8% $\Delta P$ : 10 in-Hg	<b><u>Filter medium</u></b> W#41 (20-25 $\mu\text{m}$ )	dt/dV vs. V dt/dV vs. t

Case No.	Experiment No.	Operational parameters*		Data analysis
		Constant	Variable	
		PS: 200-210 $\mu\text{m}$ M: upflow	Nylon f.m.(41 $\mu\text{m}$ ) Steel mesh (200 $\mu\text{m}$ )	t vs. V $d^2t/dV^2$ vs. t
<b>II</b>	Exp. II-A	C: 2% $\Delta P$ : 4.5 in-Hg FM:W#41(20-25 $\mu\text{m}$ ) M: upflow	<b><u>Particle size</u></b> 53-75 $\mu\text{m}$ 250-425 $\mu\text{m}$ Mixed	dt/dV vs. V dt/dV vs. t t vs. V $d^2t/dV^2$ vs. t
	Exp. II-B	C: 4% $\Delta P$ : 4.5 in-Hg FM:W#41(20-25 $\mu\text{m}$ ) M: upflow	<b><u>Particle size</u></b> 75-100 $\mu\text{m}$ 200-210 $\mu\text{m}$ 250-425 $\mu\text{m}$	dt/dV vs. V dt/dV vs. t t vs. V $d^2t/dV^2$ vs. t
<b>III</b>	Exp. III-A	C: 4% PS: 200-210 $\mu\text{m}$ FM:W#41(20-25 $\mu\text{m}$ ) M: upflow	<b><u>Pressure</u></b> 5 in-Hg 10 in-Hg	dt/dV vs. V dt/dV vs. t t vs. V $d^2t/dV^2$ vs. t
	Exp. III-B	C: 4% PS: 200-210 $\mu\text{m}$ FM: Steel (200 $\mu\text{m}$ ) M: upflow	<b><u>Pressure</u></b> 5 in-Hg 10 in-Hg	dt/dV vs. V dt/dV vs. t t vs. V $d^2t/dV^2$ vs. t

\* C: Solids concentration (by wt. %), FM: Filter medium, M: Mode of filtration,  
PS: Particle size distribution

### Case I-Filter Medium Effect

Two different sets of experiments are presented under Case I. Table 6.5 present the experimental conditions for the first data set.

Figure 6.4 is the dt/dV versus V plot and Figure 6.5 is the dt/dV versus t plot for the first data set. As can be seen from the figures, whilst the dt/dV vs. V plots show a linear trend, the dt/dV vs. t plots indicate a deviation in the initial period. The initial deviations are marked on Figures 6.6 and 6.7. The MATLAB time-volume fit results for Case I are given in Table 6.6.

**Table 6.5.** Experimental conditions-Filter medium effect (I-A)

Operational Conditions	Water + Meliodent
Slurry concentration	2%
Pressure	5 in-Hg
Particle size distribution	53-75 $\mu\text{m}$
Mode of filtration	Up-flow
Filter Medium	W#41 (20-25 $\mu\text{m}$ ) Nylon filter medium (41 $\mu\text{m}$ )

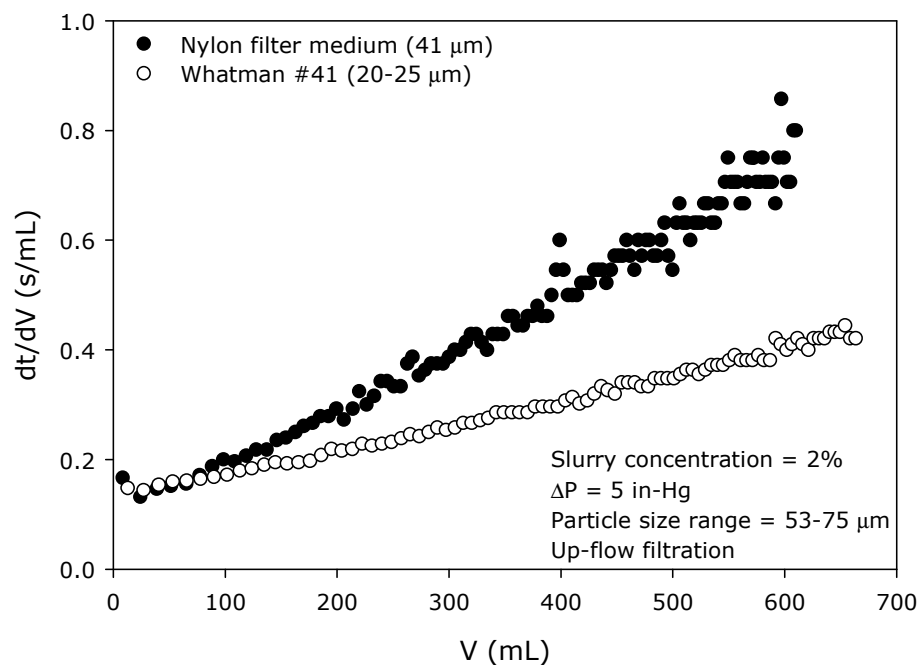


**Figure 6.4.** dt/dV vs. V plot-Filter medium effect (I-A)

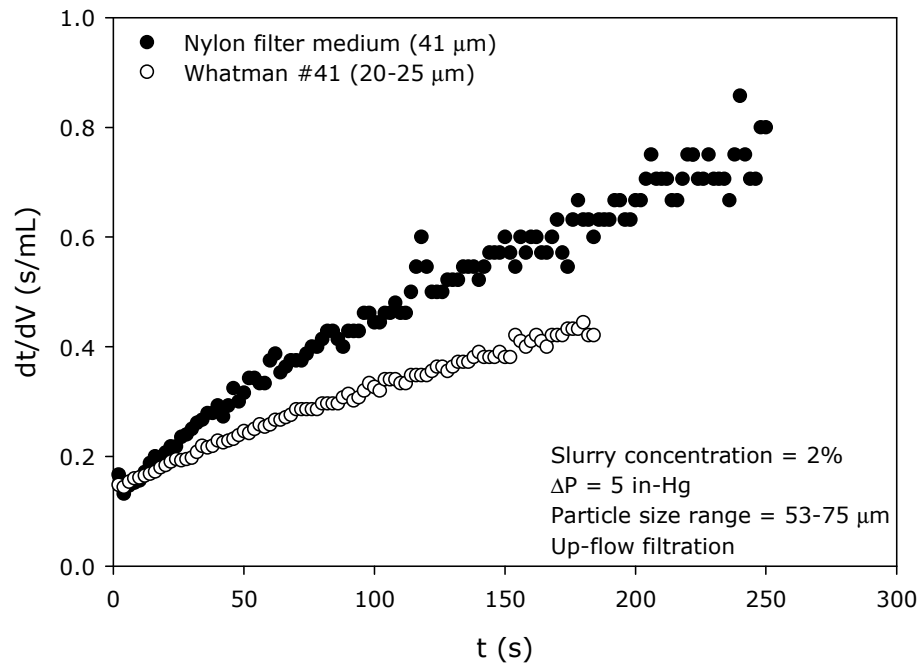


**Figure 6.5.** dt/dV vs. t plot-Filter medium effect (I-A)

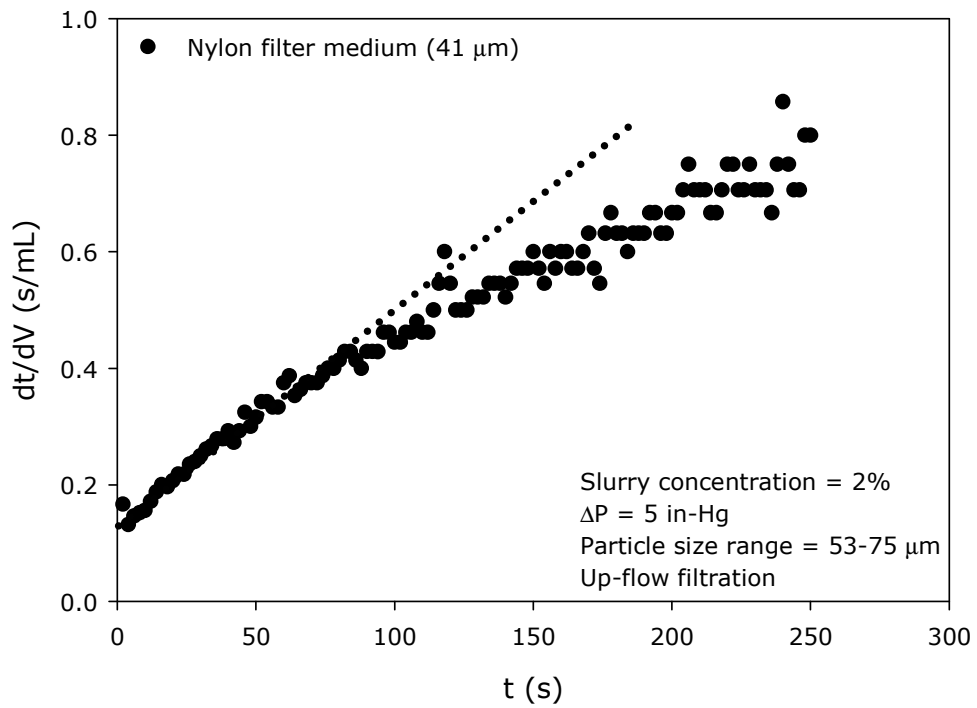


**Figure 6.6.** dt/dV vs. t plot-Filter medium effect (I-A, nylon filter medium)

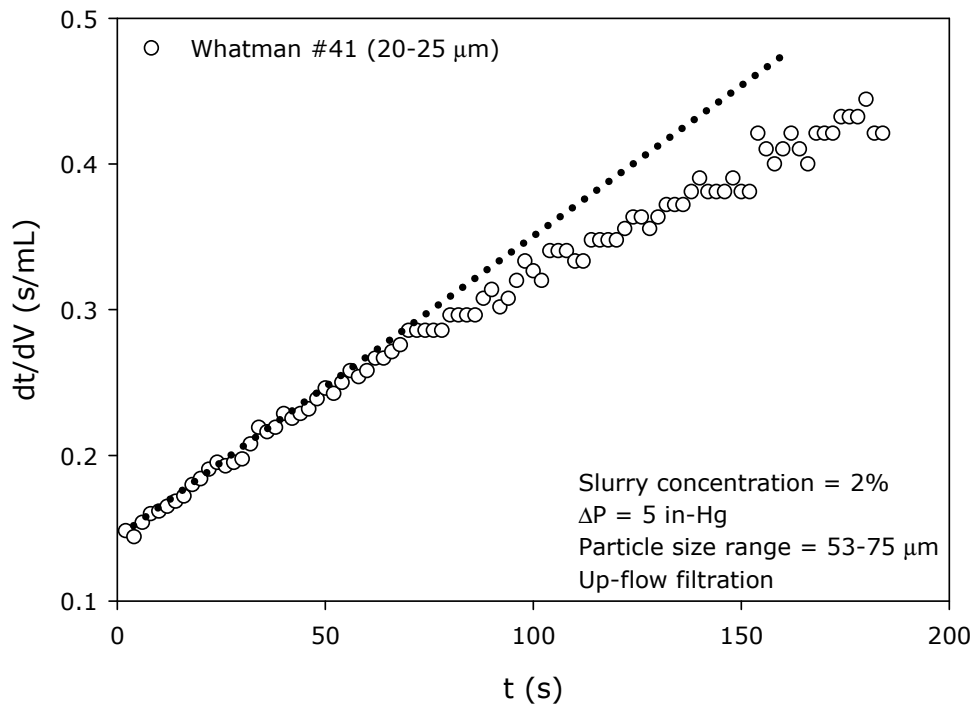


**Figure 6.7.** dt/dV vs. t plot-Filter medium effect (I-A, Whatman #41)

**Table 6.6.** MATLAB results for Case I

Case I-Filter Medium Effect	t = aV <sup>m</sup> + bV			R <sup>2</sup>	SSE <sup>a</sup>	RMSE <sup>b</sup>
	a	b*	m			
Exp. I-A, W#41	1.41 × 10 <sup>-4</sup>	0.14	2.057	0.99	43.05	0.68
Exp. I-A, Nylon	9.81 × 10 <sup>-5</sup>	0.13	2.239	1.00	6.99	0.24
Exp. I-B, W#41	4.42 × 10 <sup>-4</sup>	0.16	1.957	1.00	7.84	0.21
Exp. I-B, Nylon f.m.	1.87 × 10 <sup>-4</sup>	0.11	2.021	1.00	1.92	0.17
Exp. I-B, Steel mesh	1.60 × 10 <sup>-3</sup>	0.08	1.728	1.00	4.26	0.19
Exp. I-C, W#41	6.70 × 10 <sup>-5</sup>	0.10	2.097	1.00	7.13	0.31
Exp. I-C, Nylon f.m.	3.35 × 10 <sup>-5</sup>	0.07	2.175	1.00	2.84	0.22
Exp. I-C, Steel mesh	1.05 × 10 <sup>-3</sup>	0.06	1.656	1.00	1.82	0.17
Exp. I-D, W#41	6.46 × 10 <sup>-4</sup>	0.20	1.948	1.00	6.38	0.22
Exp. I-D, Nylon f.m.	2.17 × 10 <sup>-4</sup>	0.13	2.102	1.00	1.23	0.13
Exp. I-D, Steel mesh	6.32 × 10 <sup>-4</sup>	0.21	1.941	0.99	66.07	0.68
Exp. I-E, W#41	3.45 × 10 <sup>-4</sup>	0.09	1.929	1.00	0.76	0.11
Exp. I-E, Nylon f.m.	5.42 × 10 <sup>-5</sup>	0.09	2.209	1.00	0.79	0.13
Exp. I-E, Steel mesh	8.90 × 10 <sup>-5</sup>	0.10	2.121	1.00	2.66	0.22

\* Values calculated up to 4 digits by MATLAB, but here given up to 2 digits

<sup>a</sup> Sum of Squared Errors (SSE); <sup>b</sup> Root Mean Squared Error (RMSE) (a measure of total error defined as the square root of the sum of the variance and the square of the bias)

The dt/dV vs. t plots of both the experimental data and the MATLAB-predicted data are presented in Figures 6.8 and 6.9.

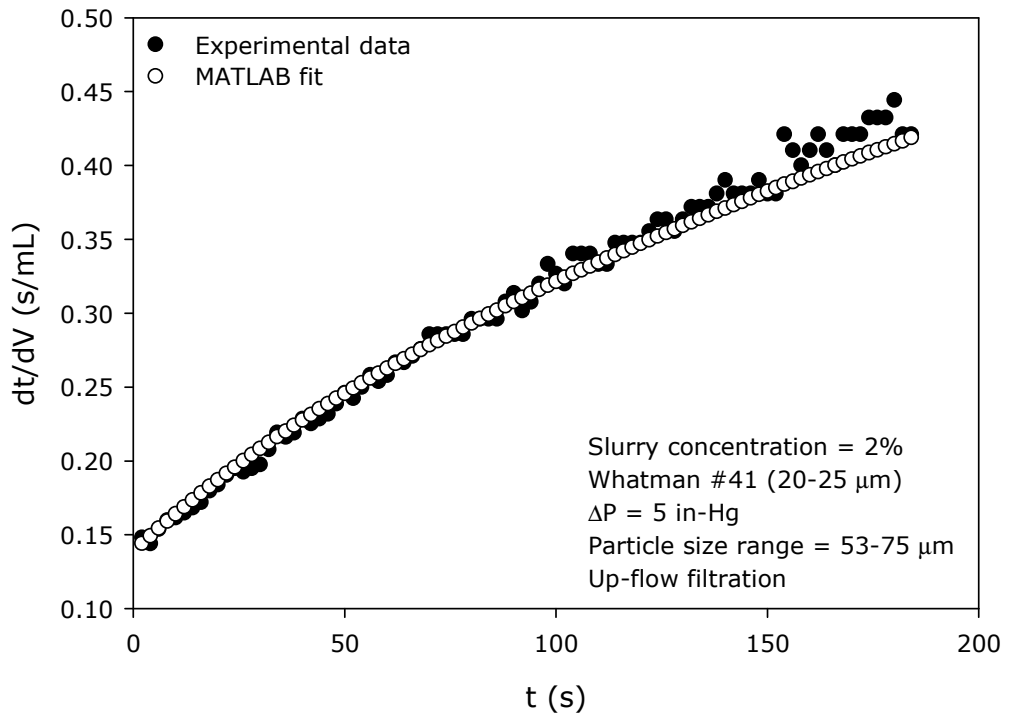


**Figure 6.8.** Comparative  $dt/dV$  vs.  $t$  plot-Filter medium effect (I-A, W#41)

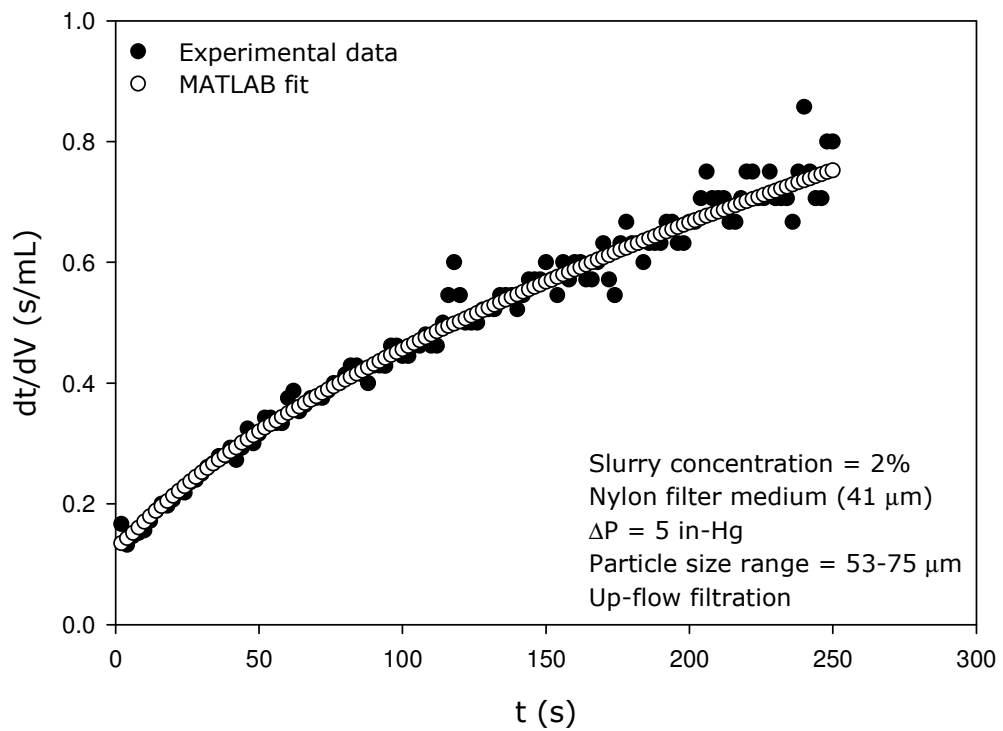


**Figure 6.9.** Comparative  $dt/dV$  vs.  $t$  plot-Filter medium effect (I-A, nylon f.m)

As Figures 6.8 and 6.9 clearly show, MATLAB predictions are in good agreement with the experimental data as also given in Table 6.6. Finally,  $d^2t/dV^2$  vs.  $t$  graphs are generated as shown in Figures 6.10 and 6.11.

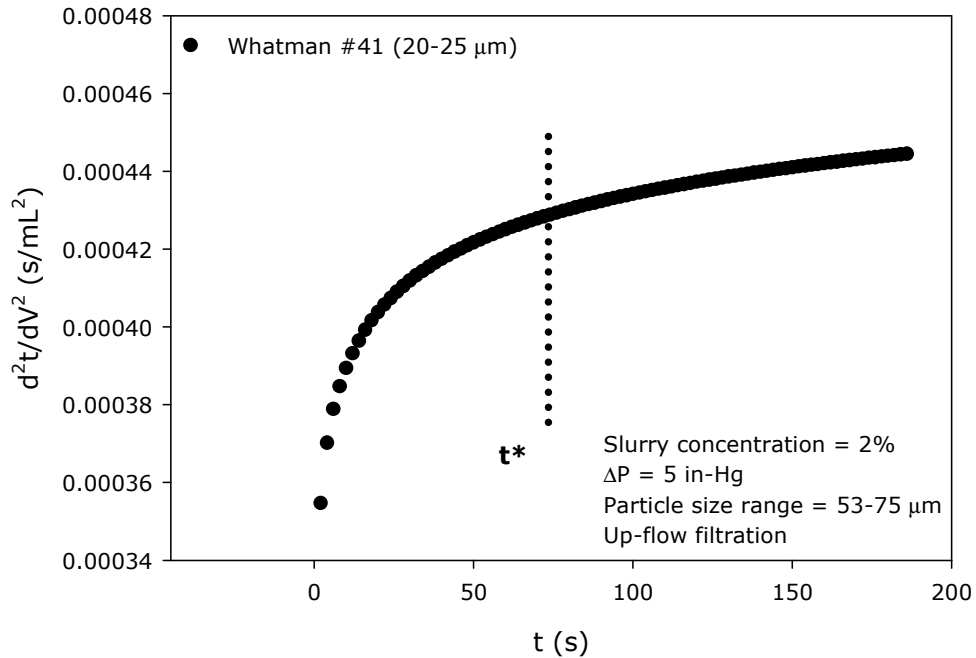


**Figure 6.10.**  $d^2t/dV^2$  vs.  $t$  plot-Filter medium effect (I-A, W#41)

As seen from Figures 6.10 and 6.11, as the filtration triggers, there is a certain time,  $t^*$ , up to which the resistance changes ( $d^2t/dV^2$  value) considerably. The  $t^*$  value is within 50 s and 100 s time interval, which actually corresponds to the interval in which deviation in  $dt/dV$  vs.  $t$  plots are seen. This time interval is believed to be the period at which the resistance at the cake-septum interface develops and reaches a nearly constant value which characterizes the overall filterability. One should note that, this cake-septum resistance is characterized not only by the slurry properties but also by the properties of the filter medium. Considering the deviations indicated in Figures 6.6 and 6.7, if  $t^*$  is to be taken as 80 s, then the data before the  $t^*$  value is excluded from the total filtration data and the  $dt/dV$  vs.  $V$  plots of the data after  $t^*$  is evaluated as given in Figure 6.12.

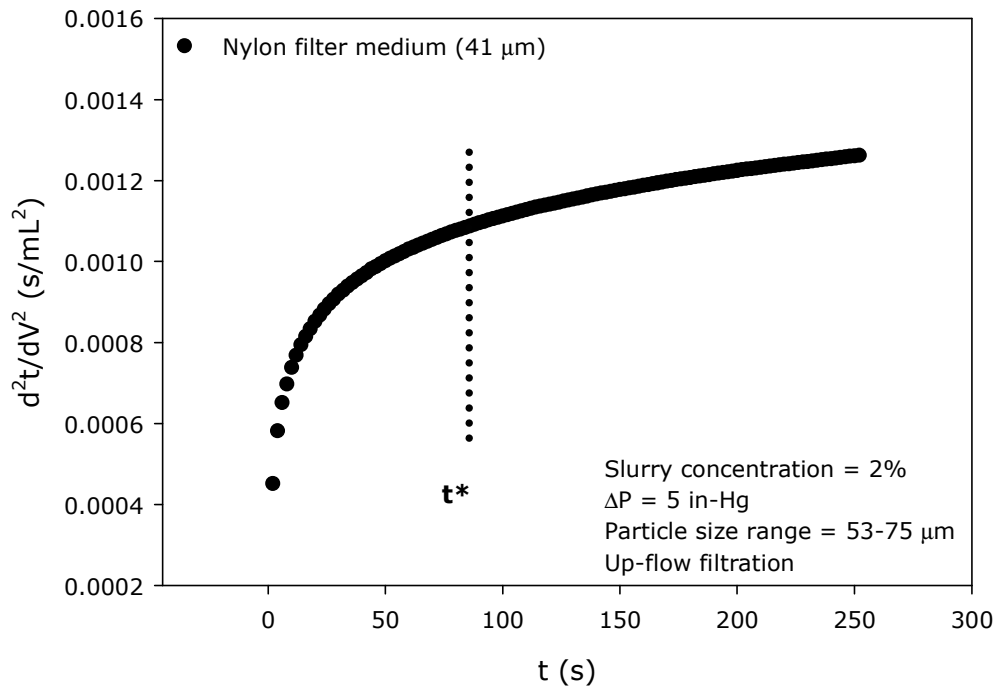


**Figure 6.11.**  $d^2t/dV^2$  vs.  $t$  plot-Filter medium effect (I-A, nylon f.m)

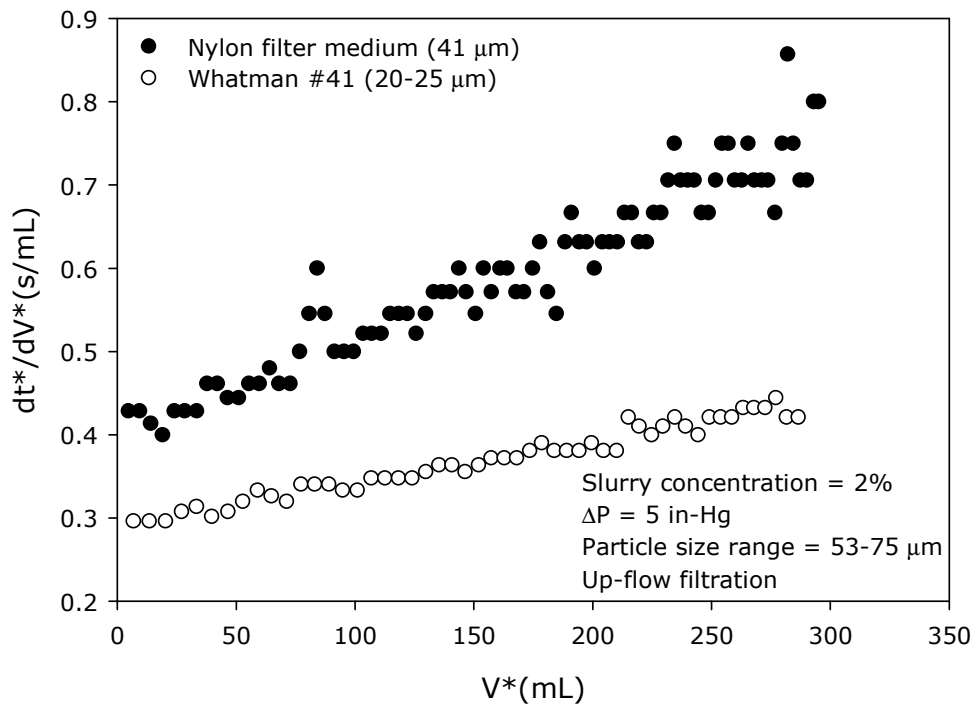


**Figure 6.12.**  $dt^*/dV^*$  vs.  $V^*$  plot-Filter medium effect (I-A)

Figure 6.12 shows that, although the initial filtration data up to  $t^*$  is eliminated,  $dt/dV$  vs.  $V$  plots still show difference in slope values which is a measure of the slurry filterability. Although the same slurry is being tested, it is not possible to obtain a slurry-specific filterability parameter as it is affected both by the slurry characteristics and the properties of the filter medium. In the analysis of the filtration test results, the initial data should be discarded as it corresponds to the stage of filtration at which the pore coverage and pore blockage mechanisms are prevailing and a certain resistance is being developed.

Figure 6.12 presents the filterability characteristics of the slurry that is passing through the filter medium plus the particles deposited above the medium up to 80 s. That is why, when the intercept values in Figure 6.12 are to be compared, it is seen that nylon filter medium results in a higher intercept value implying a lower initial passage rate of the slurry through the filter medium and the particles deposited over it. This is an expected result since the particle size distribution of the slurry is closer to the pores of the nylon filter medium resulting in the formation of a more resistant layer up to 80 s. On the other hand, it is obvious that the particle-pore coverage or blockage for Whatman #41 is not as considerable as for the nylon filter medium resulting in a higher passage rate and lower intercept value as presented in Figure 6.12.

In line with the above discussions, when Figure 6.10 and 6.11 are compared, it is seen that, the plateau value reached for the nylon filter medium is larger than Whatman #41 implying a higher resistance to filtration. Thus, the  $K_o J_o$  value (Eqn. 6.31) is higher for the Whatman #41.

It is clear that, for a specific slurry it is not correct to set typical filterability numbers as given in literature for SCR. Filterability analysis for sludge systems should be simulated at lab scale tests as close as possible to the real scale applications in terms of the operational conditions to have accurate and reliable results. Otherwise, it is for sure that filterabilities will be either underestimated or overestimated.

#### *Case II-Particle Size Effect*

Two different sets of experiments are presented under Case II as given in Table 6.4. The detailed graphical analyses for the experiments are given in Appendix B

(Figure B.36-B.51). The results of time-volume analysis in MATLAB are presented in Table 6.7.

**Table 6.7.** MATLAB results for Case II

Case II- Particle Size Effect	$t = aV^m + bV$			$R^2$	SSE <sup>a</sup>	RMSE <sup>b</sup>
	a	b*	m			
Exp. II-A, 53-75 $\mu\text{m}$	$1.41 \times 10^{-4}$	0.14	2.057	0.99	43.05	0.68
Exp. II-A, 250-425 $\mu\text{m}$	$1.84 \times 10^{-5}$	0.12	2.112	0.99	6.94	0.39
Exp. II-A, Mixed	$1.77 \times 10^{-5}$	0.16	2.35	1.00	1.64	0.13
Exp. II-B, 75-100 $\mu\text{m}$	$6.03 \times 10^{-5}$	0.16	2.226	1.00	6.83	0.22
Exp. II-B, 200-210 $\mu\text{m}$	$4.42 \times 10^{-4}$	0.16	1.957	1.00	7.84	0.21
Exp. II-B, 250-425 $\mu\text{m}$	$1.68 \times 10^{-5}$	0.16	2.383	1.00	3.09	0.21

\* Values calculated up to 4 digits by MATLAB, but here given up to 2 digits

<sup>a</sup> Sum of Squared Errors (SSE); <sup>b</sup> Root Mean Squared Error (RMSE) (a measure of total error defined as the square root of the sum of the variance and the square of the bias)

As given in Appendix B, the experimental  $dt/dV$  vs.  $t$  data and the MATLAB predictions are in good agreement.

Especially for the first data set, when the plateau values are compared, the effect of particle size distribution on the overall filterability is clearly seen. It is found out that the resistance developed at the cake-septum interface is nearly 5 times higher for the fine slurry (53-75  $\mu\text{m}$ ) when compared to the coarse slurry (250-425  $\mu\text{m}$ ) and nearly 6 times higher for the mixed slurry when compared to the coarse slurry.

#### *Case III-Pressure Effect*

Two different sets of experiments are presented under Case III as given in Table 6.4. The detailed graphical analyses for the experiments are given in Appendix B. The results of time-volume analysis in MATLAB is presented in Table 6.8.

**Table 6.8.** MATLAB results for Case III

Case III- Pressure Effect	$t = aV^m + bV$			$R^2$	SSE <sup>a</sup>	RMSE <sup>b</sup>
	a	b*	m			
Exp. III-A, 5 in-Hg	$4.42 \times 10^{-4}$	0.16	1.957	1.00	7.84	0.21
Exp. III-A, 10 in-Hg	$6.70 \times 10^{-5}$	0.10	2.097	1.00	7.13	0.31
Exp. III-B, 5 in-Hg	$1.60 \times 10^{-3}$	0.08	1.728	1.00	4.26	0.19
Exp. III-B, 10 in-Hg	$1.05 \times 10^{-3}$	0.06	1.656	1.00	1.82	0.17

\* Values calculated up to 4 digits by MATLAB, but here given up to 2 digits

<sup>a</sup> Sum of Squared Errors (SSE); <sup>b</sup> Root Mean Squared Error (RMSE) (a measure of total error defined as the square root of the sum of the variance and the square of the bias)

For Exp. III-A with W#41 filter paper, it is observed that decreasing the vacuum level from 10 in-Hg to 5 in-Hg results in nearly 4 times higher resistance developed at the cake-septum interface. This fact can be explained by the possible pile up during the filtration process. At a lower vacuum level the particles may come and block more pores resulting in a lower  $K_0$  value (permeability at the cake-septum interface) and higher overall resistance considering the product  $K_0J_0$ . For Exp. III-B with steel mesh, decreasing the vacuum level from 10 in-Hg to 5 in-Hg results in 3 times higher resistance developed at the cake-septum interface. Thus, with steel mesh, lowering of the  $K_0$  is not so considerable and the change in the product  $K_0J_0$  is less as compared to W#41 filter paper.

### 6.3.2. Real Sludge Systems

The data analysis procedure outlined above is also adapted to real sludge systems.

#### *Activated Sludge*

As an example, activated sludge filtered through a commercial filter cloth under 5 in-Hg vacuum in both down-flow and up-flow modes of filtration are given below. Figures 6.13 and 6.15 are the  $t$  vs.  $V$  plots for the experiments, 6.14 and 6.16 are the resulting  $d^2t/dV^2$  vs.  $t$  graphs. As observed for Meliodent slurries, after an initial sharp change in the resistance, a plateau level is reached. A

higher value is reached with the up-flow mode as compared to the down-flow mode. This is practically the result of interaction of the particle size distribution of the sludge and the pore size distribution of the filter cloth which determines the resistance developed at the cake-septum interface. Practically speaking, since the up-flow mode of filtration is closer to the rotary drum filters, it is clear that if the sludge is to be tested at lab scale with the same filter cloth as in the field scale operation, it will result in nearly 5 times lower resistance (down-flow) than that will be experienced in the real scale application (up-flow).

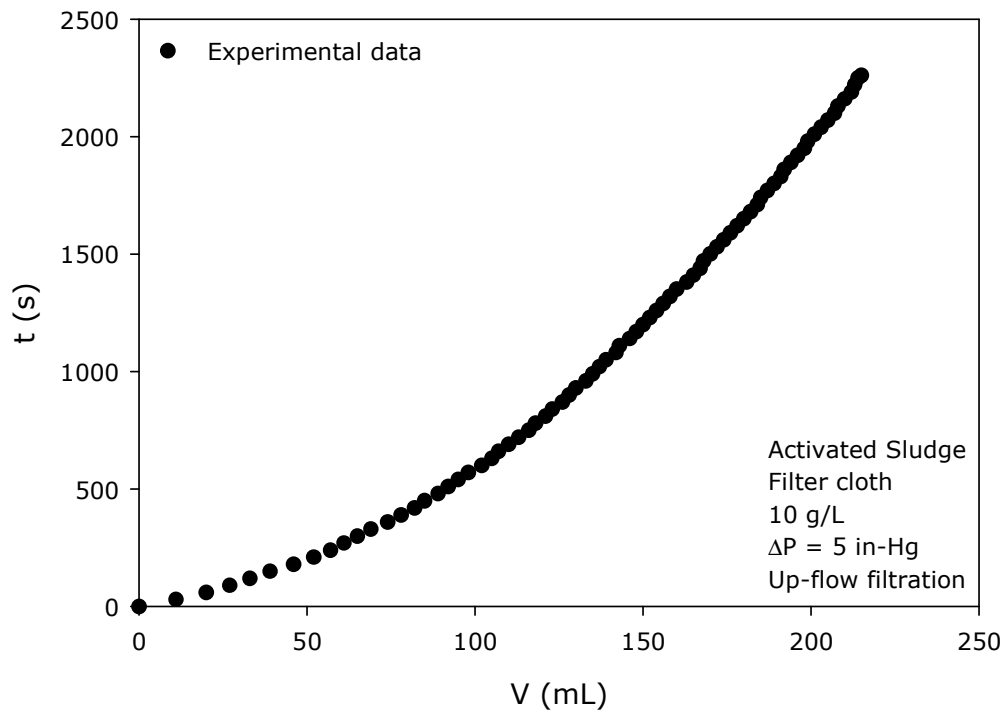


**Figure 6.13.** t vs. V plot-Activated sludge (up-flow)

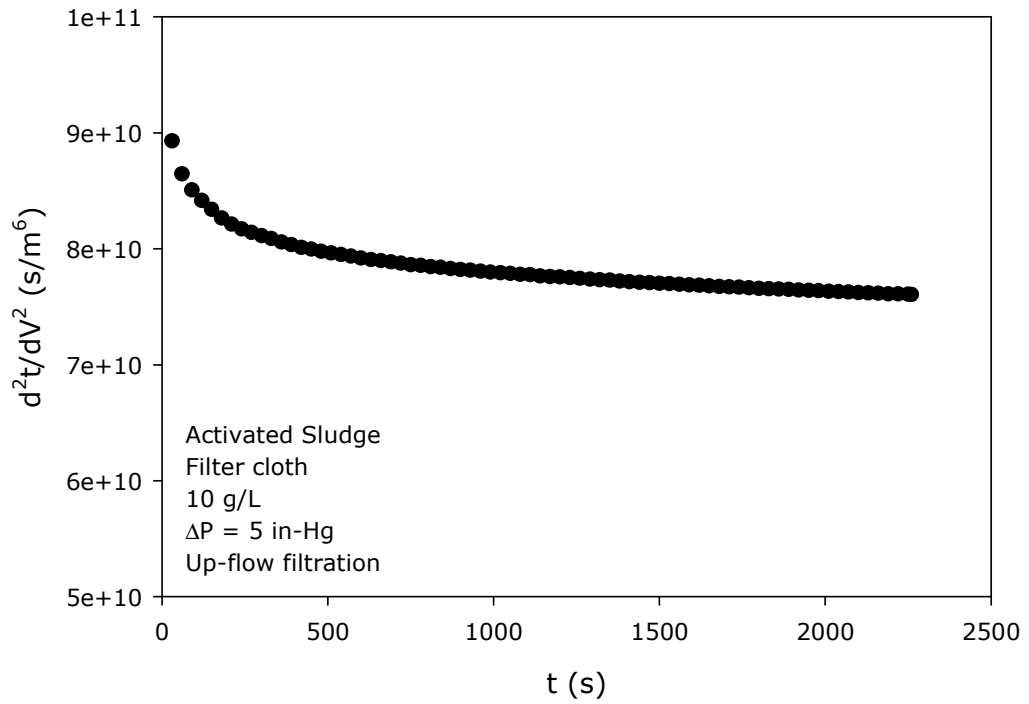


**Figure 6.14.**  $d^2t/dV^2$  vs.  $t$  plot-Activated sludge (up-flow)

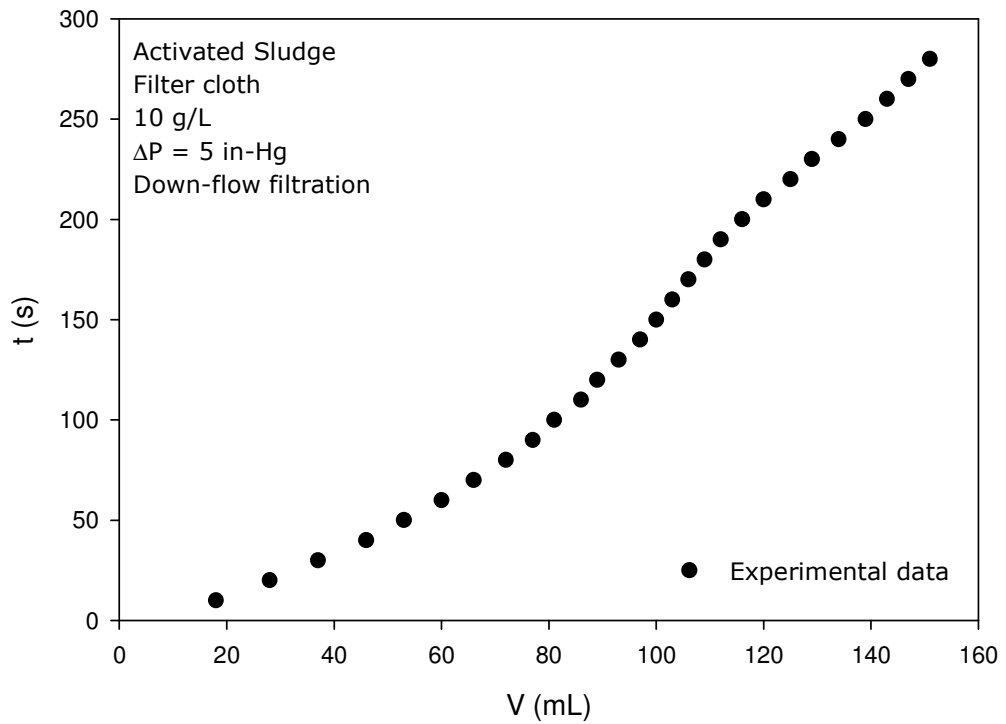


**Figure 6.15.**  $t$  vs.  $V$  plot-Activated sludge (down-flow)

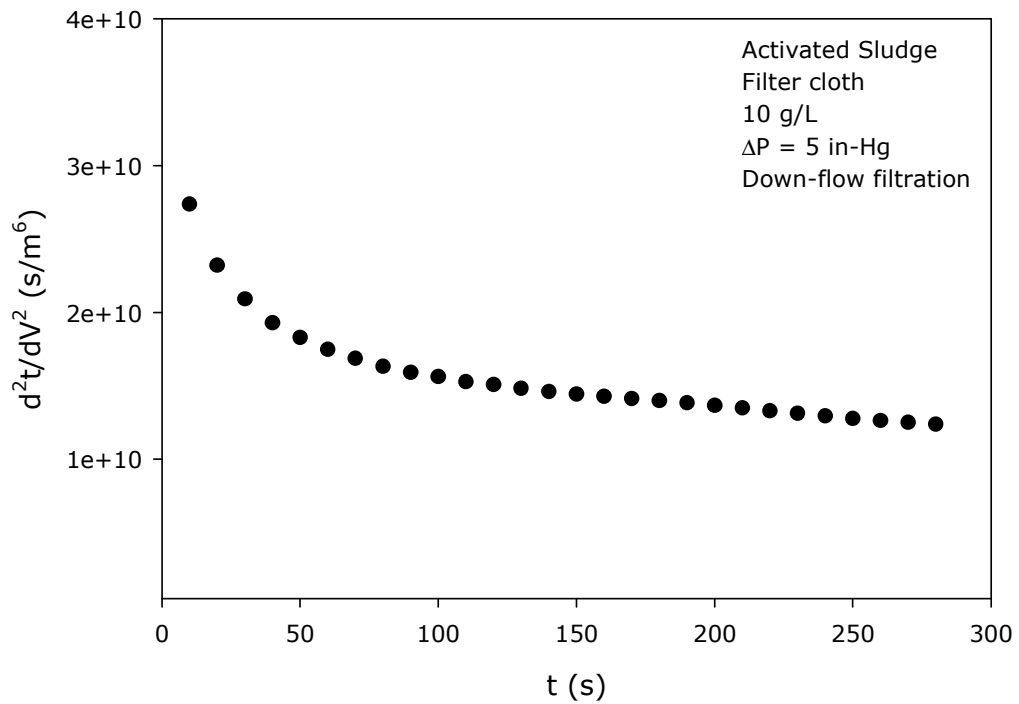


**Figure 6.16.**  $d^2t/dV^2$  vs.  $t$  plot-Activated sludge (down-flow)

*Chemical Sludge*

The applicability of the methodology is also tested with alum sludge. Figure 6.17 is the  $t$  vs.  $V$  plot and Figure 6.18 is the  $dt/dV$  vs.  $t$  plot which clearly shows the deviation at 200 s. As mentioned before, this point also corresponds to the start of the plateau in  $d^2t/dV^2$  vs.  $t$  plots as can be seen in Figure 6.19.

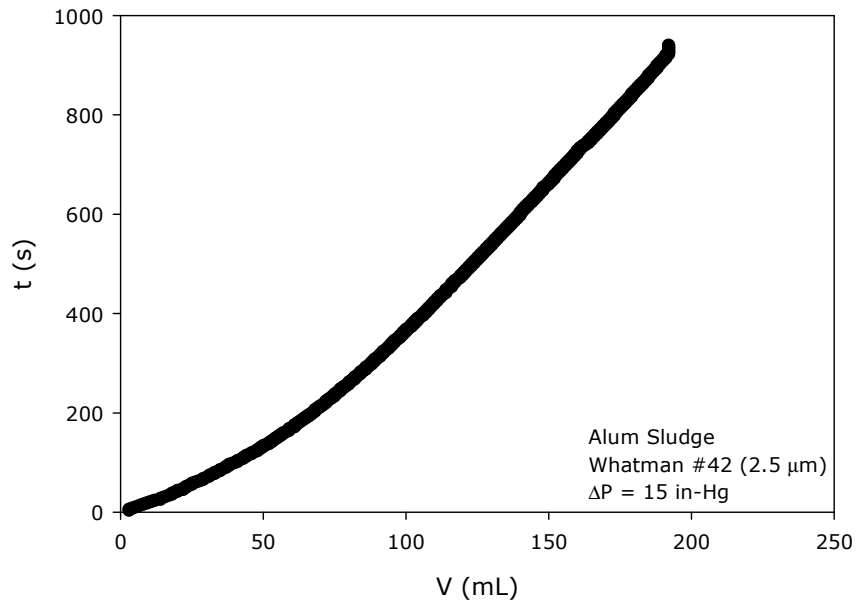


**Figure 6.17.**  $t$  vs.  $V$  plot-Chemical sludge (down-flow)

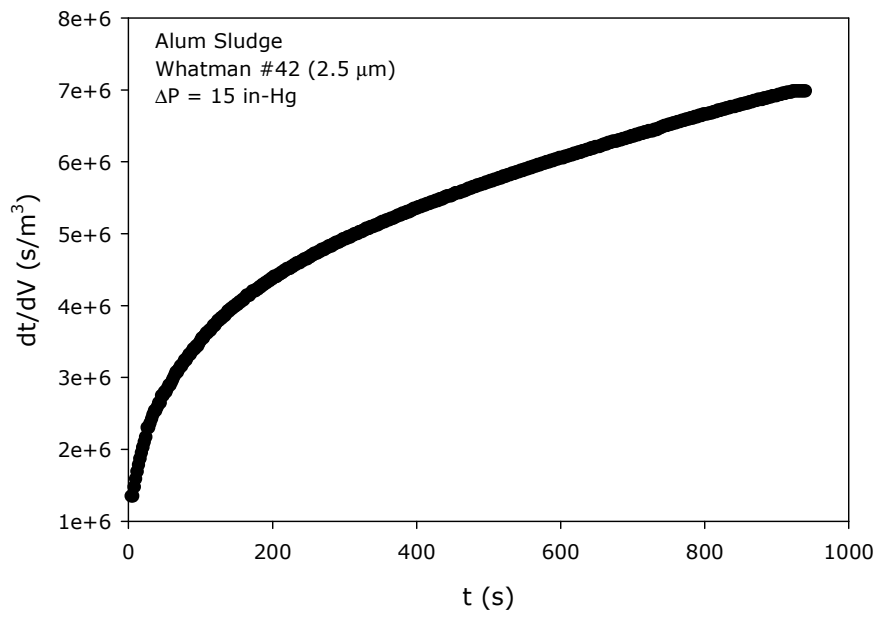


**Figure 6.18.**  $dt/dV$  vs.  $t$  plot-Chemical sludge (down-flow)

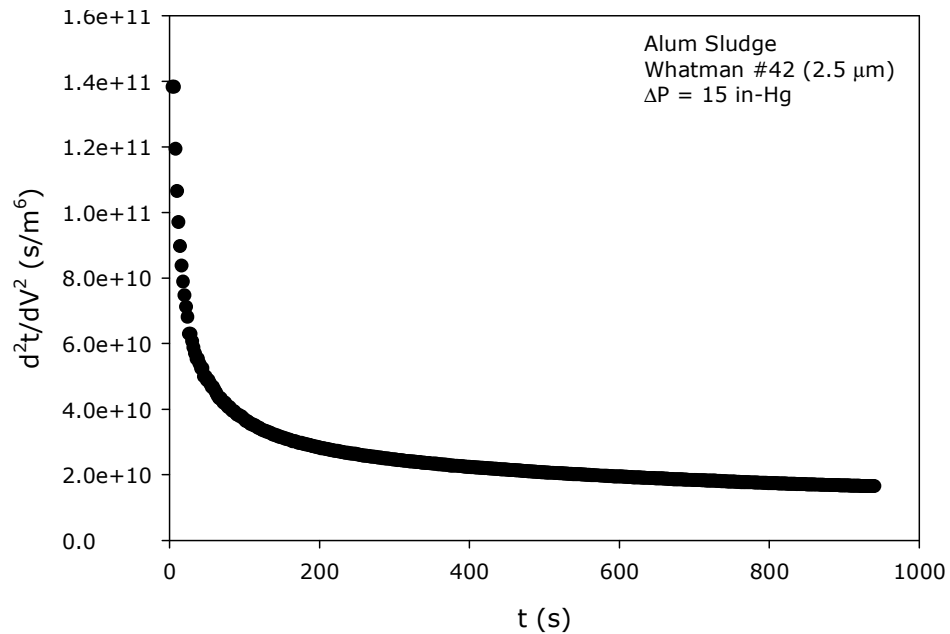


**Figure 6.19.**  $d^2t/dV^2$  vs.  $t$  plot-Chemical sludge (down-flow)

### 6.3.3. Blocking Filtration Law Analysis

The analysis presented below is the first application of the blocking filtration laws for the analysis of filterability of sludge systems. The results gathered were compared to the currently used classical filtration theory and it was found out that the blocking law analysis resulted in a slurry-specific characterization parameter that is superior to the commonly used SCR.

A set of up-flow filtration tests carried out using Meliodent – water suspensions are categorized under 3 groups for blocking law analysis: effect of slurry concentration, effect of filter medium and effect of pressure.

#### A. Effect of slurry concentration

Figure 6.20 is the log-scale plot of Eq. (6.32) for Meliodent slurry of 175-250 μm particles through Whatman #41 (20-25 μm) filter paper under a constant vacuum pressure of 4.5 in-Hg at different slurry concentrations. As can be seen from the figure, although the particles are larger than the pores of the filter medium, there is a certain time at which a climax is reached beyond which a value of zero or negative  $n$  is experienced. The period after the climax is referred

to as “cake filtration” and this data will be used in  $dt/dV$  vs.  $V$  analysis. This shift in the dominant mechanism clearly points out that at short filtration times, when the particles in the slurry and the filter medium are in direct contact and a cake is not formed yet, it will be erroneous to involve this period of time in the cake filtration analysis.

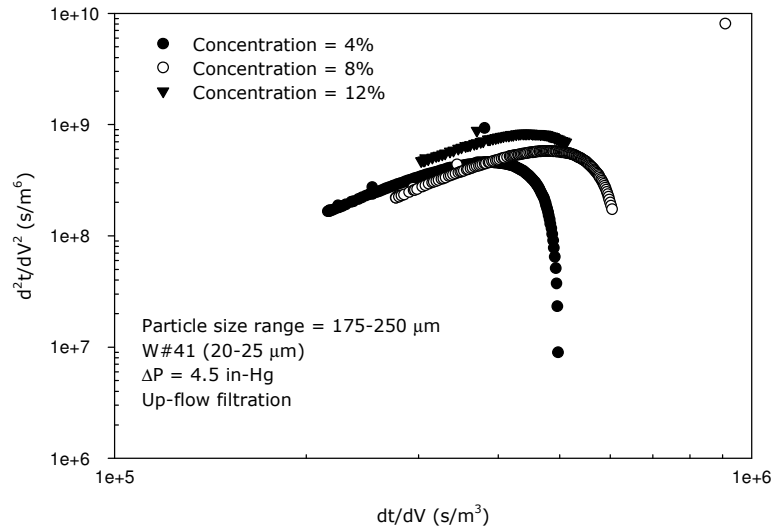


**Figure 6.20.**  $d^2t/dV^2$  vs.  $dt/dV$  plot at different slurry concentrations

Table 6.9 summarizes the  $dt/dV$  vs.  $V$  analyses of the raw filtration data and the data treated with the aforementioned method. The slope values of  $dt/dV$  vs.  $V$  plots, which indicate the resistance to filtration, have been normalized based on the slurry concentrations. A comparison of the normalized slope values suggests that with the new approach, the slope values representing the cake filtration period are almost identical to each other indicating a better description of sludge dewaterability. The fact that the resistance to filtration would be independent of slurry concentration and specific to the slurry, as long as the filter medium pore size is not variable, better describes the filterability. In order to come up with a slurry-specific parameter to replace the commonly used SCR of the classical approach, the filtration results are analyzed in terms of the cake filtration constant,  $K_{CF}$ , as given in Table 6.2.

Table 6.10 is the  $t/V$  vs.  $V$  results for the raw filtration data and  $t^*/V^*$  vs.  $V^*$  for the cake filtration phase which are used for the evaluation of  $K_{CF}$ . Whilst the  $K_{CF}$

values determined considering the raw filtration data show a wide variation, the  $K_{CF}$  values for the cake filtration phase are found to be almost identical to each other. This is a very important outcome of this analysis since  $K_{CF}$  appear to be a slurry-specific parameter.

### **B. Effect of filter medium**

Table 6.11 presents the  $t/V$  vs.  $V$  results for Meliodent slurry of 200-210  $\mu\text{m}$  particles filtered through 3 different medium, Whatman #41 (20-25  $\mu\text{m}$ ), nylon filter medium (41  $\mu\text{m}$ ) and steel mesh (200  $\mu\text{m}$ ), under a constant vacuum pressure of 5 in-Hg at a slurry concentration of 8%. As can be seen from Table 6.11, when the initial blocking phase of the data is discarded,  $K_{CF}$  values obtained for the same slurry filtered through different filter mediums yield quite similar values. This result is a clear indication of how the particle size and pore size interactions affect the overall filtration rate and that elimination of the effect of the initial phase results in a slurry-specific filtration number.

### **C. Effect of pressure**

Table 6.12 presents the  $t/V$  vs.  $V$  results for Meliodent slurry of 100-250  $\mu\text{m}$  particles at a concentration of 8% filtered through Whatman #41 (20-25  $\mu\text{m}$ ) filter paper under three different constant vacuum pressures of 4.5 in-Hg, 9 in-Hg and 18 in-Hg. The effect of eliminating the initial phase of the data on  $K_{CF}$  values is more pronounced since here the only variable is the applied pressure. Calculated  $K_{CF}$  values are much closer to each other than  $K_{CF}$  with all data, yielding a value specific to the slurry being filtered.

**Table 6.9.** Filtration test results-Effect of slurry concentration

Slurry Conc.	Raw filtration data	Slope value normalized with concentration	Filtration data after climax (cake filtration)	Slope value normalized with concentration
4%	$\frac{dt}{dV} = 1.18 \times 10^{-3} V + 0.153$	0.295	$\frac{dt^*}{dV^*} = 1.28 \times 10^{-3} V^* + 0.118$	0.320
8%	$\frac{dt}{dV} = 1.57 \times 10^{-3} V + 0.206$	0.196	$\frac{dt^*}{dV^*} = 2.20 \times 10^{-3} V^* - 0.045$	0.275
12%	$\frac{dt}{dV} = 2.19 \times 10^{-3} V + 0.252$	0.183	$\frac{dt^*}{dV^*} = 3.22 \times 10^{-3} V^* + 0.050$	0.268

**Table 6.10.**  $K_{CF}$  analysis-Effect of slurry concentration

Slurry Conc.	Raw filtration data	$K_{CF}$ normalized with concentration	Filtration data after climax (cake filtration)	$K_{CF}$ normalized with concentration
4%	$\frac{t}{V} = 5.18 \times 10^{-4} V + 0.182$	0.0157	$\frac{t^*}{V^*} = 6.91 \times 10^{-4} V^* + 0.616$	0.0018
8%	$\frac{t}{V} = 6.80 \times 10^{-3} V + 0.243$	0.0058	$\frac{t^*}{V^*} = 1.12 \times 10^{-3} V^* + 0.708$	0.0011
12%	$\frac{t}{V} = 9.34 \times 10^{-4} V + 0.279$	0.0040	$\frac{t^*}{V^*} = 1.99 \times 10^{-3} V^* + 0.616$	0.0018

**Table 6.11.**  $K_{CF}$  analysis-Effect of filter medium

Filter Medium	Raw filtration data	$K_{CF}$ (all data)	Filtration data after climax (cake filtration)	$K_{CF}$ (cake filtration)
Whatman#41 (20-25 $\mu\text{m}$ )	$\frac{t}{V} = 4.27 \times 10^{-4}V + 0.221$	0.0351	$\frac{t^*}{V^*} = 4.62 \times 10^{-4}V^* + 0.516$	0.0069
Nylon filter medium (41 $\mu\text{m}$ )	$\frac{t}{V} = 3.90 \times 10^{-4}V + 0.133$	0.0887	$\frac{t^*}{V^*} = 4.50 \times 10^{-4}V^* + 0.376$	0.0127
Steel mesh (200 $\mu\text{m}$ )	$\frac{t}{V} = 4.08 \times 10^{-4}V + 0.227$	0.0318	$\frac{t^*}{V^*} = 4.87 \times 10^{-4}V^* + 0.488$	0.0082

**Table 6.12.**  $K_{CF}$  analysis-Effect of pressure

Pressure	Raw filtration data	$K_{CF}$ normalized with pressure (all data)	Filtration data after climax (cake filtration)	$K_{CF}$ normalized with pressure (cake filtration)
18 in-Hg	$\frac{t}{V} = 0.85 \times 10^{-4}V + 0.077$	0.014	$\frac{t^*}{V^*} = 0.99 \times 10^{-4}V^* + 0.164$	0.004
9 in-Hg	$\frac{t}{V} = 2.49 \times 10^{-4}V + 0.146$	0.024	$\frac{t^*}{V^*} = 3.74 \times 10^{-4}V^* + 0.393$	0.005
4.5 in-Hg	$\frac{t}{V} = 5.67 \times 10^{-4}V + 0.236$	0.041	$\frac{t^*}{V^*} = 7.32 \times 10^{-4}V^* + 0.667$	0.007

The analysis of cake filtration data with Hermia's approach seems to be superior to the Ruth's classical approach in terms of being closer to the physical reality of the filtration process. Upon identification of the cake filtration phase, the calculated  $K_{CF}$  values appear to be slurry-specific.

As contrary to the common acceptance, the existence of particles greater in size than the pore size of the filter medium does not imply that there will not be any pore blocking mechanism. Filtration test results with particles larger than the pore size of the filter medium reveal an initial phase of filtration which could be described by one or a combination of the blocking mechanisms.

A further contribution to the Hermia's approach is the analysis of the cake filtration data after discarding the data belonging to the initial phase of filtration or in other words the data before climax of  $d^2t/dV^2$  vs.  $dt/dV$  plots. The justification behind this data elimination is the fact that at real scale applications of sludge dewatering process such as rotary drums, the filter cloth reaches a certain blocking on continuous operation. The scraping of sludge from the surface of the filter cloth and subsequent washing will not completely clean the medium. Practically, after the filter cloth is washed and submerged into the drum, the operation starts from the climax point that is shown in lab scale experiments. In order to verify this speculation, filtration tests with textile dyeing wastewater are conducted. The dyeing wastewater having a wide range of particles in it is first filtered through clean nylon filter medium of 41  $\mu\text{m}$  pore size. Then the medium is spray washed with 80 mL of distilled water and then submerged again into the wastewater for the second run of the test. The same procedure continued for 6 runs. The filtration test results are given in Figures 6.21 and 6.22.

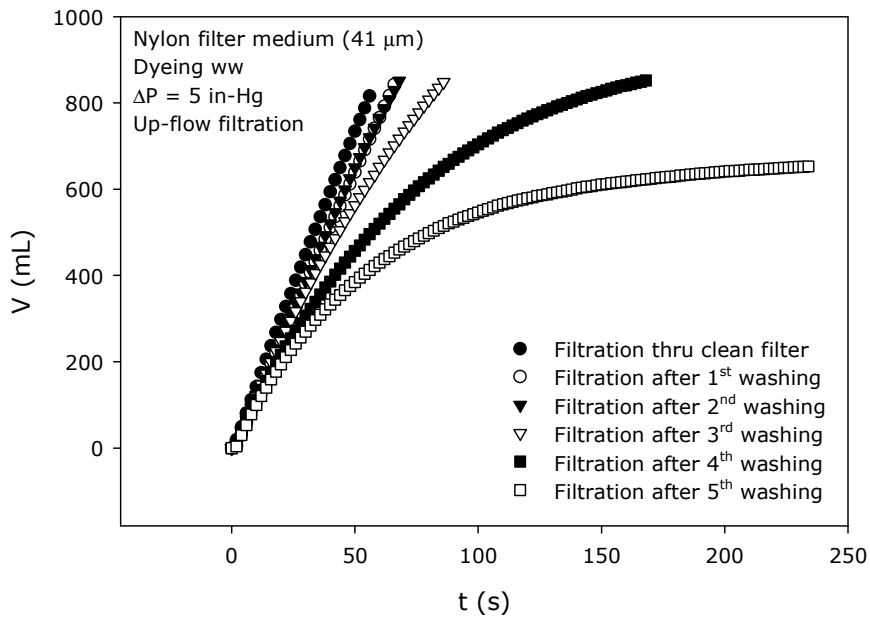


**Figure 6.21.** V vs. t plot for textile wastewater

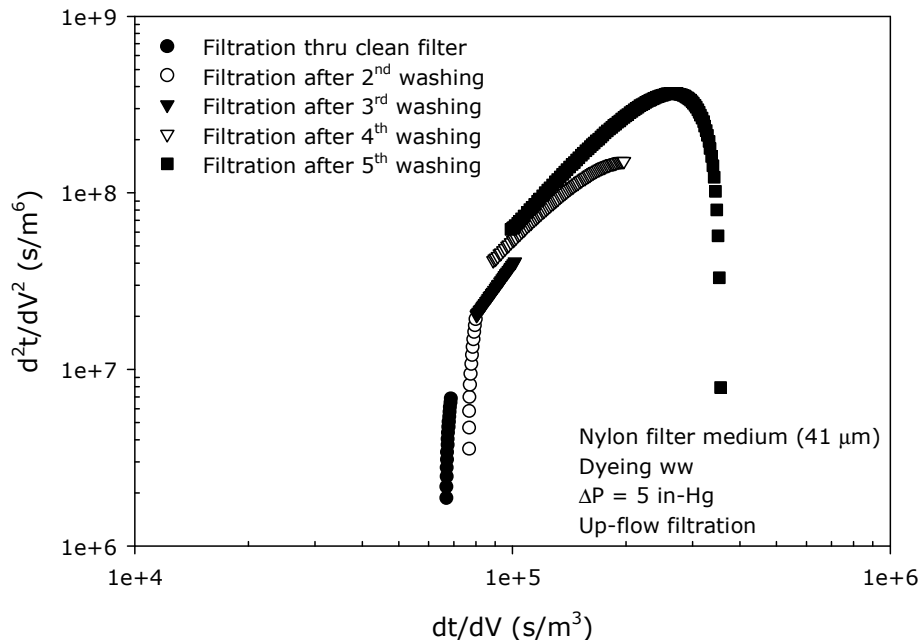


**Figure 6.22.**  $d^2t/dV^2$  vs.  $dt/dV$  plot for textile wastewater

Figure 6.21 presents the V vs. t trend; which clearly implies that as the filter medium gets clogged, the amount of filtrate collected per unit time decreases. On the other hand, Figure 6.22 shows the shift in the dominant mechanism

during continuous operations; from solely pore blocking-dominant runs with clean filter medium to pore blocking-cake filtration dominant cases with used filter medium. It is important to note that, during continuous operations, the filter medium will reach such a level of pore blockage that afterwards the scraping and washing procedures will not “clean” those blocked pores to a considerable extent. Thus, the filter medium will reach a certain level of saturation in terms of blockage. Therefore, the phase before the climax becomes unimportant in the assessment of the overall filterability of the slurry under consideration.

#### **6.4. Conclusions**

The present chapter reveals several important conclusions:

- A first application of the blocking filtration laws to the analysis of cake filtration data result in a better characterization parameter compared to the commonly used SCR.
- The  $dt/dV$  vs.  $t$  plots indicate an initial deviation of the data which is believed to be the time period at which the cake-septum resistance develops. Further analysis of data in the form of  $d^2t/dV^2$  vs.  $t$  reveal an initial sharp increase or decrease beyond which a nearly constant  $d^2t/dV^2$  value is achieved which is the KoJo value that characterizes the filtration run. The time period up to which a deviation is observed in  $dt/dV$  vs.  $t$  plots and the time period beyond which a plateau is reached in  $d^2t/dV^2$  vs.  $t$  plots are found out to be coincident.
- In continuous operations, this initial phase becomes unimportant since the filter medium will reach a certain level of pore blockage in time. Although washed and re-used, it will not act as a clean filter medium. Practically, the operation will start from the point at which deviation is seen.
- The filterability is controlled by the cake-septum interface which results from the filter medium plus the particles that deposit above the medium which cover and/or block the pores and form a skin layer. This coupled

effect is responsible for the overall resistance. This phenomenon is clearly seen in the initial deviations of  $dt/dV$  vs.  $t$  and  $d^2t/dV^2$  vs.  $t$  plots.

- It is not possible to foresee the resulting behavior of the interaction of the particles in the slurry and the pores of the filter medium which determine the overall filterability. Thus, it is not correct and possible to give ranges of slurry-specific filterability numbers.

## CHAPTER 7

### CONCLUSIONS

The present study is undertaken for the overall assessment and in-depth analysis of filterability of sludge systems. Initially, the inadequacy of the classical filtration theory and the currently used testing methodology in representing filterability of real sludge systems is investigated. The effect of slurry characteristics and operational conditions on the filterability is studied using synthetic slurries formed by Meliodent particles. Buchner funnel filtration tests both in down-flow and up-flow mode using different types of filter media are conducted. The experimental data gathered is analyzed in terms of the multiphase filtration theory for the assessment of the filterability performance in terms of the KoJo parameter.

The present study reveals several important conclusions:

- Activated and chemical sludge experiments indicate that, the expected straight line fit of  $t/V$  vs.  $V$  plots with a positive slope by the classical filtration theory is not satisfied all the time. Deviations from the straight line behavior and negative intercepts are observed for some of the filtration tests.
- The slopes of the  $t/V$  vs.  $V$  plots are found out to be strongly affected by the operational conditions, i.e., filter medium, filtration area, mode of filtration.
- Mathematically,  $dt/dV$  vs.  $V$  analysis is the correct way to analyze filtration data since  $t/V$  vs.  $V$  relationship results from integration of  $dt/dV$  vs.  $V$  assuming concentration, SCR and filter medium resistance values constant (which do not necessarily be constants during a filtration run).
- Up-flow and down-flow filtration tests reveal different filterability characteristics for the same sludge filtered under the same operational

conditions. This is attributed to the different particle deposition and pile up over the filter medium.

- SCR is not a slurry specific characterization parameter as depicted by the classical filtration theory. It provides only qualitative and comparative information. Quantitative results are subject to question since they are valid only for the conditions under which the test is being carried out.
- Filtration test results show that, filterability is not cake-driven as predicted by the classical approach; it is affected by the cake-septum interface as stated by the multiphase theory.
- The filterability of a specific slurry is a strong function of the filter medium; moreover, the particle size distribution relative to the pore size of the filter medium is found to affect the filtration performance. It is not possible to foresee the resulting behavior of the interaction of the particles in the slurry and the pores of the filter medium which determine the overall filterability. Thus, it is not correct and possible to give ranges of slurry-specific filterability numbers.
- The lab scale BF test does not actually represent the field scale applications of dewatering in terms of the filter medium and the mode of filtration. Hence, the SCR values obtained at lab scale studies do not reflect the real plant scale performance. Lab scale tests should be conducted by real scale filter medium, in up-flow mode (so as to mimic the real scale units such as rotary drums and to eliminate the sedimentation effect during filtration) and the data should be collected by a computer for the accuracy of the results.
- The intercept of  $dt/dV$  vs.  $V$  plots is defined as the reciprocal rate of the initial passage of slurry through the clean filter medium. The filtration test results show that, the magnitude of the intercept is affected not only by the pore size of the filter medium but also by the concentration of the slurry being filtered.

- Filtration is a very complex phenomenon even for the model slurries and it is very hard to predict the particle-pore interactions at the cake-septum interface which is the major rate determining part.
- Mathematical analysis of filtration via the blocking law analysis reveal a better characterization as compared to the currently used classical approach.
- Mathematically, the analysis of filtration data by the multiphase filtration theory better describes the physical reality behind the overall phenomenon. The KoJo parameter reflects the coupled effect of the particles in the slurry and the pore size of the filter medium in determining the filterability.
- The filtration test results should be analyzed in terms of  $dt/dV$  vs.  $t$ ,  $d^2t/dV^2$  vs.  $t$  and  $dt/dV$  vs.  $V$  plots.
- The  $dt/dV$  vs.  $t$  plots indicate an initial deviation of the data which is believed to be the time period at which the cake-septum resistance develops. Further analysis of data in the form of  $d^2t/dV^2$  vs.  $t$  reveal an initial sharp increase or decrease beyond which a nearly constant  $d^2t/dV^2$  value is achieved which is the KoJo value that characterizes the filtration. The time period up to which a deviation is observed in  $dt/dV$  vs.  $t$  plots and the time period beyond which a plateau is reached in  $d^2t/dV^2$  vs.  $t$  plots are found out to coincide.
- In continuous operations, this initial phase becomes unimportant since the filter medium will reach a certain level of pore blockage in time. Although washed and re-used, it will not act as a clean filter medium. Practically, the operation will start from the point at which deviation is seen.
- The coupled effect of the filter medium plus the particles that deposit above the medium which cover and/or block the pores and form a skin layer is responsible for the overall resistance.

## REFERENCES

- Atsumi, K. and Akiyama, T. (1975). A study of cake filtration-formulation as a Stefan problem, *J. Chem. Engr. Japan*, **8**, 487-492.
- Aoustin, E., Schafer, A.I., Fane, A.G. and Waite, T.D. (2001). Ultrafiltration of natural organic matter, *Separation and Purification Technology*, **22-23**, 63.
- Baskerville, R.C. and Gale, R.S. (1968). A simple automatic instrument for determining the filterability of sewage sludges, *Water Pollution Control*, **67**, 233.
- Bear, J. (1972). *Hydrodynamics of Fluids in Porous Media*, Elsevier, New York.
- Benesch, T., Meier, U. and Schütz, W. (2004). Modeling filtration with superimposed sedimentation. *Separation and Purification Technology*, **35**, 37-46.
- Bowen, W.R., Calvo, J.I. and Hernandez, A. (1995). Steps of membrane blocking in flux decline during protein microfiltration, *Journal of Membrane Science*, **101**, 153.
- Bürger, R., Concha, F. and Karlsen, K.H. (2001). Phenomenological model of filtration process: 1. Cake formation and expression. *Chem. Eng. Sci.*, **56**, 4537.
- Carman, P. C. (1938). Fundamental principles of industrial filtration, *Trans.Inst.Chem.Engrs.*, **16**, 168-188.
- Casey, T.J. (1997). *Unit Treatment Processes in Water and Wastewater Engineering*, Wiley.

- Chi, S., Klinzing, G. E., Chang, S. and Wen, W. W. (1985). Effect of entrapped air bubbles on fine coal dewatering via filtration, *Powder Technology*, **45**, 25-34.
- Coackley, P. and Jones, B. R. S. (1956). Vacuum sludge filtration: Interpretation of results by the concept of specific resistance, *Sewage and Industrial Wastes*, **28**, 963-968.
- Costa, A.R., de Pinho, M.N. and Elimelech, M. (2006). Mechanisms of colloidal natural organic matter fouling in ultrafiltration, *Journal of Membrane Science*, **281**(1-2), 716.
- Dentel, S. K. (1997). Evaluation and role of rheological properties in sludge management, *Water Science and Technology*, **36**(11), 1-8.
- Drew, D.A. (1970). Derivation and application of average equations for two-phase media. Ph.D Thesis, Rensselaer Polytechnic Institute, Troy, New York.
- Eckenfelder, W.W. (1989). *Industrial Water Pollution Control*, 2<sup>nd</sup> Ed., McGraw-Hill, Singapore.
- Gala, H. B. and Chiang, S. H. (1980). Filtration and Dewatering: Review of Literature, prepared for U. S. Department of Energy Office of Coal Mining.
- Gale, R. S. (1967). Filtration theory with special reference to sewage sludges, *Water Pollution Control*, **66**, 622-632.
- Gray, W.G. and Lee, P.C.Y. (1977). On the theorems for local volume averaging of multiphase systems, *Int. J. Mult. Flow*, **3**, 333-340.
- Guan, J., Amal, R. and Waite, T.D. (2001). Effects of aggregate size and structure on specific resistance of biosolids filter cakes. *Water Science and Technology*, **44**(10), 215-220.

- Hermans, P.H. and Bredée, H.L. (1936). Principles of the mathematical treatment of constant-pressure filtration, *J. Soc. Chem. Industry*, **55**, 1T-4T.
- Hermia, J. (1982). Constant pressure blocking filtration laws-application to power-law non-Newtonian fluids, *TransI ChemE.*, **60**, 183.
- Hwang, K. J. and Lu, W. M. (1997). Hydrodynamic analysis on the mechanism of cross-flow filtration of power-law slurry, *J. Chem. Eng. Japan*, **30**, 698-705.
- Hwang, K. J., Wu, Y. S. and Lu, W. M. (1997a). Effect of the size distribution of spheroidal particles on the surface structure of a filter cake, *Powder Technology*, **91**, 105-113.
- Hwang, K. J., Hwang, G. Y. and Lu, W. M. (1997b). Constant-pressure filtration of a viscoelastic slurry, *Proc. 1997 Symp. Transport Phenomena and Applications*, pp. 295-300.
- Iritani, E., Mukai, Y., Tanaka, Y. and Murase, T. (1995). Flux decline behavior in dead-end microfiltration of protein solutions, *Journal of Membrane Science*, **103**, 181.
- Kavanagh, B. V. (1980). The dewatering of activated sludge: Measurement of specific resistance to filtration and capillary suction time, *Water Pollution Control*, **79**, 388-398.
- Konieczny, K. and Raja, J. (2000). Modeling of the membrane filtration process of natural waters, *Polish J. Env. Studies*, **9**(1), 57.
- Lee, D. J., Wang, C. H. (2000). Theories of cake filtration and consolidation and implications to sludge dewatering, *Water Research*, **34**(1), 1-20.
- Leonard, J.I. and Brenner, H. (1965). Experimental studies of three-dimensional filtration on a circular leaf, *AIChE Journal*, **11**(6), 965.

- Lu, W. M. and Hwang, K. J. (1993). Mechanism of cake formation in constant pressure filtrations, *Sep. Technol.*, **3**, 122.
- Lu, W., Tiller, F. M., Cheng, F. and Chien, C. (1970). A new method to determine local porosity and filtration resistance of filter cakes, *J. Chinese Inst. Chem. Engrs.*, **1**, 45-53.
- Mihoubi, D. (2004). Mechanical and thermal dewatering of residual sludge. *Desalination*, **167**, 135-139.
- Mohammadi, T., Kazemimoghadam, M. and Saadabadi, M. (2003). Modeling of membrane fouling and flux decline in reverse osmosis during separation of oil in water emulsions, *Desalination*, **157**, 369.
- Novak, J. T., Agerbaek, M. L., Sorensen, B. L. and Hansen, J. A. (1999). Conditioning, filtering and expressing waste activated sludge, *Journal of Environmental Engineering*, **125**(9), 816-824.
- Orsello-Duclos, C., Li, W. and Ho, C. C. (2006). A three mechanism model to describe fouling of microfiltration membranes, *Journal of Membrane Science*, **280**, 856-866.
- Rawling, F. L., Boylan, D. R. and David, H. T. (1970). Effect of wall friction in compression-permeability testing, *Ind. Eng. Chem. Process Des. Develop*, **9**, 161-164.
- Roorda, J.H. (2004). Filtration characteristic in dead-end ultrafiltration of WWTP effluent, PhD Dissertation, TU-Delft, The Netherlands.
- Ruth, B. F., Montillon, G. H., Montonna, R. E. (1933). Studies in Filtration-I. Critical Analysis of Filtration Theory, *Industrial and Engineering Chemistry*, **25**(1), 76-82.
- Ruth, B. F., Montillon, G. H., Montonna, R. E. (1933). Studies in Filtration-II. Fundamental Axiom of Constant-Pressure Filtration, *Industrial and Engineering Chemistry*, **25**(2), 153-161.

- Ruth, B. F. (1935). Studies in Filtration-III. Derivation of General Filtration Equation, *Industrial and Engineering Chemistry*, **27(6)**, 708-723.
- Ruth, B. F. (1946). Correlating filtration theory with industrial practice, *Industrial and Engineering Chemistry*, **38**, 564-571.
- Scales, P. J., Dixon, D. R., Harbour, P. J. and Stickland, A. D. (2004). The fundamentals of wastewater sludge characterization and filtration, *Water Science and Technology*, **49 (10)**, 67-72.
- Shirato, M., Aragaki, T., Mori, R. and Sawamoto, K. (1968). Prediction of constant pressure and constant rate filtrations based on the appropriate correction for side-wall friction in compression-permeability cell data, *J. Chem. Eng. Japan*, **1**, 86-90.
- Shirato, M., Sambuichi, M., Kato, H. and Aragaki, T. (1969). Internal flow mechanism in filter cakes, *AIChE Journal*, **13**, 405-409.
- Smiles, D. E. (1970). A theory of constant pressure filtration, *Chem. Eng. Sci.*, **25**, 985-996.
- Smiles, D. E. and Kirby, J. M. (1987). Aspects of one dimensional filtration, *Sep. Science and Technology*, **22**, 1405-1423.
- Swanwick, J.D. and Davidson, M.F. (1961). Determination of specific resistance to filtration, *The Water and Waste Treatment Journal*, **8**, 386-389.
- Tchobanoglous, G. (1979). *Wastewater Engineering: Treatment, disposal, reuse*, 2<sup>nd</sup> Ed., McGraw-Hill, New York.
- Tenney, M.W., Eckelberger, W.F., Coffey, J.J. and McAloon, T.J. (1970). Chemical conditioning of biological sludges for vacuum filtration, *J. Water Pollut. Control Fed.*, **42**, R1-R20.
- Tiller, F. M. and Cooper, H. R. (1960). The role of porosity in filtration IV. Constant pressure filtration, *AIChE Journal*, **6**, 595-601.

- Tiller, F. M. and Green, T. C. (1973). Skin effect with highly compressible materials, *AIChE Journal*, **19**, 1266-1269.
- Tiller, F. M., Haynes, S. and Lu, W. (1972). Effect of side wall friction in compression-permeability cells, *AIChE Journal*, **18**, 13-20.
- Tiller, F. M. and Huang, C. J. (1961). Theory, *Industrial and Engineering Chemistry*, **53**, 529-537.
- Tosun, İ. (1986). Formulation of cake filtration, *Chem. Eng. Sci.*, **41**(10), 2563-2568.
- Tosun, İ. (2005). Simulation of cake filtration by the Compression-permeability cell - How good is it?, American Filtration and Separations Society 18th Annual Conference, April 10-13, Atlanta, GA, USA.
- Tosun, İ., Yetiş, Ü., Willis, M. S., Chase, G. C. (1993). Specific cake resistance: Myth or Reality, *Water Science and Technology*, **28(1)**, 91-101.
- Vesilind, P.A. (1979). *Treatment and Disposal of Wastewater Sludges*, 2<sup>nd</sup> Ed., Ann Arbor Science Pub., Ann Arbor, Michigan.
- Vesilind, P. A. (1988). Capillary suction time as a fundamental measure of sludge dewaterability, *Journal of Water Pollution Control Federation*, **60**(2), 215-220.
- Vesilind, P.A. (2003). *Wastewater Treatment Plant Design*, Water Environment Federation, IWA Publishing, USA.
- Wakeman, R. J. (1978). A numerical integration of the differential equations describing the formation of and flow in compressible filter cakes, *Trans. Inst. Chem. Engrs.*, **56**, 258-265.
- Willis, M. S. (1959). Compression-permeability testing with calcium carbonate, M. S. Thesis, Iowa State University, Ames, Iowa.

- Willis, M. S., Tosun, İ. (1980). A Rigorous Cake Filtration Theory, *Chem. Eng. Sci.*, **35**, 2427-2438.
- Wu, C.C., Huang, C.P. and Lee, D.J. (1997). Effect of polymer dosage on alum sludge dewatering characteristics and physical properties, *Colloids and Surfaces A*, **122**, 89-96.
- Wu, C. C., Lee, D. J. and Huang, C. (2000). Determination of the optimal dose of polyelectrolyte sludge conditioner considering particle sedimentation effects, *Advances in Environmental Research*, **4**, 245-249.
- Yuan, W., Kocic, A. and Zydney, A.L. (2002). Analysis of humic acid fouling during microfiltration using a pore blockage-cake filtration model, *Journal of Membrane Science*, **198**, 51-62.

## **APPENDIX A**

### **FILTRATION TEST RESULTS OF MODEL SLURRY**

This appendix provides the supplementary data for the filtration test results of model slurries discussed in Chapter 5.

**I. Effect of particle settling rate (buoyant vs. non-buoyant slurries)**

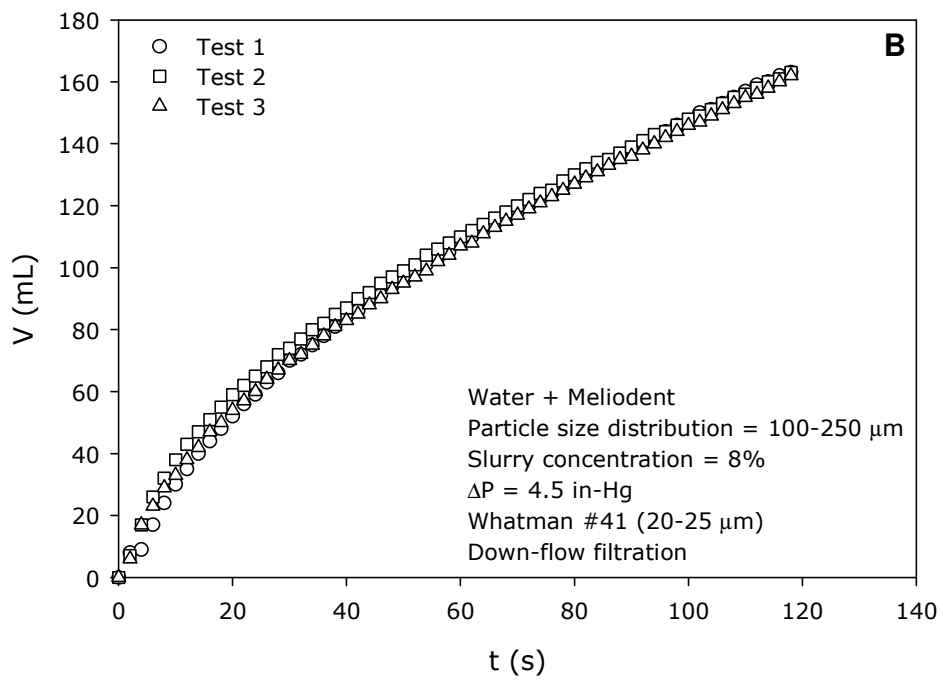
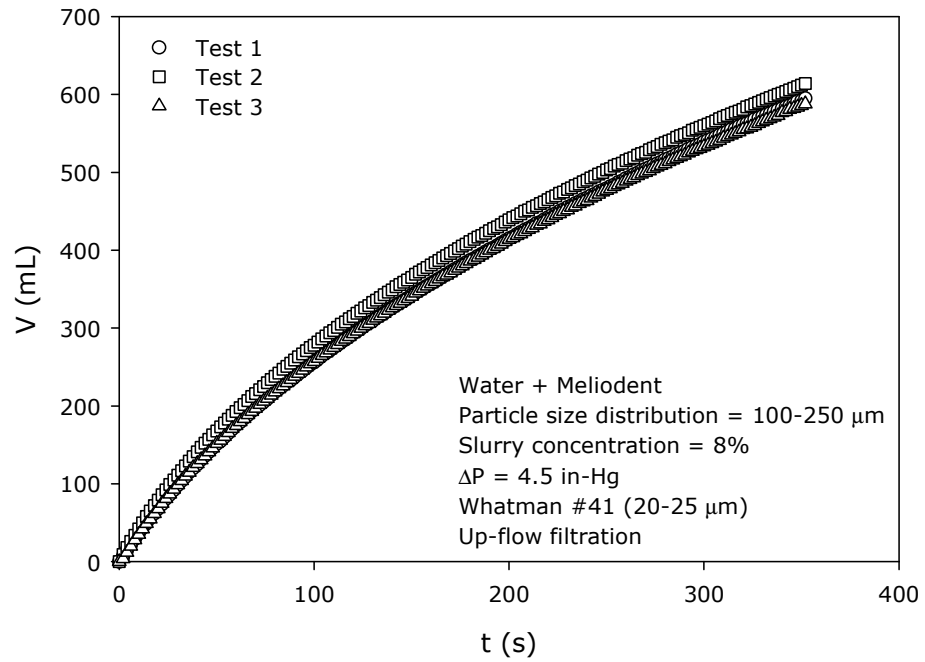


**Figure A.1.** V vs. t for water + Meliodent (A) Up-flow mode (B) Down-flow mode

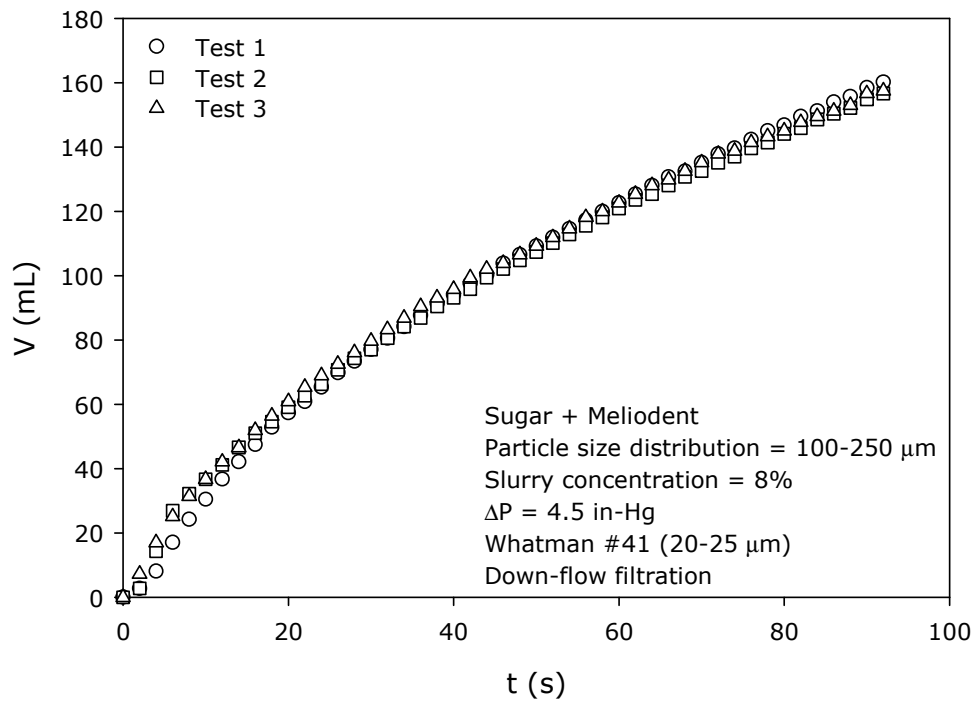
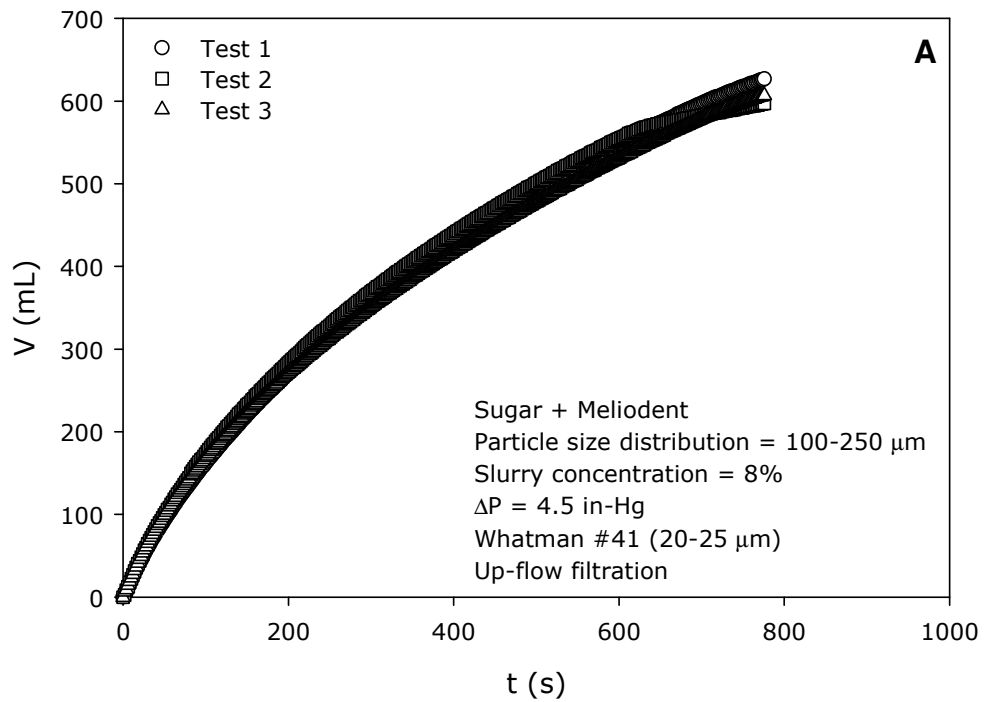


**Figure A.2.** V vs. t for sugar + Meliodent (A) Up-flow mode (B) Down-flow mode

## II. Effect of particle size distribution

**Table A.1.** Effect of particle size distribution (I)

Operational conditions		Water+Meliodent	Water+Meliodent	Water+Meliodent
<b>Particle Size Distribution</b>		75-100 μm	175-250 μm	Mixed (50%, 175-250 μm + 50%, 75-100 μm)
<b>Slurry concentration</b>		4%	4%	4%
<b>Filter Paper</b>		Whatman #41	Whatman #41	Whatman #41
<b>P (in-Hg)</b>	<b>Mode</b>			
<b>4.5</b>	<b>Up</b>	$\frac{dt}{dV} = 0.6 \times 10^{-3}V + 0.1$	$\frac{dt}{dV} = 0.7 \times 10^{-3}V + 0.1$	$\frac{dt}{dV} = 0.6 \times 10^{-3}V + 0.1$
	<b>Down</b>	$\frac{dt}{dV} = 1.8 \times 10^{-3}V + 0.2$	$\frac{dt}{dV} = 1.3 \times 10^{-3}V + 0.2$	$\frac{dt}{dV} = 1.2 \times 10^{-3}V + 0.2$
<b>9</b>	<b>Up</b>	$\frac{dt}{dV} = 0.4 \times 10^{-3}V + 0.1$	$\frac{dt}{dV} = 0.3 \times 10^{-3}V + 0.1$	$\frac{dt}{dV} = 0.3 \times 10^{-3}V + 0.1$
	<b>Down</b>	$\frac{dt}{dV} = 0.5 \times 10^{-3}V + 0.1$	$\frac{dt}{dV} = 3.5 \times 10^{-3}V + 0.1$	$\frac{dt}{dV} = 0.6 \times 10^{-3}V + 0.1$

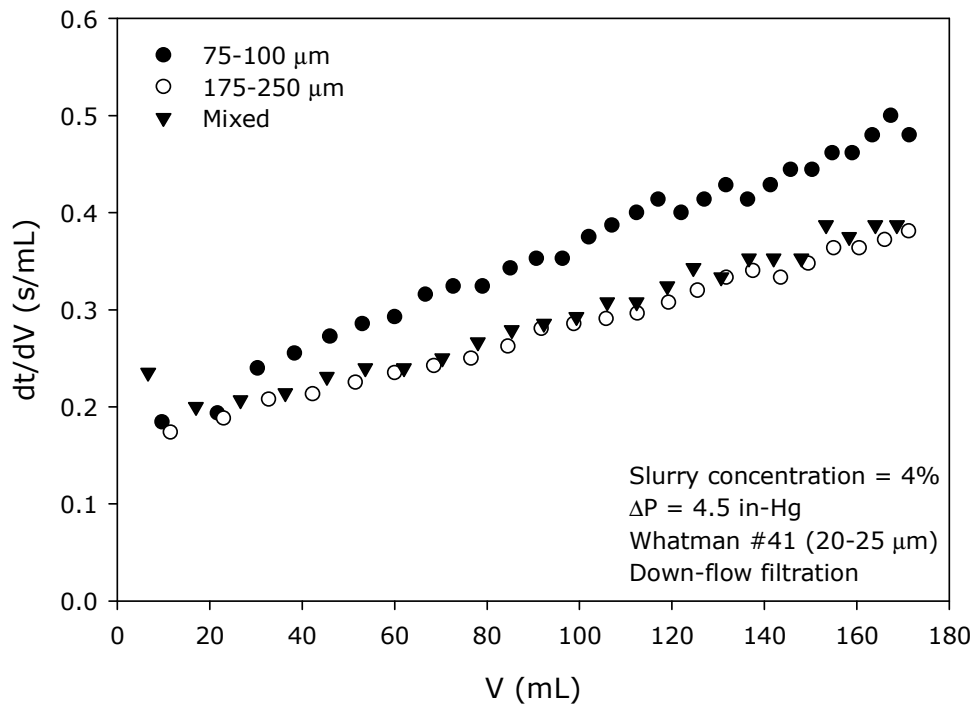


**Figure A.3.** dt/dV vs. V plot for different particle sized slurries at 4.5 in-Hg

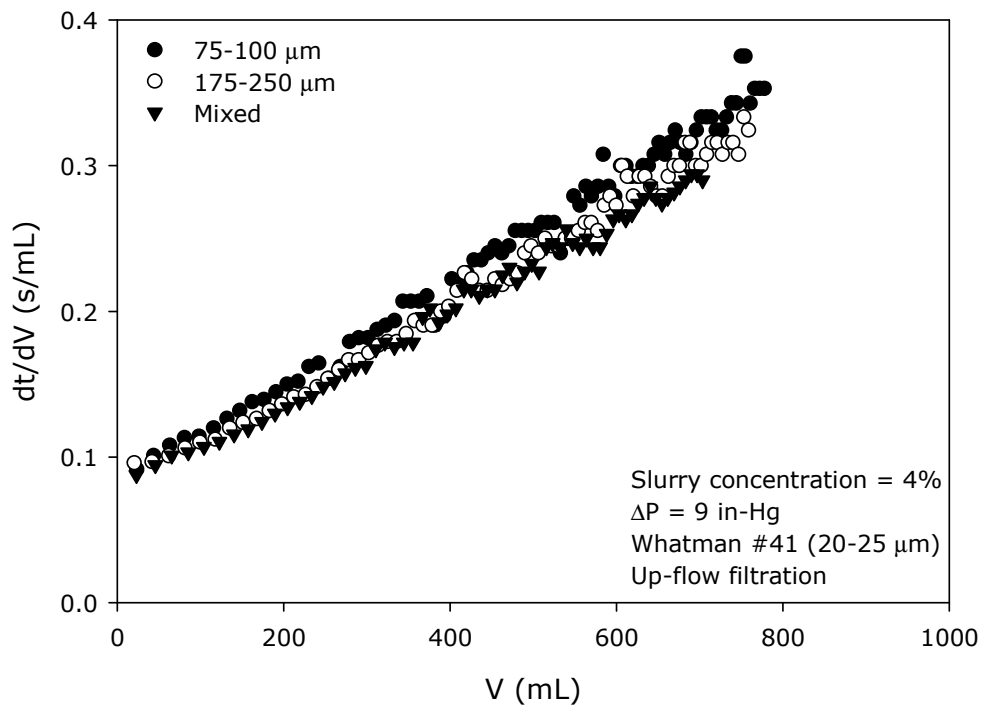


**Figure A.4.** dt/dV vs. V plot for different particle sized slurries at 9 in-Hg (up-flow mode)

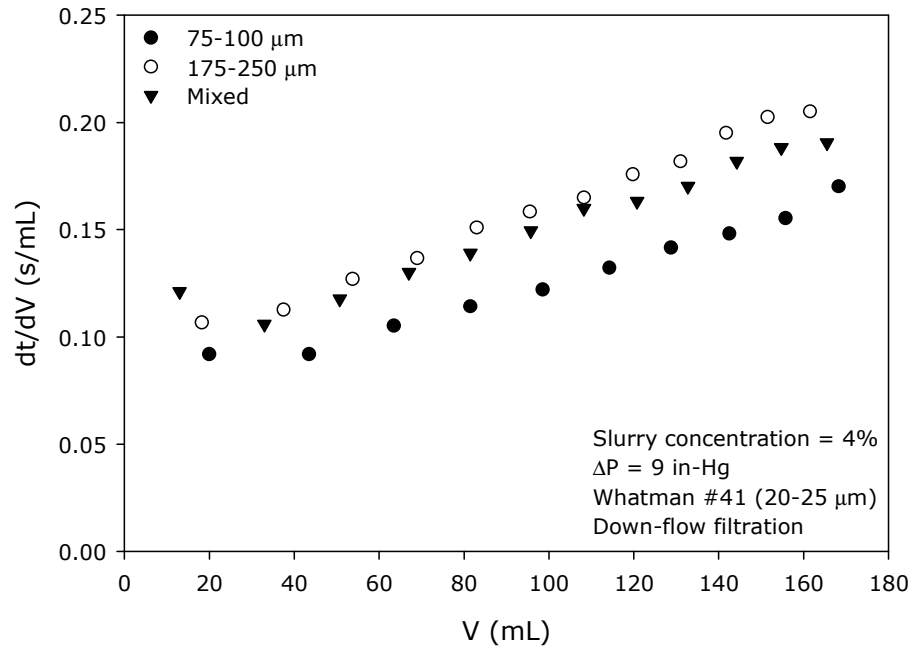


**Figure A.5.** dt/dV vs. V plot for different particle sized slurries at 9 in-Hg (down-flow mode)

### III. Effect of slurry concentration

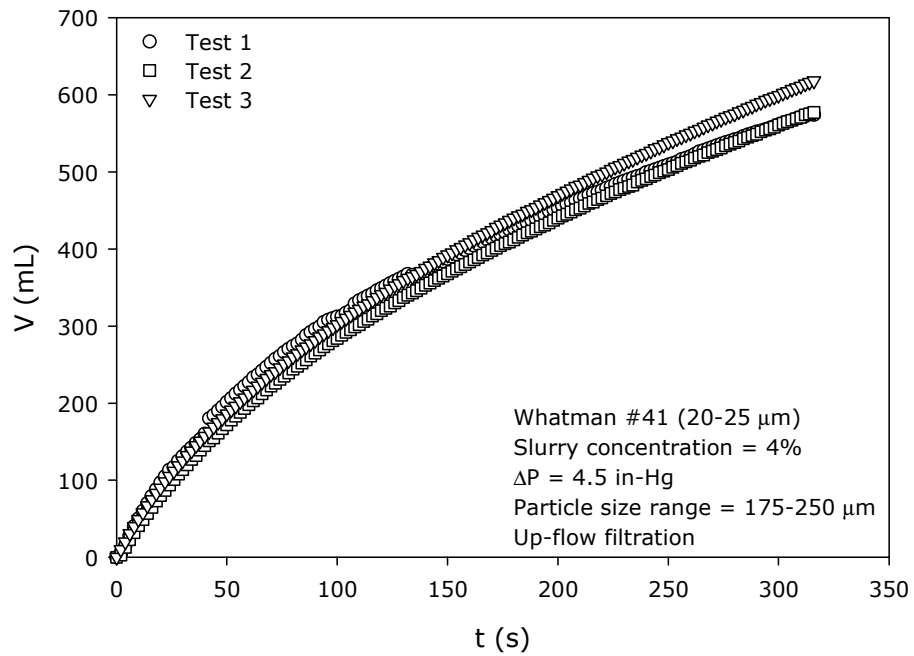


**Figure A.6.** V vs. t plot for 4% slurry at 4.5 in-Hg- Effect of slurry concentration

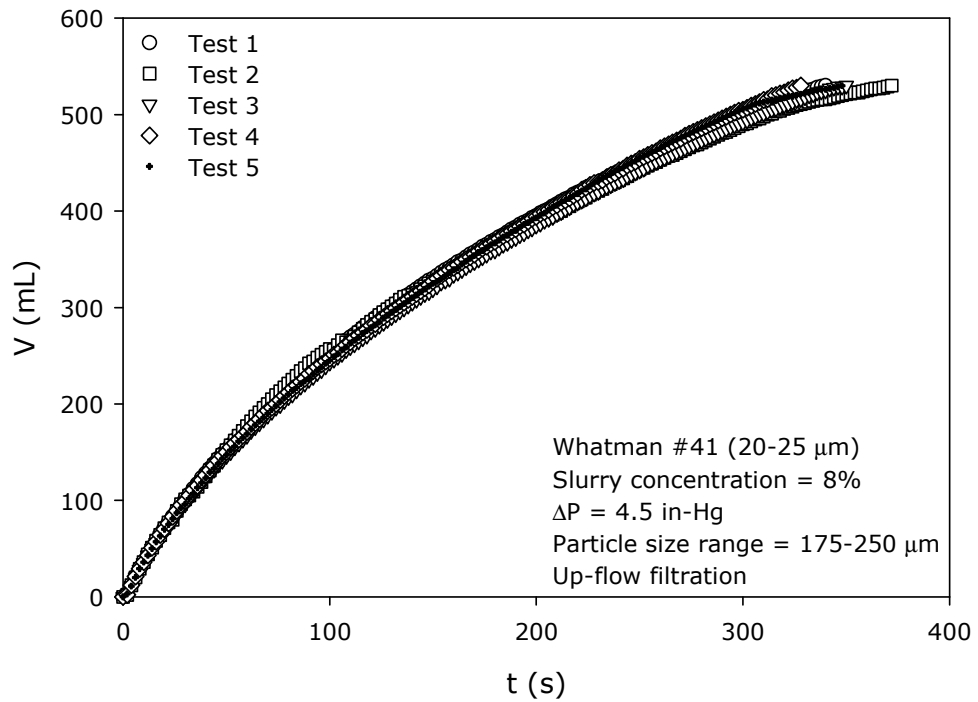


**Figure A.7.** V vs. t plot for 8% slurry at 4.5 in-Hg- Effect of slurry concentration

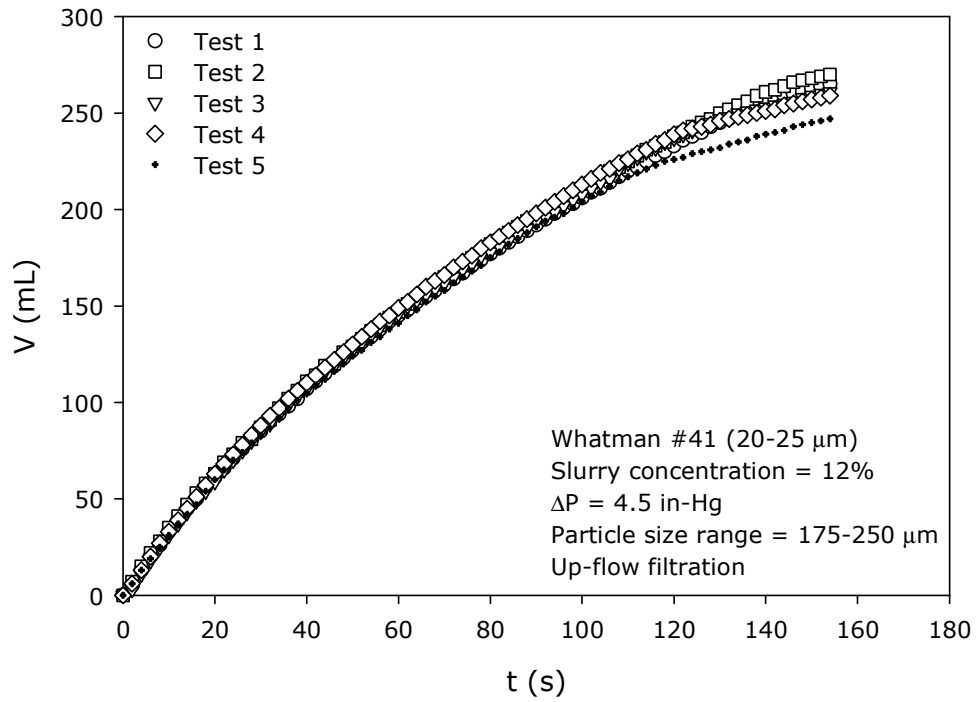


**Figure A.8.** V vs. t plot for 12% slurry at 4.5 in-Hg- Effect of slurry concentration

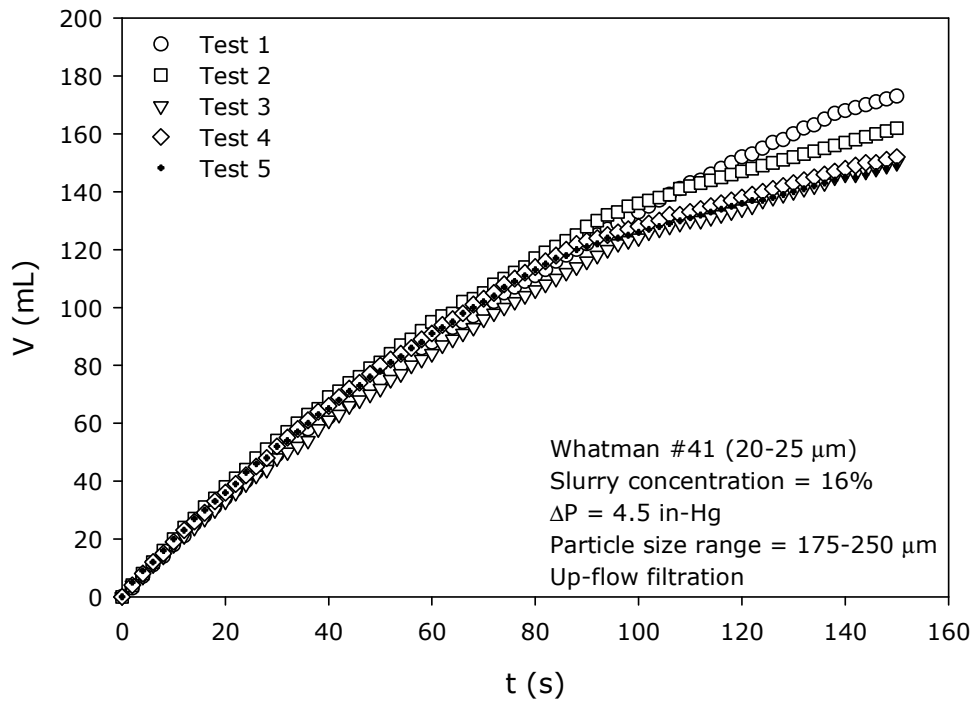


**Figure A.9.** V vs. t plot for 16% slurry at 4.5in-Hg- Effect of slurry concentration

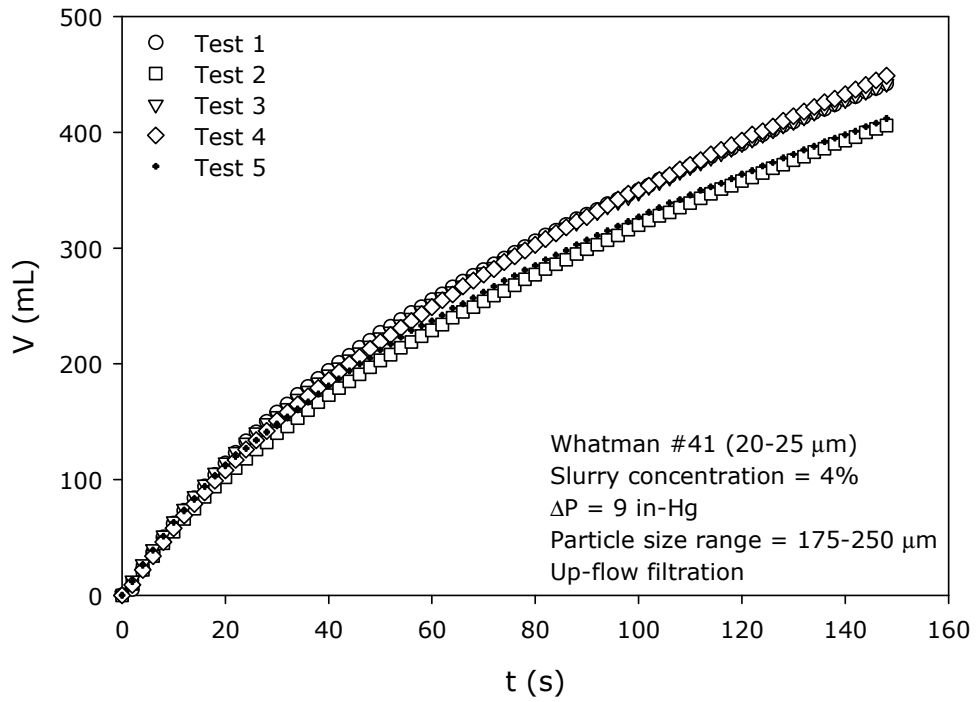


**Figure A.10.** V vs. t plot for 4% slurry at 9 in-Hg - Effect of slurry concentration

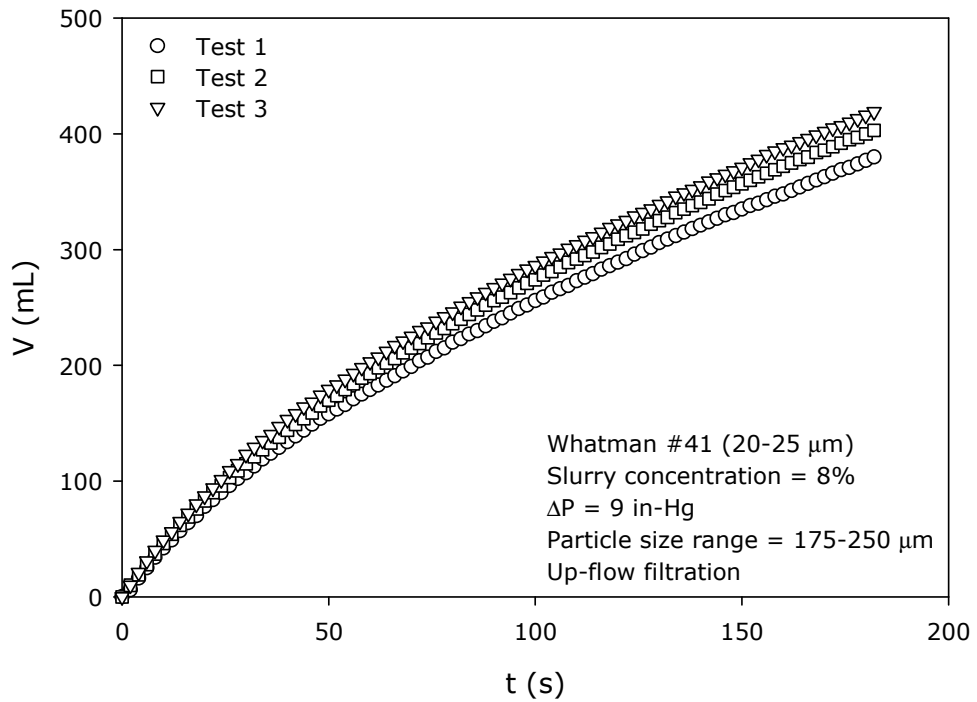


**Figure A.11.** V vs. t plot for 8% slurry at 9 in-Hg - Effect of slurry concentration

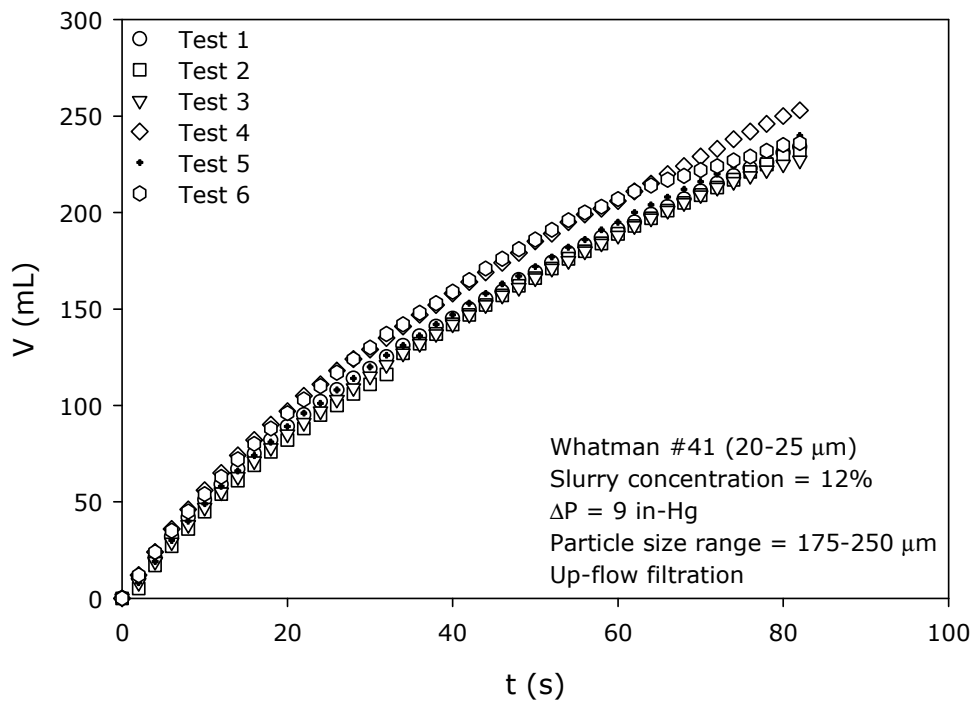


**Figure A.12.** V vs. t plot for 12% slurry at 9 in-Hg-Effect of slurry concentration

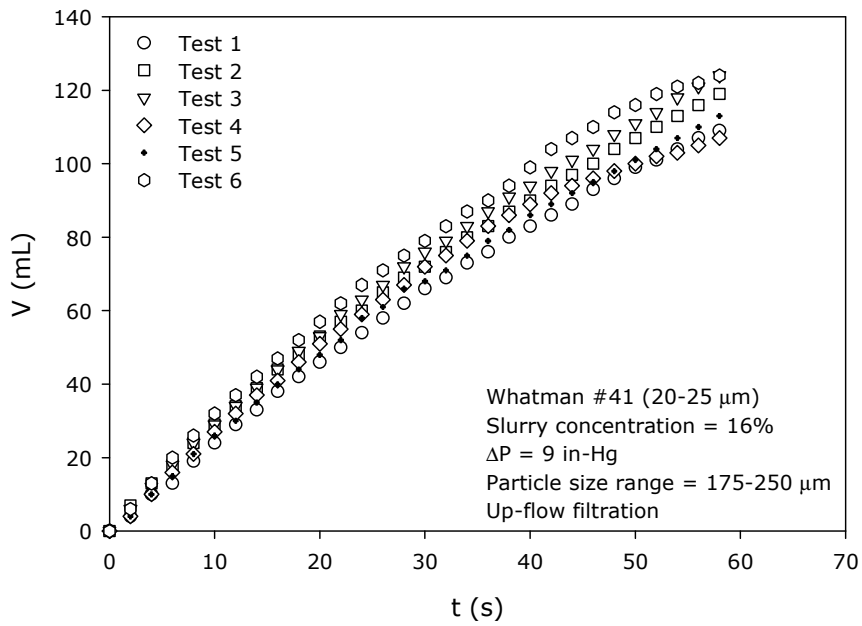


**Figure A.13.** V vs. t plot for 16% slurry at 9 in-Hg-Effect of slurry concentration

**IV. Effect of particle size and pore size of the filter medium**

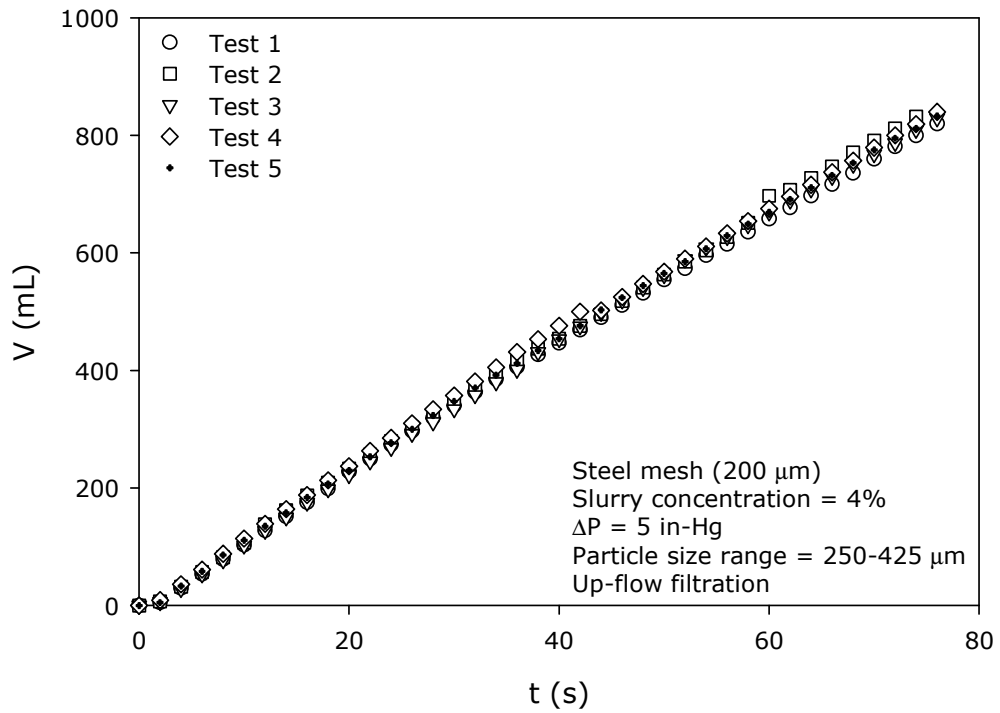


**Figure A.14.** V vs. t plot for steel mesh-Effect of particle size-pore size (I)

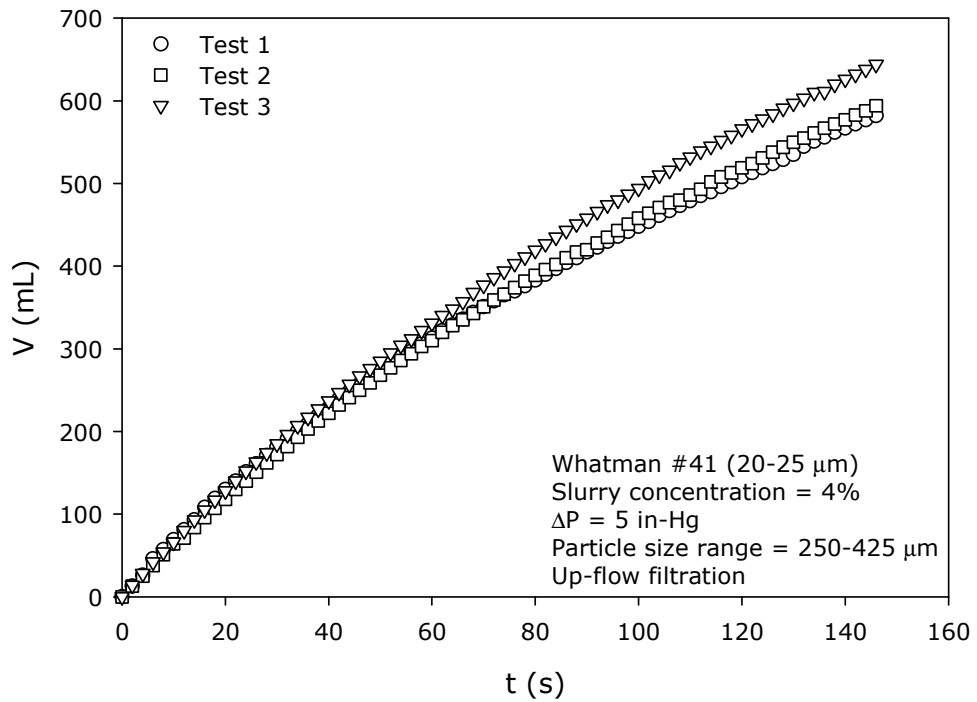


**Figure A.15.** V vs. t plot for W#41-Effect of particle size-pore size (I)

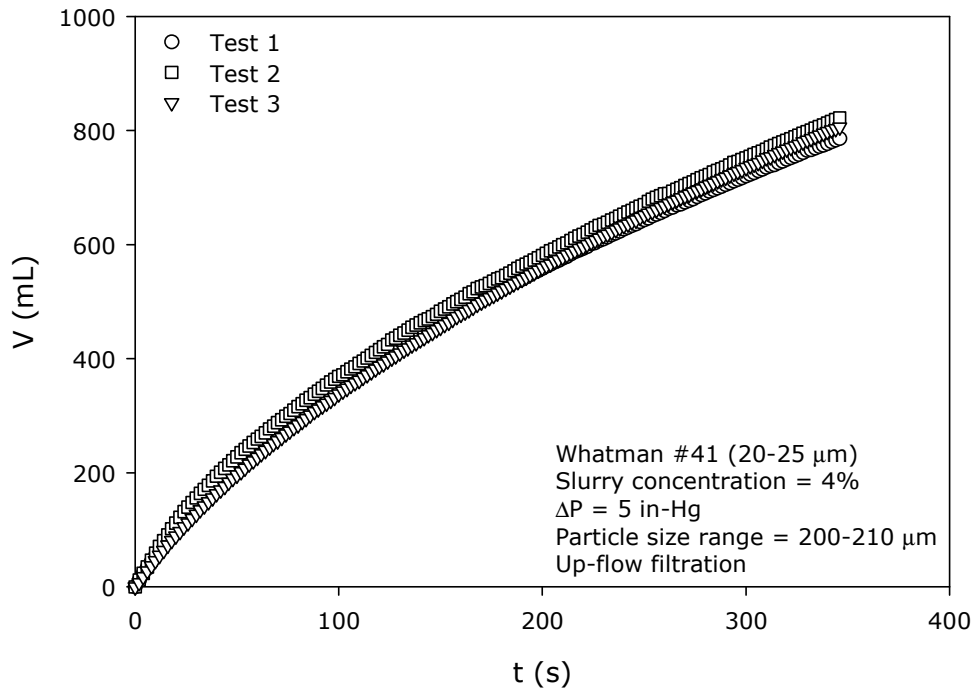


**Figure A.16.** V vs. t plot for W#41 (4%, 5 in-Hg)-Effect of particle size-pore size (III)

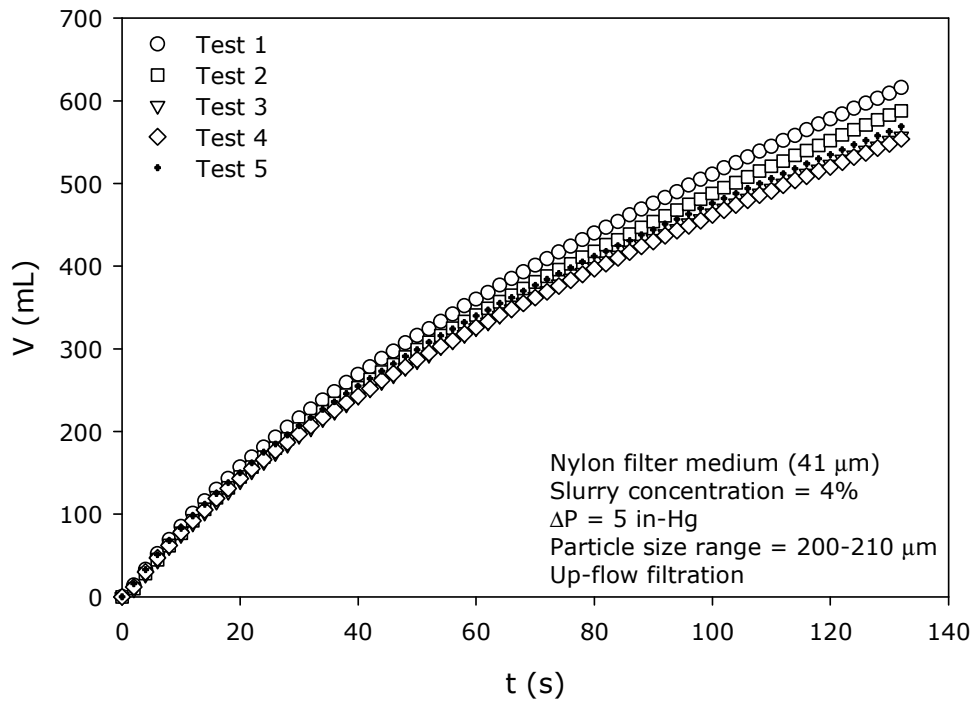


**Figure A.17.** V vs. t plot for nylon filter medium (4%, 5 in-Hg)-Effect of particle size-pore size (III)

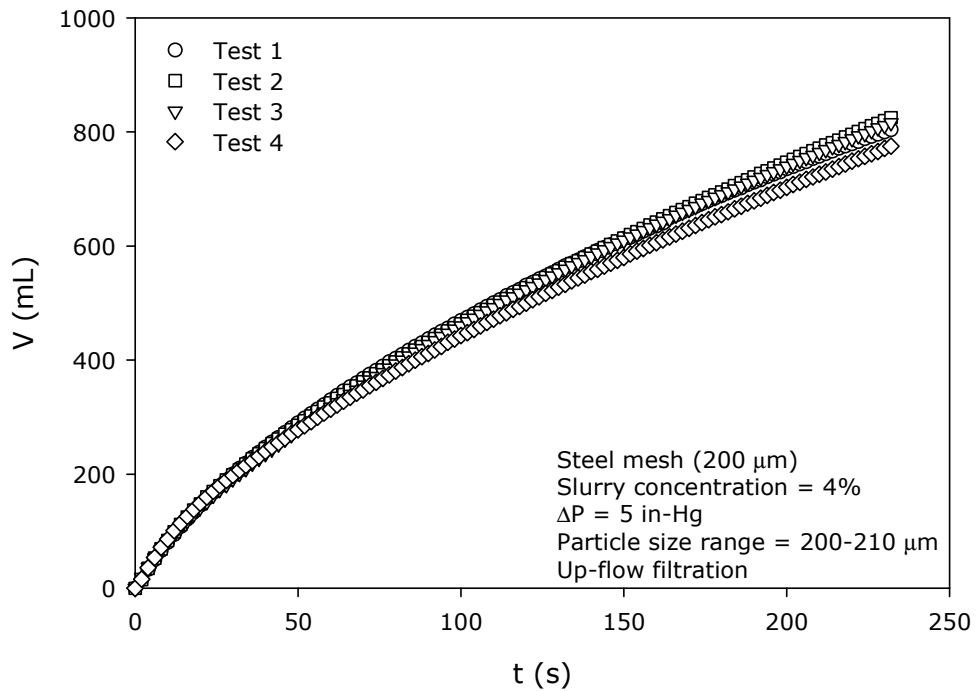


**Figure A.18.** V vs. t plot for steel mesh (4%, 5 in-Hg)-Effect of particle size-pore size (III)

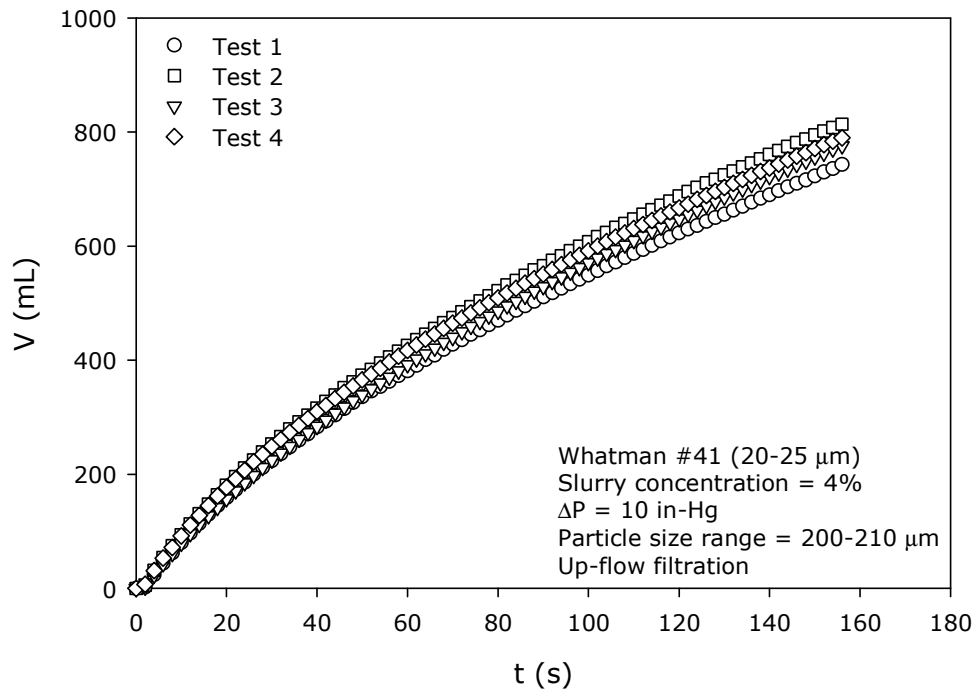


**Figure A.19.** V vs. t plot for W#41 (4%, 10 in-Hg)-Effect of particle size-pore size (III)

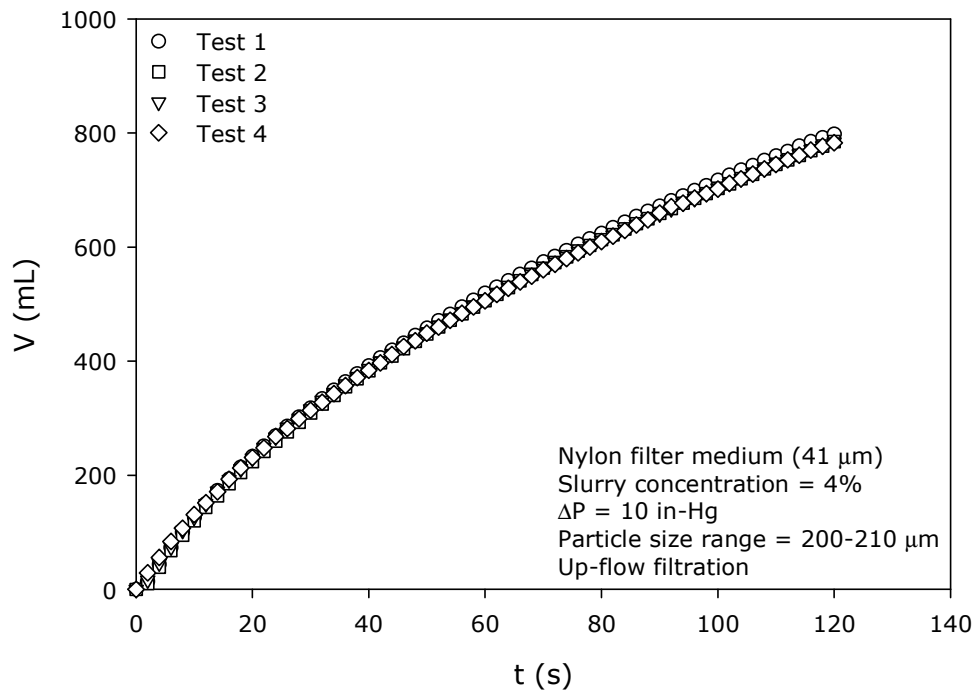


**Figure A.20.** V vs. t plot for nylon filter medium (4%, 10 in-Hg)-Effect of particle size-pore size (III)

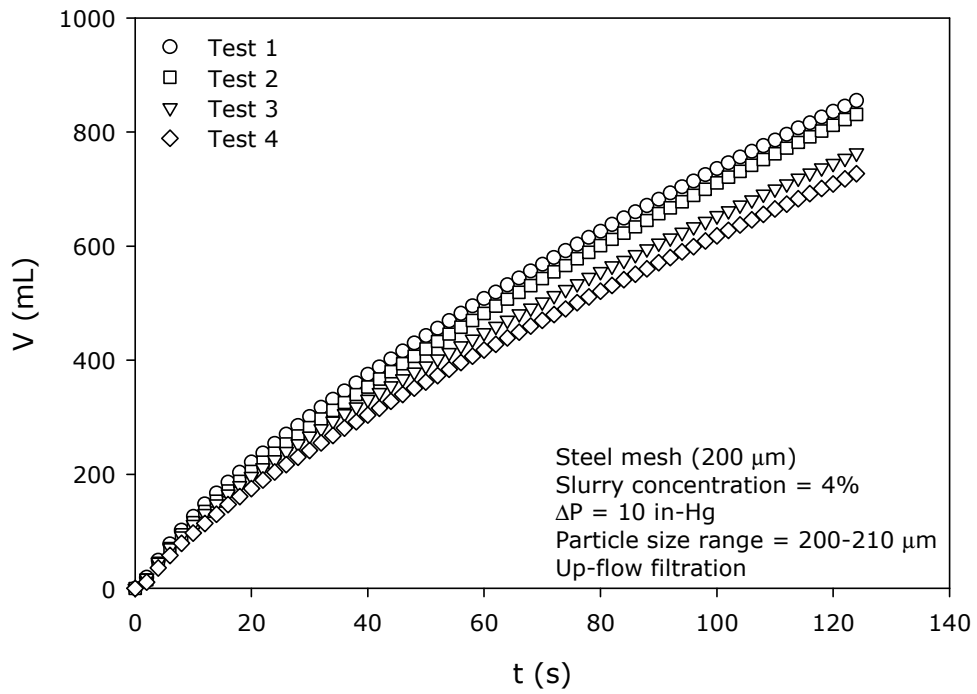


**Figure A.21.** V vs. t plot for steel mesh (4%, 10 in-Hg)-Effect of particle size-pore size (III)

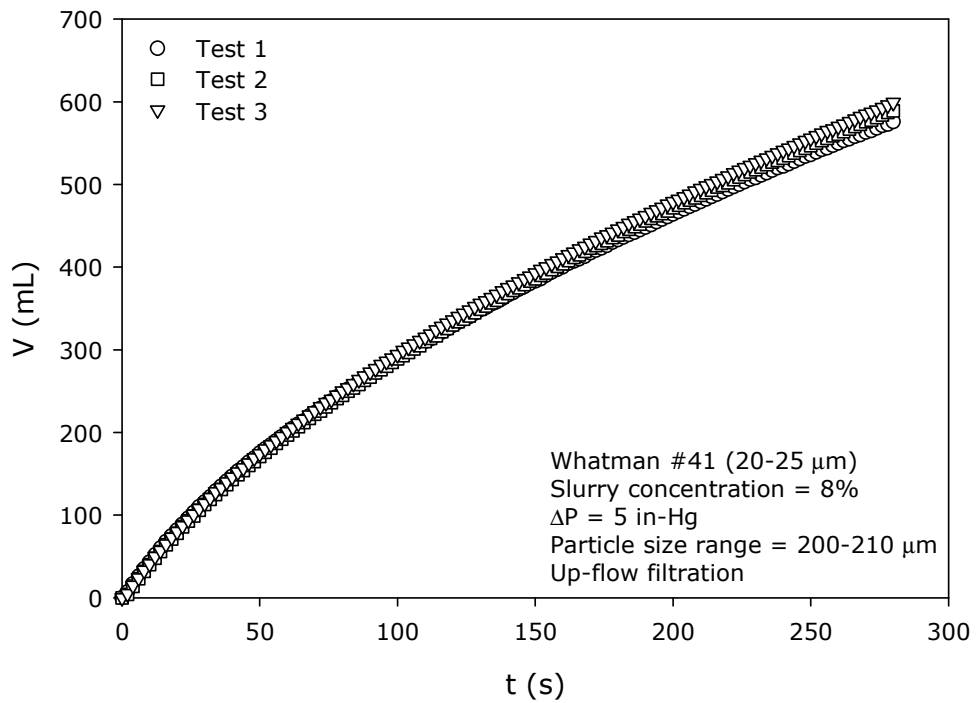


**Figure A.22.** V vs. t plot for W#41 (8%, 5 in-Hg)-Effect of particle size-pore size (III)

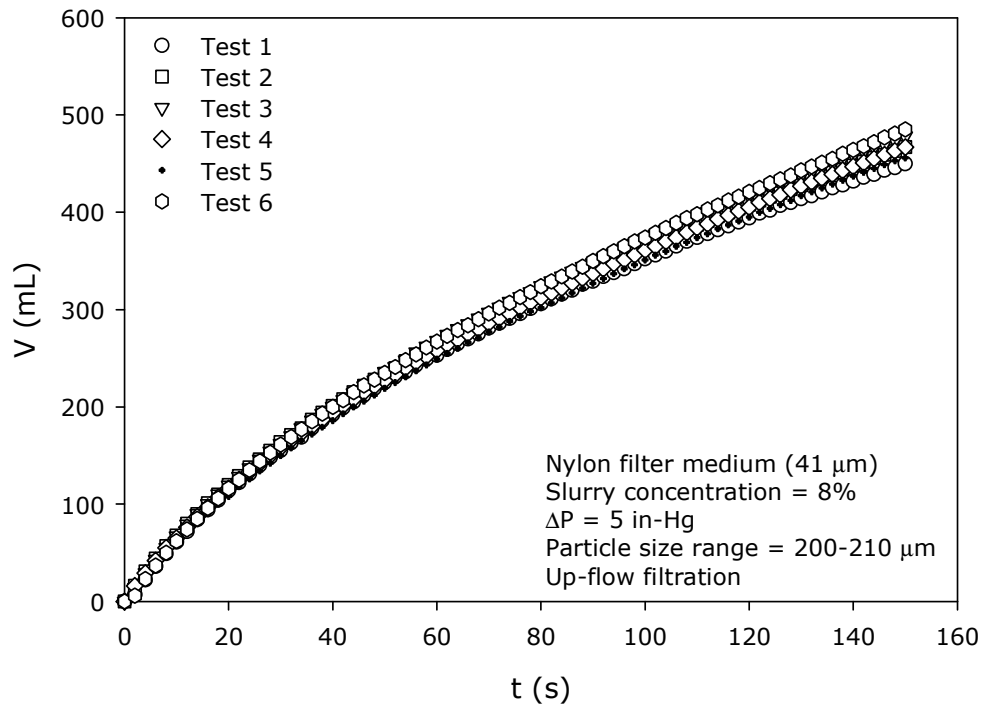


**Figure A.23.** V vs. t plot for nylon filter medium (8%, 5 in-Hg)-Effect of particle size-pore size (III)

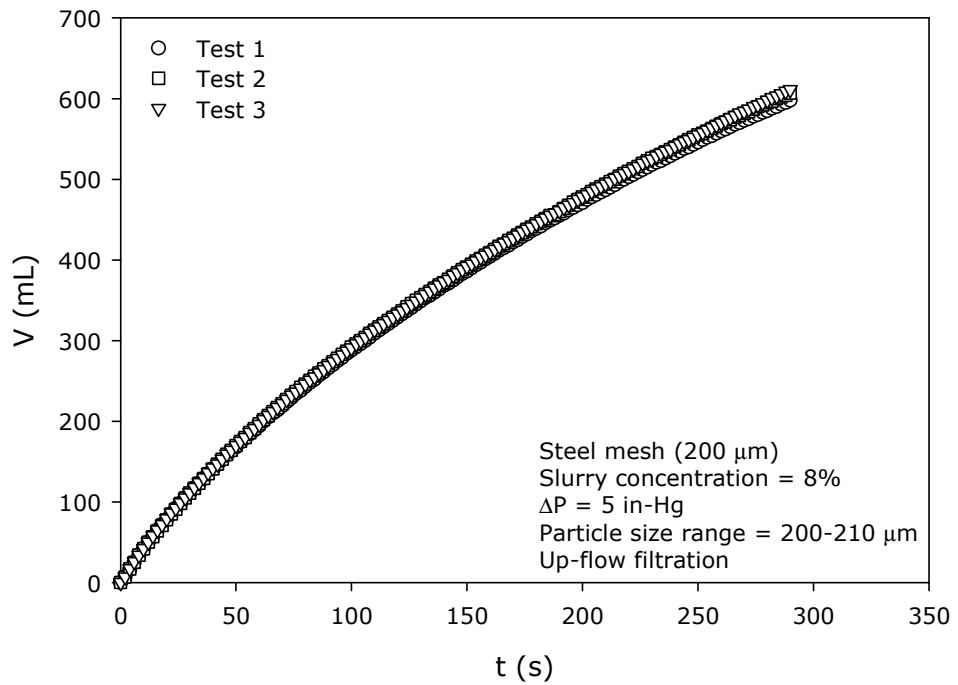


**Figure A.24.** V vs. t plot for steel mesh (8%, 5 in-Hg)-Effect of particle size-pore size (III)

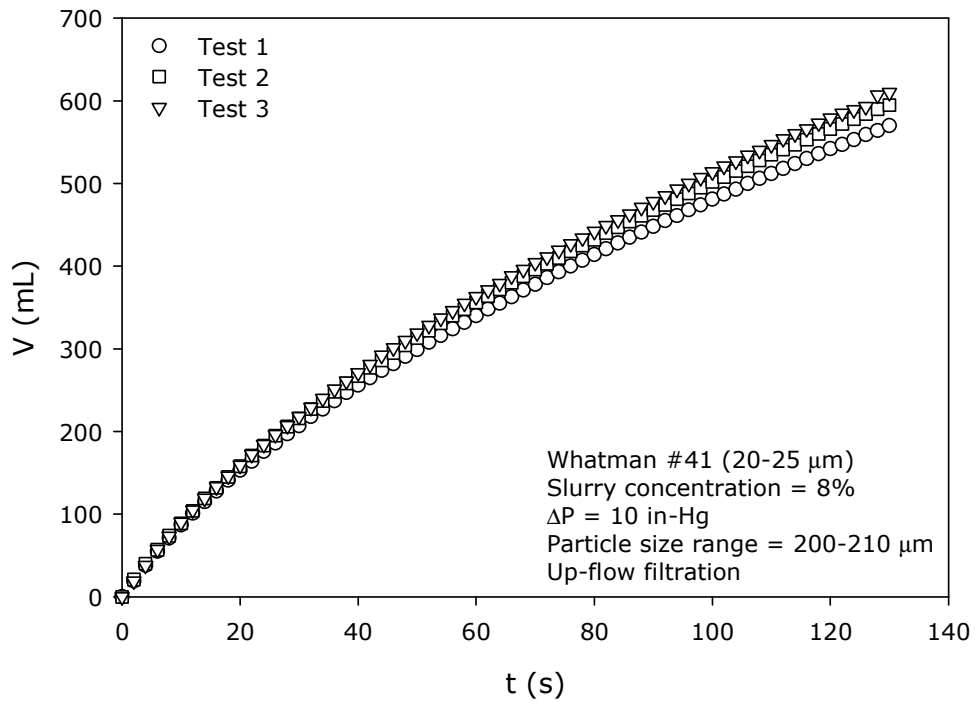


**Figure A.25.** V vs. t plot for W#41 (8%, 10 in-Hg)-Effect of particle size-pore size (III)

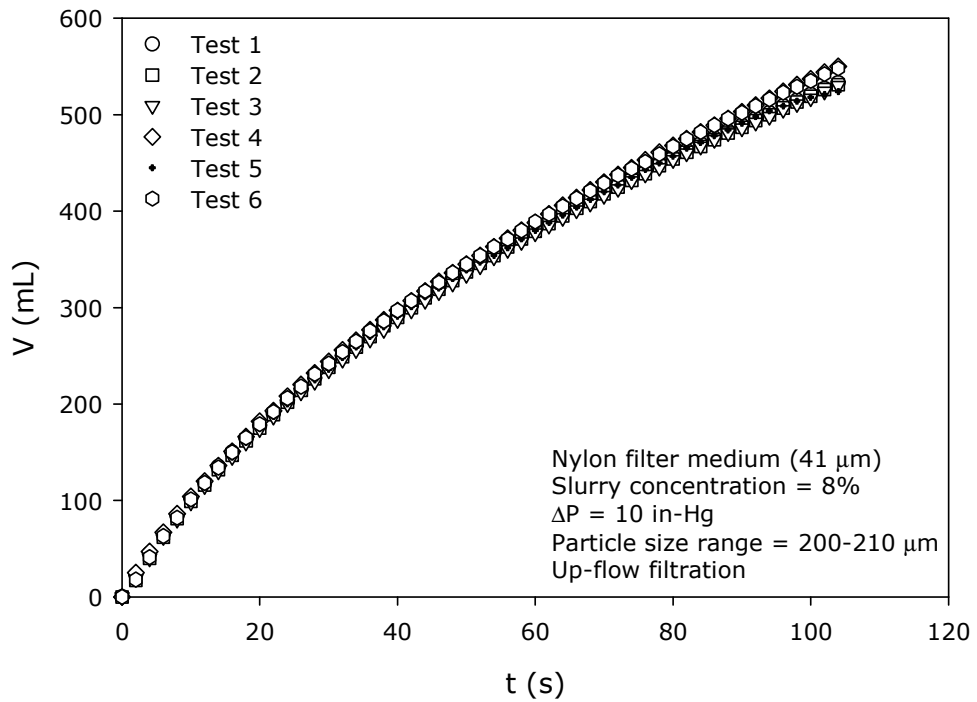


**Figure A.26.** V vs. t plot for nylon filter medium (8%, 10 in-Hg)-Effect of particle size-pore size (III)

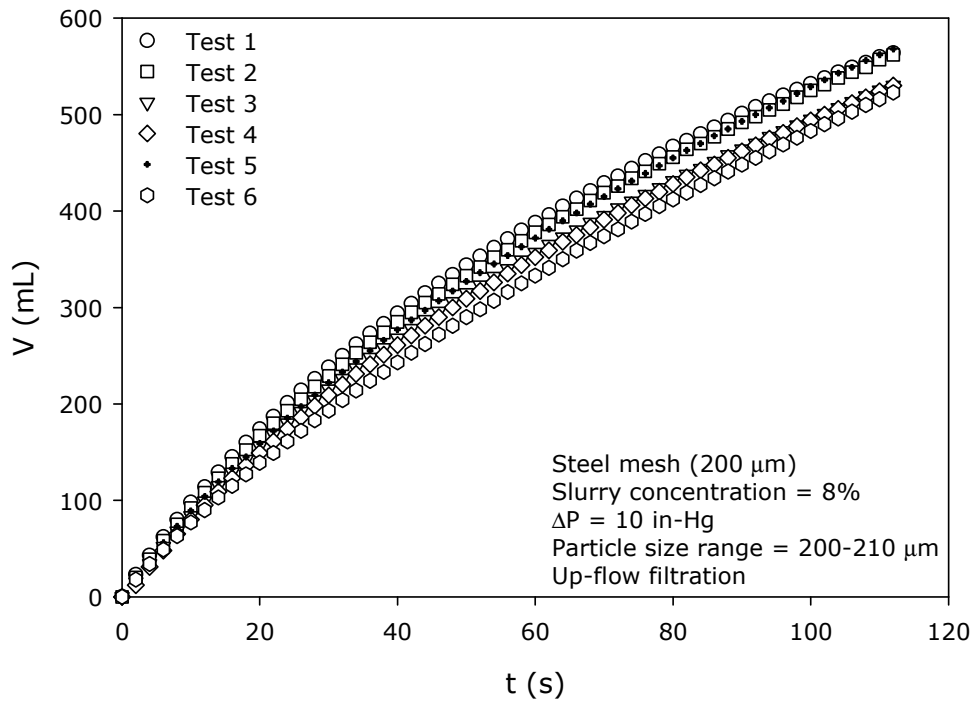


**Figure A.27.** V vs. t plot for steel mesh (8%, 10 in-Hg)-Effect of particle size-pore size (III)

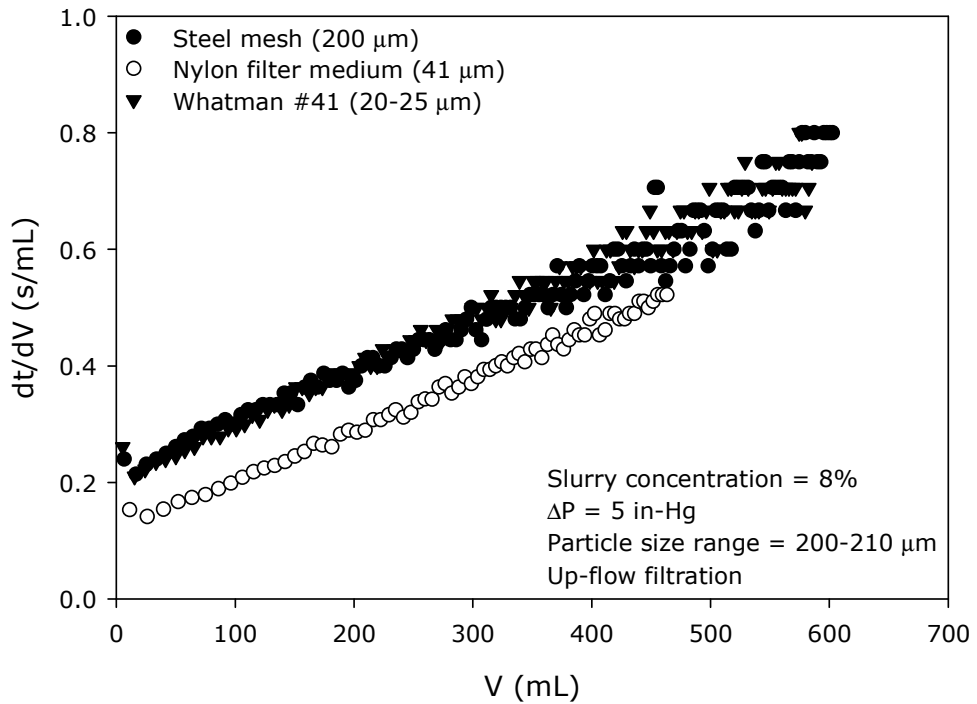


**Figure A.28.** dt/dV vs. V plot for 8% slurry at 5 in-Hg -Effect of particle size-pore size (III)

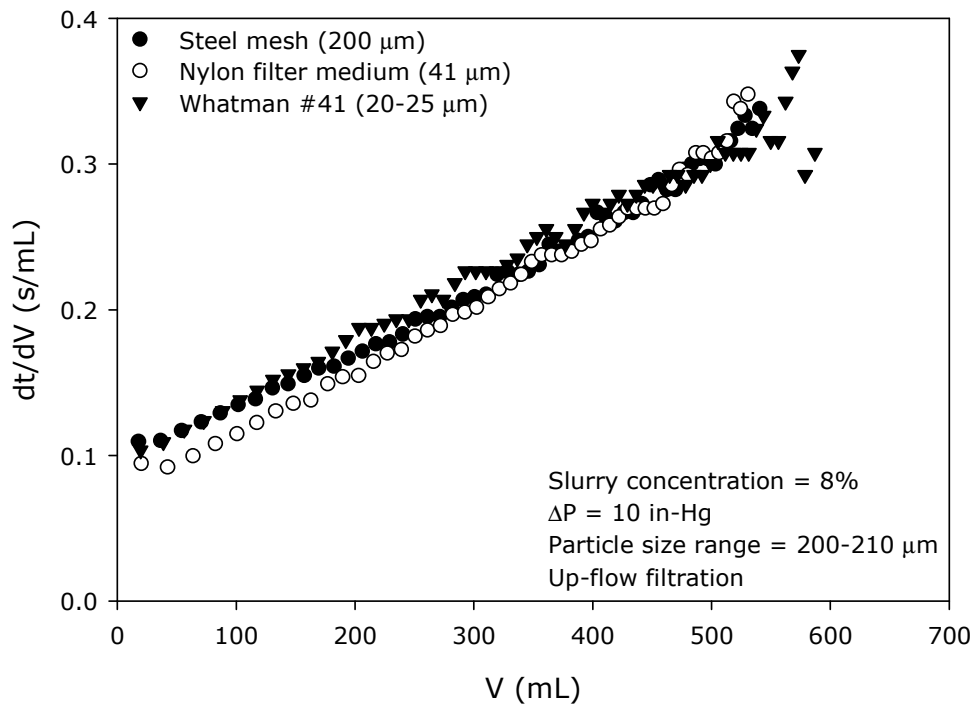


**Figure A.29.** dt/dV vs. V plot for 8% slurry at 10 in-Hg -Effect of particle size-pore size (III)

## **APPENDIX B**

### **MULTIPHASE FILTRATION LAW ANALYSIS**

This appendix provides the necessary data regarding the mathematical analysis of filtration process by the multiphase approach as given in Chapter 6, Section 6.3.

## Data Analysis Procedure

1. The experimental volume-time relationship is used to generate  $dt/dV$  vs.  $t$  plots ( $dt/dV$  values are calculated from experimental data as the ratio of time difference to volume difference). These plots indicate the deviation in the initial phase of the filtration process.
2. Time-volume data is best fitted in MATLAB and the resulting equations in the form  $t = aV^m + bV$  are obtained (the constraint for the parameter “ $b$ ” is set by considering the passage of particle-free water through the clean filter medium).
3. The  $d^2t/dV^2$  vs.  $t$  plots are generated from the fitted time-volume relationship ( $d^2t/dV^2$  physically represents the “change in resistance to flow”, thus, the change of this value with time shows the change of resistance developed at cake-septum interface with time). The time after which a nearly constant  $d^2t/dV^2$  value is reached is the  $K_oJ_o$  value that characterizes the overall filtration process (Eqn. 6.31).
4. The data belonging to this constant  $d^2t/dV^2$  phase predicts the filterability of the slurry under the defined operational conditions.
5. This procedure is followed both for the model slurries and the real sludge systems.

## I. Model Slurry Systems

### *Case I-Filter Medium Effect*

As a continuation of the first data set presented in Chapter 6, filtration tests under the conditions described in Table B.1, B.2, B.3 and B.4 are conducted.

**Table B.1.** Experimental conditions-Filter medium effect (I-B)

<b>Operational Conditions</b>	<b>Water + Meliodent</b>
Slurry concentration	4%
Pressure	5 in-Hg
Particle size distribution	200-210 $\mu\text{m}$
Mode of filtration	Up-flow
	W#41 (20-25 $\mu\text{m}$ )
Filter Medium	Nylon filter medium (41 $\mu\text{m}$ ) Steel mesh (200 $\mu\text{m}$ )

Figure B.1 is the  $dt/dV$  vs.  $V$  plot and Figures B.2, B.3, B.4 and B.5 are the  $dt/dV$  vs.  $t$  plots.

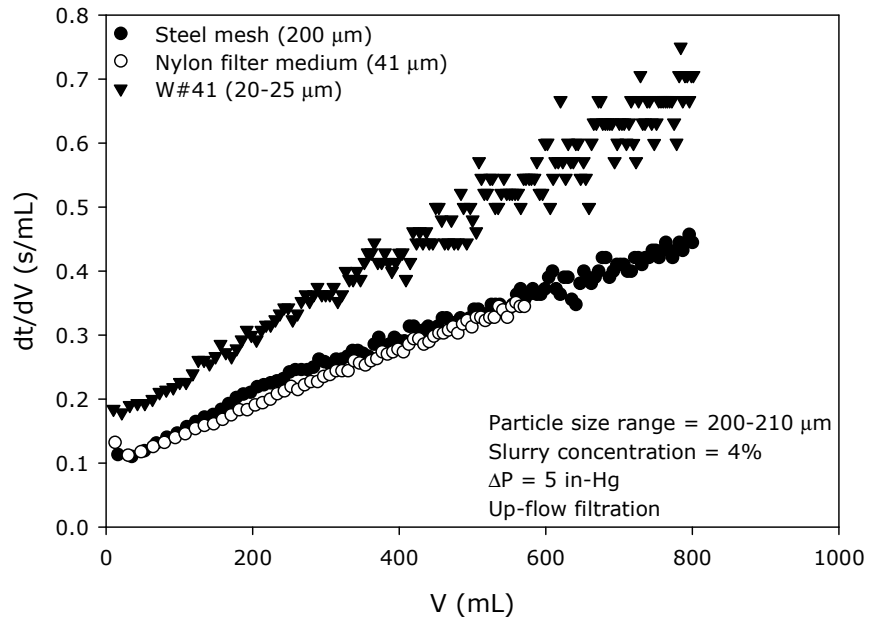


**Figure B.1.**  $dt/dV$  vs.  $V$  plot-Filter medium effect (I-B)

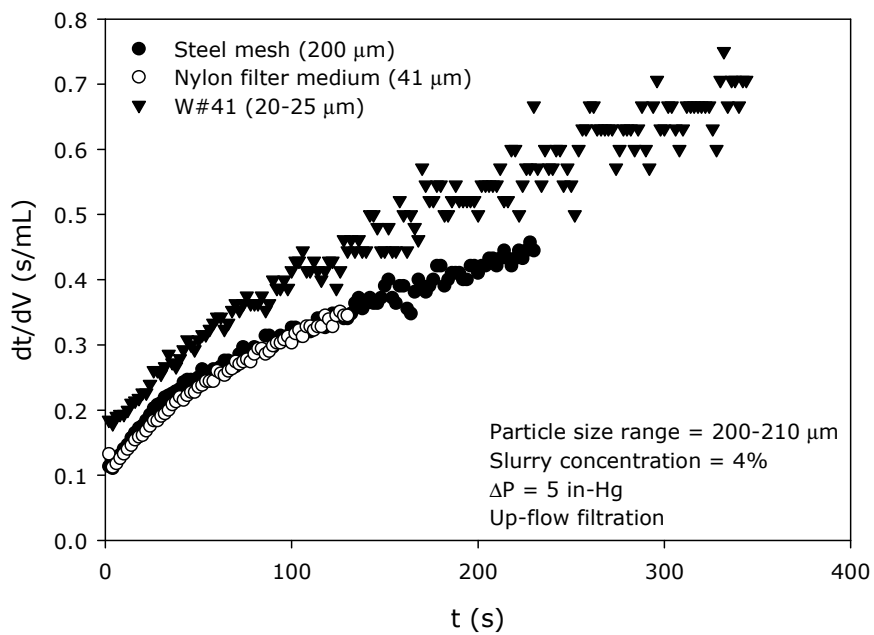


**Figure B.2.**  $dt/dV$  vs.  $t$  plot-Filter medium effect (I-B)

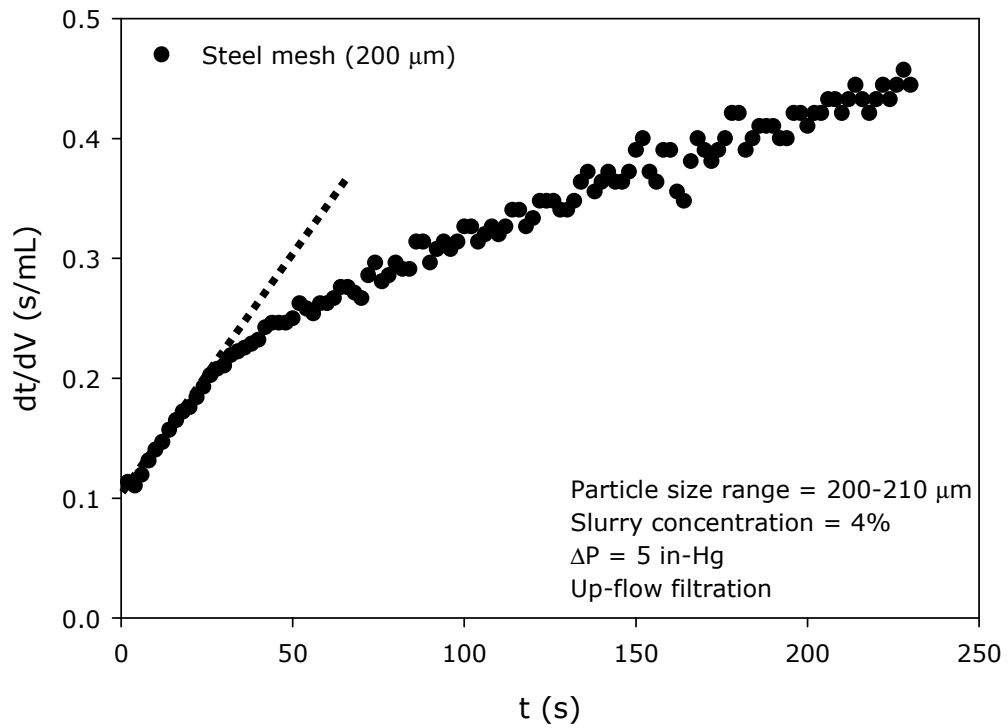


**Figure B.3.** dt/dV vs. t plot-Filter medium effect (I-B, steel mesh)

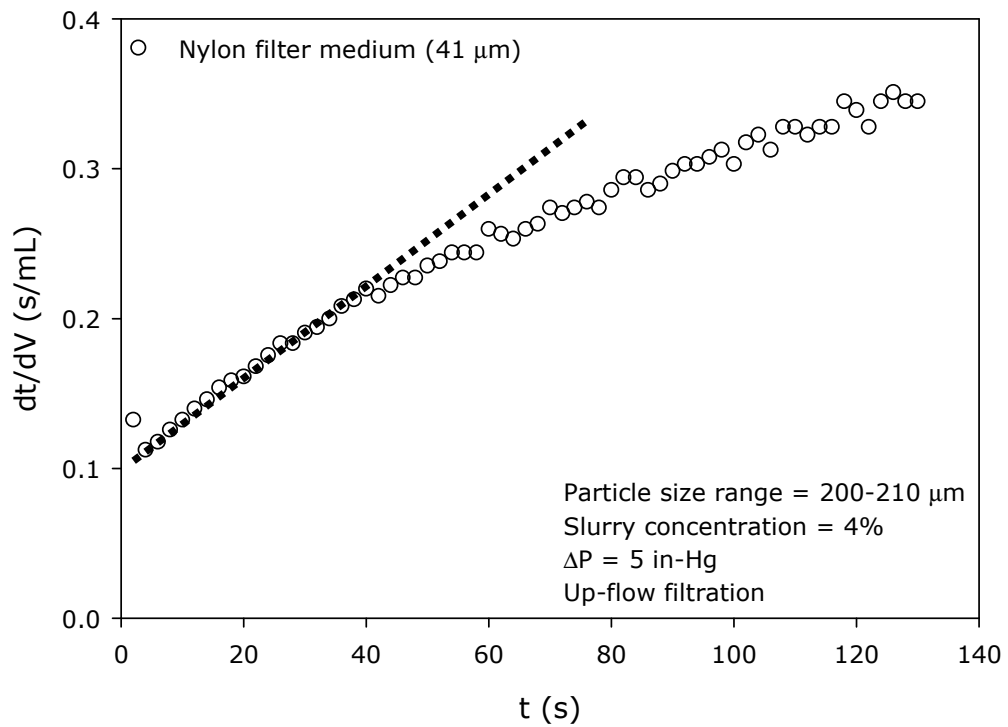


**Figure B.4.** dt/dV vs. t plot-Filter medium effect (I-B, nylon filter medium)

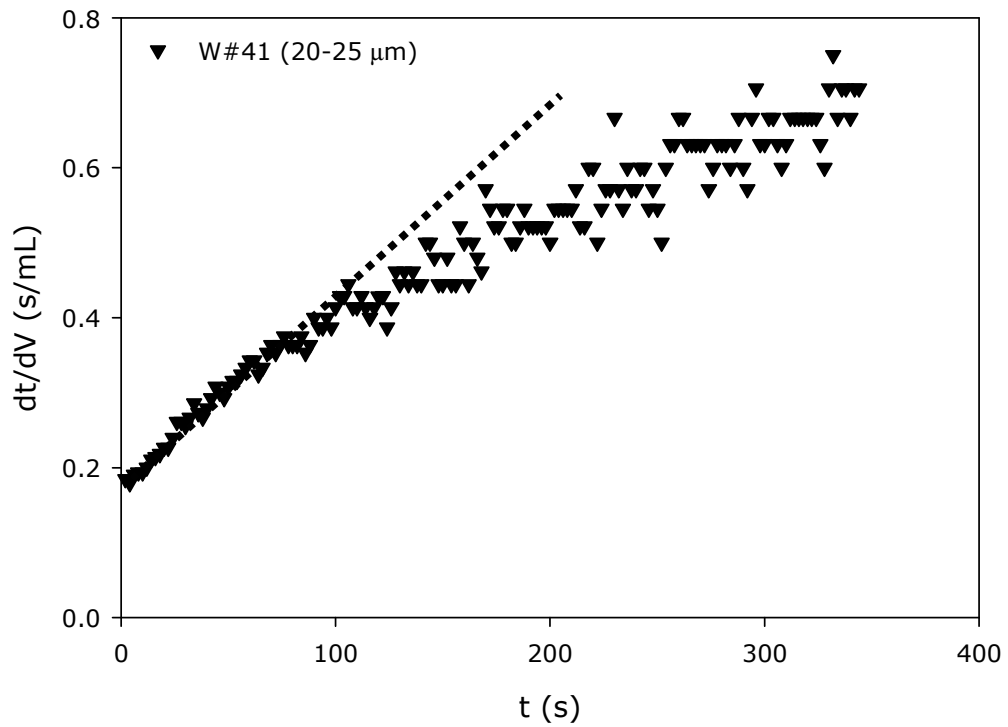


**Figure B.5.** dt/dV vs. t plot-Filter medium effect (I-B, W#41)

The MATLAB time-volume fit results for Case I are given in Table 6.6. The dt/dV vs. t plots of both the experimental data and the MATLAB-predicted data are presented in Figures B.6, B.7 and B.8 which show a good agreement. The  $d^2t/dV^2$  vs. t graphs are given in Figures B.9, B.10 and B.11.

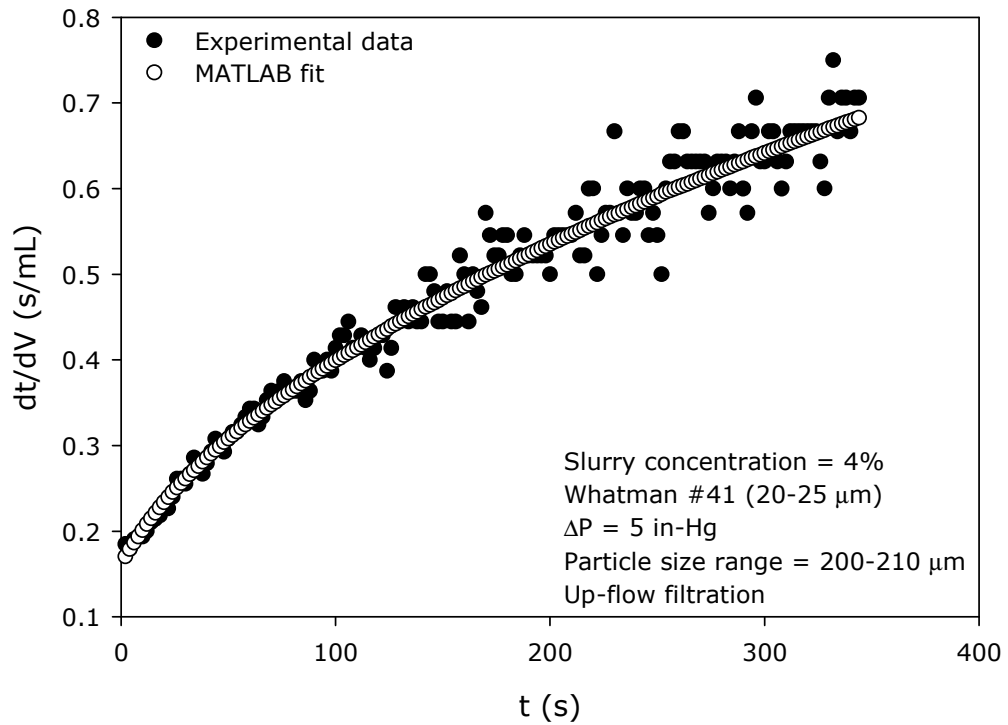


**Figure B.6.** Comparative  $dt/dV$  vs.  $t$  plot-Filter medium effect (I-B, W#41)

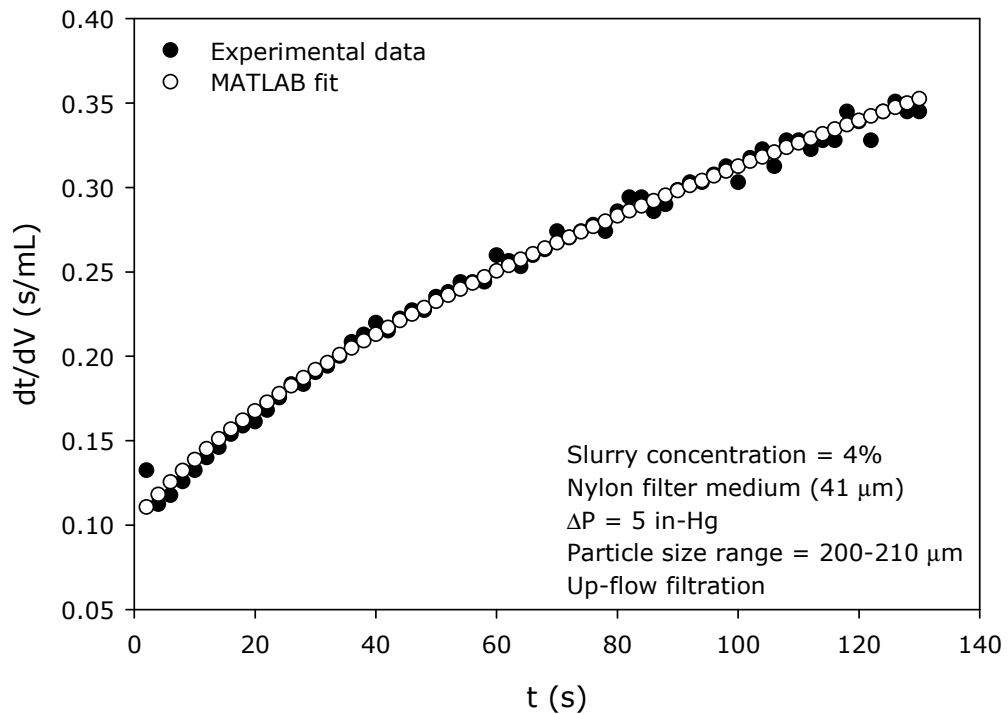


**Figure B.7.** Comparative  $dt/dV$  vs.  $t$  plot-Filter medium effect (I-B, nylon f.m)

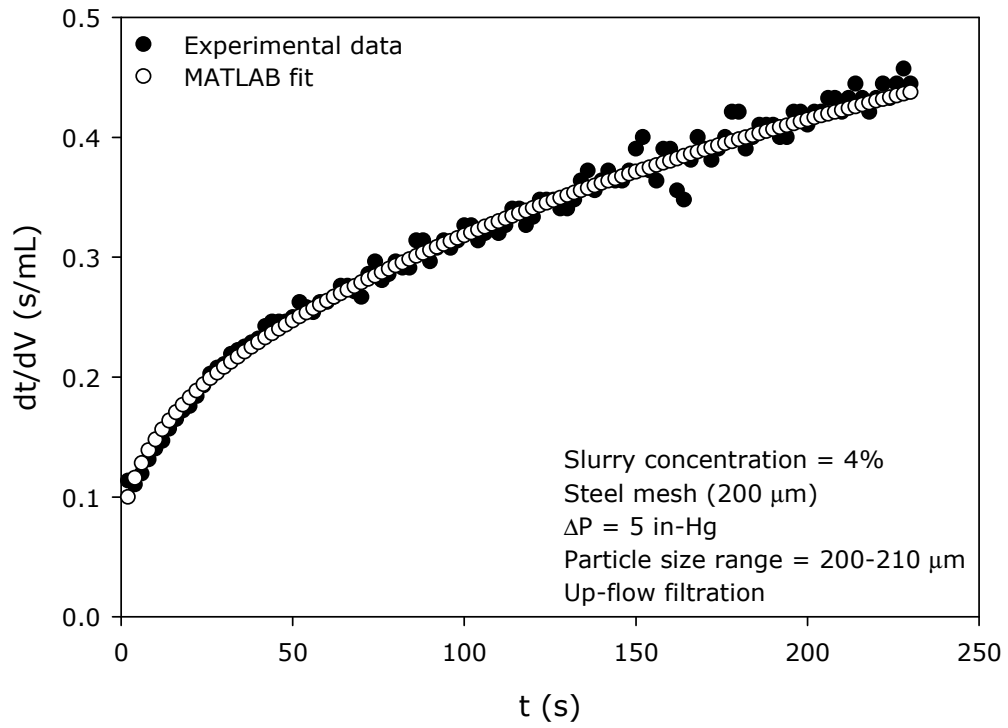


**Figure B.8.** Comparative  $dt/dV$  vs.  $t$  plot-Filter medium effect (I-B, steel mesh)

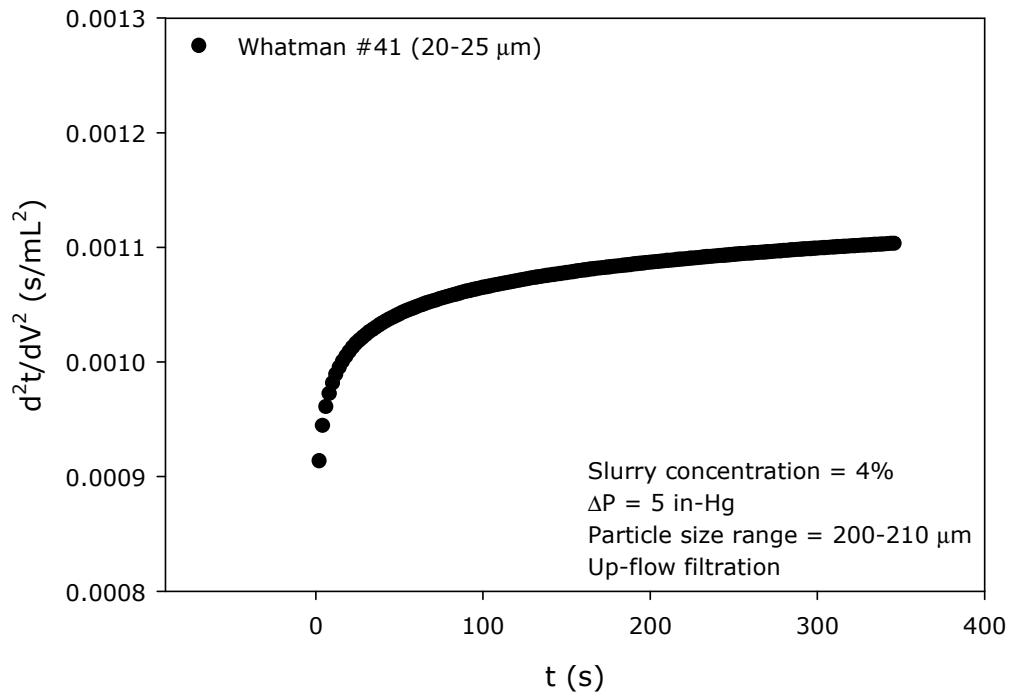


**Figure B.9.**  $d^2t/dV^2$  vs.  $t$  plot-Filter medium effect (I-B, W#41)

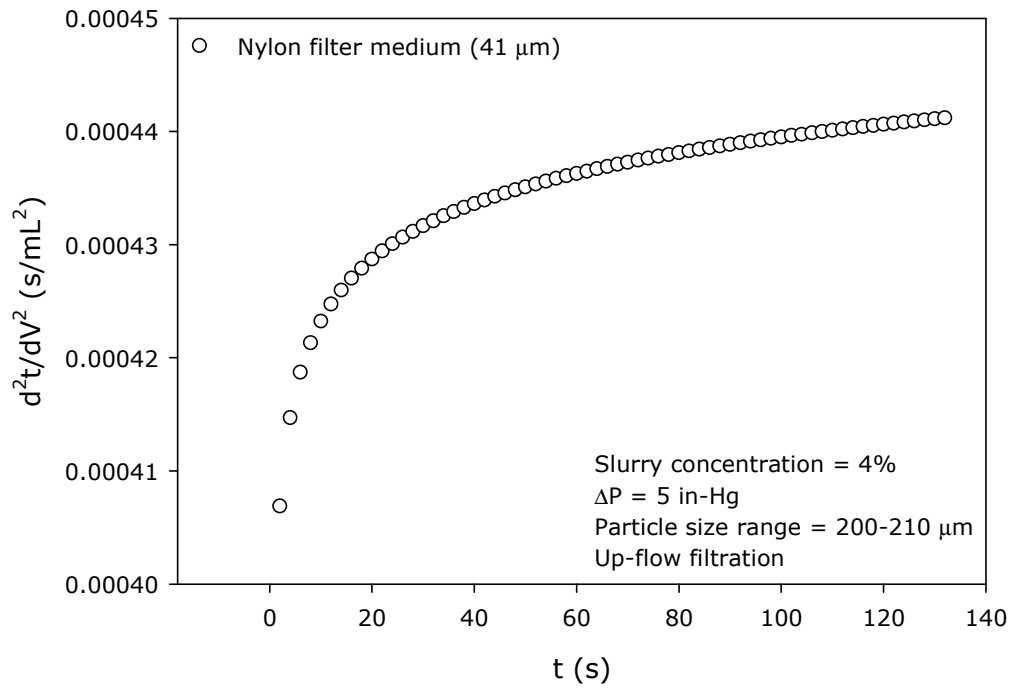


**Figure B.10.**  $d^2t/dV^2$  vs.  $t$  plot-Filter medium effect (I-B, nylon f.m)

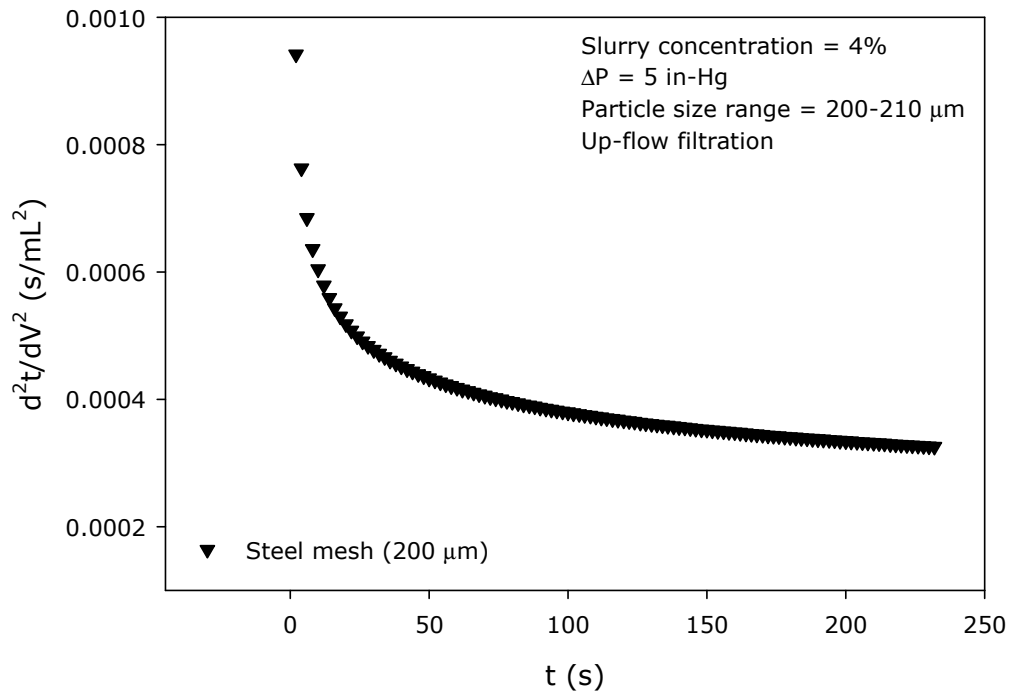


**Figure B.11.**  $d^2t/dV^2$  vs.  $t$  plot-Filter medium effect (I-B, steel mesh)

**Table B.2.** Experimental conditions-Filter medium effect (I-C)

Operational Conditions	Water + Meliodent
Slurry concentration	4%
Pressure	10 in-Hg
Particle size distribution	200-210 $\mu\text{m}$
Mode of filtration	Up-flow
Filter Medium	W#41 (20-25 $\mu\text{m}$ ) Nylon filter medium (41 $\mu\text{m}$ ) Steel mesh (200 $\mu\text{m}$ )

Figure B.12 is the  $dt/dV$  vs.  $V$  plot and Figure B.13 is the  $dt/dV$  vs.  $t$  plot.

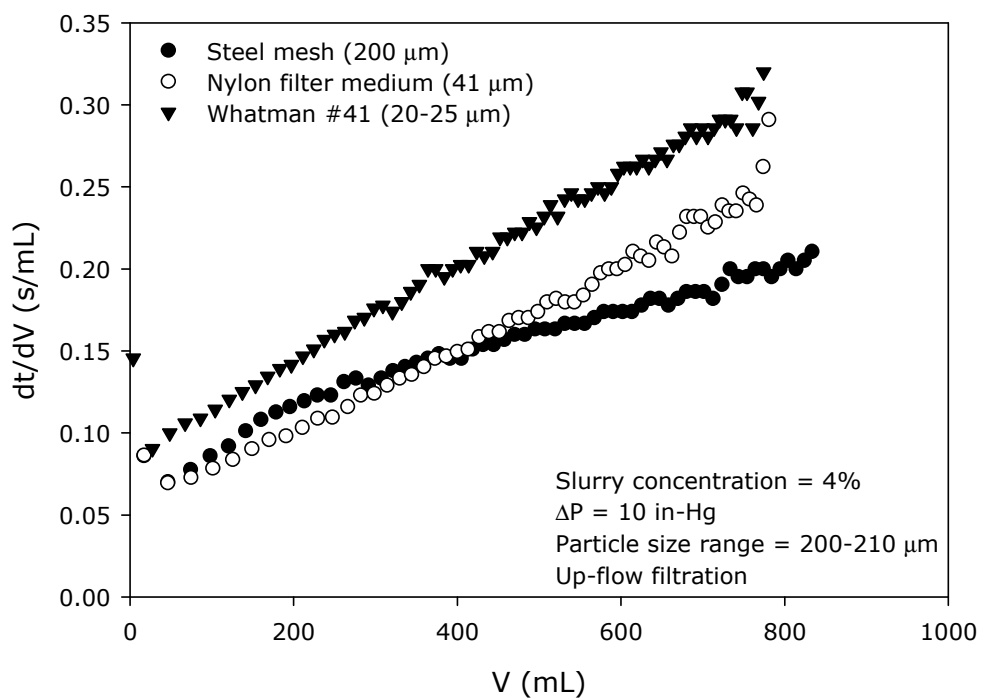


**Figure B.12.**  $dt/dV$  vs.  $V$  plot-Filter medium effect (I-C)

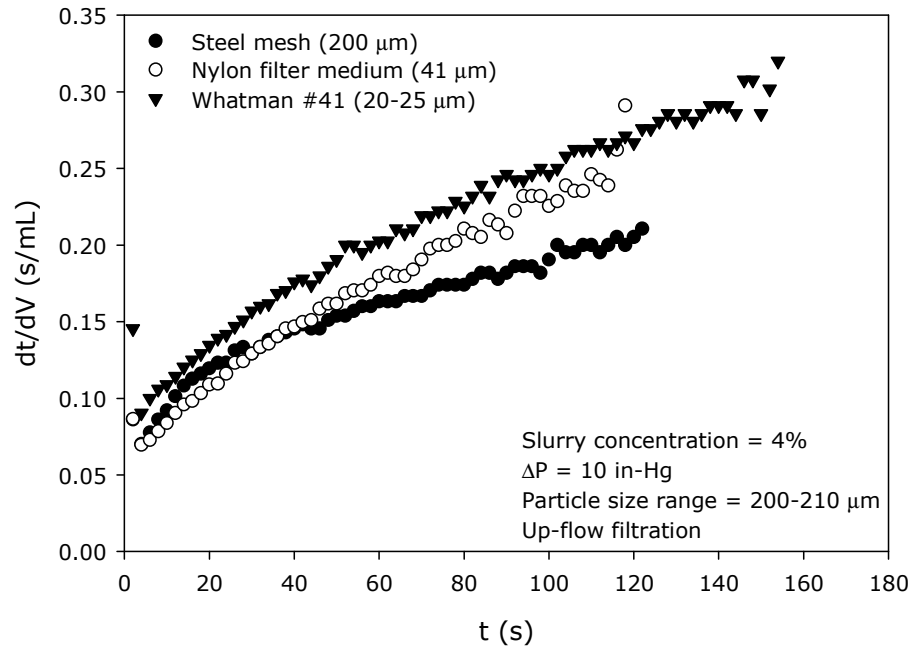


**Figure B.13.** dt/dV vs. t plot-Filter medium effect (I-C)

The dt/dV vs. t plots of both the experimental data and the MATLAB-predicted data are presented in Figures B.14, B.15 and B.16 which show a good agreement. The  $d^2t/dV^2$  vs. t graphs are given in Figures B.17, B.18 and B.19.

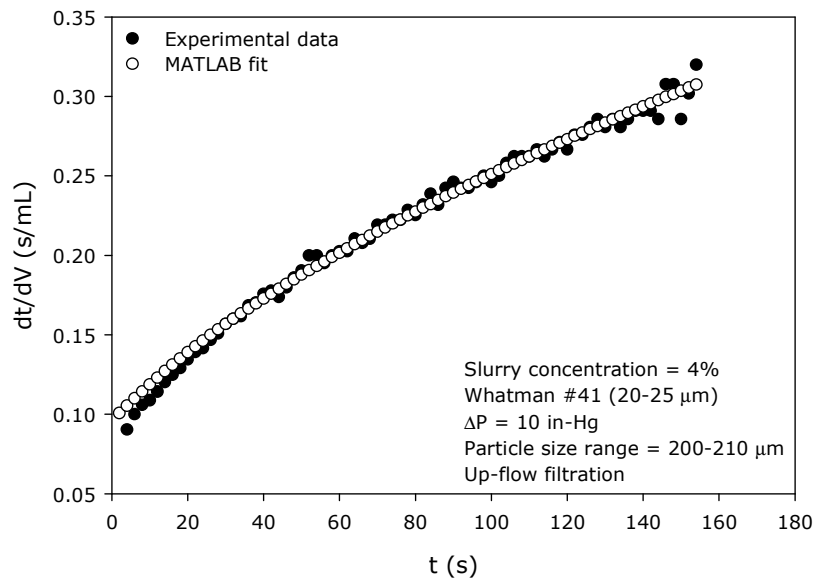


**Figure B.14.** Comparative dt/dV vs. t plot-Filter medium effect (I-C, W#41)

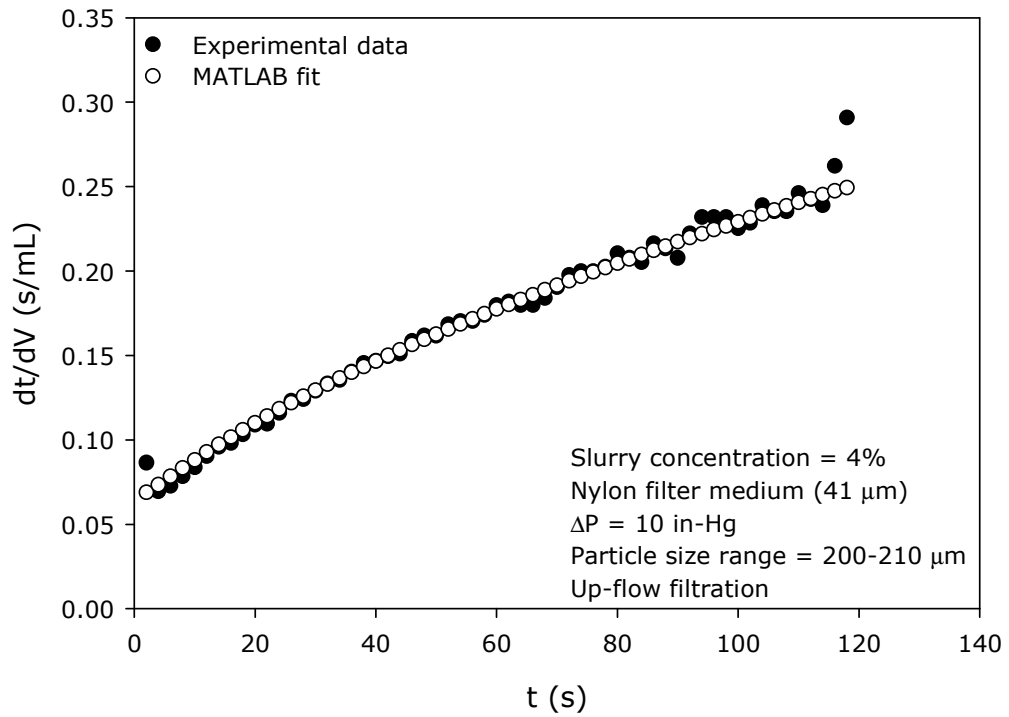


**Figure B.15.** Comparative dt/dV vs. t plot-Filter medium effect (I-C, nylon f.m)

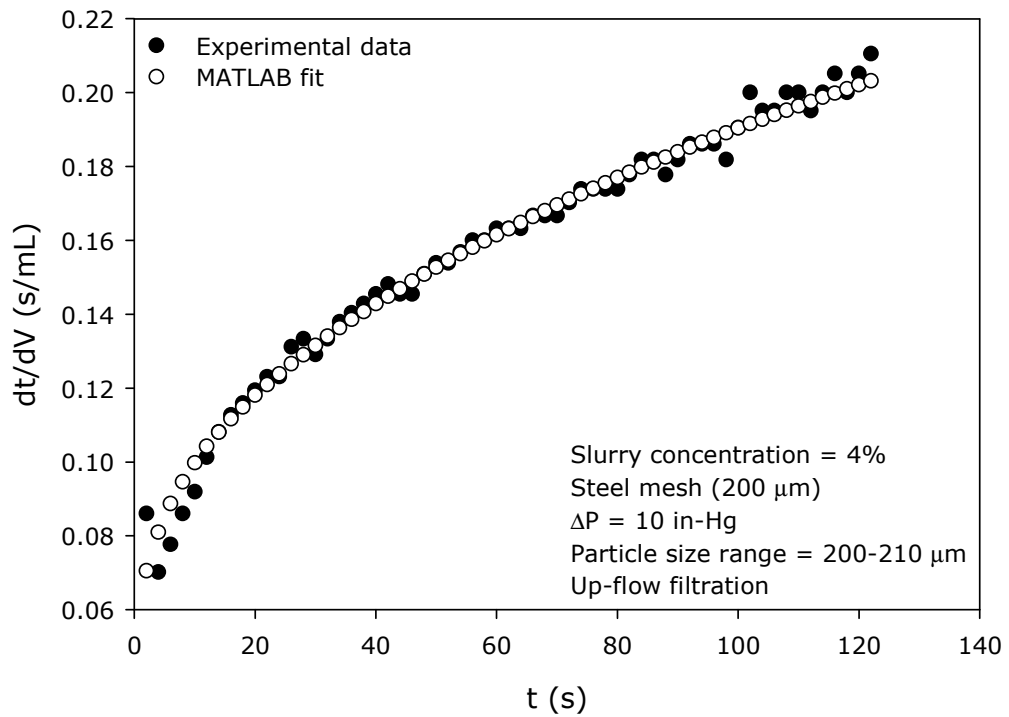


**Figure B.16.** Comparative dt/dV vs. t plot-Filter medium effect (I-C, steel mesh)

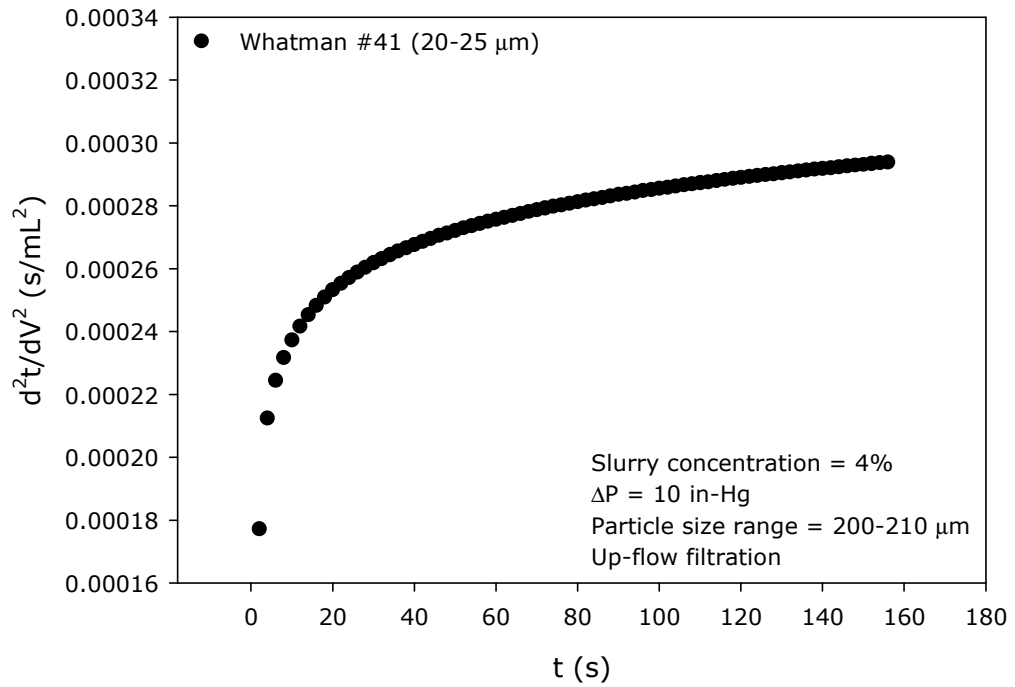


**Figure B.17.**  $d^2t/dV^2$  vs.  $t$  plot-Filter medium effect (I-C, W#41)

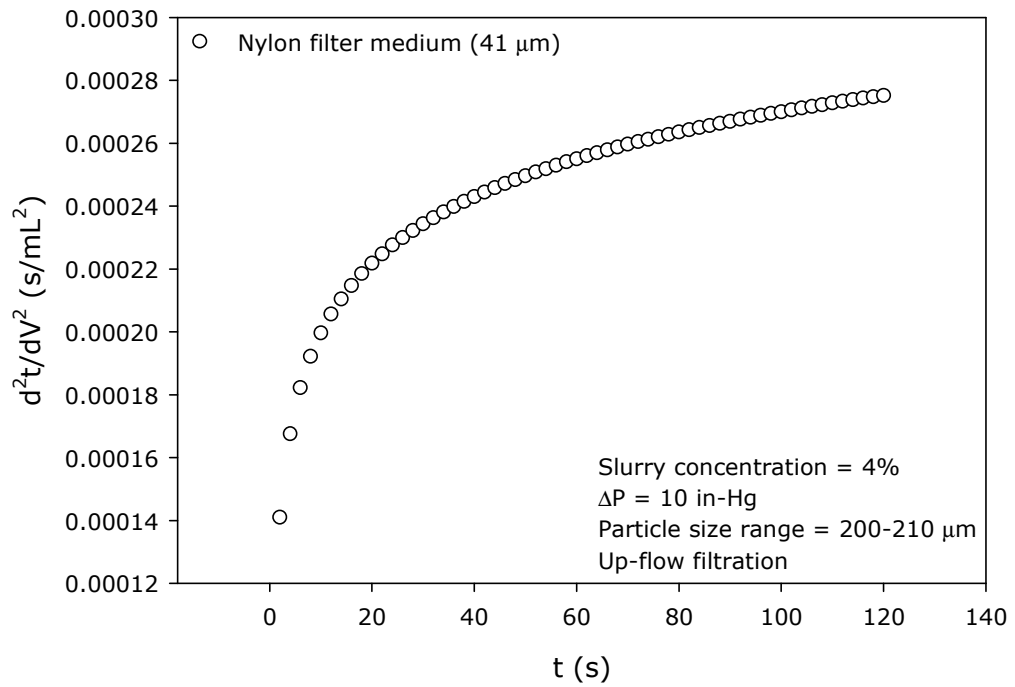


**Figure B.18.**  $d^2t/dV^2$  vs.  $t$  plot-Filter medium effect (I-C, nylon f.m)

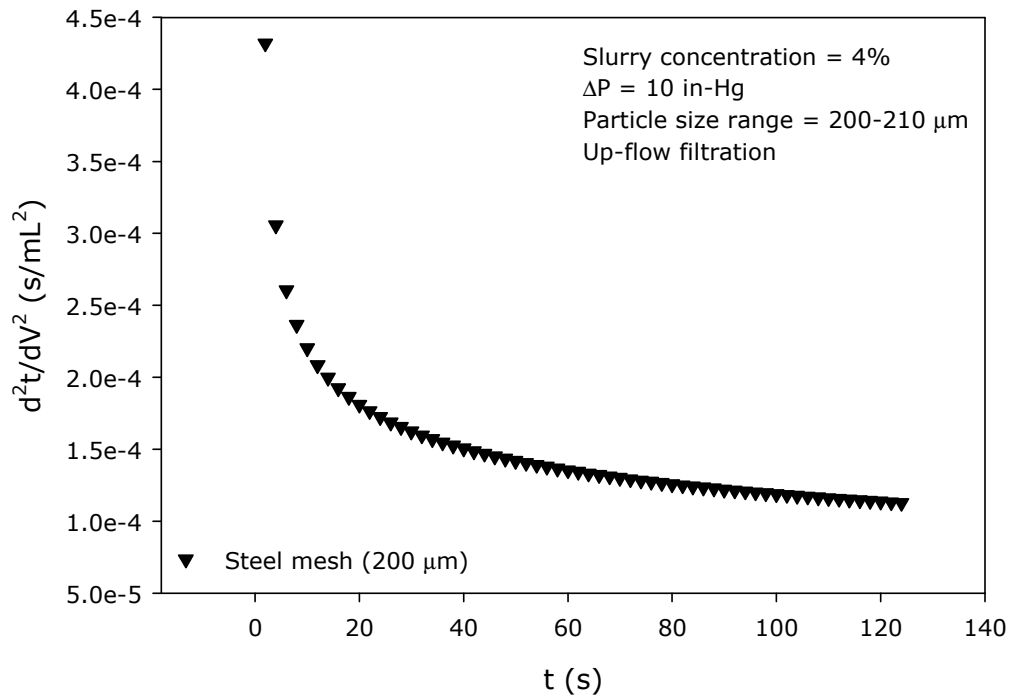


**Figure B.19.**  $d^2t/dV^2$  vs.  $t$  plot-Filter medium effect (I-C, steel mesh)

**Table B.3.** Experimental conditions-Filter medium effect (I-D)

<b>Operational Conditions</b>	<b>Water + Meliodent</b>
Slurry concentration	8%
Pressure	5 in-Hg
Particle size distribution	200-210 $\mu\text{m}$
Mode of filtration	Up-flow
Filter Medium	W#41 (20-25 $\mu\text{m}$ )
	Nylon filter medium (41 $\mu\text{m}$ )
	Steel mesh (200 $\mu\text{m}$ )

Figure B.20 is the  $dt/dV$  vs.  $V$  plot and Figure B.21 is the  $dt/dV$  vs.  $t$  plot.

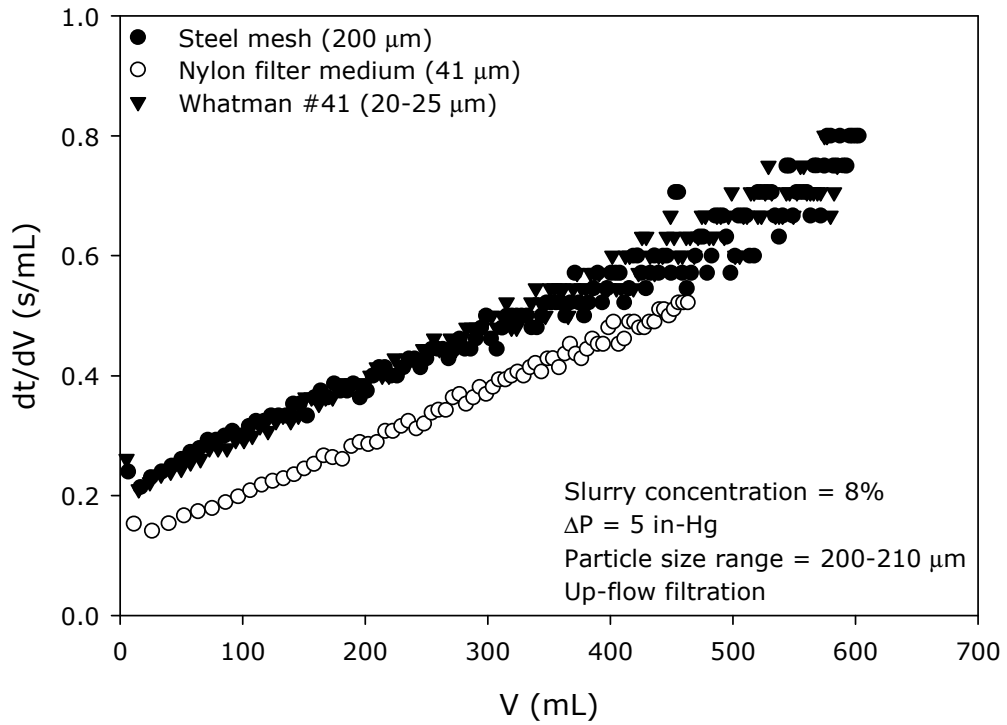


**Figure B.20.** dt/dV vs. V plot-Filter medium effect (I-D)

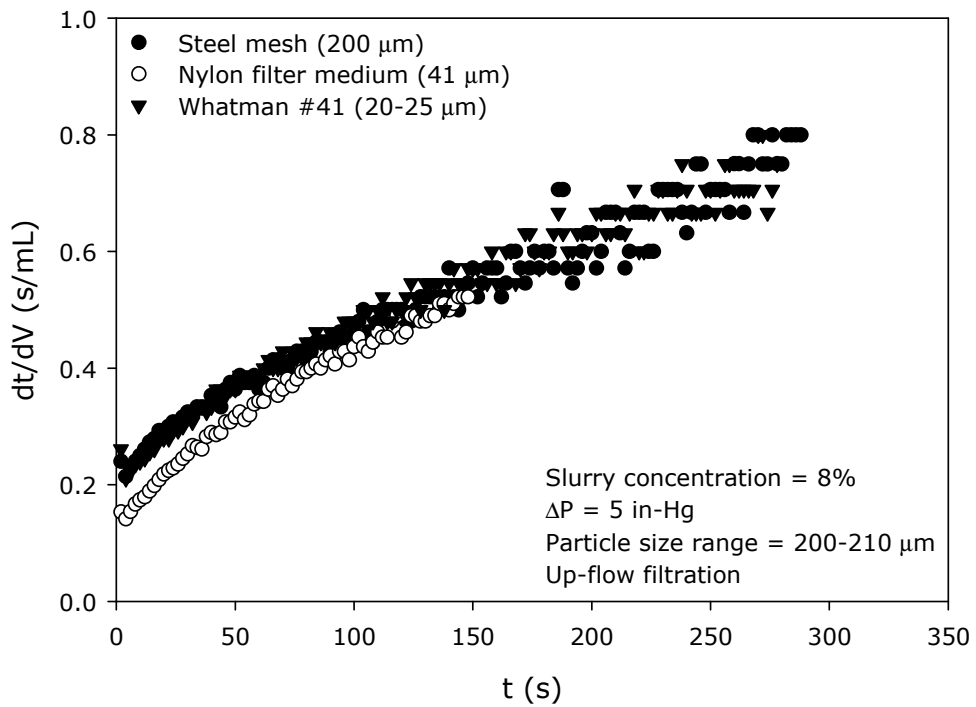


**Figure B.21.** dt/dV vs. t plot-Filter medium effect (I-D)

The  $dt/dV$  vs.  $t$  plots of both the experimental data and the MATLAB-predicted data are presented in Figures B.22, B.23 and B.24 which show a good agreement. The  $d^2t/dV^2$  vs.  $t$  graphs are given in Figures B.25, B.26 and B.27.

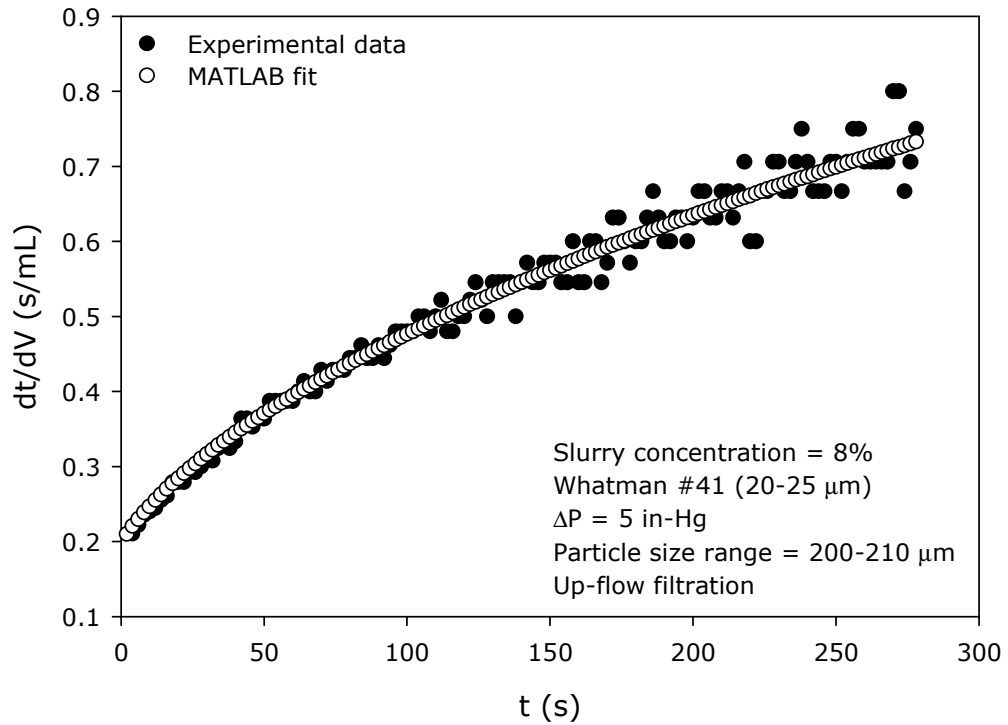


**Figure B.22.** Comparative  $dt/dV$  vs.  $t$  plot-Filter medium effect (I-D, W#41)

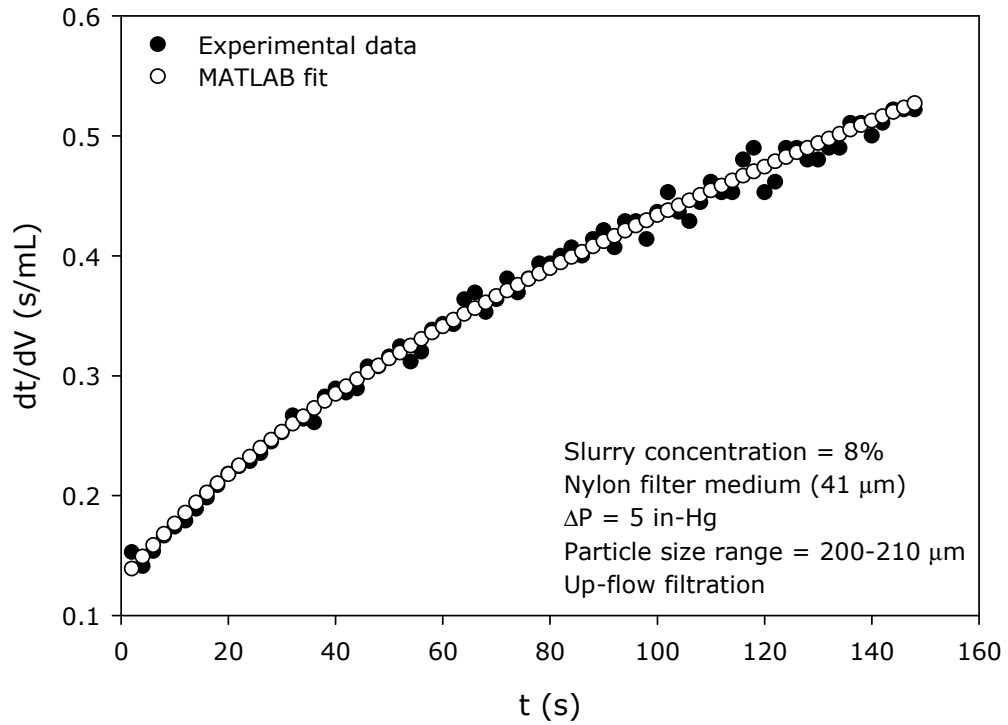


**Figure B.23.** Comparative dt/dV vs. t plot-Filter medium effect (I-D, nylon f.m)

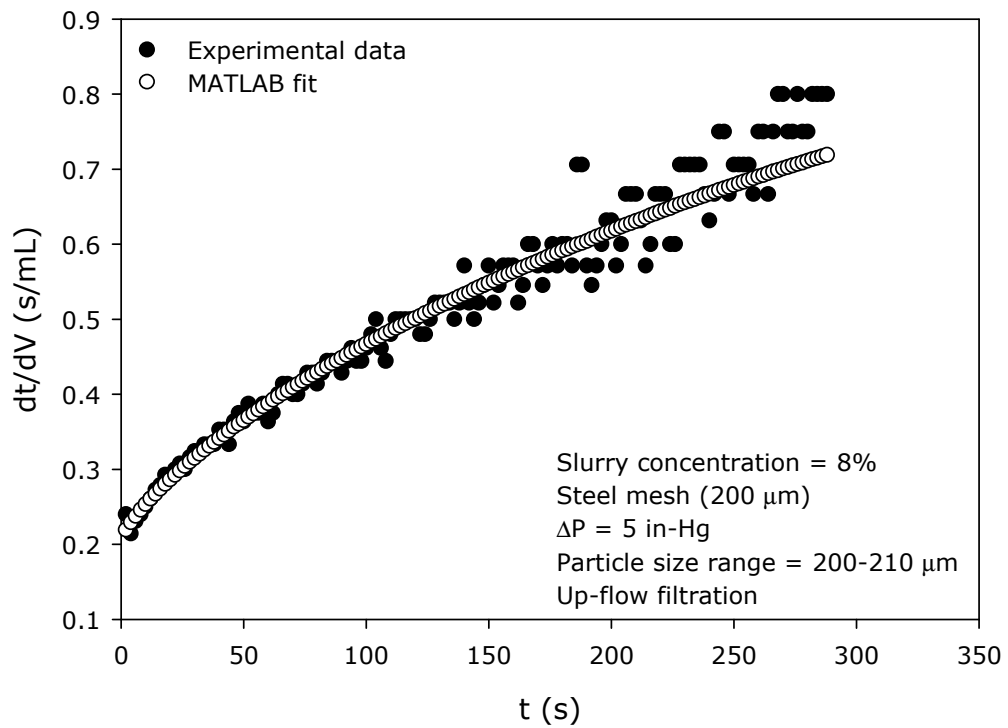


**Figure B.24.** Comparative dt/dV vs. t plot-Filter medium effect (I-D, steel m.)

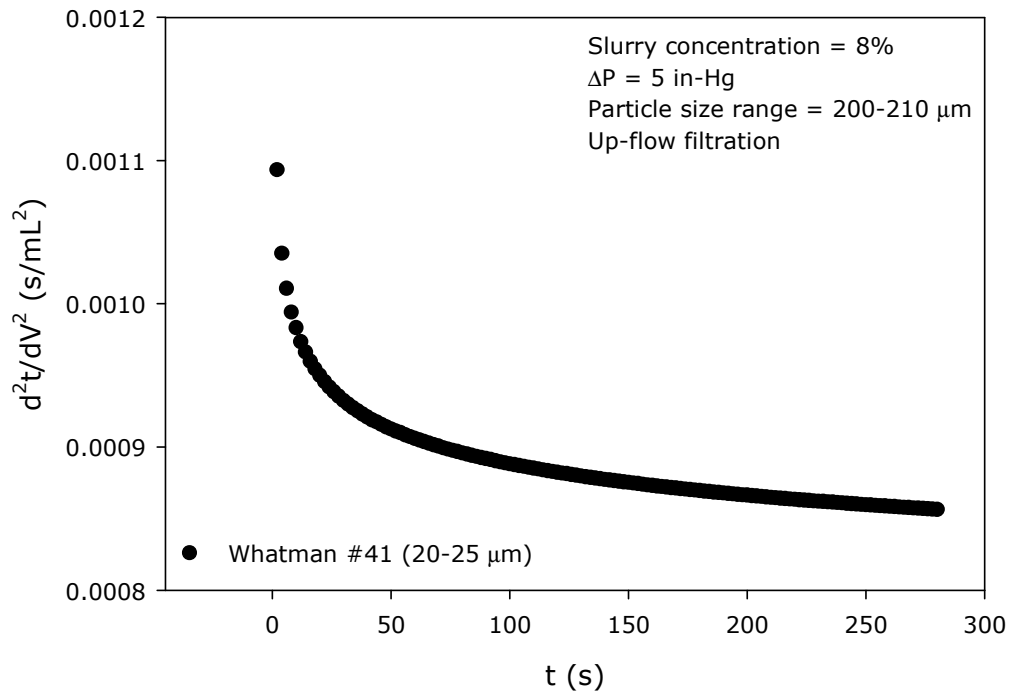


**Figure B.25.**  $d^2t/dV^2$  vs.  $t$  plot-Filter medium effect (I-D, W#41)

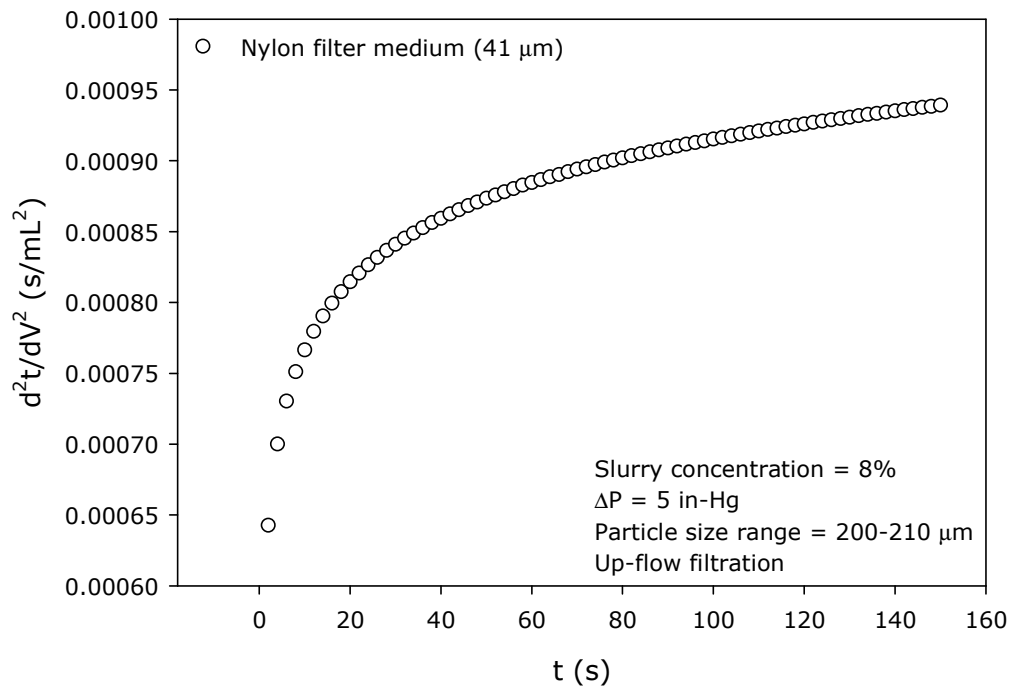


**Figure B.26.**  $d^2t/dV^2$  vs.  $t$  plot-Filter medium effect (I-D, nylon f.m)

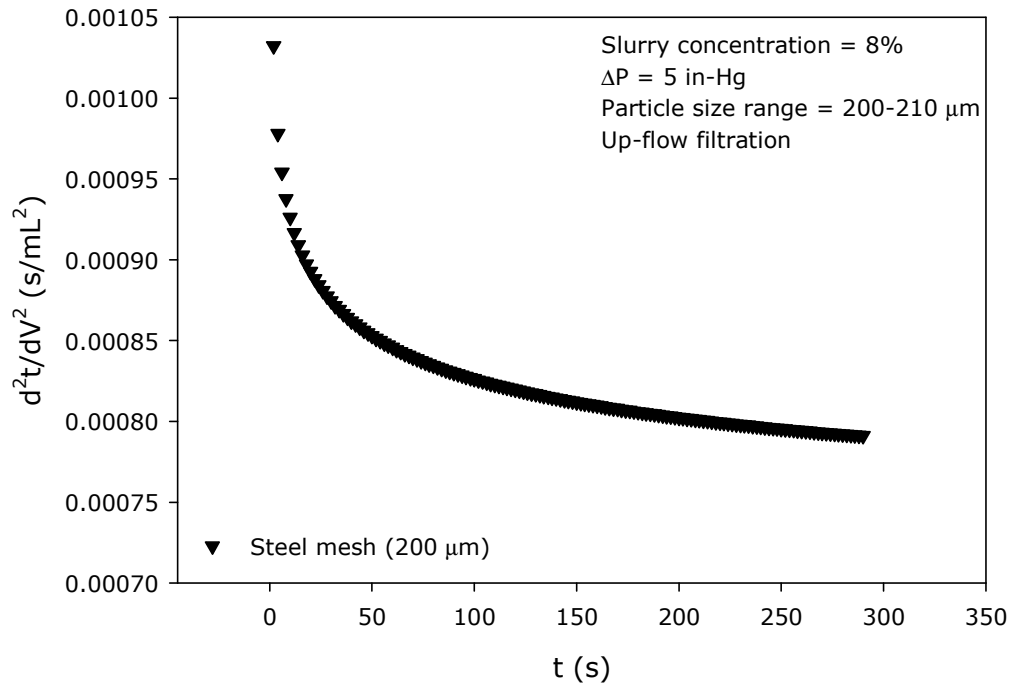


**Figure B.27.**  $d^2t/dV^2$  vs.  $t$  plot-Filter medium effect (I-D, steel mesh)

**Table B.4.** Experimental conditions-Filter medium effect (I-E)

<b>Operational Conditions</b>	<b>Water + Meliodent</b>
Slurry concentration	8%
Pressure	10 in-Hg
Particle size distribution	200-210 $\mu\text{m}$
Mode of filtration	Up-flow
Filter Medium	W#41 (20-25 $\mu\text{m}$ ) Nylon filter medium (41 $\mu\text{m}$ ) Steel mesh (200 $\mu\text{m}$ )

Figure B.28 is the  $dt/dV$  vs.  $V$  plot and Figure B.29 is the  $dt/dV$  vs.  $t$  plot.

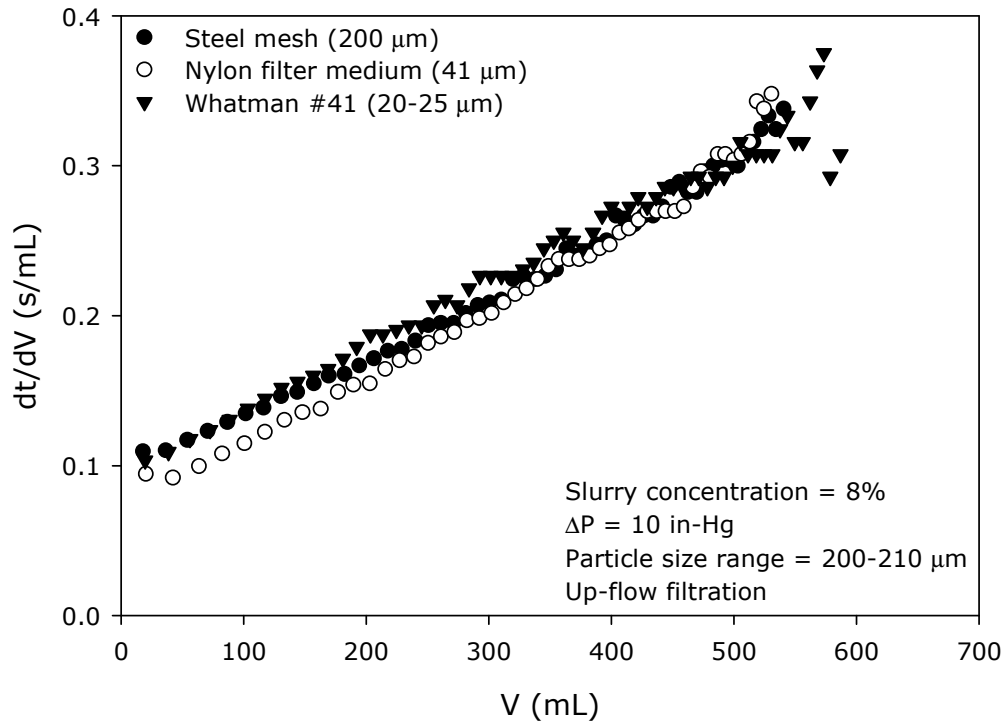


**Figure B.28.** dt/dV vs. V plot-Filter medium effect (I-E)

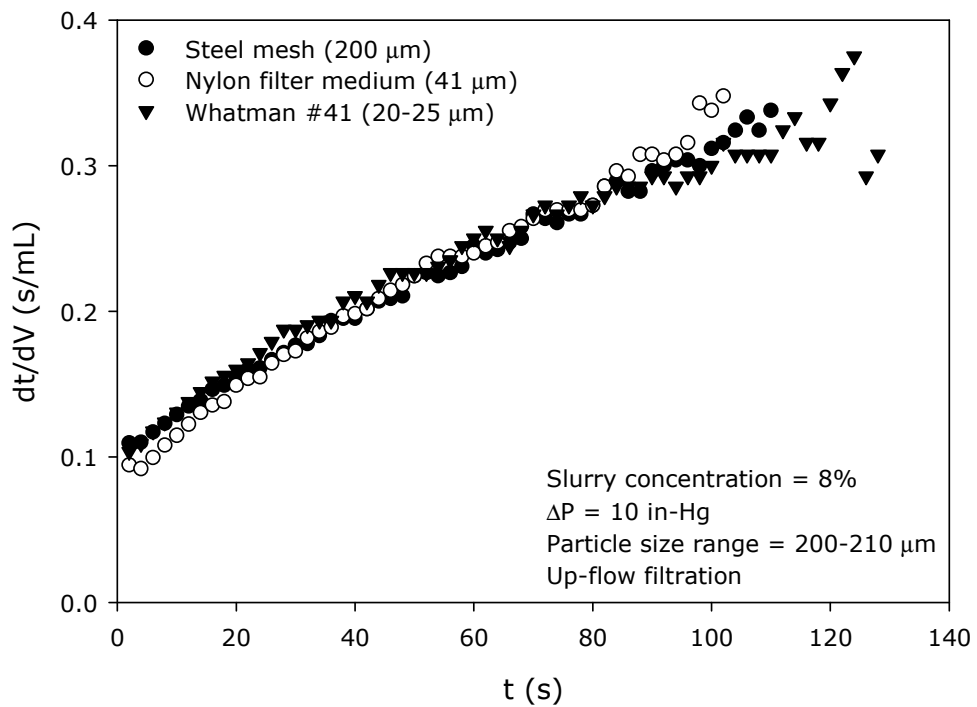


**Figure B.29.** dt/dV vs. t plot-Filter medium effect (I-E)

The  $dt/dV$  vs.  $t$  plots of both the experimental data and the MATLAB-predicted data are presented in Figures B.30, B.31 and B.32 which show a good agreement. The  $d^2t/dV^2$  vs.  $t$  graphs are given in Figures B.33, B.34 and B.35.

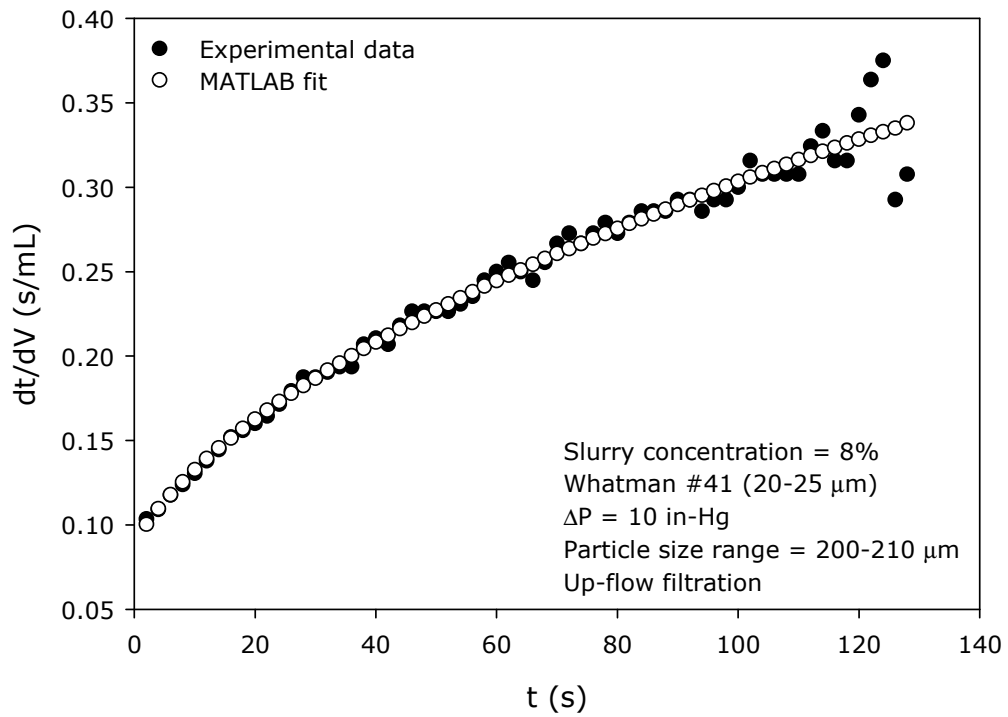


**Figure B.30.** Comparative  $dt/dV$  vs.  $t$  plot-Filter medium effect (I-E, W#41)

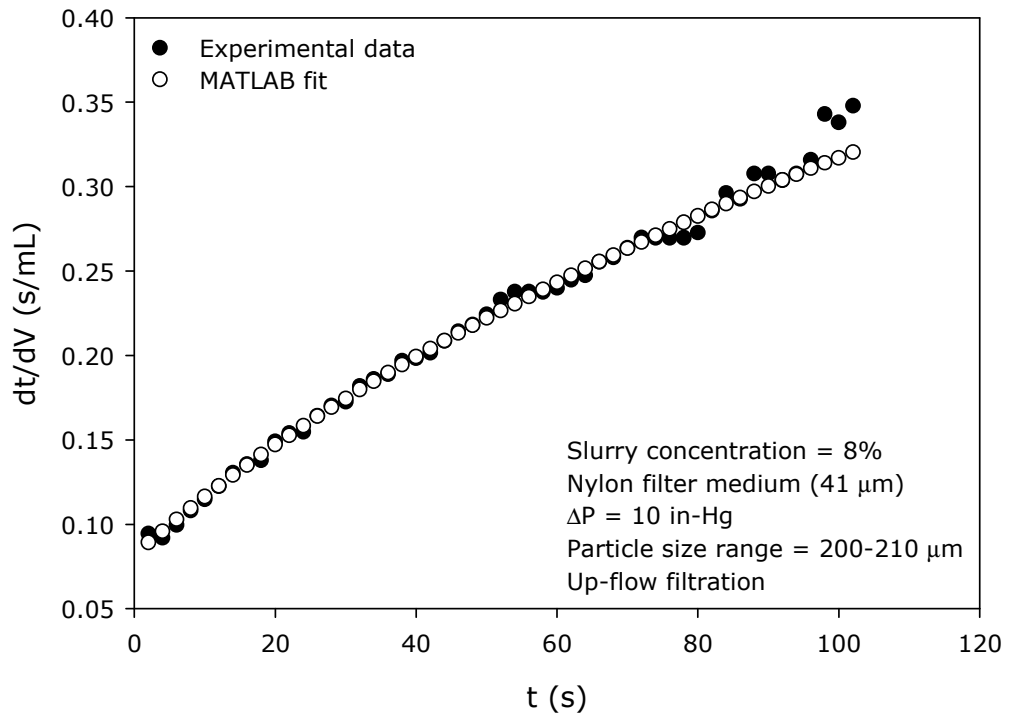


**Figure B.31.** Comparative dt/dV vs. t plot-Filter medium effect (I-E, nylon f.m)

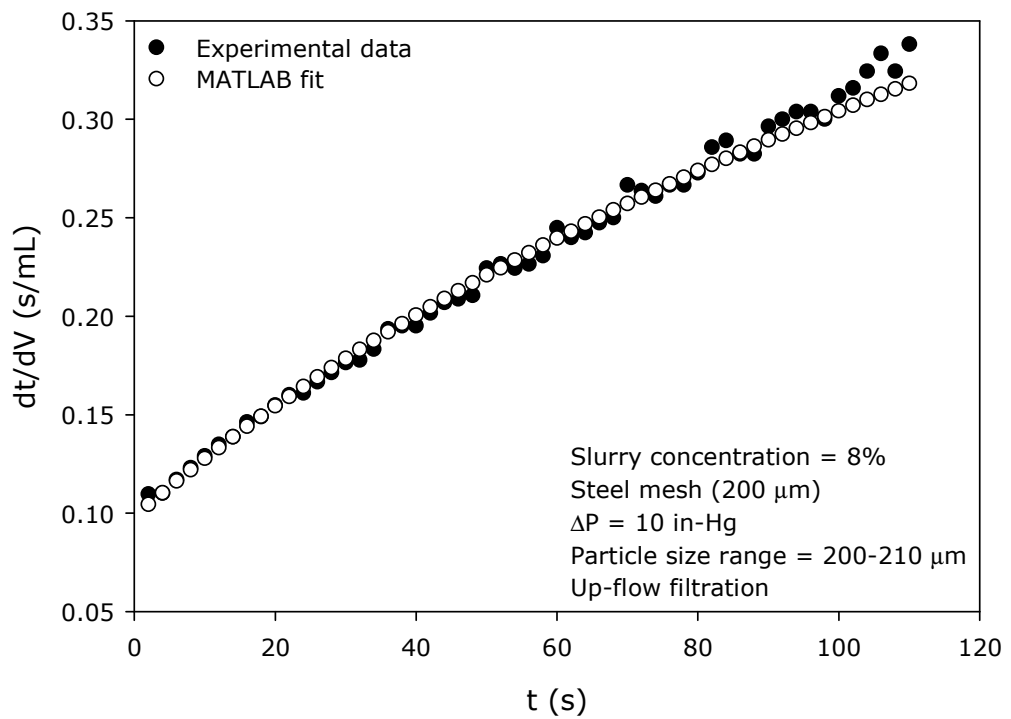


**Figure B.32.** Comparative dt/dV vs. t plot-Filter medium effect (I-E, steel mesh)

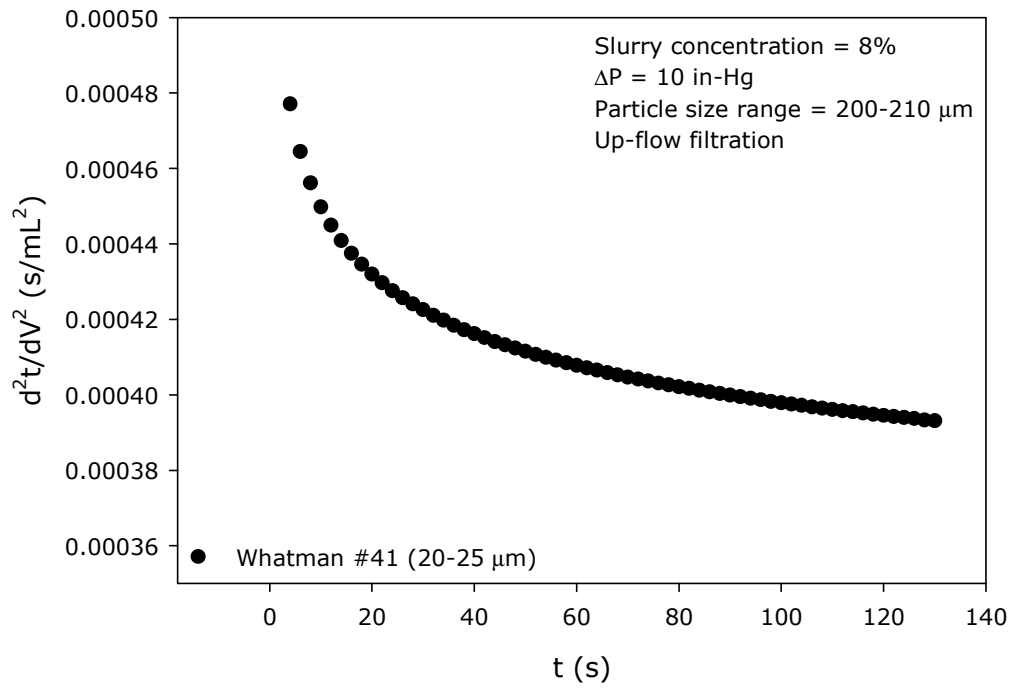


**Figure B.33.**  $d^2t/dV^2$  vs.  $t$  plot-Filter medium effect (I-E, W#41)

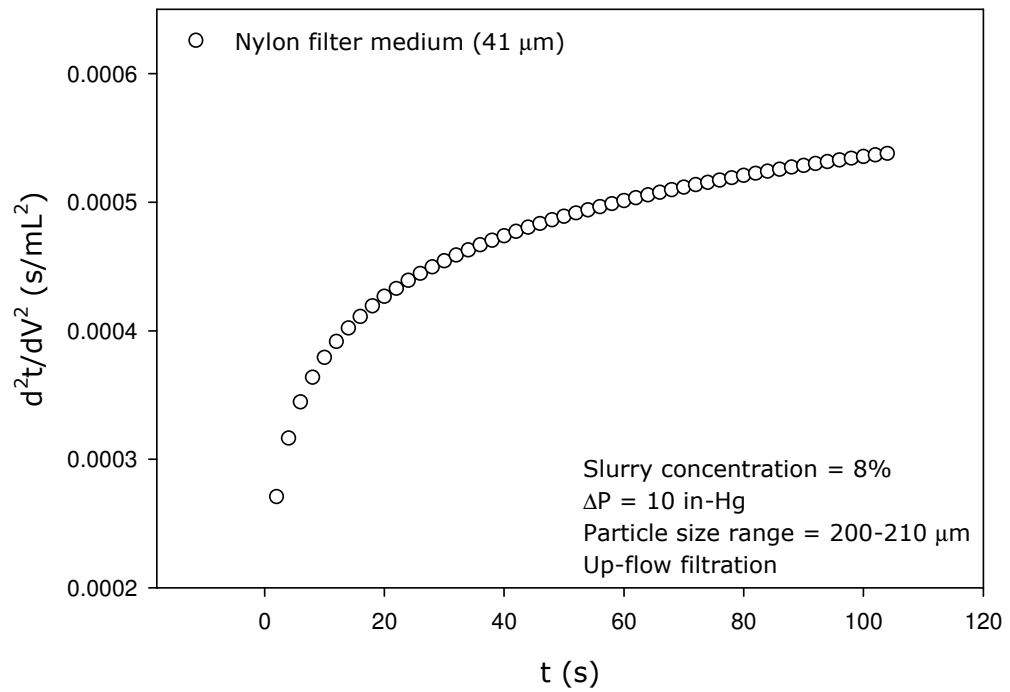


**Figure B.34.**  $d^2t/dV^2$  vs.  $t$  plot-Filter medium effect (I-E, nylon f.m)

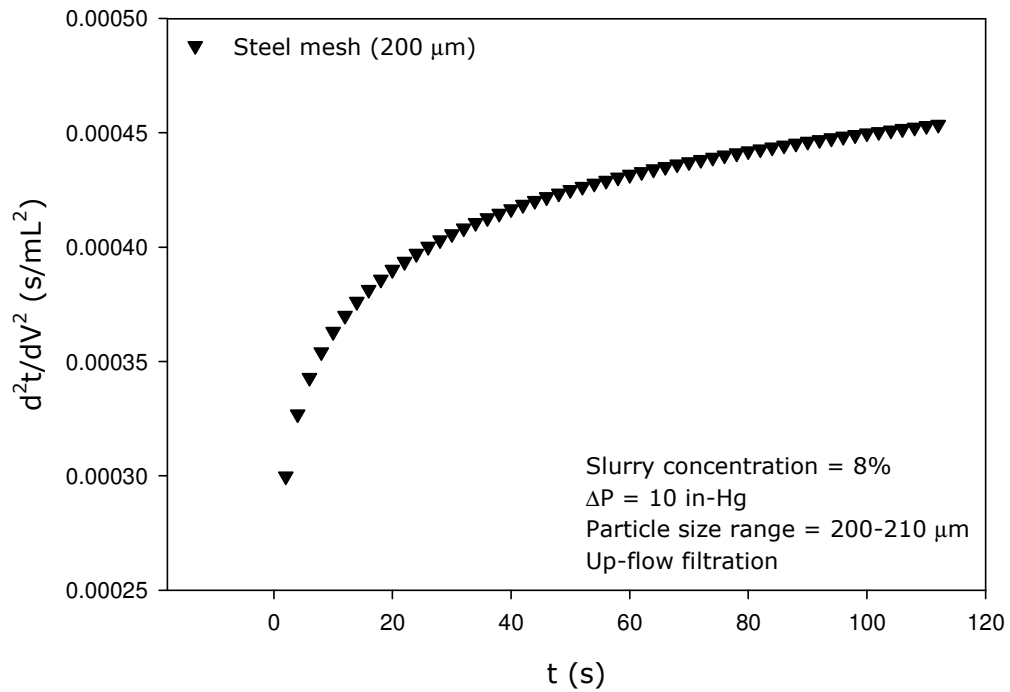


**Figure B.35.**  $d^2t/dV^2$  vs.  $t$  plot-Filter medium effect (I-E, steel mesh)

*Case II-Particle Size Effect*

**Table B.5.** Experimental conditions-Particle size effect (II-A)

<b>Operational Conditions</b>	<b>Water + Meliodent</b>
Slurry concentration	2%
Pressure	4.5 in-Hg
Mode of filtration	Up-flow
Filter Medium	W#41 (20-25 $\mu\text{m}$ )
	53-75 $\mu\text{m}$
Particle size distribution	250-425 $\mu\text{m}$
	Mixed
	(both sizes in equal wt %)

Figure B.36 is the  $dt/dV$  vs.  $V$  plot and Figure B.37 is the  $dt/dV$  vs.  $t$  plot.

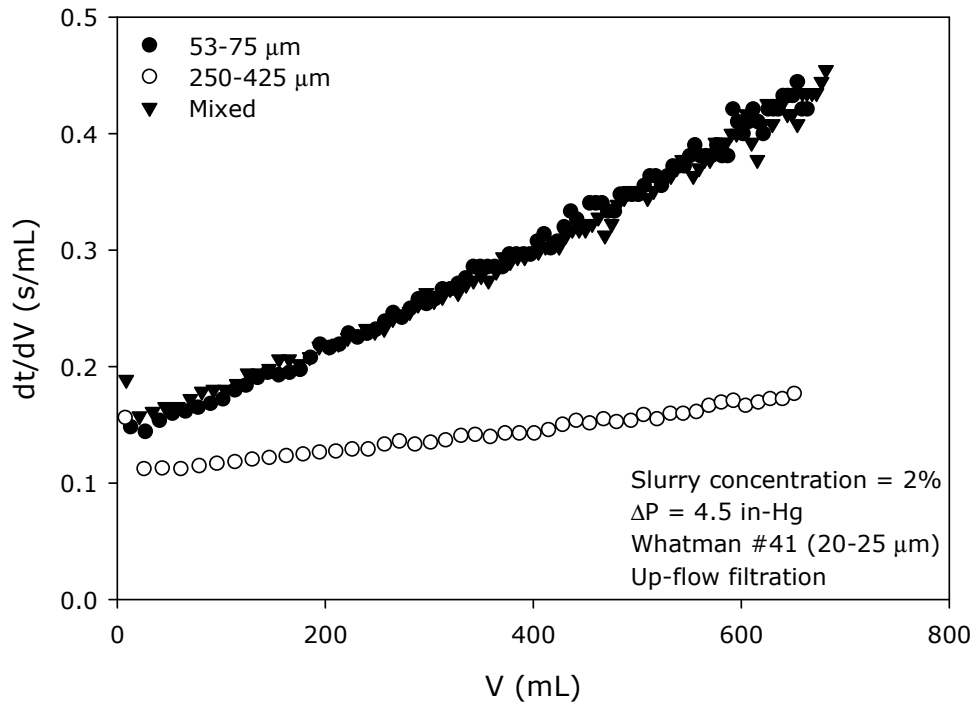


**Figure B.36.** dt/dV vs. V plot-Particle size effect (II-A)

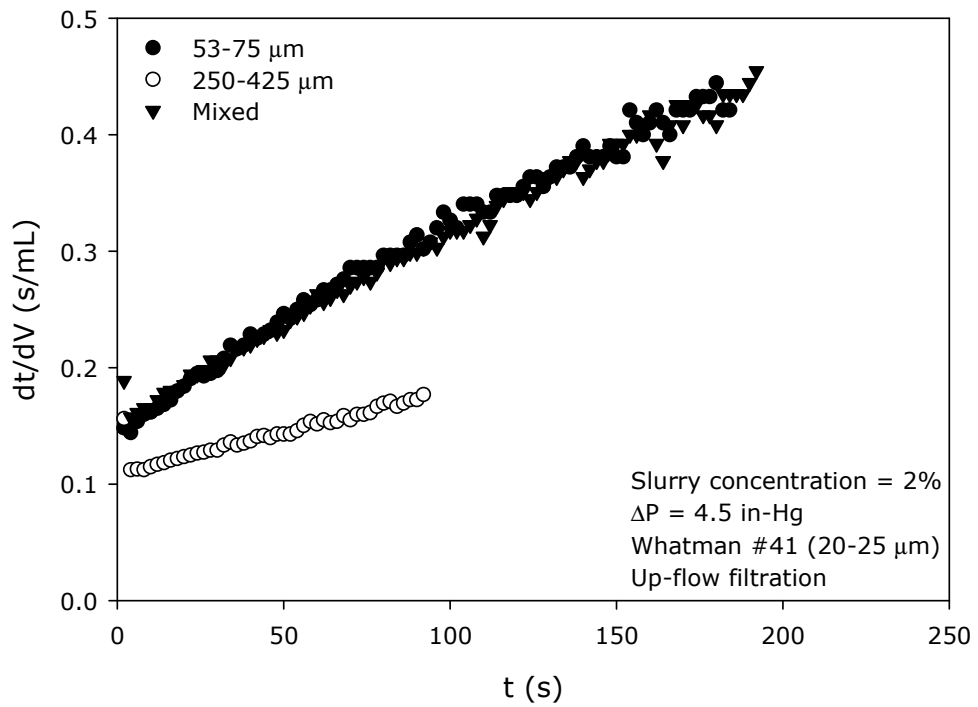


**Figure B.37.** dt/dV vs. t plot-Particle size effect (II-A)

The  $dt/dV$  vs.  $t$  plots of both the experimental data and the MATLAB-predicted data are presented in Figures B.38, B.39 and B.40. The  $d^2t/dV^2$  vs.  $t$  graphs are given in Figures B.41, B.42 and B.43.

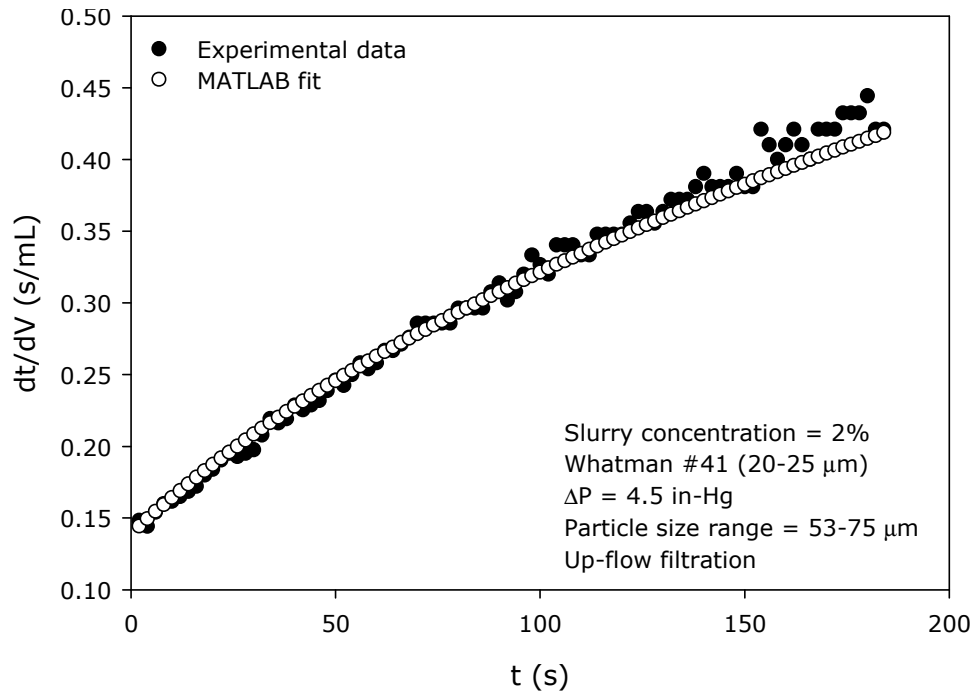


**Figure B.38.** Comparative  $dt/dV$  vs.  $t$  plot-Particle size effect (II-A, 53-75  $\mu\text{m}$ )

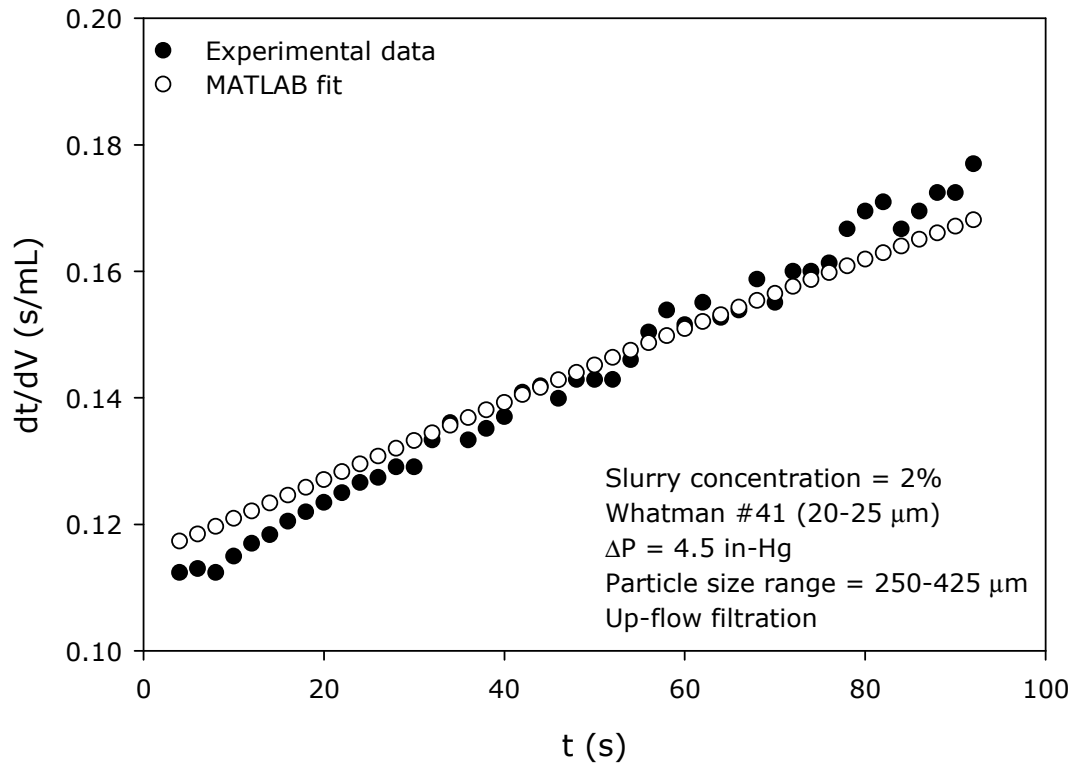


**Figure B.39.** Comparative  $dt/dV$  vs.  $t$  plot-Particle size effect (II-A, 250-425 $\mu\text{m}$ )

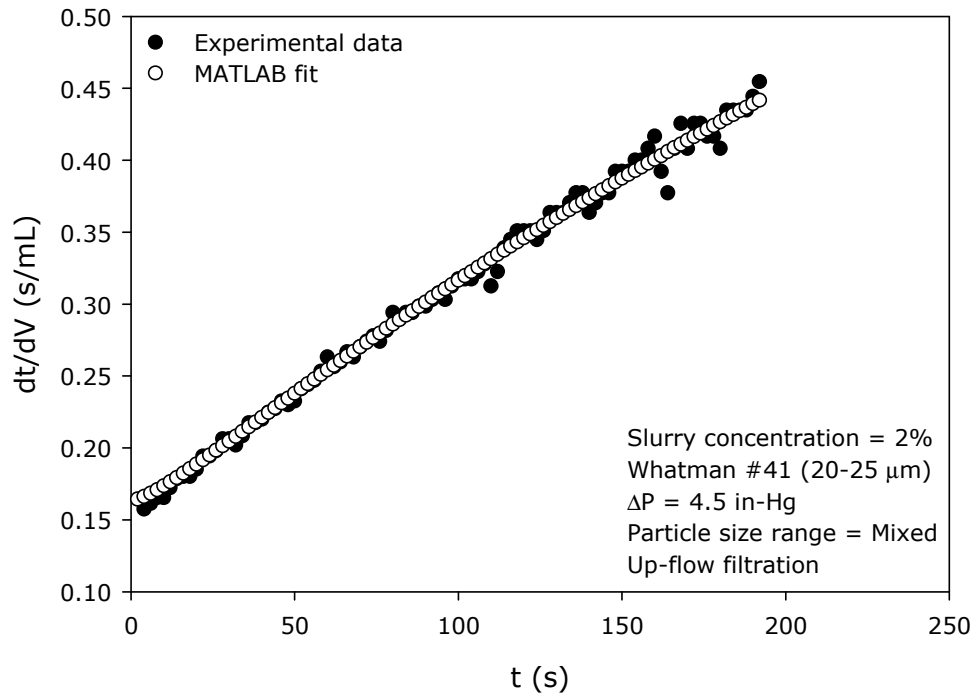


**Figure B.40.** Comparative  $dt/dV$  vs.  $t$  plot-Particle size effect (II-A, mixed)

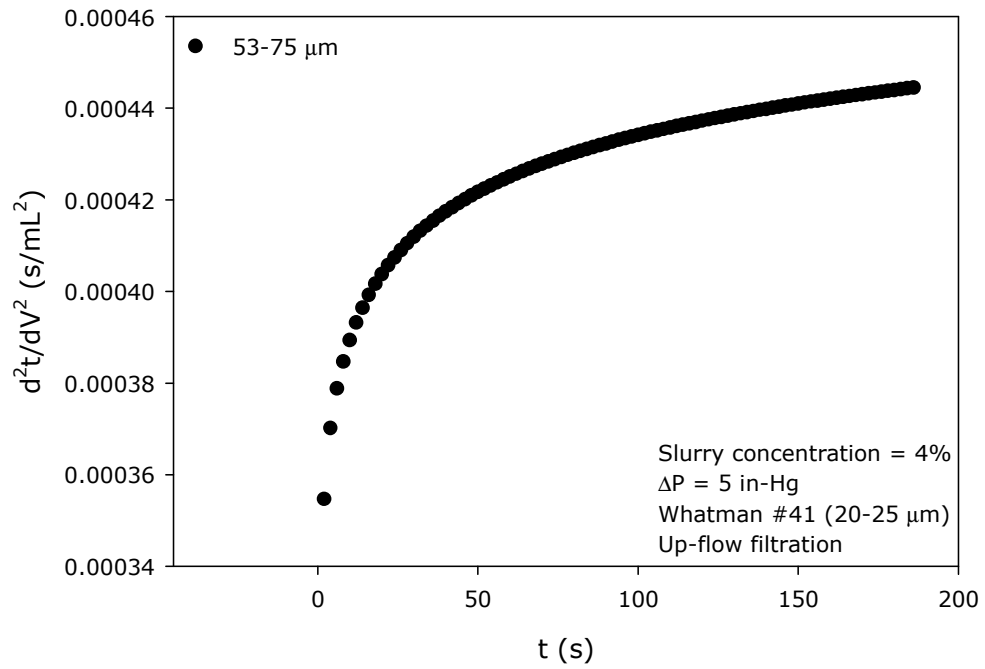


**Figure B.41.**  $d^2t/dV^2$  vs.  $t$  plot-Particle size effect (II-A, 53-75  $\mu\text{m}$ )

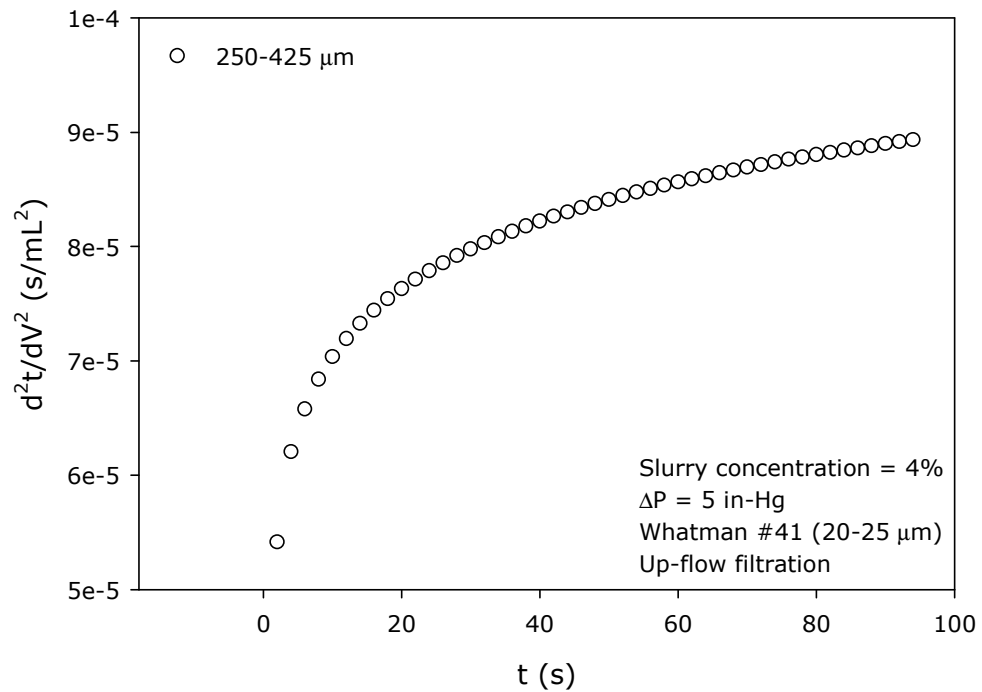


**Figure B.42.**  $d^2t/dV^2$  vs.  $t$  plot-Particle size effect (II-A, 250-425  $\mu\text{m}$ )

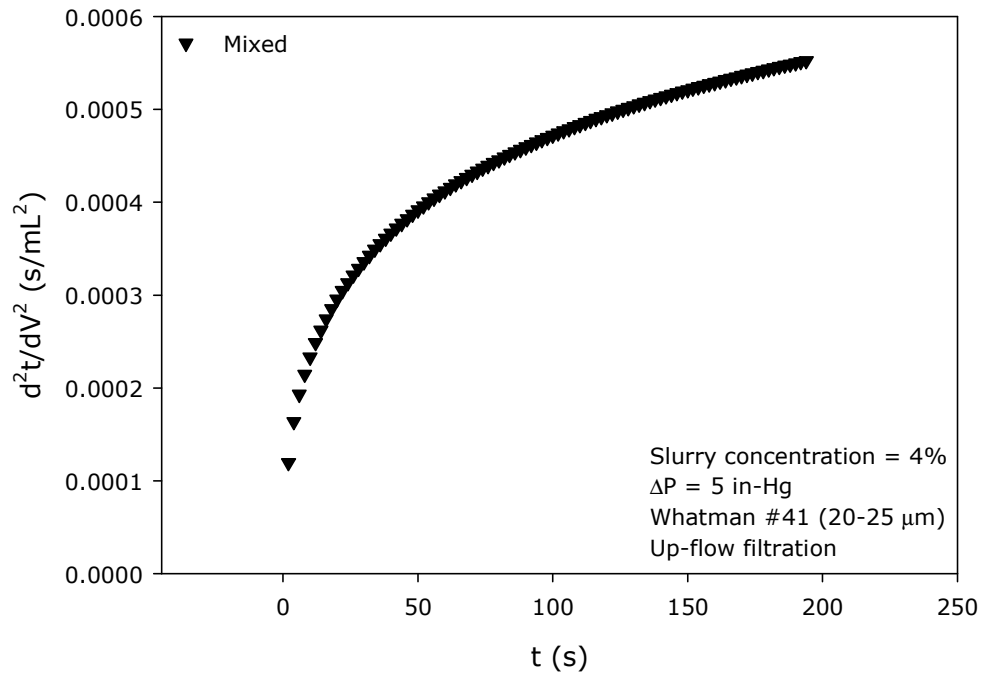


**Figure B.43.**  $d^2t/dV^2$  vs.  $t$  plot-Particle size effect (II-A, mixed)

**Table B.6.** Experimental conditions-Particle size effect (II-B)

<b>Operational Conditions</b>	<b>Water + Meliodent</b>
Slurry concentration	4%
Pressure	4.5 in-Hg
Mode of filtration	Up-flow
Filter Medium	W#41 (20-25 $\mu\text{m}$ )
Particle size distribution	75-100 $\mu\text{m}$
	200-210 $\mu\text{m}$
	250-425 $\mu\text{m}$

Figure B.44 is the  $dt/dV$  vs.  $V$  plot and Figure B.45 is the  $dt/dV$  vs.  $t$  plot.

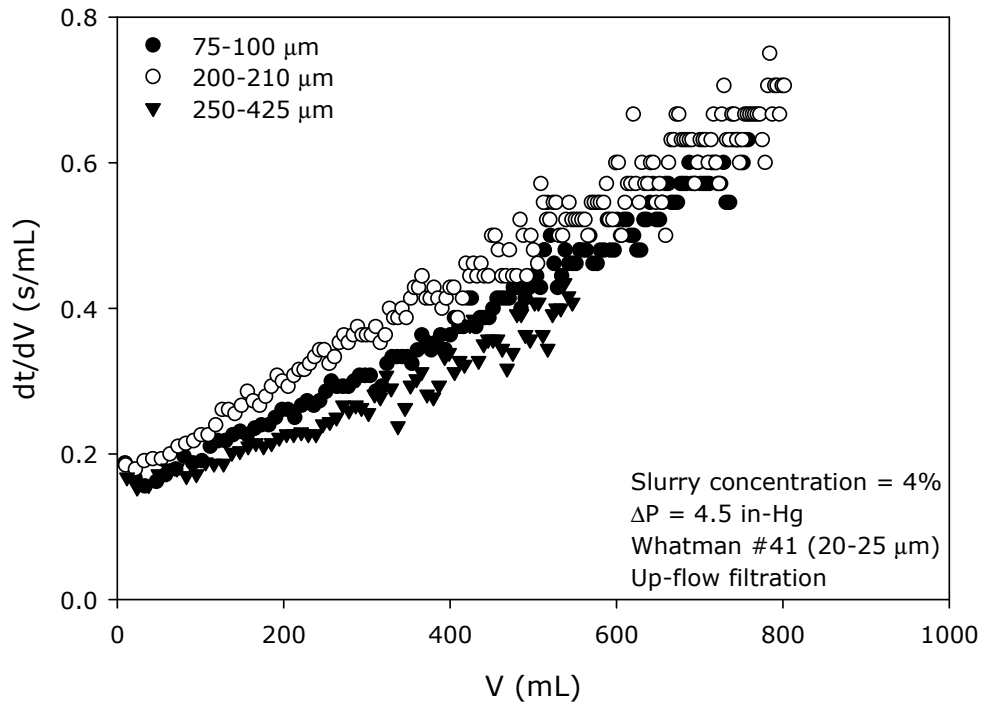


**Figure B.44.** dt/dV vs. V plot-Particle size effect (II-B)

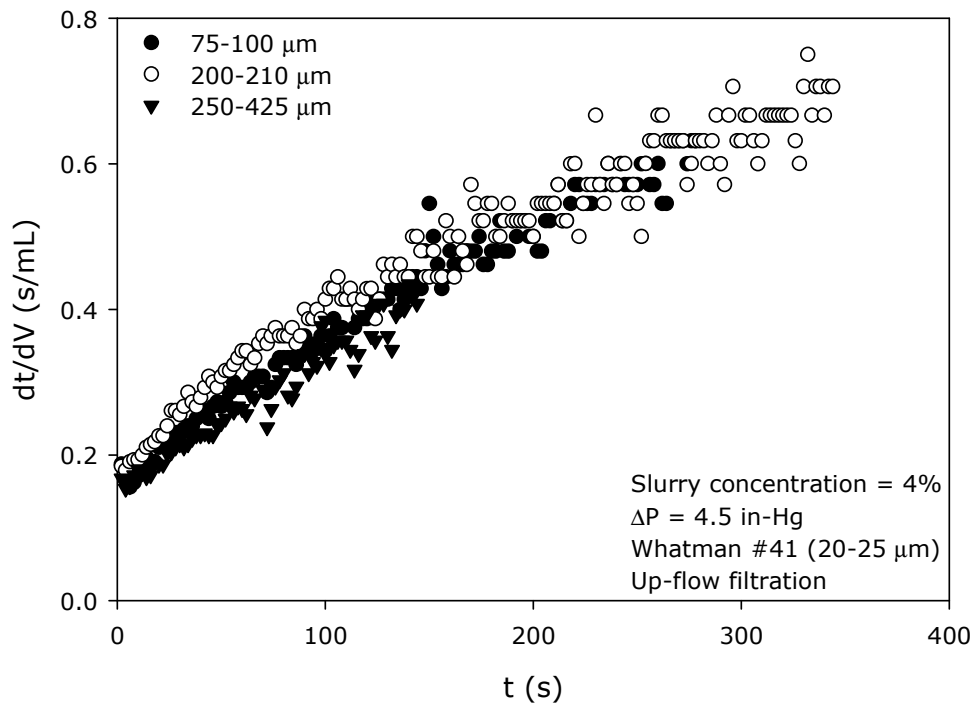


**Figure B.45.** dt/dV vs. t plot-Particle size effect (II-B)

The  $dt/dV$  vs.  $t$  plots of both the experimental data and the MATLAB-predicted data are presented in Figures B.46, B.47 and B.48. The  $d^2t/dV^2$  vs.  $t$  graphs are given in Figures B.49, B.50 and B.51.

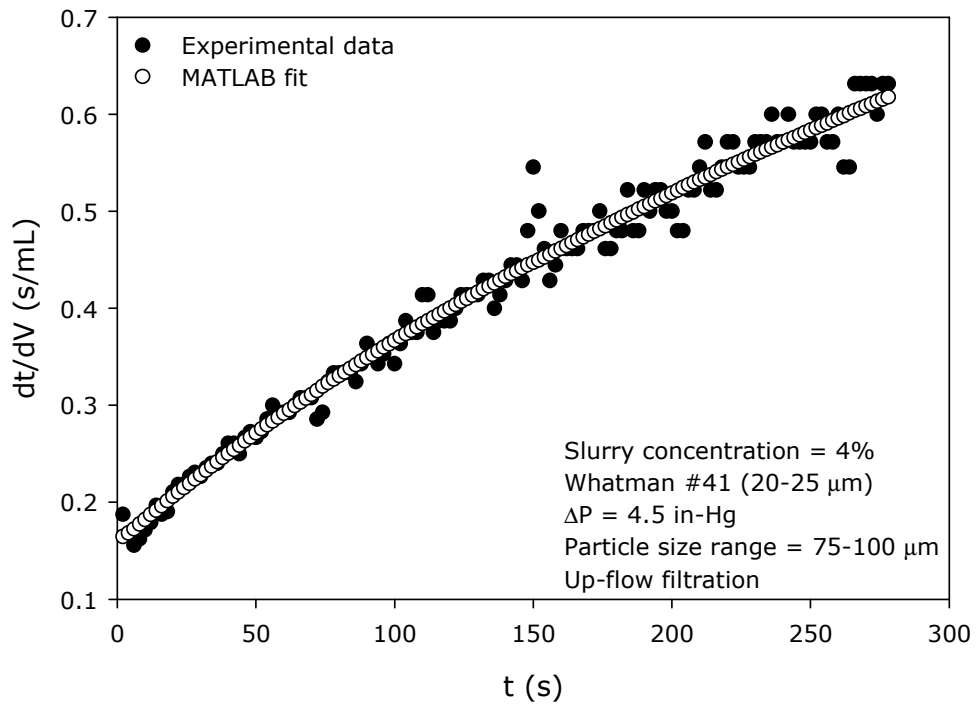


**Figure B.46.** Comparative  $dt/dV$  vs.  $t$  plot-Particle size effect (II-B, 75-100  $\mu\text{m}$ )

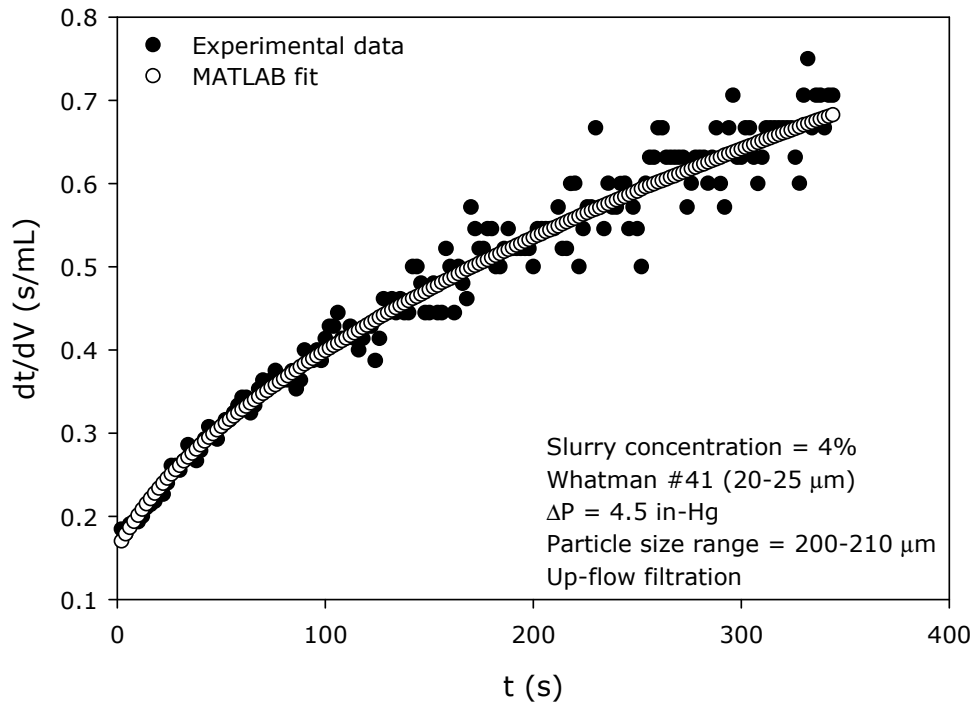


**Figure B.47.** Comparative  $dt/dV$  vs.  $t$  plot-Particle size effect (II-B, 200-210 $\mu\text{m}$ )

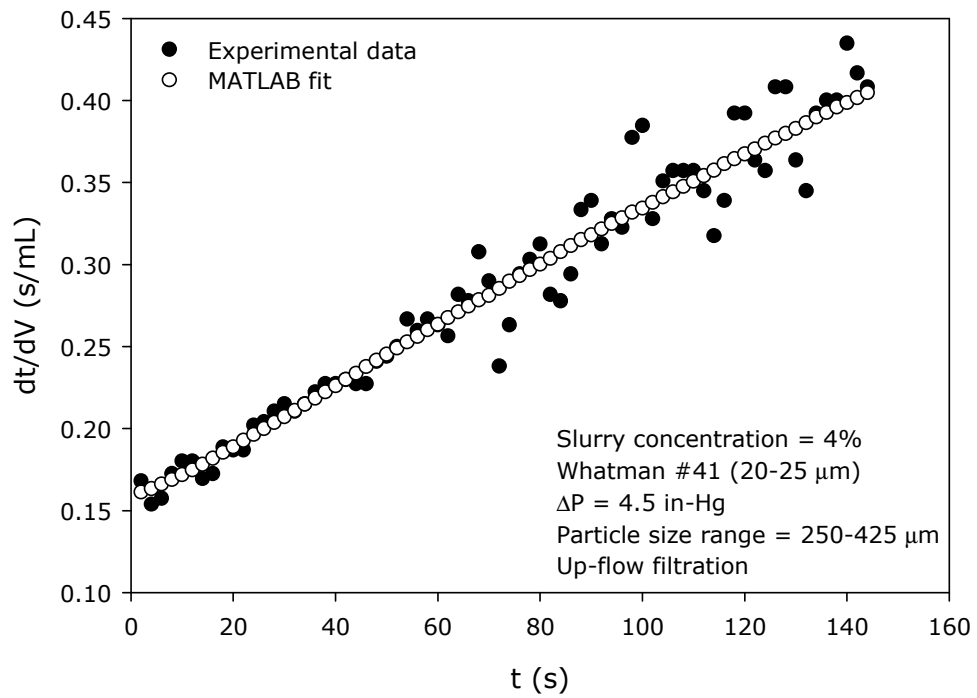


**Figure B.48.** Comparative  $dt/dV$  vs.  $t$  plot-Particle size effect (II-B, 250-425 $\mu\text{m}$ )

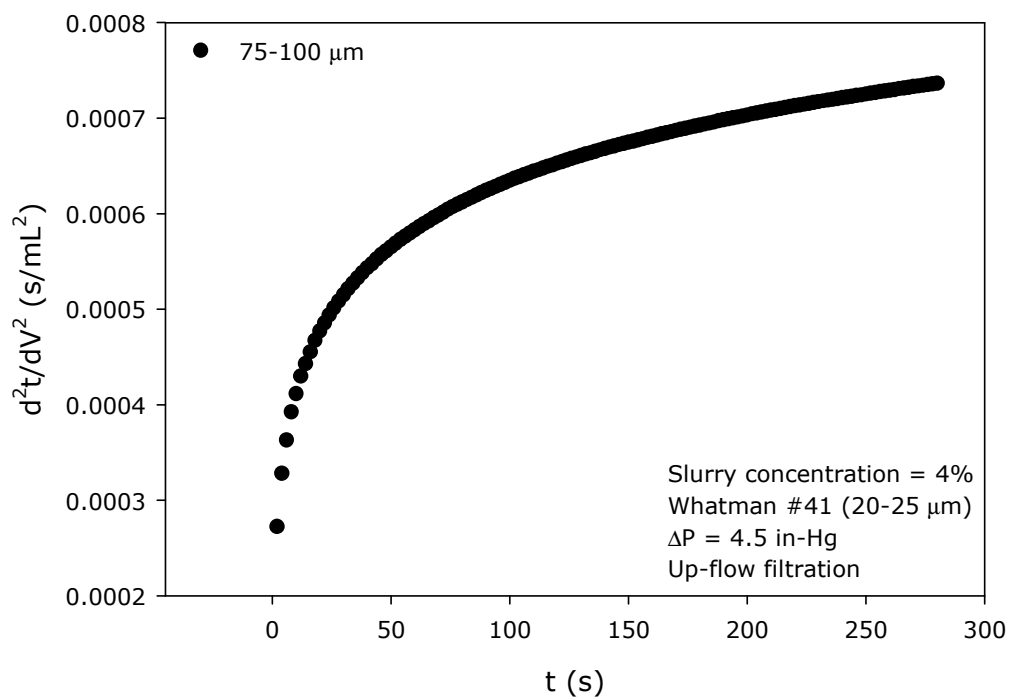


**Figure B.49.**  $d^2t/dV^2$  vs.  $t$  plot-Particle size effect (II-B, 75-100  $\mu\text{m}$ )

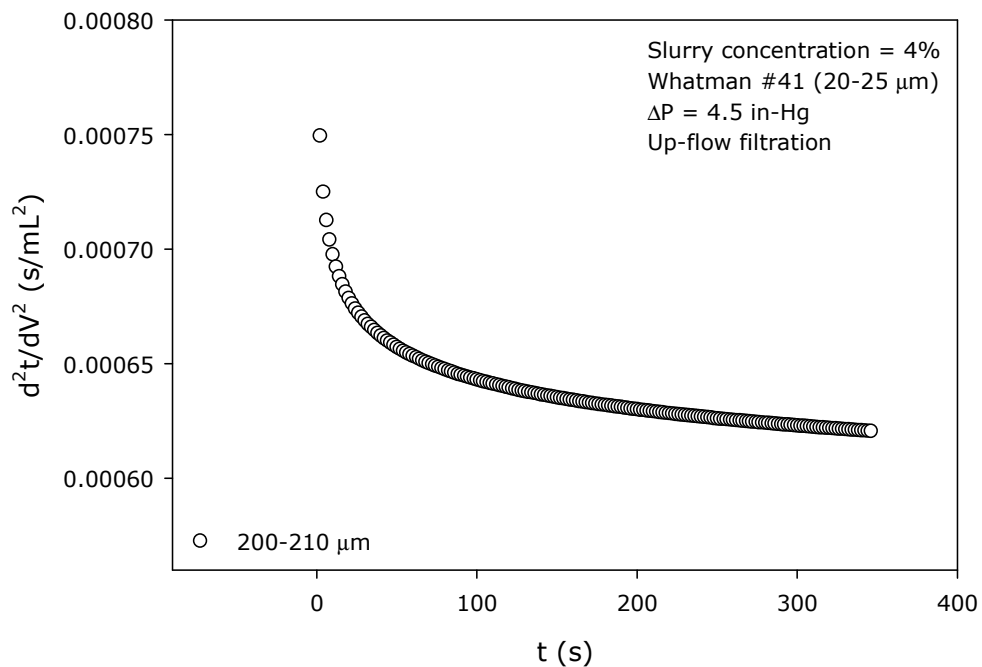


**Figure B.50.**  $d^2t/dV^2$  vs.  $t$  plot-Particle size effect (II-B, 200-210  $\mu\text{m}$ )

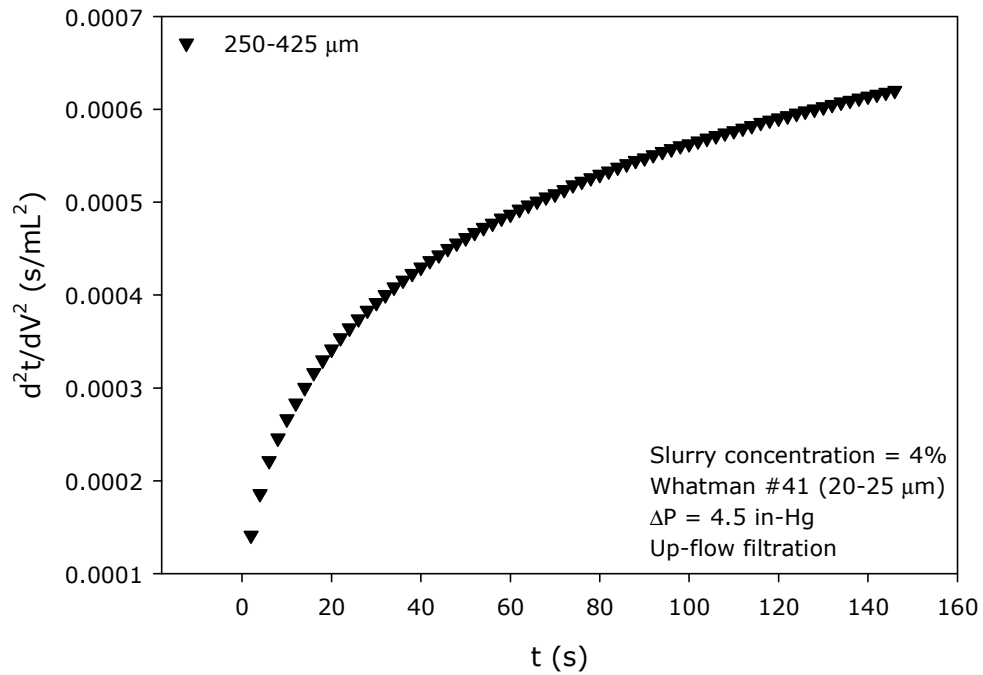


**Figure B.51.**  $d^2t/dV^2$  vs.  $t$  plot-Particle size effect (II-B, 250-425  $\mu\text{m}$ )

*Case III-Pressure Effect*

**Table B.7.** Experimental conditions-Pressure effect (III-A)

<b>Operational Conditions</b>	<b>Water + Meliodent</b>
Slurry concentration	4%
Filter Medium	W#41 (20-25 $\mu\text{m}$ )
Particle size distribution	200-210 $\mu\text{m}$
Mode of filtration	Up-flow
Pressure	5 in-Hg 10 in-Hg

Figure B.52 is the  $dt/dV$  vs.  $V$  plot and Figure B.53 is the  $dt/dV$  vs.  $t$  plot.

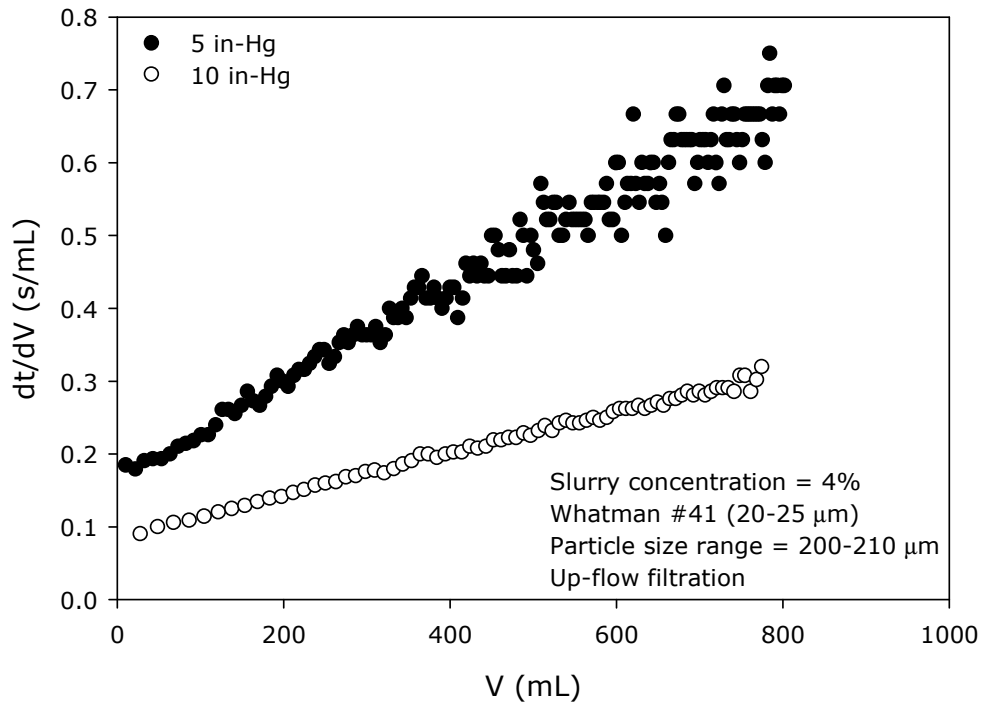


**Figure B.52.** dt/dV vs. V plot-Pressure effect (III-A)

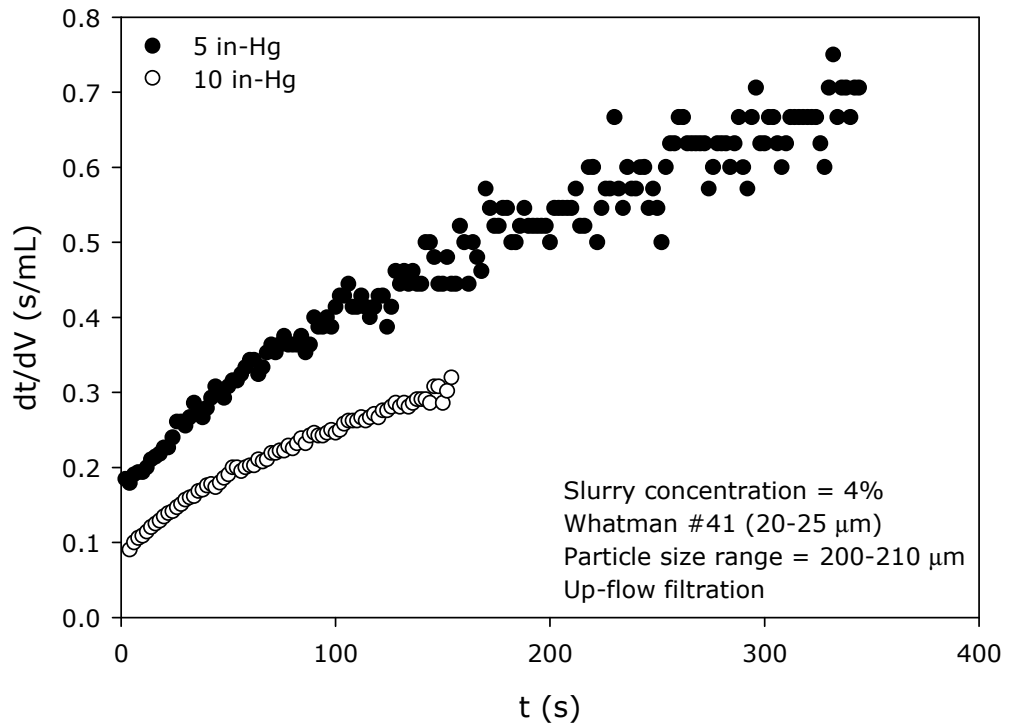


**Figure B.53.** dt/dV vs. t plot-Pressure effect (III-A)

The  $dt/dV$  vs.  $t$  plots of both the experimental data and the MATLAB-predicted data are presented in Figures B.6 and B.14. The  $d^2t/dV^2$  vs.  $t$  graphs are given in Figures B.9 and B.17.

**Table B.8.** Experimental conditions-Pressure effect (III-B)

<b>Operational Conditions</b>	<b>Water + Meliodent</b>
Slurry concentration	4%
Filter Medium	Steel mesh (200 $\mu\text{m}$ )
Particle size distribution	200-210 $\mu\text{m}$
Mode of filtration	Up-flow
Pressure	5 in-Hg 10 in-Hg

Figure B.54 is the  $dt/dV$  vs.  $V$  plot and Figure B.55 is the  $dt/dV$  vs.  $t$  plot.

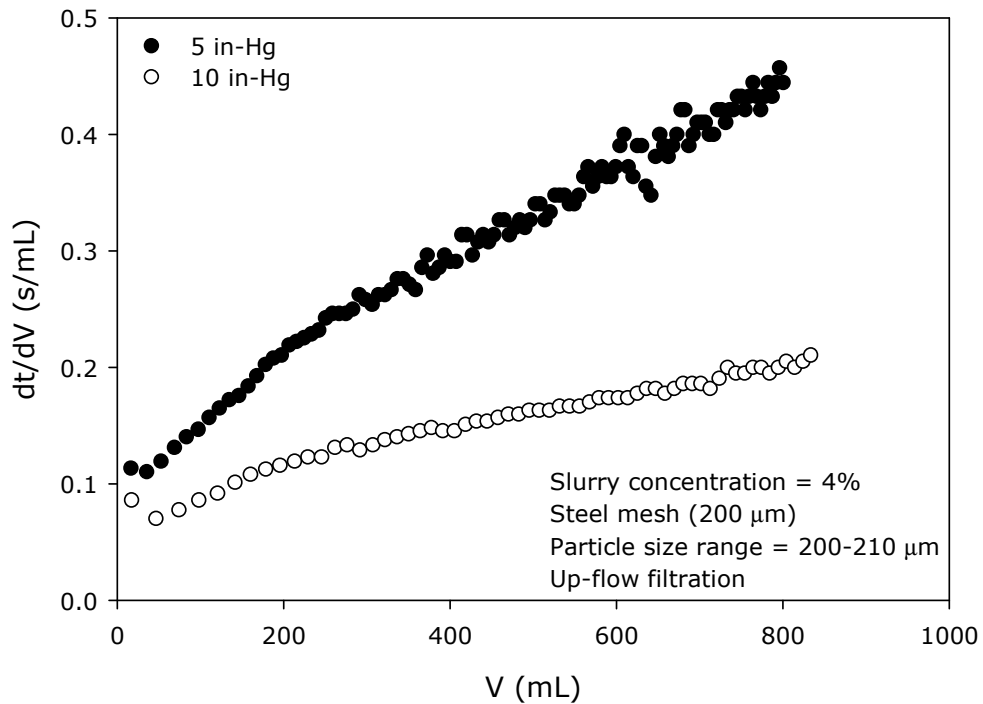


**Figure B.54.**  $dt/dV$  vs.  $V$  plot-Pressure effect (III-B)

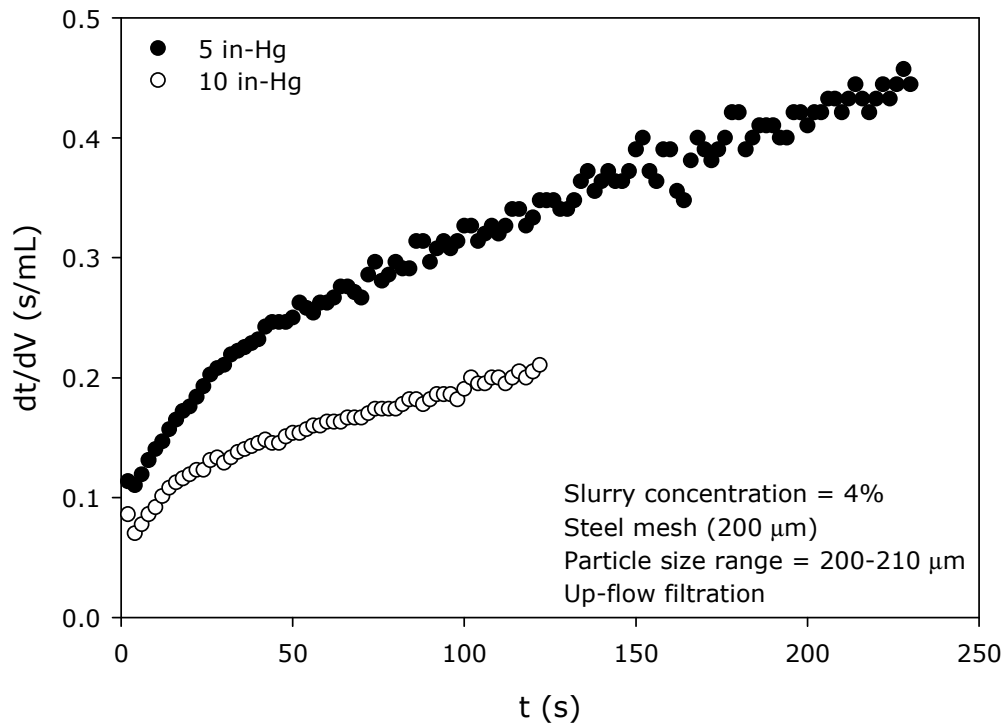


**Figure B.55.** dt/dV vs. t plot-Pressure effect (III-B)

The dt/dV vs. t plots of both the experimental data and the MATLAB-predicted data are presented in Figures B.8 and B.16. The  $d^2t/dV^2$  vs. t graphs are given in Figures B.11 and B.19.

## CURRICULUM VITAE

### PERSONAL INFORMATION

Surname, Name: Yükseler, Hande

Nationality: Turkish (TC)

Date and Place of Birth: November 6<sup>th</sup>, 1980, Ankara

Marital Status: Single

Phone: (+90) 312 292 1622

Fax: (+90) 312 287 1648

e-mail: hande.yukseler@mfa.gov.tr, hande\_yukseler@yahoo.co.uk

### EDUCATION

Degree	Institution	Year of Graduation
MS	METU Environmental Engineering	2004
BS	METU Environmental Engineering	2001
High School	TED Ankara College	1997

### WORK EXPERIENCE

Year	Place	Enrollment
7/2007-Present	Republic of Turkey Ministry of Foreign Affairs, Deputy General Directorate of Energy, Water and Environment	Advisor
9/2001-7/2007	METU Department of Environmental Engineering	Teaching Assistant

### FOREIGN LANGUAGES

English (fluent), French (basic)

### PUBLICATIONS

1. Yükseler, H., Tosun, I. and Yetis, U., 2007. "A New Approach in Assessing Slurry Filterability", *Journal of Membrane Science*, in press.

2. H. Yukseler, N. Uzal, M. Unlu, C. Varol, E. Sahinkaya, N. O. Yigit, L. Yilmaz, G. N. Demirer, M. Kitis, F. B. Dilek and U.Yetis, "*Integrated Wastewater Management in a Denim Manufacturing Textile Mill - Implementation of EU's IPPC Directive*", 6<sup>th</sup> IWA Specialist Conference on Wastewater Reclamation and Reuse for Sustainability, October 9-12, 2007, Antwerp, Belgium (*accepted for long presentation*).

3. U. Yetis, H. Yukseler S. Valatka, D.Semeniene, M. Kerestecioglu, M. Jacobsen, "*Implementation of the EU's Bathing Water Directive in Turkey*", 3<sup>rd</sup> International Conference on Environmental Science and Technology, August 6-9, 2007, Houston, Texas, USA (*accepted for oral presentation*).

4. H. Yukseler, N. Uzal, E. Şahinkaya, M. Unlu, C. Varol, O. Yilmaz, F. Morova, S. Alanya, E. Ozturk, N.O. Yigit, A. M. Kocabas, M. Mungan, M. Kerestecioglu, L. Yilmaz, M. Kitis, G.N. Demirer, F.B. Dilek, U. Yetis, "*Implementation of EU's IPPC Directive to a Denim Textile Mill in Turkey-Performance Evaluation of BAT Options*", 3<sup>rd</sup> International Conference on Environmental Science and Technology, August 6-9, 2007, Houston, Texas, USA (*accepted for oral presentation*).

5. M. Unlu, H. Yükseler, N. Uzal, M. Kitis, G.N. Demirer, F.B. Dilek, U.Yetis, "*Indigo Dyeing Wastewater Reclamation By Microfiltration and Coagulation Processes*", PERMEA 2007, September 2-6, 2007, Siofok, Hungary (*accepted for oral presentation*).

6. N.O. Yigit, N. Uzal, H. Koseoglu, I. Harman, H. Yukseler, U. Yetis, G. Civelekoğlu, M. Kitis, "*Treatment of a Denim Producing Textile Industry Wastewater Using Pilot-Scale Membrane Bioreactor*", PERMEA 2007, September 2-6, 2007, Siofok, Hungary (*accepted for oral presentation*).

7. N.O. Yigit, I. Harman, N. Uzal, H. Yukseler, U. Yetis, G. Civelekoglu, M. Kitis, "*Treatment of Textile Industry Wastewater Using Pilot-Scale Membrane Bioreactor*", UCS2007, National Environment Symposium 2007, Mersin University, April 18<sup>th</sup>-21<sup>st</sup>, 2007, Mersin, Turkey (*in Turkish, oral presentation*).

8. H. Yükseler, I. Tosun, Ü. Yetiş, "A New Approach in Analyzing Cake Filtration Data", IWA Specialist Conferences, Facing Sludge Diversities: Challenges, Risks and Opportunities, March 28<sup>th</sup>-30<sup>th</sup>, 2007, Antalya, Turkey (*oral presentation*).
9. H. Yükseler, Ü. Yetiş, I. Tosun, "Cake Filtration: Effect of Cake-Septum Interface", IWA Specialist Conferences, Facing Sludge Diversities: Challenges, Risks and Opportunities, March 28<sup>th</sup>-30<sup>th</sup>, 2007, Antalya, Turkey (*poster presentation*).
10. U. Onwusogh, H. Yükseler, N. Uzal, D. Marinkova, P. Pholchan, D. Yordanov, L. Yotova, "Svilozza AD Wastewater Treatment Plant Design", STaR City Training Programme, Technical Feedback Meeting and Public Event, October 24<sup>th</sup>-26<sup>th</sup>, 2006, The Island of Alderney, Channel Islands, United Kingdom (*oral and poster presentation*).
11. U. Onwusogh, D. Santana, J. Go, H. Yükseler, "Design and application of reed beds in wastewater treatment", STaR City Training Programme, Technical Feedback Meeting and Public Event, October 24<sup>th</sup>-26<sup>th</sup>, 2006, The Island of Alderney, Channel Islands, United Kingdom (*poster presentation*).
12. N. Uzal, H. Yükseler, M. Ünlü, Ö. Yılmaz, C. Varol, G.N. Demirer, F. B. Dilek, Ü. Yetiş, "Water reuse and recycling opportunities in dyeing process of a denim producing factory", The Seventh International Symposium On Waste Management Problems In Agro-Industries, September 27<sup>th</sup>-29<sup>th</sup>, 2006, Amsterdam RAI, The Netherlands (*Proceedings Book, pp.167-174*).
13. H. Yükseler, N. Uzal, M. Ünlü, Ö. Yılmaz, C. Varol, G.N. Demirer, F. B. Dilek, Ü. Yetiş, "Adoption of EU's IPPC Directive: Determining BAT In A Turkish Denim Manufacturing Plant", The Seventh International Symposium On Waste Management Problems In Agro-Industries, September 27<sup>th</sup>-29<sup>th</sup>, 2006, Amsterdam RAI, The Netherlands. (*poster presentation*)
14. Yükseler, H., Ü. Yetiş, İ. Tosun, "Characterization of Sludge Filtration", The American Filtration and Separations Society 2006 Annual Meeting, 9-11 May, 2006, Illinois, USA (*oral presentation*).

15. Yükseler, H., Ü. Yetiş, İ. Tosun, 2005. "Current Status of Filtration Theory", *Journal of Residuals Science and Technology*, 2(4), pp. 211-220.
16. Yükseler, H., Ü. Yetiş, İ. Tosun, "Sludge Dewatering", Proceedings of the 1<sup>st</sup> National Sludge Symposium, pp. 201-210, 23-25 March 2005, İzmir, Turkey (*oral presentation*).
17. Yükseler, H., Ü. Yetiş, İ. Tosun, "Filtration of Activated Sludge", The American Filtration and Separation Society, 9<sup>th</sup> World Filtration Congress, Abstract Book p.25, 18-22 April, 2004, New Orleans, USA (*oral presentation*).
18. İ. İmamoğlu, S. Girgin, F.D. Sanin, F.B. Dilek, Ü. Yetiş, H. Yükseler, C.F. Gökçay, "Municipal Wastewater Management in Turkey: Impacts & Reuse", Best Practice Examples for Reuse of Wastewaters in Agricultural Irrigation in the World 2004, International Workshop on Implementation and Operation of Municipal Wastewater Reuse Plants, Thessaloniki, Greece (*poster presentation*).
19. Kerestecioglu, M., İ. İmamoğlu, E. Tokcaer, and H. Yükseler "Evaluation of a Treatment Plant Design Course", Proceedings of the 2nd Environmental Pollution Control Symposium, pp.291-298, 22-24 October 2003, Ankara, Turkey (*oral presentation*).
20. Yükseler, H., Ö. Yılmaz, İ. Tosun, Ü. Yetiş, "Sludge Filtration", Proceedings of the 5th National Environmental Engineering Congress, pp.411-422, 1-4 October 2003, Ankara, Turkey (*oral presentation*).